



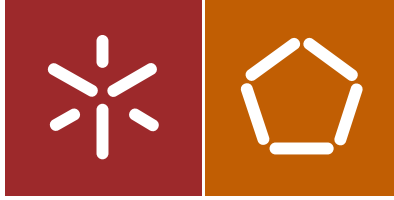
David Jefferson Cardoso Araújo

Production of cellulose-based bioplastics from  
agroindustrial residues

Universidade do Minho  
Escola de Engenharia







Universidade do Minho  
Escola de Engenharia

David Jefferson Cardoso Araújo

Production of cellulose-based bioplastics from  
agroindustrial residues

Tese de Doutoramento  
Gestão e Tratamento de Resíduos

Trabalho efetuado sob a orientação de  
Professora Doutora Ana Vera Alves Machado  
Professora Doutora Maria Cândida Lobo Guerra  
Vilarinho

## **DECLARAÇÃO**

### **DIREITOS DE AUTOR E CONDIÇÕES DE UTILIZAÇÃO DO TRABALHO POR TERCEIROS**

Este é um trabalho académico que pode ser utilizado por terceiros desde que respeitadas as regras e boas práticas internacionalmente aceites, no que concerne aos direitos de autor e direitos conexos. Assim, o presente trabalho pode ser utilizado nos termos previstos na licença abaixo indicada. Caso o utilizador necessite de permissão para poder fazer o uso do trabalho em condições não previstas no licenciamento indicado, deverá contactar o autor, através do RepositórioUM da Universidade do Minho.

#### **Licença concedida aos utilizadores deste trabalho**



#### **Atribuição-NãoComercial-SemDerivações**

CC BY-NC-ND

<https://creativecommons.org/licenses/by-nc-nd/4.0/>

## ACKNOWLEDGEMENTS

Esse desafiador percurso acadêmico não teria sido tão gratificante sem a ajuda de diversas pessoas e instituições, as quais manifesto os meus sinceros agradecimentos. Primeiramente, gostaria de agradecer às minhas supervisoras, Professora Ana Vera Machado e Professora Cândida Vilarinho, pela oportunidade de trabalho em parceria, bem como por todos os ensinamentos adquiridos ao longo desse doutoramento. Gostaria ainda de expressar a minha gratidão a ambas professoras por me terem recebido em seus grupos de pesquisa e instituições parceiras, o qual considero uma experiência de enorme ganho profissional e pessoal.

Os meus mais sinceros agradecimentos a todos os meus colegas do programa doutoral e membros dos laboratórios pelo acolhimento e convívio. Um especial agradecimento à Doutora Cidália Castro, pelas orientações e ajuda laboratorial, bem como à Pedro Rodrigues, que sempre se mostrou disposto a ajudar com as análises de caracterização. Gostaria ainda de expressar a minha gratidão aos meus amigos Flávio Bartolomeu, Lucas Nascimento, Rafael Pereira e Driano Rezende pela amizade e companheirismo sempre, e por terem tornado mais descontraída essa longa jornada.

Agradeço aos funcionários e técnicos da Universidade que sempre se mostraram disponíveis e prestativos. Ao CNPq (Conselho Nacional de Desenvolvimento Científico e Tecnológico) e ao governo do Brasil pelo suporte financeiro no consentimento da bolsa 201940/2015-9. Obrigada à FCT (Fundação para a Ciência e Tecnologia) pelo apoio financeiro no âmbito dos projetos TSSiPRO (technologies for sustainable and smart innovative products-norte-01-0145-FEDER-000015) e UID/CTM/50025/2019 (UID/EEA/04436/2019 e NORTE-01-0145-FEDER-000018-HAMaBICo).

Por último, mas não menos importante, gostaria de agradecer à minha companheira e esposa, Caroline, por me ter inserido nessa jornada, pela ajuda e conselhos, pelo amor oferecido e por ser simplesmente, Ela. À minha filha, Eva, por me preencher com tudo que há de melhor na vida. À minha família, especialmente meus pais, pelo amor e incentivo sempre, e por compreender a minha ausência.

## **STATEMENT OF INTEGRITY**

I hereby declare having conducted this academic work with integrity. I confirm that I have not used plagiarism or any form of undue use of information or falsification of results along the process leading to its elaboration.

I further declare that I have fully acknowledged the Code of Ethical Conduct of the University of Minho.

University of Minho, 31 of October of 2019

---

David Jefferson Cardoso Araújo

## RESUMO

### **Production of cellulose-based bioplastics from agroindustrial residues**

O desenvolvimento de plásticos biodegradáveis e de base biológica desempenham um papel fundamental na transição para uma economia circular, nomeadamente em aplicações de caso único, como embalagens. Esta tipologia de materiais baseia-se no uso de matérias-primas renováveis, na possibilidade de reciclagem orgânica e na economia de recursos por reprocessamento. A biomassa lignocelulósica destaca-se como uma fonte promissora de biopolímeros naturais, sendo os resíduos agroindustriais uma fonte atraente devido à sua disponibilidade, baixo custo e alto teor de celulose. Paralelamente, é igualmente importante que os produtos emergentes de base biológica acompanhem as tendências do mercado, nomeadamente no uso de técnicas de processamento ecológicas e no desenvolvimento de materiais com propriedades ativas. No presente trabalho pretendeu-se desenvolver bioplásticos de base celulósica a partir de resíduos agroindustriais. Estes foram identificados com base num diagnóstico e na implementação de um modelo linear, tendo sido seleccionado o caroço do milho como matéria prima a estudar. Um pré-tratamento combinado de dois estágios (tratamento hidrotérmico seguido da reacção com solução diluída de hidróxido de sódio) foi realizado para extrair a sua fração celulósica. A celulose extraída foi utilizada para produção de acetato de celulose através de uma técnica acetilação sem a presença de um meio solvente para dissolução. Na síntese do acetato de celulose obteve-se um grau de substituição de 2,68 e um rendimento de 60%. O acetato de celulose produzido apresentou ainda características adequadas para a preparação de filmes com características mecânicas significativas. Avaliação do ciclo de vida foi realizada para contabilizar os impactos ambientais associados à aplicação conjunta das técnicas de pré-tratamento e acetilação. A análise de ciclo de vida mostrou que as técnicas utilizadas repercutiram em impactos ambientais menos significativos que os gerados por abordagens convencionais. Um bionanocompósito foi produzido através da dissolução do acetato de celulose sinterizado em uma suspensão coloidal contendo nanopartículas de dióxido de titânio e óxido de magnésio, obtida a partir da ablação a laser dos metais percussores em diclorometano. A técnica utilizada possibilitou a produção de filmes bioplásticos sem o uso de qualquer outro reagente químico ou geração de subprodutos.

**Keywords** Resíduos agroindustriais; bioplásticos; celulose; pré-tratamentos verdes; acetato de celulose; bionanocompósitos; análise de ciclo de vida

## ABSTRACT

### **Produção de plásticos baseados em celulose a partir de resíduos agroindustriais**

Bio-based and biodegradable plastics play a key role towards the successful transition to a circular economy, namely regarding the application of single-use products, such as packaging. The benefits brought by this class of materials rest on the use of renewable resources of raw-materials, organic recycling and resource-saving by reprocessing. Lignocellulosic biomass stands out as a promising source of natural biopolymers, being the agroindustrial residues are especially attractive alternative due to their availability, low-cost and high cellulose content. On top of that, it is likewise important that the emerged bio-based products keep up with the latest trends on the market, which are focused on the use of eco-friendly processing techniques and development of active materials. In this regard, the present thesis is intended to develop cellulose-based bioplastics from agroindustrial residues. Potential agroindustrial residues were identified based on a diagnosis study and on the implementation of a linear model, from which corncob was selected as the raw material to be studied. A combined two-stage liquid hot water/dilute-NaOH pretreatment was carried out to extract its cellulose content. Furthermore, cellulose acetate (CA), a recognized biodegradable polymer, was synthesized from the extracted cellulose by a solvent-free method using iodine as catalyst. The cellulose acetate synthesis resulted in substitution degree of 2.68 and yield of 60%. The synthesized CA was suitable to produce films with remarkable mechanical properties. A life cycle assessment (LCA) was modeled in order to count the environmental impacts resulting from the joint application of pretreatment/acetylation techniques. The LCA showed that, in response to the less consumption of chemicals and high yield of acetylation, the proposed techniques have environmental impacts less significant than those of conventional approaches. A bionanocomposite was produced via the direct dissolution of the synthesized CA in a colloidal suspension containing titanium dioxide and magnesium oxide, the latter obtained through the laser ablation of bare metal targets in an appropriate solvent. The processing technique used allowed the production of bioplastic films without the use of any other chemical reagent or generation of byproducts.

**Keywords:** Agroindustrial residues; bioplastics; cellulose; green pretreatments; cellulose acetate; bionanocomposites; life cycle assessment



# CONTENTS

<b>ACKNOWLEDGEMENTS</b>	<b>iii</b>
<b>RESUMO</b>	<b>v</b>
<b>ABSTRACT</b>	<b>vi</b>
<b>CONTENTS</b>	<b>vii</b>
<b>LIST OF FIGURES</b>	<b>xii</b>
<b>LIST OF TABLES</b>	<b>xv</b>
<b>Chapter 1. Introduction</b>	<b>1</b>
1.1. Study background and motivation	2
1.2. Objectives and structure of the thesis	5
References	8
<b>Chapter 2. State of the art</b>	<b>10</b>
2.1. Lignocellulosic Biomass: structure and sources	11
2.1.1. Hemicellulose	12
2.1.2. Lignin	13
2.1.3. Cellulose – structure and morphology	14
2.2. Pretreatments of lignocellulosic biomass	17
2.2.1. Liquid hot water	18
2.2.2. Pretreatment of lignocellulosic biomass with Ionic liquid	19
2.2.3. Sodium hydroxide pretreatment	24
2.2.4. Combined pretreatments	25
2.3. Cellulose modification and derivatives	25
2.3.1. Cellulose acetate	26
2.4. Cellulose-based packaging emerged from agroindustrial residues	28
2.5. Active packaging and additives	29
2.6 Pulsed laser ablation of metal/metal oxides in liquids	32
2.7 Life cycle assessment	34

References	37
<b>Chapter 3. Availability and suitability of agroindustrial residues as feedstock for cellulose-based materials: Brazil case study</b>	<b>56</b>
Abstract	57
3.1. Introduction	57
3.2. Methodology	59
3.2.1. Crop Residues Production and Chemical Composition	59
3.2.3. Availability of Agricultural Residues	61
3.2.4. Suitability of Agroindustrial Residues to Develop Cellulose-based Products	63
3.3. Results and discussion	63
3.3.1. Agricultural Production and Harvested Area	63
3.3.2. Chemical Composition of Agroindustrial Residues	65
3.3.3. Availability of Agroindustrial Residues	67
3.3.4. Suitability of Agroindustrial Residues	70
3.4. Conclusion	73
Acknowledgements	73
References	74
<b>Chapter 4. Effect of combined dilute-alkaline and green pretreatments on corncob fractionation: pretreated biomass characterization and regenerated cellulose film production</b>	<b>86</b>
Abstract	87
4.1. Introduction	87
4.2. Materials and methods	91
4.2.1. Materials	91
4.2.2. Liquid Hot Water treatment	91
4.2.3. Alkali treatment of corncob	91
4.2.4. Ionic liquid treatment and regeneration of treated biomass	92
4.2.5. Characterization of untreated and treated corncob	93

4.2.6. Preparation of regenerated cellulose film	94
4.2.7. Dynamic mechanical analysis	94
4.3. Results and discussion	95
4.3.1. Compositional analysis	95
4.3.2. Fourier-transformed Infrared spectroscopy	97
4.4.3. X-ray Diffraction Analysis	100
4.3.4. Scanning electron microscopy	102
4.3.5. Thermogravimetric properties	103
4.3.6. Dynamic mechanical analysis and chemical characterization of regenerated film	106
4.4. Conclusions	108
Acknowledgements	109
Reference	109
<b>Chapter 5. Green synthesis of cellulose acetate from corncob: physicochemical properties and assessment of environmental impacts</b>	<b>119</b>
Abstract	120
5.1. Introduction	121
5.2. Materials and methods	123
5.2.1. Materials	123
5.2.2. Isolation of cellulose from corncob	123
5.2.3 Synthesis of cellulose acetate	124
5.2.4. Chemical characterization	125
5.2.5. Chemical composition of untreated and treated biomass	125
5.2.6. Cellulose acetate film preparation	126
5.2.7. Morphological analysis	126
5.2.8. Dynamic mechanical analysis	126
5.2.9. Life cycle assessment	126
5.3. Results	130

5.3.1. Effect of combined pretreatment on corncob fractionation – compositional analysis	130
5.3.2. Cellulose acetate syntheses – degree of substitution and yield	130
5.3.3. Fourier Transformed Infrared analysis	132
5.3.4. Thermogravimetric analysis	133
5.3.5. Scanning Electron Microscopy Analysis	135
5.3.6. Dynamic mechanical analysis	136
5.3.7. Life Cycle assessment	137
4. Conclusions	143
Acknowledgements	144
Reference	144
<b>Chapter 6. A novel eco-friendly synthesis processing to produce cellulose acetate/ TiO<sub>2</sub>/MgO bionanocomposite films</b>	<b>152</b>
Abstract	153
6.1. Introduction	153
6.2. Materials and methods	157
6.2.1. Materials	157
6.2.2. Isolation of cellulose from corncob	157
6.2.3. Synthesis of cellulose acetate	157
6.2.4. Production of Nanoparticles/colloidal solution	158
6.2.5. Cellulose acetate/TiO <sub>2</sub> /MgO nanocomposite film preparation	158
6.2.6. Material characterization	159
6.2.7. Dynamic mechanical analysis of the bionanocomposite film	161
6.3. Results	161
6.3.1. Cellulose extraction from corncob	161
6.3.2. Cellulose acetate synthesis	161
6.3.3. Characterization of nanoparticles	162

6.3.4. Fourier-transformed infrared spectroscopy	165
6.3.5. X-ray diffraction analysis	166
6.3.6. Scanning electron microscopy of the films	167
6.3.7. Thermogravimetry analysis of films	169
6.3.8. Dynamic mechanical analysis	170
6.4. Conclusions	172
Acknowledgements	173
References	173
<b>Chapter 7. Conclusion and Future Work</b>	<b>183</b>
7.1 General conclusions	184
7.2 Suggestions for future works	186
<b>Appendix A</b>	<b>187</b>
<b>Appendix B</b>	<b>204</b>
References	208

## LIST OF FIGURES

Figure 2-1. Structure of lignocellulosic biomass. ....	12
Figure 2-2. Chemical structure of cellulose chain.....	14
Figure 2-3. Morphological hierarchy of cellulose fibers.....	16
Figure 2-4. Pretreatment effect on lignocellulosic biomass.....	17
Figure 2-5. Schematic illustration of metal nanoparticles formation by PLAL. ....	33
Figure 3-1. Average production of permanent crops in Brazil. a) Average percentage of the main crops produced by each macroregion. b) Average production of permanent crops from 2004 to 2014 and average percentage of permanent crop production by macroregions. .	64
Figure 3-2. Annual evolution of temporary agricultural crops production from 1990 to 2014. ...	65
Figure 3-3. Availability and cellulose content of the major agroindustrial residues identified. ....	69
Figure 3-4. Annual evolution of availability of residues in Brazil. ....	70
Figure 3-5. Suitability of agrosidues for cellulose-based materials production. ....	72
Figure 4-1. Schematic representation of pretreatments performed. ....	92
Figure 4-2. Photographs of (a) corncob, (b) ground corncob, (c) ionic liquid treated corncob, (d) LHW treated corncob, (e) NaOH treated corncob, (f) LHW-NaOH treated corncob, (g) LHW- NaOH-IL treated corncob, (h) NaOH-IL treated corncob and (i) LHW-IL treated corncob....	97
Figure 4-3. FTIR spectra of (a) cellulose pulp, corncob and single pretreatments and (b) combined pretreatments. Abbreviation Ar in graphs means aromatic ring. ....	99
Figure 4-4. X-ray diffractograms of (a) cellulose pulp, corncob and single pretreatments and (b) combined pretreatments. ....	101
Figure 4-5. SEM micrographs of (a) untreated corncob, (b) LHW-CC, (c) NaOH-CC, (d) LHW- NaOH-CC, (e) IL-CC, (f) LHW-IL-CC, (g) NaOH-IL-CC, (h) LHW-NaOH-IL-CC and (i) Cellulose Pulp.....	103
Figure 4-6. (a) TGA, (b) DTG and DSC (inset plot in the graph 5b) curves of the cellulose pulp, untreated and treated corncob.....	105
Figure 4-7. (a) Dynamic mechanical analysis, (b) X-ray diffraction and FTIR spectra (inset graph in figure 7b) and (c) SEM cross section of (d) regenerated cellulose film produced from LHW- NaOH pretreated corncob.....	108

Figure 5-1. Flow chart of product systems: Left branch – modeled green approach scenario; right branch – modeled conventional approach scenario. Inputs highlighted with an asterisk do not exist in Ecoinvent database and had to be modeled in OpenLCA.....	128
Figure 5-2. <sup>1</sup> H NMR spectra of cellulose acetate synthesized by (a) green and (b) standard acetylation methods. ....	132
Figure 5-3. FTIR spectra of cellulose pulp, commercial CA, extracted cellulose (LHW-dilute NaOH pretreatment) and CA synthesized by green and standard acetylation. ....	133
Figure 5-4. (a) TG and (b) DTG (as well as inset plot in the graph 4b of DTG ranging from 330 °C to 390 °C) curves of cellulose pulp, commercial CA, extracted cellulose (LHW-dilute NaOH pretreatment) and CA synthesized by green and standard acetylation. ....	134
Figure 5-5. SEM micrographs of (a) untreated corncob, (b) LHW-dilute NaOH pretreated corncob, as well as the (c) surface and (d) cross-section of the cellulose acetate film. ....	135
Figure 5-6. (a) Dynamic mechanical analysis of cellulose acetate film produced and (b) cellulose acetate film. ....	137
Figure 5-7. (a) Potential environmental impacts of cellulose acetate synthesized by green and conventional approaches and (b) proportional contributions of green approach processing steps on each environmental impact category. ....	139
Figure 5-8. Potential impact contribution in PE/10g of cellulose acetate of the green and conventional approach. ....	140
Figure 5-9. Influence of pretreatments and acetylation techniques on environmental impacts. Comparison of reference scenarios with Modeled intermediate one constituted by LHW-dilute NaOH pretreatment and acetic acid acetylation process. ....	141
Figure 5-10. Potential impact differences in all categories due to possible changes in the acetylation yield of the conventional approach. Impact increment was calculated taking as baseline scenario the green approach. WG means weight gain. ....	143
Figure 6-1. Schematic representation of the eco-friendly approach to produce bionanocomposite films. ....	159
Figure 6-2. Nanoparticles characterization. (a) SEM image of TiO <sub>2</sub> NPs, (b) SEM image of MgO, (c) NPs distribution histogram of TiO <sub>2</sub> , (d) NPs distribution histogram of MgO and (e) UV-vis spectra of colloidal TiO <sub>2</sub> /MgO ablated nanoparticles in DCM (the inset graph shows the Tauc plot for $\alpha h\nu^{1/n}$ versus $h\nu$ and the respective band gap). ....	165

Figure 6-3. FTIR spectra of the extracted cellulose (LHW-dilute NaOH pretreatment), commercial CA, synthesized CA and CA/MgO/TiO <sub>2</sub> bionanocomposite film. ....	166
Figure 6-4. (a) Schematic representation of disorder caused in the cellulose structure due to acetate groups insertion and (b) XRD diffractograms of the synthesized CA and CA/MgO/TiO <sub>2</sub> films. ....	167
Figure 6-5. SEM micrographs and EDS analysis of the produced films: (a), (b), (c) refer to synthesized CA surface, cross-section and EDS analysis, respectively, and (d), (e), (f) refer to CA/TiO <sub>2</sub> /MgO surface, cross section and EDS, respectively.....	169
Figure 6-6. TG (upper graph) and DTG (lower graph) curves of the synthesized CA and CA/TiO <sub>2</sub> /MgO films. ....	170
Figure 6-7. Dynamic mechanical analysis of the (a) synthesized CA and (b) CA/TiO <sub>2</sub> /MgO film. ....	172



## LIST OF TABLES

Table 3.1. Residues generation rates of agroindustrial residues. ....	60
Table 3.2. Competitive uses of agroresidues. ....	62
Table 3.3. Chemical composition of lignocellulosic biomass derived from temporary crops .....	65
Table 3.4. Chemical composition of lignocellulosic biomass derived from permanent crops. ....	66
Table 3.5. Average availability of agricultural residues.. ....	67
Table 3.6. Availability of residues, Cellulose content and cellulose-to-lignin ratio normalized values. ....	71
Table 4.1. Chemical composition of untreated and pretreated corncob. ....	97
Table 4.2. FTIR absorbance bands and the respective functional groups in cellulose pulp, untreated and treated corncob. ....	98
Table 4.3. Thermogravimetric results for cellulose pulp, untreated and treated corncob samples. ....	104
Table 5.1. Environmental impact categories and normalization references used.....	129
Table 5.2. Thermogravimetric results for cellulose pulp, commercial CA, extracted cellulose (LHW-dilute NaOH pretreatment) and CA synthesized by green and standard acetylation.....	134

## Chapter 1. Introduction

---

This chapter aims to clarify the scope of this PhD project by enlightening the motivation, the objectives and the structure of the thesis.

---

## 1.1. Study background and motivation

Synthetic plastics have long since played an important role throughout many application domains, namely science, technology, industry and household, whether as an advanced or basic material. Their wide applicability, easy and low-cost processability, versatility and physical-chemical properties (e.g. tensile strength, durability, flexibility, low weight, resistance to the action of microorganisms and weathering) have contributed to their attractiveness and demand, which fostered the rapid development of polymer industry in the last decades. In 2017, over 348 million tonnes of synthetic plastics (mainly derived from fossil resources) were manufactured around the world [1]. From this total, the polyolefins accounted for more than 50%, which were mainly used for packaging production [2]. However, the same properties that make synthetic plastics a ubiquitous class of material, can also unleash negative environmental effects if they are mismanaged or littered. For instance, a great share of macroplastics-related findings in the ocean or in coastal areas corresponds well with the main sources of short-lived consumer goods ending up in municipal solid waste systems, which include mainly packaging [2].

Recently, the growing concerns over economic and environmental issues regarding synthetic plastics' value chain, namely oil market price fluctuations, finiteness of fossil raw materials and biotic/abiotic pollution of earth's compartments, have become nucleation supports for new sustainable thoughts on polymers' life cycle. At the same time, the narrowing of legal frameworks regarding the production, consumption and disposal of plastics has increasingly forced a change of position at the social and organizational level. The progress of good practices in this area tends to continue as governments and businesses are narrowing and driving their policies towards a circular economy model.

Ongoing practical applications of circular economy are dated since the late 1970s, but only recently it gained notoriety and momentum [3]. The idea of circular economy emphasizes that, by employing a regenerative approach through reuse, refurbishment, repair and recycling, the value and time of materials would be maximized, while the demand of resources and waste generation would decrease [4]. As a part of public policy, the change of a linear economy to a circular one could provide economy grow and opportunities in line with social development and environmental protection. A promisor route identified in countries trying to promote circular economy as national policy deals with the substitution of non-renewable resources by biomaterials. This aspect is in synergy with the principles of bioeconomy, which, conceptually, comprises any value chain that uses biomaterials as starting point, such as agriculture and forestry sources [5]. In the field of

polymers, the development of biopolymers has shown a dynamically growing market and a central theme of research in countless vehicles of scientific communication. Bioplastics can be bio-based, biodegradable or feature both properties. Bio-based polymers have been one of the most relevant drivers for the development of the European Union bioeconomy, with recognized potential to accelerate the transition to a circular economy. Global production capacities of bioplastics are predicted to grow from around 2.11 million tonnes in 2018 to approximately 2.62 million tonnes by 2023 [6].

To date, the bio-based plastics with highest growth rates on the market are bio-based polyethylene (PE), bio-based polyethylene terephthalate (PET), polylactic acid (PLA) and polyhydroxyalkanoates (PHA) [6,7]. Although they do have better environmental performance in comparison to the oil-based options, they have been still criticized for being not completely bio-based, nonbiodegradable or derived from first-generation products. In response to the aforementioned issues, there has been a growing interest in the development of biodegradable plastics from renewable polymer sources that have technological, economic and environmental viability, and that are also not eligible for feed or food production. In this context, lignocellulosic biomass has been pointed out as one of the most promising renewable alternatives since it is mainly composed by natural polymers (cellulose, hemicellulose and lignin) and available worldwide in the form of agroindustrial, forestry and municipal residues.

Annually, billions of tons of agroindustrial residues are generated by agri-food industries operations. These residues are largely available in the form of harvesting residues or byproducts and, despite some of them are used for added-value applications, the largest share is typically collected, burned, left on the ground to decompose or disposed of in municipal solid waste systems. Therefore, in addition to be a low-cost and neutral-carbon alternative, the agroindustrial residues are also greatly available as a biopolymer source, and their valorization could help to prevent environmental pollution and would foster the circular economy.

Among the main components of lignocellulosic biomass, the cellulose stands out as the most abundant renewable organic material in the biosphere [8]. Its availability and numerous properties (e.g. renewability, low cost, biodegradability, biocompatibility, chemical and thermal stability as well as its ability to form derivatives) makes it an especially attractive biopolymer [9, 10]. However, in the cell wall of plants, cellulose is incorporated (and tightly bound by covalent bonds) into a matrix of lignin and hemicellulose and, when it comes to the production of cellulose-based bioplastics, the coexistence of these other constituents may difficult cellulose accessibility and

entail undesirable properties to the final products. As a result, pretreatments are usually carried out to disrupt the compact structure of agroindustrial residues and extract the cellulose content.

There are different techniques available to pretreat lignocellulosic biomass (LCB), which may pose distinct effects on extraction efficiency of biomass components and on their physicochemical properties. In addition to influencing subsequent processing of LCB components, the pretreatment step is also considered one of the main bottlenecks within LCB valorization. For instance, in terms of environmental feasibility, the most conventional and commonly applied pretreatments make use of harsh, toxic and corrosive chemicals, and usually demand long processing times. As these issues may jeopardize the environmental sustainability of bio-plastic production, in recent decades there has been a growing interest in the use of “green” technologies for cellulose extraction, among which stand out liquid hot water (LHW), ionic liquids (IL), as well as combined pretreatments. The potential application of cellulose-enrich samples emerged from agroindustrial residues to produce bio-based packaging have already been presented in various studies [11–16]. Notwithstanding, conventional pretreatments (e.g. alkali-acid treatments) are still commonly applied to extracted cellulose-enrich pulp from biomass.

Another issue that challenges the processing of pure cellulose for bio-based packaging production arises from its non thermoplasticity and poor solubility in many organic solvents. Consequently, cellulose is usually derivatized in order to enhance its physical-chemical properties and widen its functionalities and applications. To date, cellulose acetate is one of the most important cellulose derivatives. For commercial purpose, the largest fraction of cellulose acetate is synthesized from wood and cotton pulp and manufactured through the acetic acid process route. Recently, some methodologies claimed as green (e.g. iodine-catalyzed solvent-free method and homogeneous acetylation in ionic liquid [17, 18]), were successfully applied to synthesize cellulose acetate from lignocellulosic biomass. However, most of them lack environmental assessment studies, and their eco-friendly aspect is simply assumed based on the substitution of catalysts.

Taking into account the commercial value and properties of cellulose acetate films (including thermoplasticity, chemical resistance, low water permeability and biodegradability), they come across as an interesting option for food packaging applications. Nevertheless, it is important to bear in mind that, recently, new classes of packages with additional active and smart properties are increasingly being demanded by market constituencies. Active packages with antimicrobial properties have been one of the most explored products. At scientific research level, the nanotechnologies have been greatly harnessed to this purpose. Recent studies have shown

excellent results at the level of metal/metal oxide nanoparticles (NPs) synthesis (such as silver, zinc, titanium dioxide and magnesium oxide) and their antimicrobial effects when embedded into potential polymer-based packages (synthetic or bio-based) [19–21].

However, although substantial advances have already been made in the field of active packaging, namely in antimicrobial packaging containing metal/metal oxide NPs, the development of such products making use of renewable polymer sources along with eco-friendly techniques throughout the production chain is still lacking. Far less attention has been given to the implementation of environmental assessment studies to support the eco-friendly aspect of the concerned products and the integrated manufacturing techniques used. An effective and standardized tool suitable for this purpose is the Life Cycle Assessment (LCA) methodology. Depending on the significance of the data and methods used in the LCA construction, the results obtained may present sufficient validity and provide reliable justifications to support the choice of the best alternatives studied.

## **1.2. Objectives and structure of the thesis**

Based on the foregoing considerations, this work proposes the development of cellulose-based bioplastics from agroindustrial residues by using environmentally friendly experimental procedures, with potential to be applied as packaging component. To achieve this, key tasks have been performed with the aim of: (i) making a diagnosis of the Brazilian agroindustrial sector with the view of identifying residues suitable for the concerned application; (ii) performing appropriate pretreatments technologies to extract cellulose from the selected agroindustrial residue; (iii) modifying the extracted cellulose into cellulose acetate by an eco-friendly synthesis route, thereby widening commercial acceptability ; (iv) investigating, by life cycle assessment, the environmental impact of the whole production process applied to synthesize the cellulose acetate (including pretreatment and acetylation steps); (v) and designing a novel eco-friendly processing technique to produce cellulose acetate/metal oxides bionanocomposites with potential to be applied as active packaging.

This thesis is organized into seven main chapters stemming from research papers published and submitted in international ISI-indexed books and journals. The current chapter (**Chapter 1**) is composed by the motivation, objectives and structure of the thesis, which seeks to provide context to the following discussed issues and to give an overview about the subject addressed in each section of the thesis.

Fundamental concepts and general aspects related with the main topics covered by the thesis are revised in **Chapter 2**. Particular focus is given to the main resources and techniques applied in this work, including structure and sources of lignocellulosic biomass, properties of cellulose, green pretreatments, cellulose acetate, cellulose-based packaging derived from agroindustrial residues, pulsed laser ablation in liquids and life cycle assessment. This chapter was partially derived from the following conference proceeding:

- Araújo, D. J. C., Vilarinho, M. C. L. G., Machado, A. V. Agroindustrial residues as cellulose source for food packaging applications. 5th International Conference: Wastes: solutions, treatments and opportunities III. Vilarinho et al. (Eds). Taylor and Francis, pp. 217-223, 4-6 September, Lisbon, Portugal, 2020. ISBN: 978-0-367-257774.

**Chapter 3** presents a diagnosis of the Brazilian agroindustrial sector and highlights the main agroindustrial residues produced in the country. In this research, besides the data collection and estimation of residues availability, a linear model was applied to identify the most suitable residues to the concerned application. This chapter was based on the following conference proceeding (oral presentation) and paper:

- Araújo, D. J. C., Vilarinho, M. C. L. G., Machado, A. V. Suitability of agroindustrial residues for cellulose-based materials production. 4th International Conference: Wastes: solutions, treatments and opportunities II. Vilarinho et al. (Eds). Taylor and Francis, pp. 417-423, 25-26 September, Porto, Portugal, 2017. ISBN: 9781138196698.
- Araújo, D.J.C., Machado, A.V. & Vilarinho, M.C.L.G. Availability and suitability of agroindustrial residues as feedstock for cellulose-based materials: Brazil case study. Waste Biomass Valorization, 10: 2863, (2019). <https://doi.org/10.1007/s12649-018-0291-0>

**Chapter 4** is related to the pretreatment of a selected agroindustrial residue (corn cob). In this chapter, combined green pretreatments were performed individually and in combination in order to extract cellulose, and their fractionation capacity were assessed via physicochemical characterization. The best pretreatment technique was selected based, primarily, on the cellulose content and on the physicochemical properties of the pretreated samples. A preliminary assessment regarding the suitability of the obtained enriched-cellulose sample to produce bioplastics was attested via the production of a regenerated cellulose film. This chapter was based on the following and paper:

- Araújo, D.J.C., Machado, A.V. & Vilarinho, M.C.L.G. Effect of combined dilute-alkaline and green pretreatments on corn cob fractionation: Pretreated biomass characterization and

regenerated cellulose film production. *Industrial crops and products*, 141, 111785, (2019).  
<https://doi.org/10.1016/j.indcrop.2019.111785>.

In **Chapter 5** the extracted cellulose was derivatized into cellulose acetate: a recognized biodegradable material with higher commercial significance and applicability. This was accomplished by applying a claimed eco-friendly acetylation synthesis, which preceded the pretreatment step proposed in chapter 4. The suitability of the synthesized cellulose acetate was also verified by the production of films and their assessment through dynamic mechanical analysis. On top of that, the environmental performance of the integrated pretreatment/acetylation techniques was evaluated via life cycle assessment and compared with a conventional approach. This chapter was based on the following submitted paper:

- David Araújo, M. Cidália R. Castro, Aline Figueiredo, Maria Vilarinho, Ana Machado. Green synthesis of cellulose acetate from corncob: physicochemical properties and assessment of environmental impacts. *Journal of Cleaner Production*, (2019).

**Chapter 6** address the production of a bio-based cellulose acetate/TiO<sub>2</sub>/MgO nanocomposite. In this chapter, a novel eco-friendly and versatile synthesis route is proposed. A colloidal suspension containing TiO<sub>2</sub> and MgO nanoparticles was prepared via pulsed laser ablation in a liquid media suitable to dissolve the previously synthesized cellulose acetate, and a bionanocomposite film was successfully produced by solvent casting method. The nanoparticle synthesis and nanocomposite film properties were assessed by physicochemical characterization and dynamic mechanical analysis. TiO<sub>2</sub> and MgO nanoparticles are known from literature to confer additional active properties (e.g. biodegradability and antimicrobial activity) when embedded into polymeric matrices, and therefore the proposed approach stands out as a promising route for developing active food packaging. This chapter was based on the following submitted paper:

- David Araújo, M. Cidália R. Castro, Maria Vilarinho, Ana Machado. A novel eco-friendly synthesis processing to produce cellulose acetate/TiO<sub>2</sub>/MgO bionanocomposite films. *International journal of environment, agriculture and biotechnology*, (2019).

Finally, **Chapter 7** sets out the main findings of the developed work, followed by recommendations for future work.



## References

1. Statista: Global plastic production from 1950 to 2017 (in million metric tons), <https://www.statista.com/statistics/282732/global-production-of-plastics-since-1950/>
2. UN Environment: Mapping of global plastics value chain and plastics losses to the environment (with a particular focus on marine environment). Ryberg, M., Laurent, A., Hauschild, M. United Nation Environment Programme. Nairobi, Kenya (2018)
3. Ellen McArthur Foundation: Towards a circular economy: business rationale for an accelerated transition. pp. 20. Ellen McArthur Foundation (2015)
4. Korhonen, J., Honkasalo, A., Seppala, J.: Circular Economy: The Concept and its Limitations. *Ecol. Econ.* 143, 37–46 (2018)
5. Birner, R.: Bioeconomy concepts. In: Lewandoski, I. (ed.) *Bioeconomy*. pp. 17–38. Springer, Cham. (2018)
6. European Bioplastics: Bioplastics: facts and figures. Berlin (2018)
7. Baltus, W., Beckmann, J., Carrez, D., Carus, M.: Market study on Bio-based Polymers in the World Capacities, Production and Applications: Status Quo and Trends towards 2020. Huerth (2013)
8. Klemm, D., Heublein, B., Fink, H.P., Bohn, A.: Cellulose: Fascinating biopolymer and sustainable raw material. *Angew. Chemie - Int. Ed.* 44, 3358–3393 (2005). <https://doi.org/10.1002/anie.200460587>
9. Wang, B., Li, D.: Strong and optically transparent biocomposites reinforced with cellulose nanofibers isolated from peanut shell. *Compos. Part A Appl. Sci. Manuf.* 79, 1–7 (2015). <https://doi.org/10.1016/j.compositesa.2015.08.029>
10. Habibi, Y., Lucia, L.A., Rojas, O.J.: Cellulose nanocrystals: Chemistry, self-assembly, and applications. *Chem. Rev.* 110, 3479–3500 (2010). <https://doi.org/10.1021/cr900339w>
11. Reddy, K.O., Maheswari, C.U., Dhlamini, M.S., Mothudi, B.M., Zhang, J., Zhang, J., Nagarajan, R., Rajulu, A.V.: Preparation and characterization of regenerated cellulose films using borassus fruit fibers and an ionic liquid. *Carbohydr. Polym.* 160, 203–211 (2017). <https://doi.org/10.1016/j.carbpol.2016.12.051>
12. Zhang, Q., Hu, J., Lee, D.J.: Pretreatment of biomass using ionic liquids: Research updates. *Renew. Energy.* 111, 77–84 (2017). <https://doi.org/10.1016/j.renene.2017.03.093>

13. Oun, A.A., Rhim, J.: Isolation of cellulose nanocrystals from grain straws and their use for the preparation of carboxymethyl cellulose-based nanocomposite films. *Carbohydr. Polym.* 150, 187–200 (2016). <https://doi.org/10.1016/j.carbpol.2016.05.020>
14. Luzi, F., Fortunati, E., Giovanale, G., Mazzaglia, A., Torre, L., Mariano, G.: Cellulose nanocrystals from *Actinidia deliciosa* pruning residues combined with carvacrol in PVA CH films with antioxidant / antimicrobial properties for packaging applications. *Int. J. Biol. Macromol.* 104, 43–55 (2017). <https://doi.org/10.1016/j.ijbiomac.2017.05.176>
15. Sánchez-Safont, E.L., Aldureid, A., María, J., Gámez-pérez, J., Cabedo, L.: Biocomposites of different lignocellulosic wastes for sustainable food packaging applications. *Compos. Part B.* 145, 215–225 (2018). <https://doi.org/10.1016/j.compositesb.2018.03.037>
16. Bilo, F., Pandini, S., Sartore, L., Depero, L.E., Gargiulo, G., Bonassi, A., Federici, S., Bontempi, E.: A sustainable bioplastic obtained from rice straw. *J. Clean. Prod.* 200, 357–368 (2018). <https://doi.org/10.1016/j.jclepro.2018.07.252>
17. Das, A.M., Ali, A.A., Hazarika, M.P.: Synthesis and characterization of cellulose acetate from rice husk: Eco-friendly condition. *Carbohydr. Polym.* 112, 342–349 (2014). <https://doi.org/10.1016/j.carbpol.2014.06.006>
18. Cao, Y., Wu, J., Meng, T., Zhang, J., He, J., Li, H., Zhang, Y.: Acetone-soluble cellulose acetates prepared by one-step homogeneous acetylation of cornhusk cellulose in an ionic liquid 1-allyl-3-methylimidazolium chloride (AmimCl). *Carbohydr. Polym.* 69, 665–672 (2007). <https://doi.org/10.1016/j.carbpol.2007.02.001>
19. Swaroop, C., Shukla, M.: International Journal of Biological Macromolecules Nano-magnesium oxide reinforced polylactic acid bio films for food packaging applications. *Int. J. Biol. Macromol.* 113, 729–736 (2018). <https://doi.org/10.1016/j.ijbiomac.2018.02.156>
20. Kaewklin, P., Siripatrawan, U., Suwanagul, A., Suk, Y.: Active packaging from chitosan-titanium dioxide nanocomposite film for prolonging storage life of tomato fruit. *Int. J. Biol. Macromol.* 112, 523–529 (2018). <https://doi.org/10.1016/j.ijbiomac.2018.01.124>
21. Dobrucka, R., Ankiel, M.: Possible applications of metal nanoparticles in antimicrobial food packaging. 1–7 (2018). <https://doi.org/10.1111/jfs.12617>

## Chapter 2. State of the art

---

This chapter aims to contextualize the main aspects discussed in the following chapters, as well as to help readers with different backgrounds to a common level of knowledge on several subjects that are fundamental to this work.

---

## 2.1. Lignocellulosic Biomass: structure and sources

Lignocellulosic biomass is the most abundant and renewable source of biomass on earth, naturally generated from available atmospheric CO<sub>2</sub>, water and sunlight through photosynthesis [1]. It encompasses all terrestrial plants, wastes (such as agroindustrial, forestry and municipal) and energy crops. With a global production capacity around 140 billion tons/year, the agroindustrial residues stand out as the main source of available lignocellulosic materials [2–4].

The term agroindustrial residues spans over two main categories, depending on the generation source: (1) crop residues and (2) industry processing residues. The crop residues include residues left in the field after the harvesting phase and comprise straw, branches, stover, leaves, stalks, roots, trimmings and pruning. On the other hand, crops such as sugarcane, grape, orange, potato, coffee, cocoa and coconut are particularly interesting to obtain processed products. From food processing industry, residues in the form of bagasse, pomace, husk, hull and peels are commonly generated. Despite the potential use of these residues to produce bio-based products (e.g. bio-energy, compost, fibers, bioactive compounds and polymers) they are still commonly disposed in landfills or burned in the field, which might cause serious pollution-associated problems. For instance, highlighted as one of the largest agricultural producers in the world, Brazil also ranks among the nations with the highest rates of CO<sub>2</sub> equivalent emissions from agricultural activities. In 2017 about 25 million tons of residues associated to the main crops produced in the country were burned, implying the emission of more than two thousand Gg (CO<sub>2</sub> equivalent) of methane and nitrous oxide [5], contributing to the global warming and health problems.

The agricultural crops can be classified accordingly to their growing cycle into temporary (those which are both sown and harvested during the same agricultural year) and permanent (plants that last for many seasons). Besides, the crop production can be geographical specific as three main factors influence its yield, namely soil fertility, water availability and climate [6]. These issues can lead to a spatio-temporal variability of residues generation and, hence, their knowledge is essential to a proper estimation of residues availability and to develop management strategies. Despite the assessment of residues availability can be done by applying Geographic information System tools [7], a more common and precise approach is based on the annual crop production and residue-to-crop ratio. Moreover, an appropriate estimative requires data on competitive uses and sustainable removal rates to meet environmental and economic issues.

As a typical lignocellulosic biomass, the agroindustrial residues are primarily composed of three natural organic polymers, namely cellulose, hemicellulose e lignin, as well as minor amounts of

proteins, pectin and extractives [8, 9]. LCB on a dry basis generally contain 50% of cellulose, 10-30% of hemicellulose and 20-40% of lignin [10]. This estimate slightly differs from chemical composition of agroindustrial residues (cellulose, 30-60%; hemicellulose, 14-40% and; lignin, 7-20%) [11, 12] as LCB also includes wood biomass, that refers to hardwood and softwood, which are denser, structurally stronger and contains larger amount of lignin [4]. In the cell wall of plants, cellulose is incorporated into a matrix of hemicellulose and lignin, linked together by covalent crosslinking, which ultimately results in the recalcitrant property of lignocellulosic biomass (Figure 2.1) [8, 13]. Cellulose is a semi-crystalline homopolymer consisting of a linear chain of several linked D-glucose units. Conversely, the hemicellulose is an amorphous heteropolymer formed by repeated polymers of pentoses and hexoses, while lignin is composed largely by three aromatic alcohols, and acts as glue by filling the gap between and around the cellulose and hemicellulose.

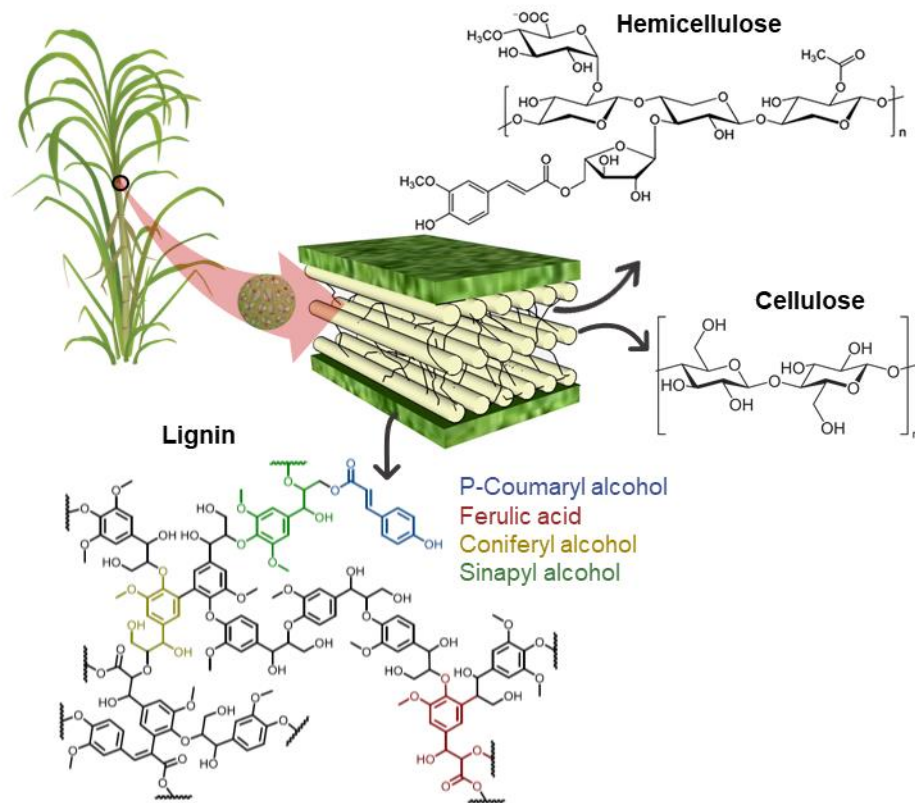


Figure 2-1. Structure of lignocellulosic biomass.

### 2.1.1. Hemicellulose

Hemicellulose is a branched heteropolymer with low polymerization degree, primarily formed by xylan and glucomannan chains intermixed with uronic acids and several kinds of

monosaccharides, including glucose, mannose, galactose and pentose (comprising arabinose and xylose) [14, 15]. The variety and amount of each component depend on the lignocellulosic source. For instance, the agroindustrial residues are mainly formed by a backbone chain of  $\beta$ -1,4-linked xylose units, containing branched points formed by arabinose and glucose chains. In the cell wall of plants, the hemicellulose matrix act as a connection between the cellulose and lignin fractions, providing rigidity to the lignocellulose structure. It is attached to cellulose through an oxygen-hydrogen bond linkage and Van der Waals forces, and interacts with lignin through a hemicellulose-ferulic acid-ether bond-lignin structure (also called lignin-carbohydrate complex (LCC)) [16]. In response to its random and amorphous structure, the disruption and dissolution of hemicellulose are easier to occur in comparison to cellulose and lignin [17]. Hemicellulose can also be used for sustainable production of value-added products, such as xylitol, polymers and ethanol, but its conversion is still challenging. Notwithstanding, the economic viability of lignocellulosic biomass valorization into cellulose-based products is highly conditioned by the effective utilization of hemicellulose [18, 19].

### 2.1.2. Lignin

Lignin is a complex, amorphous and cross-linked polymer, located mainly in the secondary cell wall of plants where provides rigidity and strength, favors the transport of water and solutes in the vascular system and protects the cell against pathogens [20]. It is comprised mainly of three monolignols as the basic building blocks, including p-coumaryl, coniferyl and sinapyl alcohols. These components are polymerized into an irregular network via different aromatic or aliphatic ether bonds ( $\beta$ -O-4, 5-5',  $\alpha$ -O-4,  $\beta$ -5, 4-O-5,  $\beta$ -1 and  $\beta$ - $\beta$ ), and are incorporated into lignin in the form of phenylpropanoids, namely p-hydroxyphenyl (H), guaiacyl (G), and syringyl (S) [14, 21]. Because of its no regular monomers sequences, lignin composition and structure are generally characterized by the relative abundance of H/G/S units, distribution of inter-unit linkages, as well as degree of condensation in the polymeric structure [22, 23]. The ratio of H:G:S constituents vary depending on the source of biomass and may play an important role during biomass pretreatment. For instance, sources of lignocellulose with high syringyl content, such as hardwood and some agroindustrial residues (i.e. rice straw, bagasse and corncob) are more easily hydrolysable via alkaline treatment than softwoods, which usually contain more guaiacyl [14, 24, 25]. This is because S-lignin features a higher level of labile  $\beta$ -O-4' linkages which are readily cleavable during pretreatment [26]. Although many studies are emerging regarding the potential uses of lignin as a

sustainable feedstock to produce value-added materials, such as polymers, fuel, aromatic compounds and carbon materials, this component is prominently complex and still challenging to study and valorize because of its variable composition and degree of cross-linking. Besides, the same beneficial recalcitrance property conferred by lignin to the plants is also largely responsible for the high cost and complexity of operations for lignocellulose conversions. Consequently, pretreatments are generally applied focused on removing the lignin, which is mainly relegated for heat and power in industrial plants [22, 23, 27, 28]. However, such as the hemicellulose, the use of lignin is a key issue for the techno-economic viability of lignocellulosic valorization.

### 2.1.3. Cellulose – structure and morphology

With an estimated annual production around  $1.5 \times 10^{12}$  tonnes, cellulose is considered the most abundant biomass-derived organic compound in nature [29]. Its main sources include plants, sea animals, algae, fungi and bacteria, over which, in most cases, it acts as a reinforcing agent [30].

Cellulose is a high molecular weight homopolymer generated from repeating D-glucopyranose ring units linked by  $\beta$ -1,4-glycosidic bonds (cellobiose unit). Consequently, each unit of the cellulose chain is turned  $180^\circ$  with respect to the adjacent molecule [29, 31]. In literature, the individual glucose monomers within the cellulose chain are also referred to as anhydroglucose units (AGU). Each AGU unit contains three reactive hydroxyl groups, a primary group at C6 and two secondary groups at C2 and C3, positioned in the plane of the ring (Figure 2.2). Moreover, as typical of polymers formed by polycondensation, the chain ends of the cellulosic are chemically different, which gives it the characteristic of polarity, particularly important in shaping its different crystalline structures [32]. One end exhibits chemically reducing functionality, in equilibrium with the aldehyde structure (subject to oxidation reactions), while at the other end the anomeric carbon is involved in a glycosidic bond (non-reducing end) [29].

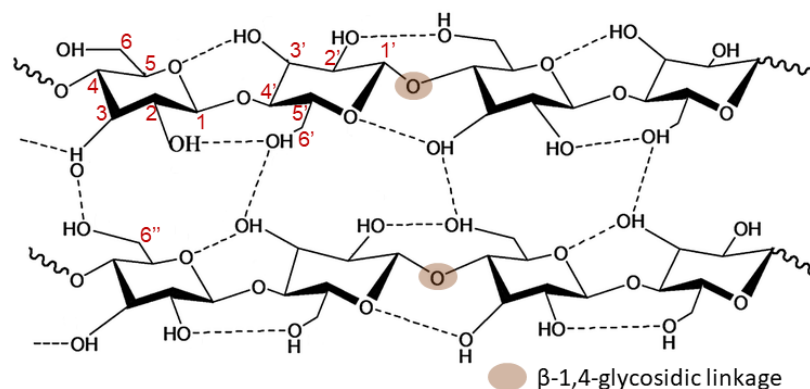


Figure 2-2. Chemical structure of cellulose chain. Source: modified from [33].

The hydroxyl groups of the AGU, along with the oxygen atoms of the D-glucopyranose ring and the glycosidic linkage, interact with each other by forming strong intermolecular and intramolecular hydrogen bonds [34]. Intramolecular bonds are formed by  $O(3')H \rightarrow O(5)$  and  $O(2)H \rightarrow O(6')$  interactions, which confer rigidity to the cellulose chain together with the  $\beta$ -1,4-glycosidic covalent linkage [33, 34] (Figure 2.2). This structural arrangement allows molecules to crystallize in a horizontal plane and parallel chains, forming microfibril bundles. In general, individual cellulose molecules are assembled into larger units, known as elementary fibrils, which are concentrated into even larger units called microfibrils, that are in turn grouped into cellulosic fibers [30, 31] (Figure 2.3).

When it comes to the interactions between cellulose chains, the intermolecular bonds are mainly produced by  $O(6'') \rightarrow O(3)$ , and allow to form rather flat ribbons [35]. All these hydrogen bonding, along with other interactions, are responsible for the assembly of cellulose in layers and for conferring low solubility in common solvents and lack of thermoplasticity. Another important feature of cellulose deals with the wide chemical variability provided by the high reactivity of the hydroxyl groups.

The cellulose elementary fibrils are comprised of crystalline regions (highly ordered) interspersed by amorphous (disordered) regions (Figure 2.3) [32]. The ordered regions are stabilized by an intra- and intermolecular hydrogen bonding network which, along with molecular orientations, can vary widely, resulting in cellulose polymorphs or allomorphs [31]. Four major crystalline cellulose structures (polymorphs), namely I, II, III and IV, are known [29].

Cellulose I can crystallize into two different crystalline phases,  $I_\alpha$  and  $I_\beta$ , coexisting in different proportions depending on the origin of the cellulose. Plant cellulose, including agroindustrial residues, mainly consists of  $I_\beta$ , while cellulose emerged from primitive organisms crystallize in the  $I_\alpha$  phase. Both exhibit parallel chain configurations, but differ in hydrogen bonding patterns, implying differences in their crystal structures. While  $I_\alpha$  presents triclinic cell unit,  $I_\beta$  exhibits monoclinic cell unit [29, 31, 34]. Cellulose II exists in a monoclinic phase and can be produced by treating cellulose I with sodium hydroxide solution (maceration) or by dissolving the cellulose followed by its regeneration [29, 36]. Unlike cellulose I, which has a parallel arrangement, cellulose II chains assume a more thermodynamically stable antiparallel arrangement [31, 37]. From different treatments (e.g. ammonia) of cellulose I or II, cellulose crystalline III<sub>i</sub> or III<sub>ii</sub> can be obtained,



respectively. The latter, when treated at high temperatures with glycerol, result in the IV<sub>i</sub> and IV<sub>ii</sub> polymorphs [31, 36].

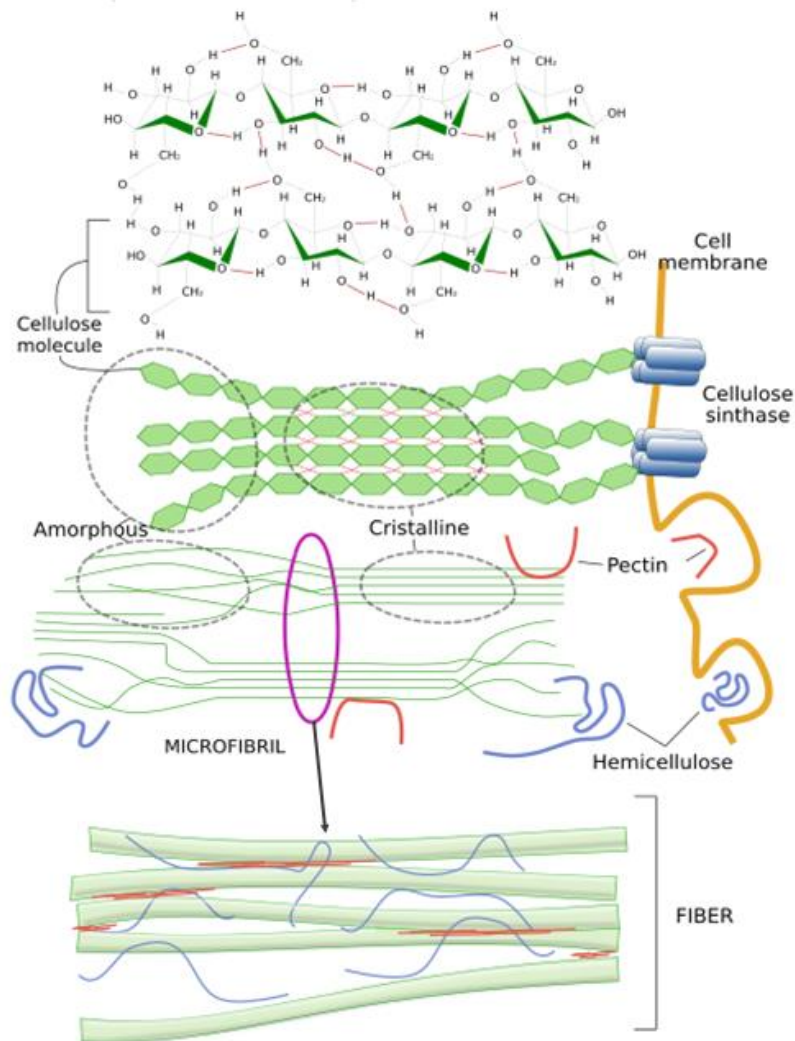


Figure 2-3. Morphological hierarchy of cellulose fibers. Source: [38]. (Accessed at September 2019)

Despite the wide availability and remarkable properties of cellulose, in the lignocellulosic residues this component is strongly linked to a matrix of lignin and hemicellulose [39]. The proportion between cellulosic and non-cellulosic constituents features a determinant role in the properties of fibers. The presence of substantial quantities of non-cellulosic materials can negatively influence their crystallinity, density, tensile strength, modulus of elasticity and moisture [40]. For instance, when not removed, these constituents can hamper chemical derivatization of fibers or endanger their application as reinforcing filler in polymeric matrices [40–42]. Therefore, for the successful use and valorization of cellulose from lignocellulosic biomass, pretreatments must be carried out to remove recalcitrant components.

## 2.2. Pretreatments of lignocellulosic biomass

Within the processes to convert LCB into value-added products, the pretreatment is an essential step, essentially carried out to disrupt the LCB compact structure and fractionate its main components [43] (Figure 2.4). Basically, the pretreatment methods can be classified into four categories, namely physical, chemical, physicochemical and biological. Each pretreatment method has specific effects on fractionation and physical-chemical properties of LCB components. In addition, several other factors may play a role in this step and directly influence downstream process, including the pretreatment settings, source of raw-material and its chemical composition, and even the climatic and geographical cultivation conditions [43, 44]. Currently, the pretreatment step is considered one of the main bottlenecks to the valorization of agroindustrial residues, and its cost may reach more than 40% of the total conversion process expanses [10, 44]. Therefore, the understanding and chosen of different techniques is imperative, and optimum selection must be led by the intended application of the pretreated sample.

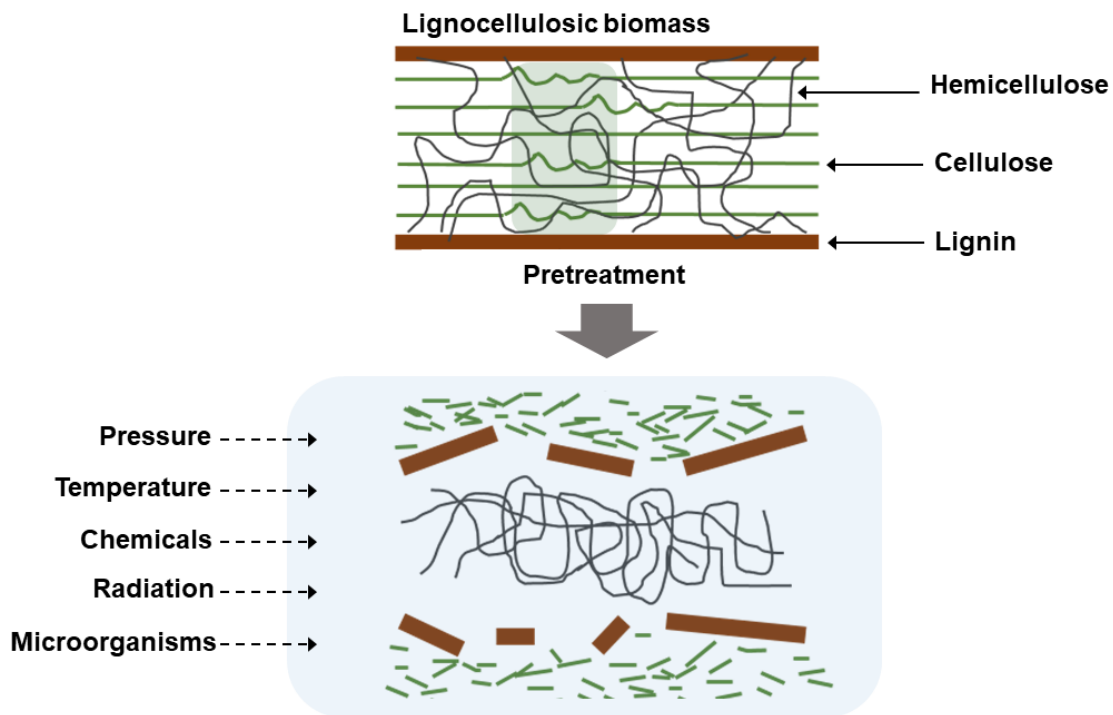


Figure 2-4. Pretreatment effect on lignocellulosic biomass. Modified from [45].

Furthermore, it is coherent that techniques with an environmental bias make up the precursor processing steps of eco-friendly products. However, the conventional techniques used for biomass pretreatments usually require harsh chemicals and extensive energy, in addition to generate excessive wastes. The most extensively used methods to pretreat LCB are acid and alkali

pretreatments. These are widely applied, followed by a bleach treatment, in bench scale experiments and pulp mills, even though atmospheric pollution and contaminants in wastewater effluent resulting from these chemical treatments are broadly documented [46, 47]. These drawbacks have induced the development of new approaches based on the “green chemistry” concept. Pretreatment techniques that fit into this concept include liquid hot water (LHW), steam explosion, wet oxidation, organosolvent, supercritical fluid, electron beam irradiation, ultrasonic energy, ionic liquids, deep eutectic solvent and biological treatment. Recently, great attention has also been focused on combining pretreatments [48]. The main advantages of the latter approach are that, by combining complementary treatments at different stages, the fractionation of specific components can occur easily, in a shorter processing time and by using less chemicals. For instance, a significant problem resulting from sodium hydroxide treatment, namely the black liquor generated as wastewater effluent, could be partially mitigated through this approach by using low concentrated solutions.

Therefore, the overall purpose of these new technologies deals with the use of non-environmentally hazardous chemicals, that can be recyclable or at least that produce less wastes [49]. Based on the foregoing, three pretreatments were selected to be applied in this work and will be discussed at some length in the next topics.

### **2.2.1. Liquid hot water**

Liquid hot water is considered one of the most promising pretreatments due to its high efficiency and low cost, as it uses only water at elevated temperature (generally between 160-240 °C) and pressure (usually <5MPa) [50, 51]. In addition, it has several advantages over other conventional treatments since no chemical is needed, equipment is little affected by erosion and, depending on the application, few inhibitory by-products are formed [52]. Depending on the LHW treatment parameters, the decomposition of main LCB components occurs at different rates. However, in general, it mainly leads to hemicellulose solubilization and hydrolysis. Conversely, lignin is only partially removed, and its insoluble fraction is almost completely retained or relocated in the solid residues along with the cellulose fraction [53].

During the LHW treatment the decomposition of hemicellulose is divided into three main steps, namely (1) surface reactions to produce primary products, (2) dissolution of primary products into the water and (3) decomposition of primary products [52]. Primary products, such as acetic acid, are released from hemicellulose as effect of water ionization, which in turn act as auto-catalysts in

the continued hemicellulose solubilization [54]. Because of the in situ generated acidic environment, the LHW pretreatment is categorized as a physicochemical method.

LHW treatment has been widely applied to pretreat agroindustrial residues [43, 44, 54–56]. Changes on microstructure and surface of LCB marked appear as cavities and cracks in the cell wall of pretreated samples in response of hemicellulose removal and lignin structural changes [53, 54]. Usually, the efficiency of LHW on biomass modification/fractionation is correlated with the severity factor (formulation that includes the combined effect of temperature and reaction time) [51]. Some expressions can also include the effect of pH (usually controlled between 4 and 7) since it may determine the formation of monomeric sugar and decomposition products. From literature, the optimal conditions for LHW treatment of agroindustrial residues are in the range of 180-220 °C and residence time varying from 5 to 30 min, at a severity factor limited to 3.64 - 4.25 [54, 56]. Under these conditions, high levels of hemicellulose solubilization and low cellulose depolymerization are expected to occur, and the accessible surface area of fibers can be substantially increased, which ultimately has a positive impact in subsequent processing. In addition, the biomass recalcitrance is greatly reduced on account of  $\beta$ -O-4' linkages disruption and removal of acetyl groups of lignin [53]. By applying a severity factor of 4.13 in the treatment of corncob, Michelin et al. [56] obtained a hemicellulose extraction yield of 74.1%. Similar result (hemicellulose extraction yield of 77%) was obtained by Li et al. [53] for the LHW treatment of poplar at a severity factor of 4.2. Higher levels of hemicellulose hydrolyzation (in the range of 80-90%) have already been reported for other agroindustrial residues, including sugar-cane bagasse and rice straw [50, 55].

### **2.2.2. Pretreatment of lignocellulosic biomass with Ionic liquid**

Ionic liquids (IL) can be defined as salts containing an organic cation and an organic or inorganic anion present in the liquid phase at temperatures relatively close to room temperature (below 100 °C) [57, 58]. In the last decades, numerous advances have been made towards understanding the synthesis, properties and mechanisms of action of ionic liquids, which has enabled its application in numerous manufacturing processes whether as components of technological devices, solvents or engineering fluids [59].

The following properties are generally reported in the literature as advantageous aspects of ionic liquids [59–61]: biodegradability, recyclability, low toxicity, low hydrophobicity, low viscosity, non-flammability, electrochemical and thermal stability, low volatility, ability to dissolve organic and

inorganic components, high polarity and wide electrochemical window. Nevertheless, through the combination of different anions and cations a wide range of ionic liquids can be synthesized, which makes it difficult to generalize their properties.

Regarding the dissolution of lignocellulosic biomass, ionic liquids have the advantage of being able to dissolve cellulose, lignin and hemicellulose under relatively moderate conditions without degrading their chemical structure [32]. Besides, they can be applied as an “environmentally friendly” technique as their low volatility minimizes the emission of pollutants.

For industrial scale use, the high cost associated with ionic liquids compared to conventional solvents represents one of the main limiting aspects of their application. However, due to their numerous properties, ionic liquids can be recycled and reused. In the literature, numerous attempts have been reported to reuse ionic liquids. Depending on the desired end product, different techniques may be employed, namely [62]: distillation, extraction of residual components, adsorption, induced phase separation, membranes and centrifugation. Good regeneration yields for few application cycles of recycled ionic liquids have already been reported [63–65]. For instance, by using a mixture of BmimCl and water for the treatment of vegetable straw, Wei et al. [63] observed a decrease in treatment efficiency only from the fourth application cycle.

The main ionic liquids currently used in cellulose dissolution are those that include the imidazole, pyridinium, ammonium and phosphonium cations [32, 66]. These may be linked to different radicals and associated with different anions, giving rise to a series of ionic liquids. When it comes to the pretreatment of lignocellulosic biomass, the main ionic liquids applied include 1-butyl-3-methylimidazolium chloride (BmimCl), 1-ethyl-3-methylimidazolium chloride (EmimCl), 1-allyl-3-methylimidazolium chloride (AmimCl) and 1-ethyl-3-methylimidazolium acetate (EmimMeCO<sub>2</sub>). Among these, it is worth mentioning BmimCl due to its power of dissolution [67–69].

Drawing from the high cellulose content available in lignocellulosic biomass, this latter has been extensively used as raw material in ionic liquid extraction processes. Two different approaches are currently used in the process of deconstructing lignocellulosic biomass with ionic liquids, namely dissolution process and ionosolv process. The dissolution process, which has the largest range of studies developed, consists in the solubilization of all components of lignocellulosic biomass. By contrast, the ionosolv process promotes the selective solubilization of LCB components. Currently, the ionosolv approach does not have fully optimized procedures, which reflects the scarcity of studies developed [66].

Within the dissolution process, ionic liquids capable of solubilizing all components of the lignocellulosic biomass are used, such as BmimCl and EmimMeCO<sub>2</sub>. Once the biomass is solubilized, an antisolvent is used to dilute the solution and promote the precipitation of the cellulose. Such precipitated material may be removed from the solution by filtration and should be washed to remove residual ionic liquid. As a subsequent step there is the recovery of the ionic liquid, carried out by distilling the antisolvent and recovering the lignin and hemicellulose fractions in the solution.

It is currently accepted and proven that the dissolution property of ionic liquids is directly related to the ability of their anions (e.g. chloride and acetate) to form hydrogen bonds with the hydroxyl group of cellulosic material [32, 60]. It is worth mentioning that, due to the complex hierarchical structure of cellulosic fibers, their dissolution occurs distinctively. During IL pretreatment, a heterogeneous swelling and dissolution takes place firstly in the secondary wall of the fibers. As the cellulose swells, the primary wall rolls up in such a way as to form collars, rings, or spirals that restricts the uniform expansion of the fiber forming balloons (Singh et al., 2015). Notwithstanding, the effective dissolution of LCB depends on the multi-component structure and content of the biomass, as well as the solvation property of the IL [70].

One possible way of predicting the solvency power of a solvent is through empirical or semi-empirical polarity scale equations, such as the Kamlet-Taft model. The Kamlet-Taft equation is formulated as a function of the parameters  $\beta$  (hydrogen bond basicity),  $\alpha$  (hydrogen bond acidity),  $\pi^*$  (polarizability) and  $\delta$  (dipolarity) [71]. More details about the Kamlet-Taft model and possible correlation of parameters can be found in Mäki-arvela et al. [71]. Especially in ionic liquids with non-functionalized cations, the parameter  $\beta$  is essentially affected by the anion. According to Brandt et al. [66], it is possible to verify that ionic liquids with a  $\beta$  value higher than 0.8 present higher cellulose dissolution capacity. Regarding the cations' role in the dissolution mechanism, this is still a subject of discussion among authors. However, increasing the alkali chain in the cation is likely to reduce cellulose solubility [66].

#### 2.2.2.1. Regeneration process

Cellulose pulp obtained through the dissolution process is called regenerated cellulose. The regeneration is one of the most important steps in the treatment process as it will directly result in the product to be used. As previously mentioned, regenerated cellulose can be obtained by the

addition of an antisolvent to the solution, such as water, acetone, methanol, ethanol as well as mixtures of water and organic solvents [63, 64, 72].

When added to the IL-dissolved biomass solution, the antisolvent surrounds the anions of the ionic liquid and promotes the breakdown of their interactions with cellulose [61]. Firstly, intermolecular hydrogen bonds (glucopyranose rings stacking by hydrophobic interactions) are reconstructed forming sheet like structures. As coagulation proceeds, many sheet-like structures are stacked by intramolecular hydrogen bonds to form thin planar crystals. Some aggregates that are tightly stacked with each other and free of defects transform into the crystalline regions, while those that incorporate defects in their structure become less ordered domains or amorphous regions [70]. These randomly dispersed structural units make contact with other units and, by a diffusion cluster-cluster aggregation mechanism, form a regenerated material with a mixture of crystalline and amorphous regions [73].

By changing the regeneration parameters (e.g. coagulating solvent, time and temperature), regenerated cellulose with different shapes (such as powder, fibers, films, hydrogels, aerogels and spheres) and properties (e.g. mechanical, thermal and barrier) can be obtained [74, 75]. Regenerated cellulose in the form of films, emerged from ionic liquid-pretreated agroindustrial residues, with suitable properties to be applied as packaging, were produced by Reddy et al. [73], Vanitijinda et al. [76] and Li et al. [77].

#### 2.2.2.2 Effect of IL treatment conditions

The first factor with direct influence on the efficiency of lignocellulosic biomass treatment with ionic liquids corresponds to the types of anions and cations. It is widely accepted that the main component responsible for cellulose dissolution is the anion. In general, the higher its basicity and the smaller its size, the greater is the dissolution capacity of the IL. Some examples of anions with superior cellulose dissolving capabilities are Cl and methylimidazolium acetate (MeCO<sub>2</sub>) [60].

Regarding the cation role, although several authors consider its contribution as a secondary factor, its influence on cellulose dissolution is mainly governed by the nature of existing functional groups, cation size and side chain unit [60]. Ionic liquids with heterocyclic aromatic functionalities, such as pyridinium and imidazole, exhibit better dissolution and fractionation of lignocellulosic components. Consequently, the largest share of studies on LCB treatment with IL make use of these cation categories [69, 73, 78–80]. The presence of allyl, methyl, ethyl and butyl radicals in the imidazole aromatic chain provides good dissolution performances. Moreover, according to the

results compiled by Badgujar and Bhanage, it is found that, by increasing the length of functional groups the dissolution capacity of ionic liquids is reduced [60]. As an example, the authors noted that the solubility property of four ionic liquids, with the same anion and cation categories, decreases in the following order: BmimCl > HexmimCl > OmimCl > DmimCl.

Due to the excellent dissolution capacity of BmimCl, as well as its lower cost relatively to ionic liquids with allyl and ethyl radicals, it has been widely applied in the treatment of lignocellulosic biomass. Abdulkhani et al. [81] used two imidazolium-cation ionic liquids, namely BmimCl and 1,3-methylimidazole dimethyl sulfate (DimimMeSO<sub>4</sub>), to dissolve three different types of lignocellulosic biomass with different cellulose contents. The BmimCl presented dissolution performance much higher than DimimMeSO<sub>4</sub>, and showed better efficiency for higher cellulose-content species. Similar result was obtained by Grävik et al. [69], in a study dedicated to evaluating four ionic liquids (BmimCl, EmimMeCO<sub>2</sub>, BmimMeCO<sub>2</sub> and BmimHSO<sub>4</sub>) for the treatment of different lignocellulosic species. The authors concluded that BmimCl has better treatment efficiency for simple cellulosic substrates. The main advantages of using BmimCl are its easy synthesis, stability and lower sensitivity to moisture compared to ionic liquids with acetate ions. However, its high viscosity and melting point may pose negative aspects.

In addition to the typology of cations and anions, several other factors, or treatment conditions, such as reaction time and temperature, particle size, biomass type and biomass / ionic ratio, as well as the presence of water in the ionic liquid or biomass may play an important role on IL treatment. Overall, the efficiency of ionic liquid treatment decreases with increasing recalcitrant biomass capacity. For instance, for the treatment of materials with high lignin content, higher reaction times and processing temperatures are required [61]. In addition, low concentrations of biomass appear to favor the dispersion of molecules in the solution and lead to a higher rate of dissolution and regeneration. Good solubility results are found in the literature with a biomass / ionic liquid mass ratio of less than 10% [82]. The use of particles smaller than 0.5 mm also appear to have better dissolution properties [66]. The temperature and reaction time required for the treatment of lignocellulosic biomass are defined primarily from the physical properties of the ionic liquid, such as its viscosity and melting point, as well as from the type of biomass. Increasing the temperature by 10 °C can significantly reduce the viscosity of ionic liquids [60]. In addition to favoring the dissolution of biomass, the increase in processing temperature is necessary because some ionic liquids are not liquid at room temperature.



### 2.2.3. Sodium hydroxide pretreatment

Sodium hydroxide (NaOH) is the most widely studied and effective alkaline reagent for LCB treatment. This chemical treatment has received great attention in the last decades as a potential pretreatment option because it is inexpensive, effective on a variety of feedstocks, and less energy intensive as compared to other pretreatment options [14]. Throughout the NaOH pretreatment of LCB, lignin is the main component affected. The main reaction mechanism for this effect is the cleavage of intermolecular ester bonds, by means disassociated hydroxide ions, between ferulic acid and the carbohydrate of the LCC [14]. The partial or total solubilization of lignin, as well as the effects over hemicellulose and cellulose fractions, depends on the pretreatment conditions (solution concentration, temperature, time and solid loading). Pretreatments performed with elevated NaOH concentrations seems to increase the solubilization of lignin and hemicellulose, but detrimental situations may also take place as hemicellulose degradation and cellulose losses can be set. High alkali concentrations can also trigger many structural and morphological changes in cellulose. Concentrations >6% can cause the swell of cellulose fibers, decrease the degree of polymerization and crystallinity index and lead to a transformation from cellulose crystalline I to II [14, 83]. At low alkaline concentrations, the lignin and hemicellulose fractions are partially solubilized, while cellulose remains relatively unaltered. Under this condition, the glycosidic linkages are alkali-stable and structural changes on cellulose are insignificant. In Haque et al. [84], the treatment of barley straw with low concentrated NaOH solution (0.5-2%) resulted in 84.8% removal of lignin and 79.5% removal of hemicellulose. In Talha et al. [85], a lignin removal around 86% was obtained by treating sugarcane bagasse with 1% NaOH solution at 100 °C for 3h.

The efficiency of NaOH treatment depends also on the lignin content and structure characteristic of the biomass, in a way that, sources of LCB containing a higher proportion of syringyl units are more easily delignified, such as rice straw, sugarcane bagasse and corncob [25]. On top of that, the alkali treatment works more effectively on low lignin content biomass, namely agroindustrial residues [44].

Some limitations regarding the sodium hydroxide pretreatment are the required long reaction times when operating in mild conditions and the production of liquors as a by-product. This liquid stream liquor contains inorganic chemicals and dissolved organic chemicals from biomass and usually features significant oxygen biological demand, which may pose risks to the environment if not treated [86]. In this regard, the use of low concentrated alkali solution, applied in combinations with other pretreatment technologies, can partially mitigate these issues.

#### **2.2.4. Combined pretreatments**

Studies have found that the combination of complementary treatments is more effective to fractionate the LCB than a single treatment. The combination of chemical, physicochemical and biological treatments, carried out as multi-stage or in simultaneous, have been extensively reported in the last few years [48]. For instance, it has been shown that the disruption of the cell wall layers induced by steam explosion and acidic hydrolysis, eases the dissolution of LCB in common solvents, such as ionic liquids [70]. High cellulose recovery was also obtained through the combination of an alkali solution (ammonia) and 1-ethyl-3-methylimidazolium acetate to pretreat rice straw [87]. In another approach, Wang et al. [88] combined biological pretreatment with LHW to pretreat *Populus tormentosa* and reported a hemicellulose removal rate of 92.33%, which could not be achieved by the individual treatments. Sun et al. [89] pretreated *cercariae* with two-step combined water and NaOH pretreatment and could increase cellulose extraction rate. By applying NaOH solution in combination with Fenton pretreatment, Zhang et al. [90] also obtained excellent recovery rates of straw cellulose. In Yoo et al. [91], a two-stage fractionation process using aqueous ammonia and hot-water efficiently fractionated the three main components of corn stover with relatively high purity. Ammonia treatment selectively removed lignin, while hot-water treatment separately hydrolyzed hemicellulose.

In addition to improve the fractionation of LCB, the combination of pretreatments can contribute to reducing costs, time of processing, as well as the use of chemicals and energy [48, 91]. However, understanding the structure of biomass, selecting a proper treatment method for target components and designing efficient process and optimal conditions are crucial prerequisites for the development of economically feasible combined process.

### **2.3. Cellulose modification and derivatives**

Despite the advantageous properties associated with cellulose, another set of characteristics, intrinsic to its molecular structure (e.g. lack of antimicrobial properties, high hydrophilicity and low dimensional stability and thermoplasticity), limits its application as a polymeric component [92]. The existence of free hydroxyl groups in the cellulosic chain ends up making lignocellulosic fibers susceptible to oxidation, hydrolysis and swelling reactions, thus compromising their physical and chemical integrity [93]. In this sense, the enhancement of the physical-chemical properties of cellulose through modification is a fundamental strategy to maximize its application range.

Cellulose modification techniques can be classified into physical and chemical methods. Physical methods are mainly applied to change the surface energy of cellulose, which may result, for instance, in a better compatibility between the cellulosic fibers and polymeric matrices. Regarding the chemical modification, it is worth mentioning that this approach is the main modification technique used to improve the properties of natural polymers, including cellulosic fibers. Through chemical modification, new properties are provided to the cellulose by replacing or activating their hydroxyl groups without compromising its natural characteristics. Chemical modification can be subdivided into two main methods [94–96]: (i) direct chemical modification, with emphasis on silanization, alkalization, esterification, etherification, maleated coupling, and permanganate and peroxide treatments; (ii) and the graft copolymerization method.

The most commercially important cellulose derivatives are synthesized through the direct chemical modification method and include cellulose esters (e.g. cellulose acetate, cellulose acetate butyrate, cellulose nitrate and cellulose acetate propionate) and ethers (e.g. methylcellulose, ethyl cellulose, hydroxypropyl methylcellulose and carboxymethyl cellulose). All of them feature a wide array of applications (ranging from coating to pharmaceutical components [42, 97–99]), and their common characteristic as a good film forming make them particularly suitable for packaging. With a projected market growth over the next years, cellulose acetate is by far the most important cellulose derivative (Malhotra, Keshwani, & Kharkwal, 2015; Zion Market Research, 2016), and this economic prospect can press forward even more its production from non-conventional sources, such as agroindustrial residues.

### **2.3.1. Cellulose acetate**

Cellulose acetate is an amorphous, colorless, tough and flexible natural polymer, widely used for industrial and consumer goods applications, such as filter, optical films, toys, eyeglass frames, home furnishings and osmotic drug delivery systems [102, 103]. It is also thermoplastic and easy to be processed into fibers and films [97]. As a film-like product, cellulose acetate also displays other particular properties, namely low haze, no odor, high moisture vapor transmission, low water permeability and excellent resistance to organic/inorganic weak acids and vegetable oils [97, 103], which are potentially desirable for semipermeable packaging.

Commercial cellulose acetate is typically produced from cotton linter or wood pulp-extracted cellulose via an esterification reaction, at which the natural cellulose is reacted with acetic anhydride and acetic acid (reaction medium) in the presence of sulfuric acid as a catalyst. In this

conventional method, known as acetic acid process, the mechanism of acetylation is mainly based on the formation of cellulose sulphate, resulting from the reaction of cellulose with sulphuric acid, which is transesterified from sulphate to acetate through a sulfoacetate intermediate stage [104, 105].

Depending on the degree of substitution (DS) of acetyl groups, the produced cellulose acetate can be classified in cellulose diacetate (DS of 2.4–2.6) or cellulose triacetate (DS>2.75) [106]. The DS corresponds to the average number of acetate groups in each AGU unit of cellulose, originally provided with three hydroxyl groups. Substitution occurs preferentially on the C-6 and C-2 carbon, and the acetyl content has an important influence on CA properties, namely on the solubilization, polarity and reactivity with other chemical species [107]. For instance, cellulose triacetate does not dissolve easily in common solvents, unlike cellulose diacetate. Notwithstanding their different DS, both cellulose acetates are widely used industrially in plastics (e.g. food packaging as a rigid wrapping film and membranes) and textiles [42, 106].

Recently, several other synthesis methods, claimed as green approaches, have been developed for cellulose acetylation, which have yielded great results even when applied to cellulose extracted from agroindustrial residues, namely sugarcane straw, rice husk, corn stover and oil palm empty fruit bunch [27, 108–110]. These methods include, for instance, the use of ionic liquids, one step heterogeneous acetylation or solvent-free methods [111, 112]. Recently, Das et al. [111] reported a great acetylation yield by applying a solvent-free method catalyzed with iodine to esterify rice husk. The iodine has the advantage of being a cheap, convenient, commercially available and environment friendly reagent. It is worth mentioning that the assumed eco-friendly aspect related to those previously mentioned methods comes mainly from the substitution of conventional catalysts and reaction medium. However, environmental assessment studies in this scope are still limited.

In addition to the existing eco-friendly processing technologies to acetylate cellulose, cellulose acetate also stands out because of its biodegradability property. Although some studies have shown that the biodegradation rate can be decreased by increasing DS, this does not imply inhibition of the biodegradation process. Currently, CA is recognized as a biodegradable polymer, and several studies have confirmed its biodegradation in natural environments, under aerobic or anaerobic conditions, independent of the acetyl content [102, 113, 114].

Therefore, as a potential plastic component for packaging food items, CA is able to meet one of the most pursued demand in the scope of packaging technology by ensuring a balance among food protection, environmental pollution and sustainable solid waste disposal options [97, 100].

#### **2.4. Cellulose-based packaging emerged from agroindustrial residues**

Polymer-based packaging play an essential role throughout the food distribution and storage chain. In addition to ensuring food safety and quality, packaging must protect against chemical and microbial contaminants, moisture, dust, light and oxygen, in order to increase the food shelf life. When it comes to cellulose-based packaging, the most innovative products released in the market, to date, are still based on high quality cellulose derived from wood pulp or cotton. However, the use of agroindustrial residues as a renewable source for that application may offers favorable environmental and economic advantages, and therefore has increasingly been encouraged. Recent developments and applications on this field include the use of cellulose fibers, regenerated cellulose and nanocellulose, which have been successfully applied to produce food packaging materials (and food packaging components) with remarkable physicochemical properties. The use of cellulosic fibers extracted from agroindustrial residues have been extensively reported, but because of their non-thermoplastic property, they are commonly applied as fillers to produce composites [115–117].

Regenerated cellulose refers to a class of materials prepared directly via the dissolution of cellulose into a solution, followed by its shaping and regeneration process [75]. Recently, regenerated cellulose materials have drawn considerable attention mainly after the novel developments in the field of green techniques and solvents, which opened up new possibilities to manufacture biodegradable, thermal and chemically stable products by using simple and sustainable processing methods [75]. Regenerated films with mechanical and barrier properties comparable with those of conventional films were prepared by simply dissolution and regeneration of pretreated sugarcane bagasse [74, 76, 118], borassus fruit fibers [73], and oil palm empty fruit bunch [119]. Recently, the development of regenerated cellulose-based hydrogels and aerogels from agroindustrial residues as components in food packaging have been an attractive subject of research, mainly due to their liquid absorption capacity [120–122].

In recent years, nanostructured cellulose has attracted considerable research attention due its potential for maximizing the mechanical and barriers properties of bio-based packaging [123]. From literature, the nanocellulose (CNC) is generally applied as a reinforcement filler for food

packaging applications. Nanocellulose from some agroindustrial residues, such as pea hull [124], mango seed [125], oil palm empty fruit bunch [126, 127], wheat straw, rice straw and barley straw [128] have already been applied in bio-based packaging with remarkable mechanical and barrier properties. Another relatively new application in food packaging is the use of nanocellulose-based aerogels and hydrogels. Absorbent aerogels applied for food packaging were produced from rice husk, oat husk and cotton stalk-extracted cellulose nanocrystals [122, 129].

Despite the recent advances and potential applications above mentioned, some technical and economic limitations still make the conversion of agroindustrial residues into nanocellulose and regenerated cellulose a difficult task. The main challenges deal with the low yield of CNC production and high costs related to cellulose dissolution. A promising alternative to overcome these drawbacks lies on the derivatization of cellulose, especially into cellulose acetate, as previously mentioned. In addition to meet the desired properties to replace the petroleum-based plastics, CA has the complementary advantage to be biodegradable (and disposed of by biological means) and can be processed on conventional injection molding machines or extruders adapted to their specific processing properties [130, 131].

The processing of agroindustrial residues extracted cellulose into derivatives is a very recent research topic, with substantial increase of published papers being verified only after 2000s. An inexpensive and biodegradable thermoplastic was developed from acetylation of rice straw, and through casting technology transparent thin films were formed [132]. Daud et al. [109], by using oil palm empty fruit bunch as cellulose source, obtained an acetone soluble cellulose acetate film with mechanical properties higher than those of commercial CA. A fully bio-based and transparent all-cellulose composite film was fabricated by simply aqueous blending of water-soluble CA synthesized from waste cotton fabrics (WCFs) and nanocelluloses [133]. The same Cao et al. authors [133] converted high yields of CA from WCFs through a quasi-homogeneous and environmental-friendly process, that required a small amount of acidic ILs as catalyst. Recently, cellulose acetate emerged from agroindustrial residues was also qualified as a suitable material to produce active packaging with enhanced and additional properties [131, 134, 135].

## **2.5. Active packaging and additives**

In recent years, the ever-growing global food trade, along with the consumers' demand for food safety and environmentally friendly products, have forced the research and development of innovative packaging with enhanced and multi-properties. Advances in engineering and materials

science have boosted the development of technologies towards this purpose [136], and the materials that falls under this scope are designated as active packaging. By definition, active packages are those intended to extend the shelf-life or to maintain or improve the condition of packaged food. This is accomplished via the embedment of components that would release or absorb substances into or from the packaged food or the environment surrounding the food [137]. Numerous active packaging systems with a multitude of functions have already been reported, namely absorbing/scavenging properties, realizing emitting properties, removing properties and microbial control [136, 138]. The main active agents responsible for conferring such functionalities include inorganic and organic materials/nanomaterials (e.g. metal/metal oxides nanoparticles, nanoclays, plant extracts, essential oils, phenolic compounds, chitosan and lysozyme) [136, 139].

Within the current explored agents, those with antimicrobial properties are one of the most studied components, since the growth of pathogenic and/or spoilage microorganisms are by far the major cause of food spoilage [136]. For this purpose, metal/metal oxides in their nanoscale form (including silver, gold, selenium, titanium dioxide, zinc oxide, copper oxide and magnesium oxide) have found to display effective responses. When incorporated in polymers, these nano-additives can also improve their original mechanical and barrier properties [139–141].

Just recently more attention has been given to the effects of embedding metal/metal oxides nanoparticles on cellulose and cellulose acetate-based polymers [142–148]. This came about as the development of active packaging is also being shifted towards the use of bio-based and ecofriendly materials. Nevertheless, very few studies are reported in literature regarding the use of cellulose/cellulose acetate derived from agroindustrial residues to produce active packaging. For instance, cellulose acetate-water soluble was synthesized from waste cotton fabrics by Cao et al. [149] and used to produce nanohybrid films containing silver nanoparticles. In addition to be effective in inhibiting the growth of bacteria, the produced film also exhibits catalytic activity. In Panis et al. [150], banana peel was used to produce CA-incorporated silver particles. The film produced exhibited enhanced tensile strength and antibacterial activity against *Staphylococcus aureus* e *Escherichia coli*. More recently, Harini and Sukumar [151], by using banana residues-extracted cellulose, developed a transparent cellulose acetate film with bioactive properties, but instead of metal/metal oxides nanoparticles they used thymol (an oregano compound) as biocidal agent. The bioactive films presented great retention of the natural compound, which infused CA films with increased antioxidant and antimicrobial properties. Several other studies also incorporated natural compound as antimicrobial agents into cellulose-based polymers (not

necessarily emerged from agroindustrial residues), namely thymol [131], murta fruit extract [152], essential oil from pink pepper [153] and carvacrol [154]. However, some drawbacks of incorporating these natural active compounds into polymers are their low chemical and thermal stability, as well as high volatility, which pose challenges to their processing [155].

In this perspective, inorganic nanoparticles, such as TiO<sub>2</sub> (TiO<sub>2</sub>-NPs) and MgO (MgO-NPs), have attracted considerable interest as they resist to harsh processing conditions and presents superior photocatalytic property with biocidal effects against foodborne pathogens [156]. Besides, their use as food additives is regulated as safe by the U.S. Food and Drug Administration and European Food Safety Authority

TiO<sub>2</sub>-NPs are among the most studied metal oxide NP to produce active packaging [139, 157]. In addition to the aforementioned characteristics, TiO<sub>2</sub> is chemically stable, cheap, durable and abundantly available [139, 156]. TiO<sub>2</sub> exist in nature as one three main polymorphs, namely anatase, rutile and brookite, which differ by their crystalline structure. The photocatalytic activity of TiO<sub>2</sub> nanoparticles is recognized in anatase and rutile, but they have been reported to exhibit antimicrobial activity only when exposed to UV light (generally in a wavelength range of 320-380 nm) [148, 156]. Upon exposure to light, reactive oxygen species (ROS), such as hydrogen peroxide (H<sub>2</sub>O<sub>2</sub>) and superoxide anions (O<sub>2</sub><sup>-</sup>), are generated through redox reactions. ROS leads to severe oxidative stress and damages to cells' macromolecules, causing lipid oxidation, inhibition of enzymes, RNA/DNA damages and cell lysis [158]. The generated ROS and oxidative radicals can also cause the photocatalytic oxidation of ethylene when TiO<sub>2</sub>-NP are incorporated in food packaging [159]. Photodegradation of CA films can be also enhanced by the embedment of TiO<sub>2</sub> NP [160].

Currently, few studies have been devoted to the application of MgO-NPs as an active agent in bio-based packaging. The key advantages of MgO-NPs rely on their high thermal stability, low cost, non-toxicity and potent antimicrobial activity [161]. Their biocidal action is also resultant from the production of reactive oxygen species and electrochemical interactions, as reported by Gold et al. [158]. In addition to antibacterial efficacy, Swaroop and Shukla [140] also observed that the incorporation of MgO-NPs in PLA improved oxygen barrier and tensile strength of the film produced.

Indeed, nanotechnology has been widely applied for developing in the field of packaging systems as it can fulfill almost all the basic functions currently demanded. However, despite all beneficial properties introduced by the nanostructure particles, the most recent researches are targeted in pursuit alternative green methods of synthesis in substitution of the chemical-conventional ones, that usually undergo multi-step process, are time-consuming and use toxic reducing agents. In this



regard, the pulsed laser ablation in liquid medium emerges as a promising alternative since it is a flexible and fast method to produce nanoparticles and does not require any chemical or stabilizer.

## **2.6 Pulsed laser ablation of metal/metal oxides in liquids**

Pulsed laser ablation in liquid medium is a relatively new method for producing nanoparticles, and has gained increasing interest because of its versatility, low cost, flexibility and easy execution. It is particularly interesting to integrate sustainable processing techniques since it meets the 12 principles of green chemistry (in briefly, the PLAL does not necessarily require chemicals or produce wastes) [162].

Concisely, PLAL consist of irradiating a pulsed laser beam onto a solid target immersed in a liquid medium. The mechanisms within the nanoparticles synthesis via PLAL can be distinguished into six main steps based on the temporal evolution of physical-chemical phenomena, as depicted in Figure 2.5 [162]. The process starts with the passage of the laser through the liquid medium. After going through the liquid, the laser reaches the bulk target, which absorbs energy through multiphoton absorption and direct photoionization. The laser photons of the laser couple with the electrons and phonons of the target and initiate the detachment of material. Detachment proceeds sustained by the immediate rise of the electron temperature, which leads to thermal process such as vaporization and phase explosion (material superheating up to the thermodynamic critical temperature) [162–164]. Simultaneously to the ablation process, the recoil pressure of the ablated material give rise to a shockwave, which heats the liquid and the target and may also promote the detachment of material [162]. As the ablated material is composed mainly by highly ionized atoms and electrons, it is considered a plasma plume. The constant absorption of photons by the plasma cause its expansion and subsequent cooling, with releasing of its energy to the solvent and target [163, 165]. During this process, nucleation and growth of nanomaterials take place, and reactions with solvent species may occur. Melted drops, with higher dimensions, can also be ejected from the target [162, 166]. The energy released from the plasma plume induces the formation of a cavitation bubble, that expands and then later collapse emitting a shockwave with possible effects over the NPs, namely aggregation, spreading or phase transition [162, 167].

Although this is a brief explanation of the nanoparticle formation process, there are still many events to be detailed that require a deep understanding of the physical and chemical processes involved in PLAL method.

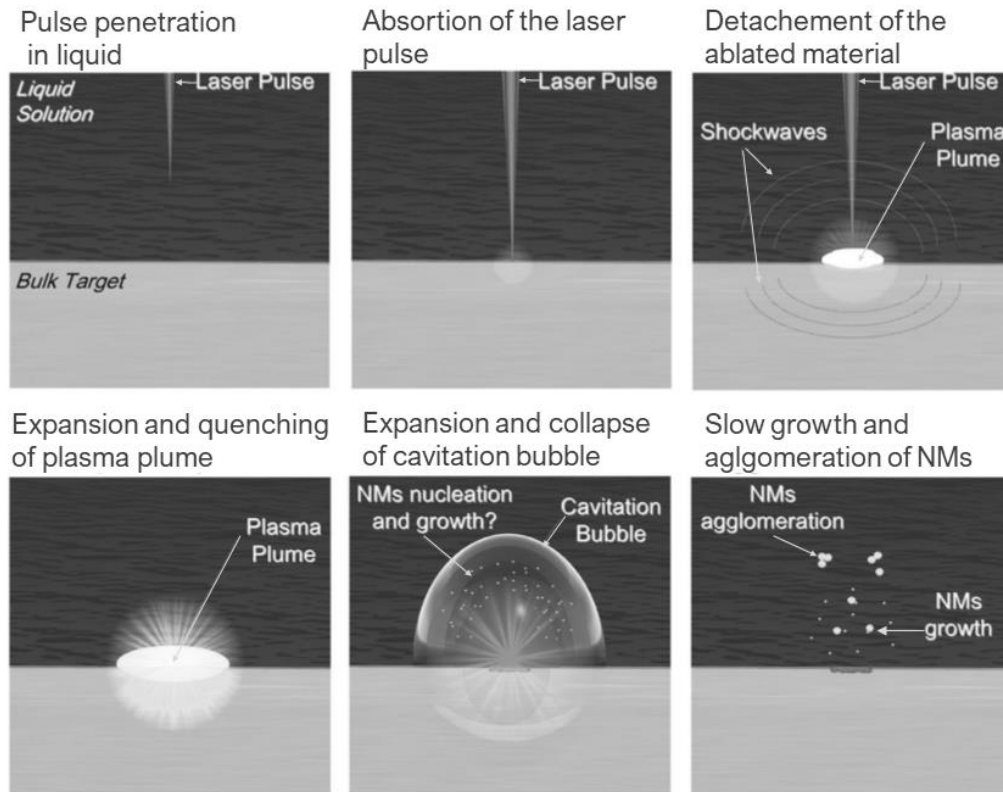


Figure 2-5. Schematic illustration of metal nanoparticles formation by PLAL. Modified from [162].

Two main processing conditions can affect the yield, composition, properties and characteristics of NPs produced by PLAL, whether material controlling and laser parameters. The bulk target and solvent composition are the main materials parameters. Several studies reported significant changes on NPs characteristic depending on the liquid medium. For instance, brucite-like  $\text{Mg}(\text{OH})_2$  particles were the primary crystalline product produced by laser ablation of Mg in deionized water, while MgO NPs were presented in higher percentage when acetone was used [168]. The same authors [168] also reported the generation of different morphologies and agglomeration patterns. Chaturvedi et al. [169] found that deionized water medium is favorable for the growth of anatase phase  $\text{TiO}_2$  nanoparticles, while surfactant added water medium is favorable for rutile phase growth. Moura et al. [171] reported the production of smaller silver NPs when ablation was carried out in deionized water instead of ethanol. The multitude of solvents suitable to be applied in PLAL opens up a range of possible applications, whether as a colloidal solution or NP powder after centrifugation.

The main laser/setup parameters influencing the NPs production and properties during PLAL are laser fluence, repetition rate, wavelength, laser energy, pulse duration and liquid depth. In

general, ablation efficiency increases with wavelength, laser fluence and pulse energy [163, 170]. Moreover, smaller metal nanoparticles are obtained by using higher laser fluence values [171].

## **2.7 Life cycle assessment**

Life cycle assessment (LCA) is an effective tool for understanding the environmental impacts associated with the development of products, processes or services. Its application can encompass all phases of a product's life, from resource extraction to final disposal, or only part of its manufacturing process.

The search for the establishment of a solid and standardized scientific base related to the application of LCA led the International Organization for Standardization (ISO) to prepare documents containing the fundamental guidelines, principles and framework for conducting this type of study, including [172, 173]: (i) definition of the goal and scope; (ii) life cycle inventory analysis (LCI); (iii) life cycle impact analysis (LCIA); and (iv) interpretation of results.

The definition of the goals and scope of the LCA study provides, among other issues, the reasons for executing the LCA, definition of functional unit (FU), the product system and system boundaries, as well as the environmental impacts categories and methodologies considered [174, 175]. The system boundaries define which unit process included in the product system will take part of the LCA study, and may extend to different stages of a product's life cycle. In the literature there are mainly projects that encompass activities from the product generation phase until the previous stages of use (cradle-to-gate), or until the end of its useful life (cradle-to-grave). Regarding the functional unit, it provides a reference to which the inputs and outputs of the product system are related. Its choice should take into consideration the type of study performed and its objectives [176]. The functional unit may be expressed, for example, in units of mass, volume, or in terms of units produced by time interval [177, 178].

The inventory analysis aims to identify and quantify the inputs (resources) and outputs (waste and emissions) of the system. Therefore, the limits of the system and subsystems (or processes) involved in the object of study must be carefully defined [174]. Once the inventory analysis is established, sufficient information is obtained to assess the contributions of resource extraction and waste emissions to potential environmental impact categories, which falls under the life cycle impact assessment [174]. As standard, the LCIA is divided into mandatory (classification and characterization) and optional (normalization, weighting, grouping and sensitivity analysis) steps (ISO 14040, 2006). In the mandatory steps, emissions from life cycle Inventory (LCI) results are

assigned to impact categories according to their potential impacts, and characterization factors are used to quantify their impact contributions. Regarding the optional steps, their application depends on the object of study and relevance of possible outcomes. In general, normalization and sensitivity analysis are usually performed, while weighting and grouping are rarely implemented since they require a subjective interpretation [179]. Through normalization, impact potentials are expressed relative to a reference situation and in a common scale, which enables comparisons across impact categories. Sensitivity analysis is highly dependent on the LCA model structure. By performing it, is possible to identify how variations on data, parameters and processing can influence the output results [179–182]. Sensitivity analysis can be performed as perturbation analysis (effect of a single parameter) or scenario analysis (effect of combination of parameters and process in a specific model layout).

There is no guideline regarding the choice of impact methodologies and categories. Most of the existing life cycle impact assessment methods (ReCiPe, Usetox, cumulative energy demand, CML, Eco-Indicator 99, TRACI 2.1 and Ecological scarcity method) can be applied for midpoint and endpoint level. Endpoint indicators are defined at the level of the areas of protection (e.g. human health and natural resources), and midpoint indicators indicate impacts somewhere between the emission and the endpoint. Naturally, on midpoint level a higher number of impact categories is differentiated and the results are more accurate and precise compared to the endpoint [183]. Consequently, most of reported studies on LCA are modeled at the midpoint level to limit uncertainties. There are many impact categories on the level of midpoint studies, and their selection must be primarily based on the purpose and type of application of the LCA [184]. The general recommendation regarding the choice of impact categories is that the obtained results must be robust enough to form a basis for further considerations or decisions. Also, the study must include impact categories for which international consensus has been reached (e.g. global warming potential, stratospheric ozone depletion, photochemical oxidant formation, acidification and resource consumption) [182]. Finally, the interpretation, significance and validity of the results are conducted. These comprise fundamental procedures as they make it possible to identify the major environmental burdens involved in the life cycle of products, processes or services.

Currently, a variety of LCA software-specific database and tools are available (e.g. GaBi, SimaPro, OpenLCA and EASETECH). These can be applied for single product evaluation or comparative studies as a means of determining environmentally preferable alternatives. Due mainly to the current expansion of the biopolymer market and the constant development of production

routes, several studies have discussed, through the application of LCA, the advantages and disadvantages of these biopolymers compared to conventional plastics. However, in addition to this application, LCA studies can be used as an important tool for identifying more sustainable production and disposal methodologies, as well as for optimizing production processes.

Recent review studies on LCA have shown that the prospects for advancement in the field of biopolymers depend mainly on the development of new materials, the application of less polluting production techniques, the use of renewable energy, and the adoption of sustainable disposal methods [179, 185–188]. Besides, the use of second-generation raw materials is mentioned in order to avoid conflicts with food production. However, the most commonly studied biopolymers via LCA are still PLA, PHA and thermoplastic starch (TPS), which are synthesized from first-generation inputs, such as corn, soybeans, sugarcane, and cassava [178, 185, 189, 190].

Overall, the most suitable disposal technologies for minimizing impacts caused by solid waste seems to be composting and recycling [185, 187, 191]. However, for the vast majority of countries, a management system that incorporates such disposal technologies still represents a utopian scenario. In many underdeveloped countries efforts still need to be made to eliminate open dumps. From this perspective, the development of biodegradable plastics seems to be the most promising alternative since, theoretically, their persistence in the natural environment is lower, and their impacts as well. Nevertheless, technically, this is not the right way to tackle this issue, as biodegradability must not be an excuse to litter. Indeed, within the circular economy approach, biodegradable plastics cannot be a sustainable solution without the infrastructure required to manufacture, collect and recycle them.

In addition to the challenges imposed by the country-specific waste management practices, several studies are focused on the development of products with applications not clearly defined, which makes decision on post-use management options a difficult task. In order to reduce model uncertainties, a coherent approach is based on the adoption of gate-to-gate perspective, with impact analysis focused on the product's processing steps [192, 193]. Besides, when comparing product systems with similar properties and manufacturing processes, common parts of the LCA may be disregarded if consistently justified.

## References

1. Isikgor, F.H., Becer, R.: Lignocellulosic biomass: a sustainable platform for the production of bio-based chemicals and polymers. *Polym. Chem.* 6, 4497–4559 (2015). <https://doi.org/10.1039/c5py00263j>
2. Forster-Carneiro, T., Berni, M.D., Dorileo, I.L., Rostagno, M.A.: Biorefinery study of availability of agriculture residues and wastes for integrated biorefineries in Brazil. *Resour. Conserv. Recycl.* 77, 78–88 (2013). <https://doi.org/10.1016/j.resconrec.2013.05.007>
3. Méridas, O.S., Coloma, A.G., Vioque, R.S.: Agricultural residues as a source of bioactive natural products. *Phytochem. Rev.* 11, 447–466 (2012). <https://doi.org/10.1007/s11101-012-9266-0>
4. Tye, Y.Y., Lee, K.T., Abdullah, W.N.W., Leh, C.P.: The world availability of non-wood lignocellulosic biomass for the production of cellulosic ethanol and potential pretreatments for the enhancement of enzymatic saccharification. *Renew. Sustain. Energy Rev.* 60, 155–172 (2016). <https://doi.org/10.1016/j.rser.2016.01.072>
5. FAOSTAT: Domain - Burning crop residues, <http://www.fao.org/faostat/en/#data/GB>
6. Kinuthia, K.J., Inoti, S.K., Nakhone, L.: Factors Influencing Farmer's Choice of Crop Production Response Strategies to Climate Change and Variability in Narok East Sub-county, Kenya. *J. Nat. Resour. Dev.* 8, 69–77 (2018). <https://doi.org/10.5027/jnrd.v8i0.07>
7. Jiang, D., Zhuang, D., Fu, J., Huang, Y., Wen, K.: Bioenergy potential from crop residues in China: Availability and distribution. *Renew. Sustain. Energy Rev.* 16, 1377–1382 (2012). <https://doi.org/10.1016/j.rser.2011.12.012>
8. Lee, H. V, Hamid, S.B. a, Zain, S.K.: Conversion of Lignocellulosic Biomass to Nanocellulose: Structure and Chemical Process Conversion of Lignocellulosic Biomass to Nanocellulose: *Sci. World J.* 2014, 1–14 (2014). <https://doi.org/10.1155/2014/631013>
9. Singh, R., Krishna, B.B., Kumar, J., Bhaskar, T.: Opportunities for utilization of non-conventional energy sources for biomass pretreatment. *Bioresour. Technol.* 199, 398–407 (2016). <https://doi.org/10.1016/j.biortech.2015.08.117>
10. Hassan, S.S., Williams, G.A., Jaiswal, A.K.: Emerging technologies for the pretreatment of lignocellulosic biomass. *Bioresour. Technol.* 262, 310–318 (2018). <https://doi.org/10.1016/j.biortech.2018.04.099>

11. Kucharska, K., Rybarczyk, P., Hołowacz, I., Łukajtis, R.: Pretreatment of Lignocellulosic Materials as Substrates for Fermentation Processes. *Molecules*. 23, 1–32 (2018). <https://doi.org/10.3390/molecules23112937>
12. Anwar, Z., Gulfranz, M., Irshad, M.: Agro-industrial lignocellulosic biomass a key to unlock the future bio-energy: A brief review. *J. Radiat. Res. Appl. Sci.* 7, 163–173 (2014). <https://doi.org/10.1016/j.jrras.2014.02.003>
13. Li, Q., Jiang, X., He, Y., Li, L., Xian, M., Yang, J.: Evaluation of the biocompatible ionic liquid 1-methyl-3-methylimidazolium dimethylphosphite pretreatment of corn cob for improved saccharification. *Appl. Microbiol. Biotechnol.* 87, 117–126 (2010). <https://doi.org/10.1007/s00253-010-2484-8>
14. Modenbach, A.A.: Effects of Sodium Hydroxide Pretreatment on Structural Components of Biomass. *Am. Soc. Agric. Biol. Eng.* 57, 1187–1198 (2014). <https://doi.org/10.13031/trans.56.10046> 1187
15. Silva, J.C. da, Oliveira, R.C. de, Neto, A. da S., Pimentel, V.C., Santos, A. de A. dos: Extraction, Addition and Characterization of Hemicelluloses from Corn Cobs to Development of Paper Properties. *Procedia Mater. Sci.* 8, 793–801 (2015). <https://doi.org/10.1016/j.mspro.2015.04.137>
16. Chen, H.: Lignocellulose biorefinery feedstock engineering. In: *Lignocellulose Biorefinery Engineering: Principles and Applications*. pp. 37–86. Woodhead Publishing (2015)
17. Bajpai, P.: Wood and Fiber Fundamentals. In: *Biermann's Handbook of Pulp and Paper - Volume 1: Raw Material and Pulp Making*. pp. 19–74. Elsevier (2018)
18. Menon, V., Prakash, G., Rao, M.: Value added products from hemicellulose: Biotechnological perspective Keywords. *Glob. J. Biochem.* 1(1), 36-67. 1, 36–67 (2010)
19. Chandel, A.K., Antunes, F.A., Terán-Hilares, R., Cota, J., Ellilä, S., Silveira, M.H., Al., E.: Bioconversion of Hemicellulose Into Ethanol and Value-Added Products: Commercialization, Trends, and Future Opportunities. In: Chandel, A.K. and Henrique, M. (eds.) *In Advances in Sugarcane Biorefinery: Technologies, Commercialization, Policy Issues and Paradigm Shift for Bioethanol and By-Products*. pp. 97–134. Elsevier (2018)
20. Lourenço, A., Pereira, H.: Compositional Variability of Lignin in Biomass. In: Poletto, M. (ed.) *Lignin: Trends and Applications*. pp. 65–98. IntechOpen (2018)

21. Ahmad, Z., Mahmood, N., Yuan, Z., Paleologou, M., Xu, C.: Effects of Process Parameters on Hydrolytic Treatment of Black Liquor for the Production of Low-Molecular-Weight Depolymerized Kraft Lignin. *Molecules*. 23, 1–17 (2018). <https://doi.org/10.3390/molecules23102464>
22. Abejón, R., Pérez-Acebo, H., Clavijo, L.: Alternatives for Chemical and Biochemical Lignin Valorization: Hot Topics from a Bibliometric Analysis of the Research Published During the 2000–2016 Period. *Processes*. 6, 1–50 (2016). <https://doi.org/10.3390/pr6080098>
23. Kathahira, R., Elder, T.J., Becham, G.T.: A Brief Introduction to Lignin Structure. In: Beckham, G.T. (ed.) *Lignin Valorization: Emerging Approaches*. pp. 1–20. The Royal Society of Chemistry (2018)
24. Guragain, Y.N., Herrera, A.I., Vadlani, P. V, Prakash, O., Magnetic, N.: Lignins of Bioenergy Crops: a review. *NPC Nat. Prod. Commun.* 10, 201–208 (2015). <https://doi.org/10.1177/1934578X1501000141>
25. Shimizu, S., Yokoyama, T., Akiyama, T., Matsumoto, Y.: Reactivity of lignin with different composition of aromatic syringyl/guaiacyl structures and erythro/threo side chain structures in  $\beta$ -O-4 type during alkaline delignification: As a basis for the different degradability of hardwood and softwood lignin. *J. Agric. Food Chem.* 60, 6471–6476 (2012)
26. Li, M., Pu, Y., Ragauskas, A.J.: Current Understanding of the Correlation of Lignin Structure with Biomass Recalcitrance. *Front. Chem.* 4, 1–8 (2016). <https://doi.org/10.3389/fchem.2016.00045>
27. Cao, L., Luo, G., Tsang, D.C.W., Chen, H., Zhang, S., Chen, J.: A novel process for obtaining high quality cellulose acetate from green landscaping waste. *J. Clean. Prod.* 176, 338–347 (2018). <https://doi.org/10.1016/j.jclepro.2017.12.077>
28. Donohoe, B.S., Decker, S.R., Tucker, M.P., Himmel, M.E., Vinzant, T.B.: Visualizing Lignin Coalescence and Migration Through Maize Cell Walls Following Thermochemical Pretreatment. *Biotechnol. Bioeng.* 101, 913–925 (2008). <https://doi.org/10.1002/bit.21959>
29. Klemm, D., Heublein, B., Fink, H.P., Bohn, A.: Cellulose: Fascinating biopolymer and sustainable raw material. *Angew. Chemie - Int. Ed.* 44, 3358–3393 (2005). <https://doi.org/10.1002/anie.200460587>
30. Lavoine, N., Desloges, I., Dufresne, A., Bras, J.: Microfibrillated cellulose – Its barrier properties and applications in cellulosic materials: A review. *Carbohydr. Polym.* 90, 735–764 (2012). <https://doi.org/https://doi.org/10.1016/j.carbpol.2012.05.026>



31. Habibi, Y., Lucia, L.A., Rojas, O.J.: Cellulose nanocrystals: Chemistry, self-assembly, and applications. *Chem. Rev.* 110, 3479–3500 (2010). <https://doi.org/10.1021/cr900339w>
32. Olsson, C., Westm, G.: Direct Dissolution of Cellulose: Background, Means and Applications. In: Van De Ven, T.G. and Godbout, L. (eds.) *Cellulose - Fundamental Aspects*. InTech (2013)
33. Kang, X., Kuga, S., Wang, L., Wu, M., Huang, Y.: Dissociation of intra / inter-molecular hydrogen bonds of cellulose molecules in the dissolution process: a mini review. *J. Bioresour. Bioprod.* 1, 58–63 (2016)
34. Heinze, T.: Cellulose Chemistry and Properties: Fibers , Nanocelluloses and Advanced Materials. In: Rojas, O.J. (ed.) *Advances in Polymer Science* 271. p. 341. Springer International Publishing Switzerland (2016)
35. Lindman, B., Karlström, G., Stigsson, L.: On the mechanism of dissolution of cellulose. *J. Mol. Liq.* 156, 76–81 (2010). <https://doi.org/10.1016/j.molliq.2010.04.016>
36. Dufresne, A.: Cellulose and potential reinforcement. In: Gruyter, W. de (ed.) *Nanocellulose: From Nature to High Performance Tailored Materials*. pp. 117–192 (2012)
37. Khalil, H.P.S.A., Davoudpour, Y., Islam, N., Mustapha, A., Sudesh, K., Dungani, R., Jawaid, M.: Production and modification of nanofibrillated cellulose using various mechanical processes: A review. *Carbohydr. Polym.* 99, 649–665 (2014). <https://doi.org/10.1016/j.carbpol.2013.08.069>
38. University of Vigo: Atlas of plan and animal histology: Cell wall. Available at: <https://bit.ly/2mE0Szm>. (2019)
39. Ravindran, R., Jaiswal, A.K.: A comprehensive review on pre-treatment strategy for lignocellulosic food industry waste: Challenges and opportunities. *Bioresour. Technol.* 199, 92–102 (2016). <https://doi.org/10.1016/j.biortech.2015.07.106>
40. Reddy, N., Yang, Y.: Biofibers from agricultural byproducts for industrial applications. *Trends Biotechnol.* 23, 22–27 (2005). <https://doi.org/10.1016/j.tibtech.2004.11.002>
41. Reddy, J.P., Rhim, J.W.: Isolation and characterization of cellulose nanocrystals from garlic skin. *Mater. Lett.* 129, 20–23 (2014). <https://doi.org/10.1016/j.matlet.2014.05.019>
42. Candido, R.G., Godoy, G.G., Gonc, A.R.: Characterization and application of cellulose acetate synthesized from sugarcane bagasse. *Carbohydr. Polym. j.* 167, 280–289 (2017). <https://doi.org/10.1016/j.carbpol.2017.03.057>

43. Bhutto, A.W., Qureshi, K., Harijan, K., Abro, R., Abbas, T., Bazmi, A.A., Karim, S., Yu, G.: Insight into progress in pre-treatment of lignocellulosic biomass. *Energy*. 122, 724–745 (2017). <https://doi.org/10.1016/j.energy.2017.01.005>
44. Baruah, J., Nath, B.K., Sharma, R., Kumar, S.: Recent Trends in the Pretreatment of Lignocellulosic Biomass for Value-Added Products. *Front. Energy Res.* 6, 1–19 (2018). <https://doi.org/10.3389/fenrg.2018.00141>
45. Koschorrek, K., Urlacher, V.B., Klose, H., Usadel, B.: BioSC - bioeconomy science center, [https://www.biosc.de/biodeg\\_en](https://www.biosc.de/biodeg_en)
46. Hoffman, E., Walker, T.R., Kim, J.S., Sherren, K., Andreou, P.: Pilot study investigating ambient air toxics emissions near a Canadian kraft pulp and paper facility in Pictou County, Nova Scotia. *Env. Sci Pollut Res.* 24, 20685–20698 (2017). <https://doi.org/10.1007/s11356-017-9719-5>
47. Hoffman, E., Alimohammadi, M., Lyons, J., Davis, E., Walker, T.R., Lake, C.B.: Characterization and spatial distribution of organic-contaminated sediment derived from historical industrial effluents. *Env. Monit Assess.* 191, 19 (2019)
48. Kumari, D., Singh, R.: Pretreatment of lignocellulosic wastes for biofuel production: A critical review. *Renew. Sustain. Energy Rev.* 90, 877–891 (2018). <https://doi.org/10.1016/j.rser.2018.03.111>
49. Capolupo, L., Faraco, V.: Green methods of lignocellulose pretreatment for biorefinery development. *Appl. Microbiol. Biotechnol.* 100, 9451–9467 (2016). <https://doi.org/10.1007/s00253-016-7884-y>
50. Mtui, G.Y.S.: Recent advances in pretreatment of lignocellulosic wastes and production of value added products. *African J. Biotechnol.* Vol. 8, 1398–1415 (2009). <https://doi.org/10.1073/pnas.1014862107/-/DCSupplemental.www.pnas.org/cgi/>
51. Xiao, L., Song, G., Sun, R.: Effect of Hydrothermal Processing on Hemicellulose Structure Chapter 3 Effect of Hydrothermal Processing on Hemicellulose Structure. In: (eds.), H.A.R. et al. (ed.) *Hydrothermal Processing in Biorefineries*. p. 51. Springer International Publishing (2017)
52. Zhuang, X., Wang, W., Yu, Q., Qi, W., Wang, Q., Tan, X., Zhou, G., Yuan, Z.: Bioresource Technology Liquid hot water pretreatment of lignocellulosic biomass for bioethanol production accompanying with high valuable products. *Bioresour. Technol.* 199, 68–75 (2016). <https://doi.org/10.1016/j.biortech.2015.08.051>

53. Li, M., Cao, S., Meng, X., Studer, M., Wyman, C.E., Ragauskas, A.J., Pu, Y.: The effect of liquid hot water pretreatment on the chemical-structural alteration and the reduced recalcitrance in poplar. *Biotechnol. Biofuels.* 10, 1–13 (2017). <https://doi.org/10.1186/s13068-017-0926-6>
54. Imman, S., Arnthong, J., Burapatana, V., Laosiripojana, N., Champreda, V.: Autohydrolysis of tropical agricultural residues by compressed liquid hot water pretreatment. *Appl. Biochem. Biotechnol.* 170, 1982–1995 (2013). <https://doi.org/10.1007/s12010-013-0320-1>
55. Singh, R., Shukla, A., Tiwari, S., Srivastava, M.: A review on delignification of lignocellulosic biomass for enhancement of ethanol production potential. *Renew. Sustain. Energy Rev.* 32, 713–728 (2014). <https://doi.org/10.1016/j.rser.2014.01.051>
56. Michelin, M., Teixeira, J.A.: Liquid hot water pretreatment of multi feedstocks and enzymatic hydrolysis of solids obtained thereof. *Bioresour. Technol.* 216, 862–869 (2016). <https://doi.org/10.1016/j.biortech.2016.06.018>
57. Weingärtner, H.: Ionic Liquids Understanding Ionic Liquids at the Molecular Level: Facts , Problems , and Controversies *Angewandte. Angew. Chem. Int. Ed.* 47, 654–670 (2008). <https://doi.org/10.1002/anie.200604951>
58. Reddy, P.: A critical review of ionic liquids for the pretreatment of lignocellulosic biomass. *S. Afr. J. Sci.* 111, 1–9 (2015). <https://doi.org/http://dx.doi.org/10.17159/sajs.2015/20150083>
59. Oliver-Bourbigou, H., Magna, L., Morvan, D.: Ionic liquids and catalysis: Recent progress from knowledge to applications. *Appl. Catal. A Gen.* 373, 1–56 (2010). <https://doi.org/10.1016/j.apcata.2009.10.008>
60. Badgujar, K.C., Bhanage, B.M.: Bioresource Technology Factors governing dissolution process of lignocellulosic biomass in ionic liquid: Current status, overview and challenges. *Bioresour. Technol. J.* 178, 2–18 (2015)
61. Lopes, A.M.C., João, K.G., Morais, A.R.C., Ł, E.B.-, Ł, R.B.-: Ionic liquids as a tool for lignocellulosic biomass fractionation. *Sustain. Chem. Process.* 1, 1–31 (2013)
62. Mai, N.L., Ahn, K., Koo, Y.: Methods for recovery of ionic liquids — A review. *Process Biochem.* 49, 872–881 (2014). <https://doi.org/10.1016/j.procbio.2014.01.016>
63. Wei, L., Li, K., Ma, Y., Hou, X.: Dissolving lignocellulosic biomass in a 1-butyl-3-methylimidazolium chloride – water mixture. *Ind. Crops Prod.* 37, 227–234 (2012). <https://doi.org/10.1016/j.indcrop.2011.12.012>

64. Wang, X., Li, H., Cao, Y., Tang, Q.: Cellulose extraction from wood chip in an ionic liquid 1-allyl-3-methylimidazolium chloride (AmimCl). *Bioresour. Technol.* 102, 7959–7965 (2011). <https://doi.org/10.1016/j.biortech.2011.05.064>
65. Financie, R., Moniruzzaman, M., Uemura, Y.: Enhanced enzymatic delignification of oil palm biomass with ionic liquid pretreatment. *Biochem. Eng. J.* 110, 1–7 (2016). <https://doi.org/10.1016/j.bej.2016.02.008>
66. Brandt, A., Gräsvik, J., Hallett, J.P., Welton, T.: Deconstruction of lignocellulosic biomass with ionic liquids. *Green Chem.* 15, 550–583 (2013). <https://doi.org/10.1039/c2gc36364j>
67. Vancov, T., Alston, A., Brown, T., Mcintosh, S.: Use of ionic liquids in converting lignocellulosic material to biofuels. *Renew. Energy.* 45, 1–6 (2012). <https://doi.org/10.1016/j.renene.2012.02.033>
68. Lopes, A.M.C., João, K.G., Rubik, D.F., Bogel-Łukasik, E., Duarte, L.C., Andreaus, J., Bogel-Łukasik, R.: Bioresource Technology Pre-treatment of lignocellulosic biomass using ionic liquids: Wheat straw fractionation. *Bioresour. Technol.* 142, 198–208 (2013). <https://doi.org/10.1016/j.biortech.2013.05.032>
69. Gräsvik, J., Winstrand, S., Normark, M., Jönsson, L.J., Mikkola, J.P.: Evaluation of four ionic liquids for pretreatment of lignocellulosic biomass. *BMC Biotechnol.* 14, 1–11 (2014). <https://doi.org/10.1186/1472-6750-14-34>
70. Singh, P., Duarte, H., Alves, L., Antunes, F., Le Moigne, N., Dormanns, J., Duchemin, B., Staiges, M.P., Medronho, B.: From Cellulose Dissolution and Regeneration to Added Value Applications – Synergism Between Molecular Understanding and Material Development. In: Poletto, M. and Ornaghi Jr, H. (eds.) *Cellulose - Fundamental Aspects and Current Trends*. pp. 1–44. IntechOpen (2015)
71. Mäki-arvela, P., Anugwom, I., Virtanen, P., Sjöholm, R., Mikkola, J.P.: Dissolution of lignocellulosic materials and its constituents using ionic liquids – A review. *Ind. Crop. Prod.* 32, 175–201 (2010). <https://doi.org/10.1016/j.indcrop.2010.04.005>
72. Swatloski, R.P., Spear, S.K., Holbrey, J.D., Rogers, R.D.: Dissolution of cellulose with ionic liquids. *J. Am. Chem. Soc.* 124, 4974–4975 (2002). <https://doi.org/10.1021/ja025790m> [pii]
73. Reddy, K.O., Maheswari, C.U., Dhlamini, M.S., Mothudi, B.M., Zhang, J., Zhang, J., Nagarajan, R., Rajulu, A.V.: Preparation and characterization of regenerated cellulose films using borassus fruit fibers and an ionic liquid. *Carbohydr. Polym.* 160, 203–211 (2017). <https://doi.org/10.1016/j.carbpol.2016.12.051>

74. Phinichka, N., Kaenthong, S.: Regenerated cellulose from high alpha cellulose pulp of steam-exploded sugarcane bagasse. *Integr. Med. Res.* 7, 55–65 (2017). <https://doi.org/10.1016/j.jmrt.2017.04.003>
75. Wang, S., Lu, A., Zhang, L.: Recent advances in regenerated cellulose materials. *Prog. Polym. Sci.* 53, 169–206 (2016). <https://doi.org/10.1016/j.progpolymsci.2015.07.003>
76. Vanitjinda, G., Nimchua, T., Sukyai, P.: International Journal of Biological Macromolecules Effect of xylanase-assisted pretreatment on the properties of cellulose and regenerated cellulose films from sugarcane bagasse. *Int. J. Biol. Macromol.* 122, 503–516 (2019). <https://doi.org/10.1016/j.ijbiomac.2018.10.191>
77. Li, J., Nawaz, H., Wu, J., Zhang, J., Wan, J.: All-cellulose composites based on the self-reinforced effect. *Compos. Commun.* 9, 42–53 (2018). <https://doi.org/10.1016/j.coco.2018.04.008>
78. Mahmood, H., Moniruzzaman, M., Yusup, S., Akil, H.M.: Pretreatment of oil palm biomass with ionic liquids: A new approach for fabrication of green composite board. *J. Clean. Prod.* 126, 677–685 (2016). <https://doi.org/10.1016/j.jclepro.2016.02.138>
79. Ang, T.N., Ngoh, G.C., Seak, A., Chua, M., Lee, M.G.: Elucidation of the effect of ionic liquid pretreatment on rice husk via structural analyses. *Biotechnol. Biofuels.* 5, 1–10 (2012)
80. Lan, W., Liu, C., Sun, R.: Fractionation of Bagasse into Cellulose, Hemicelluloses, and Lignin with Ionic Liquid Treatment Followed by Alkaline Extraction. *J. Agric. Food Chem.* 59, 8691–8701 (2011)
81. Abdulkhani, A., Hojati Marvast, E., Ashori, A., Karimi, A.N.: Effects of dissolution of some lignocellulosic materials with ionic liquids as green solvents on mechanical and physical properties of composite films. *Carbohydr. Polym.* 95, 57–63 (2013). <https://doi.org/10.1016/j.carbpol.2013.02.040>
82. Lopes, J., Bermejo, M., Martín, Á., Cocero, M.: Ionic Liquid as Reaction Media for the Production of Cellulose-Derived Polymers from Cellulosic Biomass. *ChemEngineering.* 1, 10 (2017). <https://doi.org/10.3390/chemengineering1020010>
83. Ciolacu, D.E., Popa, V.I.: Structural changes of cellulose determined by dissolution in aqueous alkali solution STRUCTURAL CHANGES OF CELLULOSE DETERMINED BY. *Cellul. Chem. Technol.* 1–22 (2005)
84. Haque, M.A., Dhirendra, N.B., Kang, T.H., Kim, M.K., Kim, J., Kim, H., Yun, H.D.: Effect of Dilute Alkali on Structural Features and Enzymatic Hydrolysis of Barley Straw (*Hordeum vulgare*)

- at Boiling Temperature with Low Residence Time. *J. Microbiol. Biotechnol.* 22, 1681–1691 (2012).  
<https://doi.org/http://dx.doi.org/10.4014/jmb.1206.06058>
85. Talha, Z., Ding, W., Mehryar, E., Hassan, M., Bi, J.: Alkaline Pretreatment of Sugarcane Bagasse and Filter Mud Codigested to Improve Biomethane Production. *Biomed Res. Int.* 2016, 11 (2016)
86. Speight, J., El-Gendy, N.S.: *Refinery Products and By-Products*. In: *Introduction to Petroleum Biotechnology*. Gulf Professional Publishing (2017)
87. Nguyen, T.D., Kim, K., Jong, S., Young, H., Woo, J., Min, S., Chan, J., Jun, S.: Pretreatment of rice straw with ammonia and ionic liquid for lignocellulose conversion to fermentable sugars. *Bioresour. Technol.* 101, 7432–7438 (2010). <https://doi.org/10.1016/j.biortech.2010.04.053>
88. Wang, W., Yuan, T., Wang, K., Cui, B., Dai, Y.: Combination of biological pretreatment with liquid hot water pretreatment to enhance enzymatic hydrolysis of *Populus tomentosa*. *Bioresour. Technol.* 107, 282–286 (2012). <https://doi.org/10.1016/j.biortech.2011.12.116>
89. Sun, S., Cao, X., Sun, S., Xu, F., Song, X., Sun, R., Jones, G.L.: Improving the enzymatic hydrolysis of thermo-mechanical fiber from *Eucalyptus urophylla* by a combination of hydrothermal pretreatment and alkali fractionation. *Biotechnol. Biofuels.* 7, 1–12 (2014). <https://doi.org/10.1186/s13068-014-0116-8>
90. Zhang, C., Pei, H., Wang, S., Cui, Z., Liu, P.: Enhanced Enzymatic Hydrolysis of Poplar after Combined Dilute NaOH and Fenton Pretreatment Chunyan. *BioResources.* 11, 7522–7536 (2016)
91. Yoo, C.G.: *Pretreatment and fractionation of lignocellulosic biomass for production of biofuel and value-added products*, (2012)
92. Roy, D., Semsarilar, M., Guthrie, J.T., Perrier, S., Tada, H., Roy, D., Semsarilar, M., Guthrie, T.: Cellulose modification by polymer grafting: a review. *Chem. Soc. Rev.* 38, 2046–2064 (2009). <https://doi.org/10.1039/b808639g>
93. Saha, P., Chowdhury, S., Roy, D., Adhikari, B., Kim, J.K., Thomas, S.: A brief review on the chemical modifications of lignocellulosic fibers for durable engineering composites. *Polym. Bull.* 73, 587–620 (2015). <https://doi.org/10.1007/s00289-015-1489-y>
94. Faruk, O., Bledzki, A.K., Fink, H., Sain, M.: Progress Report on Natural Fiber Reinforced Composites. *Macromol. Mater. Eng.* 299, 9–26 (2014). <https://doi.org/10.1002/mame.201300008>

95. Gurunathan, T., Mohanty, S., Nayak, S.K.: A review of the recent developments in biocomposites based on natural fibres and their application perspectives. *Compos. Part A Appl. Sci. Manuf.* 77, 1–25 (2015). <https://doi.org/10.1016/j.compositesa.2015.06.007>
96. Hokkanen, S., Bhatnagar, A., Sillanpää, M.: A review on modification methods to cellulose-based adsorbents to improve adsorption capacity. *Water Res.* 91, 156–173 (2016). <https://doi.org/10.1016/j.watres.2016.01.008>
97. McKeen, L.W.: Renewable Resource, Sustainable and Biodegradable Polymers. In: *The Effect of UV Light and Weather on Plastics and Elastomers*. pp. 425–438. William Andrew (2019)
98. Shokri, J., Adibkia, K.: Application of Cellulose and Cellulose Derivatives in Pharmaceutical Industries. In: Ven, van de and GM, T. (eds.) *Cellulose – Medical, Pharmaceutical and Electronic Applications to*. pp. 47–66. IntechOpen (2013)
99. Wheatley, T.A.: Water Soluble Cellulose Acetate: A Versatile Polymer for Film Coating. *Drug Dev. Ind. Pharm.* 281–290 (2008). <https://doi.org/https://doi.org/10.1080/03639040600683469>
100. Malhotra, B., Keshwani, A., Kharkwal, H.: Natural polymer based cling films for food packaging. *Int. J. Pharm. Pharm. Sci.* 7, 10–18 (2015)
101. Research, Z.M.: Cellulose Acetate Market (Cellulose Acetate Tow and Cellulose Acetate Filament) for Cigarette Filters, Textile & Apparel, Photographic Films, Tapes & Labels, Extrusion & Molding and Other Applications - Global Industry Perspective, Comprehensive Analysis. (2016)
102. Puls, J., Wilson, S.A., Ho, D.: Degradation of Cellulose Acetate-Based Materials: A Review. *J Polym Env.* 19, 152–165 (2011). <https://doi.org/10.1007/s10924-010-0258-0>
103. Polymerdatabase: Cellulose acetate, Brands/Cellulose. Available at: <http://polymerdatabase.com/Polymer>. (2019)
104. Akim, E.L.: On the mechanism of cellulose acetylation. *Pure Appl. Chem.* 14, 475–480 (1967)
105. Steinmeier, H.: Acetate manufacturing, process and technology. *Macromol. Symp.* 208, 49–60 (2004). <https://doi.org/10.1002/masy.200450405>
106. Ebnesajjad, S., Landrock, A.H.: Characteristics of Adhesive Materials. In: Ebnesajjad. pp. 84–159. William Andrew (2015)
107. Bao, C.Y.: Cellulose acetate / plasticizer systems: structure, morphology and dynamics. *Polymers*. Université Claude Bernard - Lyon I, 2015. English. NNT: 2015LYO10049. (2015)

108. Candido, R.G., Gonc, A.R.: Synthesis of cellulose acetate and carboxymethylcellulose from sugarcane straw. *Carbohydr. Polym.* 152, 679–686 (2016). <https://doi.org/10.1016/j.carbpol.2016.07.071>
109. Wan Daud, W.R., Djuned, F.M.: Cellulose acetate from oil palm empty fruit bunch via a one step heterogeneous acetylation. *Carbohydr. Polym.* 132, 252–260 (2015). <https://doi.org/10.1016/j.carbpol.2015.06.011>
110. Biswas, A., Saha, B.C., Lawton, J.W., Shogren, R.L., Willett, J.L.: Process for obtaining cellulose acetate from agricultural by-products. *Carbohydr. Polym.* 64, 134–137 (2006). <https://doi.org/10.1016/j.carbpol.2005.11.002>
111. Das, A.M., Ali, A.A., Hazarika, M.P.: Synthesis and characterization of cellulose acetate from rice husk: Eco-friendly condition. *Carbohydr. Polym.* 112, 342–349 (2014). <https://doi.org/10.1016/j.carbpol.2014.06.006>
112. Wu, J., Zhang, J., Zhang, H., He, J., Ren, Q., Guo, M.: Homogeneous acetylation of cellulose in a new ionic liquid. *Biomacromolecules.* 5, 266–268 (2004). <https://doi.org/10.1021/bm034398d>
113. Komarek, R.J., Steven, Robert M. Gardner, R.M., Buchanan, C.M., Gedon, S.: Biodegradation of radiolabeled cellulose acetate and cellulose propionate. *J. Appl. Polym. Sci.* 50, 1739–1746 (1993). <https://doi.org/https://doi.org/10.1002/app.1993.070501009>
114. Rivard, C.J., Adney, W.S., Himmel, M.E., Mitchell, D.J., Vinzant, T.B., Grohmann, K., Moens, L., Chum, H.: Effects of natural polymer acetylation on the anaerobic bioconversion to methane and carbon dioxide. *Appl. Biochem. Biotechnol.* 34, 725–736 (1992)
115. Sánchez-Safont, E.L., Aldureid, A., María, J., Gámez-pérez, J., Cabedo, L.: Biocomposites of different lignocellulosic wastes for sustainable food packaging applications. *Compos. Part B.* 145, 215–225 (2018). <https://doi.org/10.1016/j.compositesb.2018.03.037>
116. Otoni, C.G., Lodi, B.D., Lorevice, M. V, Leitão, R.C., Ferreira, M.D., Moura, M.R. De, Mattoso, L.H.C.: Industrial Crops & Products Optimized and scaled-up production of cellulose-reinforced biodegradable composite films made up of carrot processing waste. *Ind. Crop. Prod.* 121, 66–72 (2018). <https://doi.org/10.1016/j.indcrop.2018.05.003>
117. Asgher, M., Ahmad, Z., Iqbal, H.M.N.: Bacterial cellulose-assisted de-lignified wheat straw-PVA based bio-composites with novel characteristics. *Carbohydr. Polym.* 161, 244–252 (2017). <https://doi.org/10.1016/j.carbpol.2017.01.032>



118. Ghaderi, M., Mousavi, M., Yousefi, H., Labbafi, M.: All-cellulose nanocomposite film made from bagasse cellulose nanofibers for food packaging application. *Carbohydr. Polym.* 104, 59–65 (2014). <https://doi.org/10.1016/j.carbpol.2014.01.013>
119. Zailuddin, N.L.I., Husseinsyah, S.: Tensile Properties and Morphology of Oil Palm Empty Fruit Bunch Regenerated Cellulose Biocomposite Films. *Procedia Chem.* 19, 366–372 (2016). <https://doi.org/10.1016/j.proche.2016.03.025>
120. Batista, R.A., Judith, P., Espitia, P., Souza, J. De, Quintans, S., Machado, M., Ângelo, M., António, J., Cordeiro, J.: Hydrogel as an alternative structure for food packaging systems. *Carbohydr. Polym.* 205, 106–116 (2019). <https://doi.org/10.1016/j.carbpol.2018.10.006>
121. Oliveira, J., Pinheiro, G., Oliveira, K., Lisie, S., El, M., Silveira, G., Renato, A., Dias, G., Zavareze, R.: Cellulose fibers extracted from rice and oat husks and their application in hydrogel. *Food Chem.* 221, 153–160 (2017). <https://doi.org/10.1016/j.foodchem.2016.10.048>
122. Oliveira, J.P., Pinheiro, G., Lisie, S., Cleber, F., Renato, A., Dias, G., Zavareze, R.: Cellulose nanocrystals from rice and oat husks and their application in aerogels for food packaging. *Int. J. Biol. Macromol.* 124, 175–184 (2019). <https://doi.org/10.1016/j.ijbiomac.2018.11.205>
123. Azeredo, H.M.C., Rosa, M.F., Henrique, L., Mattoso, C.: Nanocellulose in bio-based food packaging applications. *Ind. Crop. Prod.* 97, 664–671 (2017). <https://doi.org/10.1016/j.indcrop.2016.03.013>
124. Chen, Y., Liu, C., Chang, P.R., Cao, X., Anderson, D.P.: Bionanocomposites based on pea starch and cellulose nanowhiskers hydrolyzed from pea hull fibre: Effect of hydrolysis time. *Carbohydr. Polym.* 76, 607–615 (2009). <https://doi.org/10.1016/j.carbpol.2008.11.030>
125. Silvério, H.A., Flauzino Neto, W.P., Dantas, N.O., Pasquini, D.: Extraction and characterization of cellulose nanocrystals from corncob for application as reinforcing agent in nanocomposites. *Ind. Crops Prod.* 44, 427–436 (2013). <https://doi.org/10.1016/j.indcrop.2012.10.014>
126. Asad, M., Saba, N., Asiri, A.M., Jawaid, M., Indarti, E.: Preparation and characterization of nanocomposite films from oil palm pulp nanocellulose / poly ( Vinyl alcohol) by casting method. *Carbohydr. Polym.* 191, 103–111 (2018). <https://doi.org/10.1016/j.carbpol.2018.03.015>
127. Lani, N.S., Ngadi, N., Johari, A., Jusoh, M.: Isolation, Characterization and Application of a Cellulose-degrading Strain *Neurospora crassa* S1 from Oil Palm Empty Fruit Bunch. *Microb. Cell Fact.* 13, 1–8 (2014). <https://doi.org/10.1155/2014/702538>

128. Oun, A.A., Rhim, J.: Isolation of cellulose nanocrystals from grain straws and their use for the preparation of carboxymethyl cellulose-based nanocomposite films. *Carbohydr. Polym.* 150, 187–200 (2016). <https://doi.org/10.1016/j.carbpol.2016.05.020>
129. Rahbar Shamskar, K., Heidari, H., Rashidi, A.: Preparation and evaluation of nanocrystalline cellulose aerogels from raw cotton and cotton stalk. *Ind. Crops Prod.* 93, 203–211 (2016). <https://doi.org/10.1016/j.indcrop.2016.01.044>
130. Ach, A.: Biodegradable Plastics Based on Cellulose Acetate. *Journal of Macromolecular Science, Part A Pure Appl. Chem.* 30, 733–740 (1993). <https://doi.org/http://dx.doi.org/10.1080/10601329308021259>
131. Rodríguez, F.J., Torres, A., Peñaloza, Á., Sepúlveda, H., Galotto, M.J., Guarda, A., Bruna, J., Rodríguez, F.J., Torres, A., Peñaloza, Á., Sepúlveda, H., Galotto, M.J., Guarda, A., Bruna, J., Rodríguez, F.J., Torres, A., Peñaloza, Á., Sepúlveda, H., Galotto, M.J., Guarda, A.: Development of an antimicrobial material based on a nanocomposite cellulose acetate film for active food packaging. *Food Addit. Contam. Part A.* 31, 342–353 (2014). <https://doi.org/10.1080/19440049.2013.876105>
132. Zhang, G., Huang, K., Jiang, X., Huang, D., Yang, Y.: Acetylation of rice straw for thermoplastic applications. *Carbohydr. Polym.* 96, 218–226 (2013). <https://doi.org/10.1016/j.carbpol.2013.03.069>
133. Cao, J., Sun, X., Lu, C., Zhou, Z., Zhang, X., Yuan, G.: Water-soluble cellulose acetate from waste cotton fabrics and the aqueous processing of all-cellulose composites. *Carbohydr. Polym.* 149, 60–67 (2016). <https://doi.org/10.1016/j.carbpol.2016.04.086>
134. Saha, N.R., Roy, I., Sarkar, G., Paul, A.K., Mishra, R.: Development of active packaging material based on cellulose acetate butyrate/polyethylene glycol/aryl ammonium cation modified clay. *Carbohydr. Polym.* 187, 8–18 (2018). <https://doi.org/10.1016/j.carbpol.2018.01.065>
135. Gemili, S., Yemeniciog, A., Altinkaya, S.A.: Development of cellulose acetate based antimicrobial food packaging materials for controlled release of lysozyme. *J. Food Eng.* 90, 453–462 (2009). <https://doi.org/10.1016/j.jfoodeng.2008.07.014>
136. Vilela, C., Kurek, M., Hayouka, Z., Röcker, B., Yildirim, S., Dulce, M., Antunes, C., Nilsen-nygaard, J., Kvalvåg, M., Freire, C.S.R.: A concise guide to active agents for active food packaging. *Trends Food Sci. Technol.* 80, 212–222 (2018). <https://doi.org/10.1016/j.tifs.2018.08.006>
137. EU: Regulation (EC) 450/2009 of 29 May 2009 on active and intelligent materials and articles intended to come into contact with food. (2009)

138. Youssef, A.M., El-sayed, S.M.: Bionanocomposites materials for food packaging applications: Concepts and future outlook. *Carbohydr. Polym.* 193, 19–27 (2018). <https://doi.org/10.1016/j.carbpol.2018.03.088>
139. Huang, Y., Mei, L., Chen, X., Wang, Q.: Recent Developments in Food Packaging Based on Nanomaterials. *Nanomaterials*. 8, 1–29 (2018). <https://doi.org/10.3390/nano8100830>
140. Swaroop, C., Shukla, M.: International Journal of Biological Macromolecules Nano-magnesium oxide reinforced polylactic acid bio films for food packaging applications. *Int. J. Biol. Macromol.* 113, 729–736 (2018). <https://doi.org/10.1016/j.ijbiomac.2018.02.156>
141. Khan, I., Saeed, K., Khan, I.: Nanoparticles: Properties, applications and toxicities. *Arab. J. Chem.* (2017). <https://doi.org/10.1016/j.arabjc.2017.05.011>
142. Pirsá, S., Shamusí, T.: Materials Science & Engineering C Intelligent and active packaging of chicken thigh meat by conducting nanostructure cellulose-polypyrrole-ZnO film. *Mater. Sci. Eng. C*. 102, 798–809 (2019). <https://doi.org/10.1016/j.msec.2019.02.021>
143. Yu, Z., Wang, W., Kong, F., Lin, M., Mustapha, A.: Cellulose nano fi bril / silver nanoparticle composite as an active food packaging system and its toxicity to human colon cells. *Int. J. Biol. Macromol.* 129, 887–894 (2019). <https://doi.org/10.1016/j.ijbiomac.2019.02.084>
144. Noshirvani, N., Ghanbarzadeh, B., Rezaei, R., Hashemi, M.: Novel active packaging based on carboxymethyl cellulose-chitosan -ZnO NPs nanocomposite for increasing the shelf life of bread. *Food Packag. Shelf Life*. 11, 106–114 (2017). <https://doi.org/10.1016/j.fpsl.2017.01.010>
145. Chook, S.W., Chia, C.H., Zakaria, S., Neoh, H.M., Jamal, R.: Effective immobilization of silver nanoparticles on a regenerated cellulose – chitosan composite membrane and its antibacterial activity. *NewJ. Chem.* 41, 5061–5065 (2017). <https://doi.org/10.1039/c7nj00319f>
146. Marrez, D.A., Abdelhamid, A.E., Darwesh, O.M.: Eco-friendly cellulose acetate green synthesized silver nano-composite as antibacterial packaging system for food safety. *Food Packag. Shelf Life*. 20, 100302 (2019). <https://doi.org/10.1016/j.fpsl.2019.100302>
147. Dairi, N., Ramos, M., Carmen, M.: Cellulose acetate / AgNPs-organoclay and / or thymol nano-biocomposite films with combined antimicrobial / antioxidant properties for active food packaging use. *Int. J. Biol. Macromol.* 121, 508–523 (2019). <https://doi.org/10.1016/j.ijbiomac.2018.10.042>
148. Xie, J., Hung, Y.: UV-A activated TiO<sub>2</sub> embedded biodegradable polymer film for antimicrobial food packaging application. *LWT - Food Sci. Technol.* 96, 307–314 (2018). <https://doi.org/10.1016/j.lwt.2018.05.050>

149. Cao, J., Sun, X., Zhang, X., Lu, C.: Homogeneous synthesis of Ag nanoparticles-doped water-soluble cellulose acetate for versatile applications. *Int. J. Biol. Macromol.* 92, 167–173 (2016). <https://doi.org/10.1016/j.ijbiomac.2016.06.092>
150. Paniz, O.G., Scheik, L.K., Silva, G.E.H. da, Gonçalves, M.R.F., Oliveira, A.D. de, Araújo, E.M., Carreño, N.L.V.: Obtenção de compósito com matriz de acetato de celulose e partículas de prata para aplicações antimicrobianas. *Matéria (Rio Janeiro)*. 23, 11 (2018). <https://doi.org/10.1590/s1517-707620180004.0578>
151. Harini, K., Sukumar, M.: Development of cellulose-based migratory and nonmigratory active packaging films. *Carbohydr. Polym.* 204, 202–213 (2019). <https://doi.org/10.1016/j.carbpol.2018.10.018>
152. Dicastillo, D., Bustos, F., Guarda, A., Jos, M.: Food Hydrocolloids Cross-linked methyl cellulose films with murta fruit extract for antioxidant and antimicrobial active food packaging. *Food Hydrocoll.* 60, 335–344 (2016). <https://doi.org/10.1016/j.foodhyd.2016.03.020>
153. Dannenberg, S., Funck, G.D., Eduardo, C., Marques, J.D.L., Padilha, W., Fiorentini, M.: LWT - Food Science and Technology Essential oil from pink pepper as an antimicrobial component in cellulose acetate film: Potential for application as active packaging for sliced cheese. 81, 314–318 (2017). <https://doi.org/10.1016/j.lwt.2017.04.002>
154. Luzi, F., Fortunati, E., Giovanale, G., Mazzaglia, A., Torre, L., Mariano, G.: Cellulose nanocrystals from *Actinidia deliciosa* pruning residues combined with carvacrol in PVA CH films with antioxidant / antimicrobial properties for packaging applications. *Int. J. Biol. Macromol.* 104, 43–55 (2017). <https://doi.org/10.1016/j.ijbiomac.2017.05.176>
155. Bautista, L., Molina, L., Niembro, S., García, J.M., López, J., Vilchez, A.: Coatings and inks for food packaging including nanomaterials. In: Busquets, R. (ed.) *Emerging Nanotechnologies in Food Science*. pp. 149–173. Elsevier (2017)
156. Hoseinnejad, M., Jafari, S.M., Katouzian, I.: Critical Reviews in Microbiology Inorganic and metal nanoparticles and their antimicrobial activity in food packaging applications. *Crit. Rev. Microbiol.* 0, 161–181 (2018). <https://doi.org/10.1080/1040841X.2017.1332001>
157. Das, C., Gebru, K.A.: Cellulose Acetate Modified Titanium Dioxide (TiO<sub>2</sub>) Nanoparticles Electrospun Composite Membranes: Fabrication and Characterization. *J. Inst. Eng. Ser. E*. 12 (2016). <https://doi.org/10.1007/s40034-017-0104-1>

158. Gold, K., Slay, B., Knackstedt, M., Gaharwar, A.K.: Antimicrobial Activity of Metal and Metal-Oxide Based Nanoparticles. *Adv. Ther.* 1700033, 1–15 (2018). <https://doi.org/10.1002/adtp.201700033>
159. Kaewklin, P., Siripatrawan, U., Suwanagul, A., Suk, Y.: Active packaging from chitosan-titanium dioxide nanocomposite film for prolonging storage life of tomato fruit. *Int. J. Biol. Macromol.* 112, 523–529 (2018). <https://doi.org/10.1016/j.ijbiomac.2018.01.124>
160. Jang, J., Lee, H., Lyoo, W.: Effect of UV Irradiation on Cellulase Degradation of Cellulose Acetate Containing TiO<sub>2</sub>. *Fibers Polym.* 8, 19–24 (2007)
161. Pilarska, A.A., Klapiszewski, Ł.: Recent development in the synthesis, modification and application of Mg(OH)<sub>2</sub> and MgO: A review. *Powder Technol.* 319, 373–407 (2017). <https://doi.org/10.1016/j.powtec.2017.07.009>
162. Amendola, V., Meneghetti, M.: What controls the composition and the structure of nanomaterials generated by laser ablation in liquid solution? *Phys. Chem. Chem. Phys.* 15, 3027–3046 (2013). <https://doi.org/10.1039/c2cp42895d>
163. Lam, J.: Pulsed Laser Ablation in Liquid: towards the comprehension of the growth processes, (2015)
164. Stauss, S., Urabe, K., Muneoka, H., Kazuo, T.: Pulsed Laser Ablation in High-Pressure Gases, Pulsed Laser Ablation in High-Pressure Gases, Pressurized Liquids and Supercritical Fluids: Pressurized Liquids and Supercritical Fluids: Generation, Generation, Fundamental Characteristics and Fundamental Cha. In: Yang, D. (ed.) *Applications of Laser Ablation - Thin Film Deposition, Nanomaterial Synthesis and Surface Modification fabrication*. pp. 221–244. IntechOpen (2016)
165. Yang, G.W.: Laser ablation in liquids: Applications in the synthesis of nanocrystals. *Prog. Mater. Sci.* 52, 648–698 (2007)
166. Zhou, R., Lin, S., Zong, H., Huang, T., Li, F., Pan, J., Cui, J.: Continuous Synthesis of Ag/TiO<sub>2</sub> Nanoparticles with Enhanced Photocatalytic Activity by Pulsed Laser Ablation. *J. Nanomater.* 2017, 10 (2017)
167. Reich, S., Schönfeld, P., Wagener, P., Letzel, A., Ibrahimkutty, S., Gökce, B., Barcikowski, S., Menzel, A., Rolo, S., Plech, A.: Pulsed laser ablation in liquids: Impact of the bubble dynamics on particle formation. *J. Colloid Interface Sci.* 489, 106–113 (2017). <https://doi.org/10.1016/j.jcis.2016.08.030>

168. Phuoc, T.X., Howard, B.H., Martello, D. V, Soong, Y., Chyu, M.K.: Synthesis of Mg (OH)<sub>2</sub>, MgO, and Mg nanoparticles using laser ablation of magnesium in water and solvents. *Opt. Lasers Eng.* 46, 829–834 (2008). <https://doi.org/10.1016/j.optlaseng.2008.05.018>
169. Chaturvedi, A., Joshi, M.P., Mondal, P., Sinha, A.K., Srivastava, A.K.: Growth of anatase and rutile phase TiO<sub>2</sub> nanoparticles using pulsed laser ablation in liquid: influence of surfactant addition and ablation time variation. *Appl. Surf. Sci.* 396, 303–309 (2017)
170. Ghaem, E.N., Dorrnian, D., Sari, A.H.: Low-dimensional Systems and Nanostructures Characterization of cobalt oxide nanoparticles produced by laser ablation method: Effects of laser fluence. *Phys. E Low-dimensional Syst. Nanostructures.* 115, (2020). <https://doi.org/10.1016/j.physe.2019.113670>
171. Moura, C.G., Pereira, R.S.F., Andritschky, M., Lopes, A.L.B., Grilo, J.P.F., Maribondo, R., Samuel, F.: Effects of laser fluence and liquid media on preparation of small Ag nanoparticles by laser ablation in liquid. *Opt. Laser Technol.* 97, 20–28 (2017). <https://doi.org/10.1016/j.optlastec.2017.06.007>
172. ISO 14040, I.: Environmental management – Life cycle assessment – Principles and framework. (2006)
173. ISO 14044: Environmental Management – Life Cycle Assessment – Requirements and Guidelines – ISO 14044. Rue de Stassart, 36, B-1050 Brussels (2006)
174. Rebitzer, G., Ekvall, T., Frischknecht, R. Hunkeler, D., Norris, G., Rydberg, T., ... & Pennington, D.W.: Life cycle assessment: Part 1: Framework, goal and scope definition, inventory analysis, and applications. *Environ. Int.* 30, 701–720 (2004)
175. Curran, M.A.: Life Cycle Assessment: A review of the methodology and its application to sustainability. *Curr. Opin. Chem. Eng.* 2, 273–277 (2013). <https://doi.org/10.1016/j.coche.2013.02.002>
176. Roy, P., Nei, D., Orikasa, T., Xu, Q., Okadome, H. Nakamura, N., Shiina, T.: A review of life cycle assessment (LCA) on some food products. *J. Food Eng.* 90, 1–10 (2009)
177. van der Harst, E., Potting, J.: A critical comparison of ten disposable cup LCAs. *Environ. Impact Assess. Rev.* 43, 86–96 (2013)
178. Papong, S., Malakul, P., Trungkavashirakun, R.: Comparative assessment of the environmental profile of PLA and PET drinking water bottles from a life cycle perspective. *J. Clean. Prod.* 65, 539–550 (2014). <https://doi.org/10.1016/j.jclepro.2013.09.030>

179. Yates, M.R., Barlow, C.Y.: Life cycle assessments of biodegradable, commercial biopolymers - A critical review. *Resour. Conserv. Recycl.* 78, 54–66 (2013). <https://doi.org/10.1016/j.resconrec.2013.06.010>
180. Bisinella, V., Conradsen, K., Christensen, T.H., Astrup, T.F.: A global approach for sparse representation of uncertainty in Life Cycle Assessments of waste management systems. *Int J Life Cycle Assess.* (2016). <https://doi.org/10.1007/s11367-015-1014-4>
181. Clavreul, J., Guyonnet, D., Christensen, T.H.: Quantifying uncertainty in LCA-modelling of waste management systems. *Waste Manag.* 32, 2482–2495 (2012). <https://doi.org/10.1016/j.wasman.2012.07.008>
182. European Commission - Joint Research Centre - Institute for Environment and Sustainability: International Reference Life Cycle Data System (ILCD) Handbook - General guide for Life Cycle Assessment - Detailed guidance. First edition March 2010. EUR 24708 EN. Luxembourg. Publications Office of the European Union; 2010
183. Van den Bossche, P., Matheys, J., Van Mierlo, J.: Battery Environmental Analysis. In: Pistoia, G. (ed.) *Electric and Hybrid Vehicles*. pp. 347–374. Elsevier (2010)
184. Stranddorf, K., Heidi, Leif, H., Schmidt, A.: Impact categories, normalisation and weighting in LCA: Updated on selected EDIP97-data. *Environ. News, Danish Environ. Prot. Agency, Copenhagen.* 78, 90 (2005). <https://doi.org/Environmental project nr. 995>
185. Spierling, S., Röttger, C., Venkatachalam, V. Mudersbach, M., Herrmann, C., Endres, H.J.: Bio-based plastics - A building block for the circular economy? *Procedia CIRP.* 69, 573–578 (2018)
186. Zhang, D., Antonio, E., Shah, N.: Life cycle assessments for biomass derived sustainable biopolymer & energy co-generation. *Sustain. Prod. Consum.* 15, 109–118 (2018). <https://doi.org/10.1016/j.spc.2018.05.002>
187. Hottle, T.A., Bilec, M.M., Landis, A.E.: Biopolymer production and end of life comparisons using life cycle assessment. *Resources, Conserv. Recycl.* 122, 295–306 (2017). <https://doi.org/10.1016/j.resconrec.2017.03.002>
188. Álvarez-Chávez, C. R. Edwards, S., Moure-Eraso, R., Geiser, K.: Sustainability of bio-based plastics: general comparative analysis and recommendations for improvement. *J. Clean. Prod.* 23, 47–56 (2012)
189. Madival, S., Auras, R., Paul, S., Narayan, R.: Assessment of the environmental profile of PLA, PET and PS clamshell containers using LCA methodology. *J. Clean. Prod.* 17, 1183–1194 (2009). <https://doi.org/10.1016/j.jclepro.2009.03.015>

190. Reddy, M.M., Vivekanandhan, S., Misra, M., Bhatia, S.K., Mohanty, A.K.: Progress in Polymer Science Biobased plastics and bionanocomposites: Current status and future opportunities. *Prog. Polym. Sci.* 38, 1653–1689 (2013). <https://doi.org/10.1016/j.progpolymsci.2013.05.006>
191. Razza, F., Farachi, F., Tosin, M., Deglinoenti, F., Guerrini, S.: Assessing the environmental performance and eco-toxicity effect of biodegradable mulch films. *n VII Int. Conf. life cycle Assess. agri-food Sect. Bari.* 4–22 (2010)
192. Walser, T., Demou, E., Lang, D.J., Hellweg, S.: Prospective environmental life cycle assessment of nanosilver T-shirts. *Environ. Sci. Technol.* 45, 4570–4578 (2011). <https://doi.org/10.1021/es2001248>
193. Arvidsson, R., Nguyen, D., Svanström, M.: Life cycle assessment of cellulose nanofibrils production by mechanical treatment and two different pretreatment processes. *Environ. Sci. Technol.* 49, 6881–6890 (2015). <https://doi.org/10.1021/acs.est.5b00888>



Chapter 3. Availability and suitability of agroindustrial residues as feedstock for cellulose-based materials: Brazil case study

---

*Published in Wastes and Biomass Valorization, 2018, 10, 2863-2878*

---

**David Jefferson Cardoso Araújo<sup>1</sup>, Ana Vera Machado<sup>2</sup>, Maria Cândida Lobo Guerra Vilarinho<sup>3</sup>**

<sup>1</sup>Institute for Polymers and Composites/I3N and Centre for Waste Valorization, University of Minho, Guimarães, Portugal.

<sup>2</sup>Institute for Polymers and Composites/i3N, University of Minho, Guimarães, Portugal.

<sup>3</sup>Mechanical Engineering and Resources Sustainability Centre, University of Minho, Guimarães, Portugal.

\*Corresponding author: David Jefferson Cardoso Araújo (david\_bct@hotmail.com)

## Abstract

Bio-based polymers have emerged as a feasible alternative to petrochemical polymers mainly due to their biodegradability and renewable feedstock. Brazil is considered one of the largest producers of agricultural commodities. Hence, the country is also distinguished by the large generation of this residue type, which can be potentially used as a source to obtain biopolymers, such as cellulose. Based on the Brazilian agriculture market, the study aims to analyze the suitability of agroindustrial residues as raw material for cellulose-based materials. A methodology for the selection of the most suitable residues is proposed, which takes into account the chemical composition of residues, namely the cellulose content and the cellulose-to-lignin ratio, as well as their availability. In order to meet conservation issues, the availability of residues is calculated as a function of sustainable removal rates and competitive uses. Taking as reference the main crops identified, the average amount of agroindustrial residues available in Brazil was estimated at 108 million tons/year. Among the most suitable residues to be used as cellulose feedstock are soybean straw, sugarcane top/leaves, maize husk and stover and sugarcane bagasse.

**Keywords:** Cellulose, lignocellulosic biomass, bio-based materials, availability of residues.

## 3.1. Introduction

In the last decades, the industrial segment of polymeric products has shaped the humankind life. Increasing demand for versatile products for several applications has been a major factor responsible for the growth of this segment. Nowadays, polymers are found throughout many sectors and industries including packaging, build and construction, automotive, electric and electronics, agriculture and consumer goods [1].

Currently, their improper disposal, persistence and fossil-based raw material represent factors with negative environmental and economic effects, namely greenhouse gas emission and land and marine pollution [2, 3]. In terms of disposal for example, only in Brazil, plastic represents around 13.5% of the total solid waste collectible [4]. Nonetheless, in 2015, from 72.5 million tons of solid waste collected, almost 30 million tons were sent to unsuitable destinations such as dumps [4]. Depending on the kind of plastic, it will take a very long time to degrade when released into the environment, enhancing its accumulation [5]. Even in the controlled environment of landfills plastics hardly degrade [6]. In the marine environment, common plastics used in packaging

degrade at a very slow rate [2, 7]. According to Eriksen et al. [8], a minimum of 5.25 trillion plastic particles weighing 268,940 tons is estimated to be floating in the world's oceans.

In this sense, the search for renewable raw materials suitable for the production of biodegradable polymeric products is imperative, especially considering the depletion of fossil resources, fluctuation of oil price and the negative environmental impacts. Indeed, bioplastics have been mentioned as a lead market by the European Commission, with global production capacity set to grow 350% by 2019 [1]. In recent years, the group of bioplastics derived from renewable and biodegradable resources has received great interest. They can be manufactured by different techniques using biopolymers as feedstock, such as cellulose, lignin and starch.

Among the available sources of renewable feedstock, lignocellulosic biomass stands out in the global scenario. Currently, this category of biomass assumes relevant importance for the generation of renewable energy, fuels and several other products (dispersants, flocculants, textile fibers and activated carbon), mainly due to its chemical constitution. Lignocellulosic biomass consists mainly of three natural organic polymers - cellulose, hemicellulose and lignin - and small amounts of proteins, pectin and extractives [9, 10]. Among the aforementioned components, cellulose is the most abundant organic polymer on earth, and owing to its mechanical and thermal properties, renewability, widely availability, non-toxic, low cost, biodegradability and derivatizability, cellulose is considered a promising feedstock for the development of sustainable materials [11–14].

Cellulose is a high molecular weight homopolymer assembled from the repetition of cellobiose units ( $\beta$  1-4 glucosidic covalent bonds between D-glucopyranose subunits) [15, 16]. Each cellobiose unit has hydroxyl groups that promote strong interactions by intra and intermolecular hydrogen bonds. This spatial structure allows the molecules to crystallize in a horizontal plane and in parallel chains, forming microfibril packages [17]. In the plant cell walls, the cellulose is embedded in a matrix of hemicellulose and lignin, bound together by covalent cross-links, which results in the recalcitrant property of the lignocellulosic biomass. Hence, the performance of physical or chemical pretreatments aiming the fractionation of lignocellulosic biomass is essential to convert cellulose into polymeric materials [10, 18]. After extraction, cellulose can be processed in the form of nanocellulose, derivatized cellulose, composites fillers or matrix and regenerated materials, such as films and gels [13, 19].

In general, lignocellulosic biomass may result from agricultural waste, forest waste, energy crops and municipal and industrial wastes [10, 20]. The set of activities associated with the

vegetable agribusiness sector stands out as one of the main residues generators. Framed worldwide as one of the leading agricultural producers, Brazil also excels due to the large waste generation originated from this type of activity. It is estimated that the production of agricultural residues in Brazil exceeds 200 million tons per year [21, 22]. Despite these residues being already applied to a range of valorization processing, a large portion is still directed to sanitarium landfills and incineration plants, or burned in the harvest field.

The first step in the sense of analyze the feasibility of agroindustrial residues valorization, regarding its application to produce cellulose-based products, consists in the identification of residues types that besides to have high content of cellulose, are also generated and available in significant quantities. Therefore, in this study, the required estimates were carried out based on the agroindustrial market of Brazil. The availability of residues was calculated as a function of the average crop production and conservative assumptions, such as sustainable removal rates and competitive uses. Then, the suitability of each residue for cellulose-based materials production was evaluated taking into consideration their availability and chemical composition.

## **3.2. Methodology**

### **3.2.1. Crop Residues Production and Chemical Composition**

Spatiotemporal characterization of agricultural crops production was performed with statistical data of Brazilian Institute of Geography and Statistics (IBGE) [23], extending from 2004 to 2014. In order to complement this previous assessment and support the selection of main crops, information about residues types and their respective cellulose, hemicellulose and lignin contents were obtained from associated literature.

The crop residues production can be calculated in terms of the average annual production of crops (AAP) and the residue generation rate (RGR). For the crops turned to processing industries, AAP corresponds to the portion of production intended for this application. For those which do not present this characteristic, the AAP values resulted directly from IBGE database. RGR values were obtained directly as default values from Natural Resource Module (NRM), as well as from other published documents. The NRM consist of a data processing and handling digital module, applied to assess the availability of bioenergy feedstock originating from crop production, agricultural residues and forestry [24].

## 3.2.2. Residue Generation Rate

The RGR can be understood as the ratio, on a dry basis, of the weight of residue produced to the total weight of the main crop product (e.g. the ratio of straw to wheat grain). RGR values may vary temporally and spatially according to several aspects, depending on the cultivation techniques, soil fertility and weather conditions [22]. Considering that RGR data used come from other studies targeted to different geographic areas, including those belonging to Natural Resource Module database, it is expected that these values encompass a technical, environmental and cultural variability, so that their application meet only a rough estimate. The diversity and variability of residues generation rates can be seen in Table 3.1.

Table 3.1. Residues generation rates of agroindustrial residues.

Crop	Residue	Residues Generation Rate				
Cotton	Hull	0.26 [24]	2.95 [22]	3.0 [25]	1.0 [26]	0.26 [27]
	Stalk	3.4 [24]				
Rice	Husk	0.25 [24]	1.49 [22]	1.0 [25]	1.0 [26]	1.55 [27]
	Straw	1.33 [24]				
Banana	Tree pruning	0.8 [28]				
Potato	Skin	0.04 [29, 30]				
Cocoa	Pod	1.5 [24]				
Coffee	Husk	1.32 [24]				
Sugarcane	Top/leaves	0.20 [24]	0.22 [22]	0.1 [25]		
	Bagasse	0.26 [24]				
Coconut	Husk	0.49 [24]				
	Shell	0.39 [24]				
Beam	Straw	1.7 [25]				
Apple	Pomace	0.30 [31]				
Cassava	Stalk	0.13 [24]	0.20 [22]			
	Cob	0.30 [24]	1.42 [22]		0.7 [26]	1.96 [27]
Maize	Husk	0.22 [24]				
	Stover	1.96 [24]		2.0 [25]		
Soybean	Straw	1.53 [24]	2.05 [22]	2.12 [27]		
	Pod	1.09 [24]				
Tomato	Pomace	0.01 [32, 33]				
Wheat	Straw	1.28 [24]	1.42 [22]	1.1 [25]	1.0 [26]	1.5 [27]
Mango	Seed	0.07 [34, 35]				
Pineapple	Peel	0.12 [34, 36]				

### 3.2.3. Availability of Agricultural Residues

After identifying the main crops produced in Brazil, the availability of crop residues ( $AR_{CR}$ ) (Equation 1) was calculated as a function of the average annual production of crops (AAP), residues generation rate (RGR), sustainable removal rate (SSR) and other competitive uses, while the availability of industry-driven crops residues ( $AR_{DC}$ ) (Equation 2) took into consideration the AAP, the portion of production turned to industrial processing (IP), RGR and other competitive uses (CU).

$$AR_{CR} = (AAP)(RGR)(SRR)(1 - CU) \quad (1)$$

$$AR_{DC} = (AAP)(IP)(RGR)(1 - CU) \quad (2)$$

#### 3.2.3.1 Sustainable Removal Rate

Sustainable removal rates (SRR) of crop residues are required to meet environmental and economic sustainability associated with the agricultural activity. The main objectives of sustainable crop residues removal consist in maintaining the natural soil fertility via incorporation of nutrients, promoting stability of upper soil layers and increase the organic matter content [37]. The percentage of crop residues that must be kept in the field depends on factors, such as the soil structure and type, planting techniques (e.g. fertilizers usage, crop rotation and till or no-till farming) and conservation practices.

In the literature is commonly suggested that a residue removal up to 30% does not imply damage to the soil [38–41]. However, estimates for sustainable residue removal may vary greatly from crop to crop, and it depends on another series of factors, such as geographical, climatic and technical/technological. For example, according to SoCo project team [42], regardless the cultivation method, it is indicated a maximum removal rate of straw around 70 percent. Karkee et al. [43] found that depending on soil characteristics, topography and farming practices (tillage, conventional and no-till), the percentage of available biomass to be removed may vary from 0% to 98%, without negative effects on the soil. In this study we adopted the sustainable removal rates of 40% for wheat straw, maize residues, rice straw and husk, bean straw and cotton stalk [44], and 30% for sugarcane top/leaves [38], cassava stalk and soybean straw and pods [44].

## 3.2.3.2 Competitive Use of Residues

Besides SRR, agroindustrial residues may be used in a range of applications, including energetic valorization, animal feed and bedding, application in the construction sector, as well as starting materials for activated carbon production [42, 45–47]. These applications represent competitive use with direct influence over the availability of residues and must be taken into account.

Generally, very little information is available on industrial processing residues used for recycling/reuse purposes. Notwithstanding, in order to proceed with conservative estimates, for those crops with no information on the percentage of residues turned to other valorization routes, it is assumed that only 50% is available. For residues that no other valorization route was identified, such as cassava stalk, rice straw, cotton stalk, soybean straw and sugarcane top/leaves, is estimated that 75% of the total generated is available (Table 3.2). It was also assumed that 35% of coconut [48], 10% of mango [49, 50], 40% of tomato [51], 10% of potato [52] and 15% of apple national production [53] are allocated to industries processing. Besides, it is verified that practically all the production of cocoa and coffee goes to processing industries [54, 55].

Table 3.2. Competitive uses of agroresidues.

Residue	Availability (%)	Competitive uses	Reference
Sugarcane bagasse	10	Fired in stem boilers in the own mill to produce electricity.	[56, 57]
Sugarcane top/leaves	75	Not identified.	—
Maize husk, cob and stover	40	Animal feed.	[56]
Rice husk	25	Drying, power generation at rice mills and chicken bedding production.	[56]
Rice straw	75	Usually burned in the harvest field.	[57]
Bean straw	50	Used to produce activated carbon and as a substrate for the production of other crops.	[58, 59]
Cassava stalk	75	Used as animal feed, but its toxic principle limits this kind of application.	[57, 60]
Orange residues	0	Aromatizing and animal feed.	[61]
Grape residues	0	Used in food, pharmaceutical and cosmetics industries.	[21, 62]
Coconut residues	90	Biomass, composites, agricultural fertilizer, activated carbon and filler for automotive banks.	[63–65]
Mango stone and husk	50	Animal feed.	[66, 67]
Tomato pomace	50	Fractionation of components, carotenoids extraction and biofuels.	[68–70]
Potato skin	50	Cattle feed.	[71]
Apple pomace	50	Organic fertilizer and animal feed.	[72]
Cocoa shell	50	Energetic valorization.	[73]
Coffee husk	50	Animal bedding.	[56]
Cotton stalk	75	Not identified.	—
Soybean straw	75	Not identified.	—

### 3.2.4 Suitability of Agroindustrial Residues to Develop Cellulose-based Products

The assessment of residues suitability has been carried out based on methodology reported by Araújo et al. [74], where the suitability scale of residues is measured (equation 3) taking into account the normalized values of three main parameters ( $\chi_j$ ): Availability of residues (AR), cellulose content (CC) and cellulose to lignin ratio ( $R_{c/L}$ ). The presence of lignin in lignocellulosic biomass can be considered as one of the major obstacles in biomass pretreatment processes [75, 76]. Therefore, the influence of lignin over the selection of residues was accounted by including the cellulose-to-lignin ratio. The greater the ratio, the greater is the cellulose percentage compared to the lignin content, and thus more efficient is the biomass treatment.

$$S_{ij}' = \sum_i^n w_i \chi_{ij}'; \text{ Lignin content} > 0 \quad (3)$$

Where,

$$\chi_{ij}' = a + \left[ \frac{(\chi_j - \chi_{\min})(b - a)}{(\chi_{\max} - \chi_{\min})} \right]; \quad (4)$$

The constants  $a$  and  $b$  in equation 4 correspond to arbitrary points, equivalent to 0.1 and 1, respectively, used to restrict the range of suitability values. Besides,  $w_j$  correspond to weights of parameters AR, CC and  $R_{c/L}$ , which are equivalent to 35, 45 and 20, respectively, and the subscript index  $j$  represents the residue under evaluation. In the same equations, the parameters designated by maximum and minimum subscripts are related to residues that present the highest and lowest values, respectively, of the parameter concerned. Thus, for each residue, the suitability index ( $S_i'$ ) may vary from 10 (lowest suitability) to 100 (highest suitability), expressed as dimensionless (Equation 3).

## 3.3. Results and discussion

### 3.3.1. Agricultural Production and Harvested Area

The crop production can be divided into two categories: (i) permanent and (ii) temporary. The permanent category includes the long-term crops that do not require replanting after harvesting, while the temporary ones generally require replanting after harvesting. Within the period from 2004 to 2014, among all permanent crops, excel the high production of orange, banana, coffee and coconut (Figure 3.1). In fact, Brazil is among the world's leading producers of these crops. Only the Southeast region is responsible for more than 80% of national orange production and 55% of



the total permanent crops production. Northeast region accounts the largest production of coconut and banana and 23% of permanent crops production (Figure 3.1a and 3.1b).

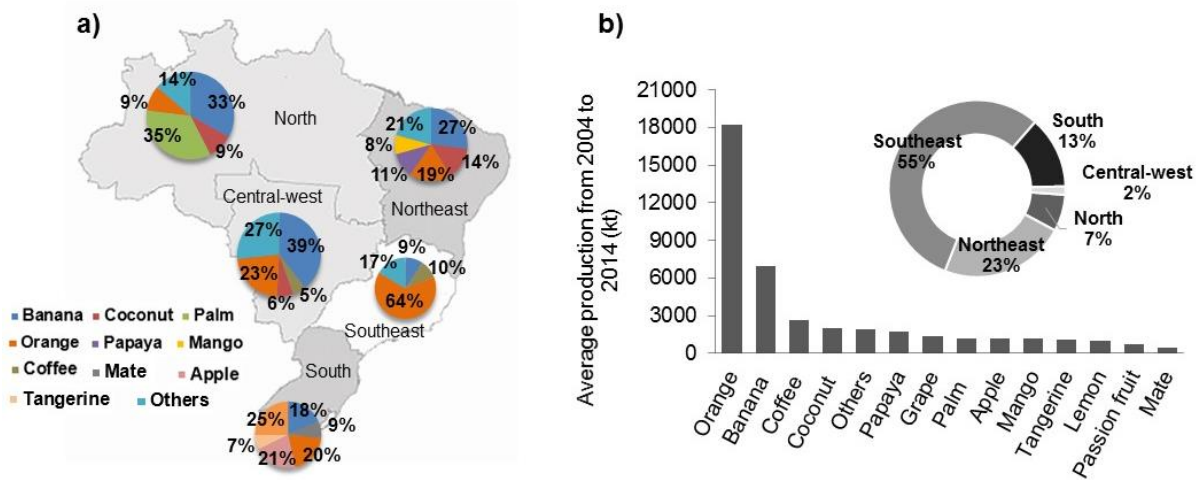


Figure 3-1. Average production of permanent crops in Brazil. a) Average percentage of the main crops produced by each macroregion. b) Average production of permanent crops from 2004 to 2014 and average percentage of permanent crop production by macroregions.

Southeast and Northeast regions accounted about 5,224,000 ha (43.43% and 39.68%, respectively), on average, of the total area used for the cultivation of permanent crops in Brazil. Around 80% of coffee plantation and 74% of orange plantation are located in the Southeast region. In the Northeast predominates plantation areas for banana, cocoa, cashew nut, coconut and sisal. In other regions, crops with lower percentage of area for cultivation prevails.

Regarding the temporary crops, over the last 11 years of data, it was possible to verify that the production almost doubled, reaching 972.2 megatons in 2014. Among all the temporary crops, sugarcane production is by far the most relevant. In 2014 were produced 737.2 Mt of sugarcane, 86.7 Mt of soybean, and 79.8 Mt of maize (Figure 3.2). These figures place Brazil among the world's largest producers of these crops. The other crops, which account for a total of 28 different types, contributed with 68.5 Mt (about 7% of the total production) (Figure 3.2). About 52% of the national temporary crops production takes place in the Southeast region. The Centre-west region presents the second higher percentage contribution, mainly due to its leadership as maize and soybean producer.

It could also be noticed that 43% of the total harvesting area were assigned to soybean plantation, 22.5% were related to maize and 14.8% to sugarcane. It is worth highlighting that, in

2014, two Brazilian regions accounted for about 45% of all harvested areas, namely Centre-west (with 24.3 million hectares) and South (with 21 million hectares).

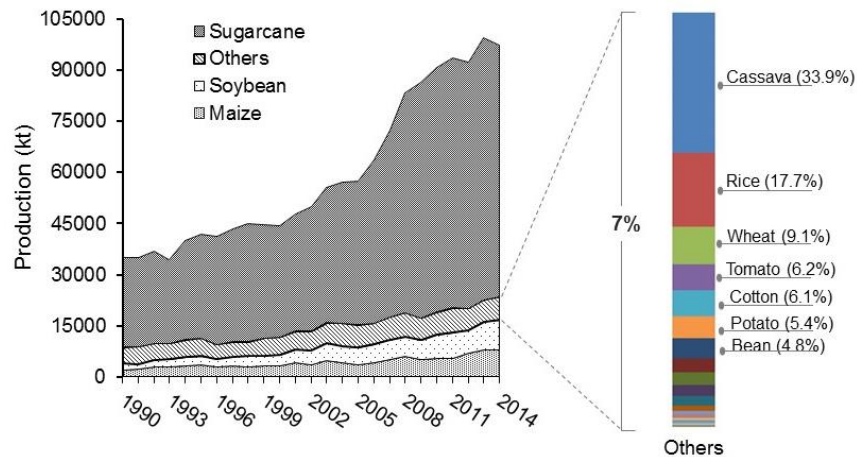


Figure 3-2. Annual evolution of temporary agricultural crops production from 1990 to 2014.

### 3.3.2. Chemical Composition of Agroindustrial Residues

Depending on the morphological structure of crops and the processing levels to which they are subject, different types of residues with specific cellulose, hemicellulose and lignin contents can be obtained (Tables 3.3 and 3.4). Cereals and oilseed crops may be mentioned as crops capable of generating wastes still in the harvesting phase. On the other hand, crops such as grape, orange, apple, potato, coconut, coffee, mango and cocoa, particularly interesting to obtain processed products, may result in the generation of wastes at different stages of industrial processing. Tables 3.3 and 3.4 present cellulose, hemicellulose and lignin values for a range of lignocellulosic residues derived from temporary and permanent agricultural crops, respectively. These tables highlight several agroindustrial residues with high cellulose content and potentially interesting to be used as sustainable resources to the production of cellulose-based materials.

Table 3.3. Chemical composition of lignocellulosic biomass derived from temporary crops

Biomass		Cellulose (%)	Hemicellulose (%)	Lignin (%)	Reference
Pineapple	Peel	21.98	74.96	2.68	[77]
Cotton	Hull	44.35	11.2	16.15	[78]
	Stalk	40.4	—	20.9	[79]
Garlic	Skin	41.7 ± 2.1	20.8 ± 1.6	34.5 ± 2.4	[80]
Peanut	shell	49.4 ± 1.4	8.1 ± 0.6	33.1 ± 1.5	[81]
Rice	Straw	39.5 - 41	24.4 - 31	15.9 - 24	[82, 83]
	Husk	35	33	23	[84]
Oat	Stalk	31 - 48	27 - 38	16 - 19	[85]
Potato	Skin	10.5	—	4.0	[86]
Sugarcane	Top/leaves	39.8	28.6	22.5	[87]
	Bagasse	43.10	22.82	24.09	[12]
Onion	Skin	41.1 ± 1.1	16.2 ± 0.6	38.9 ± 1.3	[88]
Rye (stalk)	Stalk	33 - 50	27 - 30	16 - 19	[85]
Barley	Straw	33 - 40	20 - 35	8 - 17	[10]
Pea	Hull	62.3	8.2	—	[89]
Bean	Straw	40.2	19.32	18.13	[90]
Sunflower	Straw	40.41	31.44	19.45	[90]
Jute	Stem	61 - 71.5	13.6 - 20.4	12 - 13	[91]
Flax	Stem	75.4 ± 0.2	13.4 ± 2.8	3.4 ± 0.9	[92]
Cassava	Stalk	38.8	7.2	11.8	[93]
	Husk	62.07 ± 0.86	17.93 ± 0.86	14.6 ± 0.6	[94]
Maize	Stover	40.8	34	22	[83]
	Cob	31.2 - 45	35 - 43.1	15 - 16.5	[10, 95]
Ramie	Fiber	69 - 91	5 - 17	< 1	[96, 97]
Soybean	Straw	44 - 83	24.3 ± 3.0	5.0 - 14	[98]
Sorghum	Stalk	41.7	23	18.2	[99]
Tomato	Plant	39.1	28.8	12.1	[100]
	Pomace	29.1	13.5	57.4	[101]
Wheat	Straw	30 - 40.8	38.32 - 50	15 - 22.45	[10, 90]
Triticale	Straw	32.20	—	15.02	[102]

Table 3.4. Chemical composition of lignocellulosic biomass derived from permanent crops.

Biomass		Cellulose (%)	Hemicellulose (%)	Lignin (%)	Reference
Olive	Pomace	24.1 – 14.45	11.0 - 6.63	14.1 - 8.54	[103]
	Raquis	48.7	16.1	12.2	[104]
Banana	Pseudostem	48.19 – 59.22	12.09 – 15.91	14.39 – 21.56	[105]
	Peduncle	48.31 – 60.41	10.20 – 13.99	17.56 – 20.66	
Cocoa	Shell	35.4	14.0	37	[73]
Coffee	Husk	43.0 ± 8.0	7.0 ± 3.0	9.0 ± 1.6	[106]
Coconut	Husk	37.0	–	32.5	[107]
Orange	Pell	14.4 – 37.08	10.9 – 11.04	1.33 – 7.52	[108]
Lemon	Pell	23.06 ± 2.11	8.09 ± 0.81	7.56 ± 0.54	[108]
Apple	Pomace	7.2	–	23.5	[109]
Mango	Seed	55.0 ± 1.0	20.6 ± 0.3	23.85 ± 0.21	[110]
Nut	Shell	53.9	15.4	30.7	[101]
Oil palm	Empty fruit brunch	40 - 50	20 - 30	20 - 30	[111]
Pear	Pomace	32.9 ± 0.3	22.1 ± 0.2	17.0 ± 0.4	[112]
Sisal	Fiber	64.9 - 78	10 - 25.4	8 - 11.7	[113, 114]
Grape	Pomace	27.9	9.1	63.0	[101]

### 3.3.3. Availability of Agroindustrial Residues

The availability of residues related to main crops identified in previous assessment took into consideration: (i) average annual production of crops; (ii) residue generation rate; (iii) sustainable removal rates; and (iv) other competitive uses. Table 3.6 shows the assumed values for variables encompassed in equations 1 and 2, as well as the annual residue production (RP) and the availability of residues. Exclusively for the industry-driven crops, the AAP is equivalent to the portion of production directed to industrial processing. Residues classified in this approach are highlighted in table 3.5.

Taking into account only the main residues identified, the total amount of agroindustrial residues produced in Brazil is estimated at over 589 million tons/year on average. However, in response to the conservation assumptions, the availability of residues is estimated at about 108 million tons/year (Table 3.5). The analysis of these results along with the data provided in Table 3.2 and 3.3, confirms the potential application of the accounted residues as cellulose feedstock.

Table 3.5. Average availability of agricultural residues. AAP – average annual production of crops; RGR – residue generation rate; RP – annual residue production; SRR – sustainable removal rate; AR – availability of residues; CU – competitive uses; \* production intended to industry processing.

Residues	AAP (kt/year)	RGR ( $t_{\text{residue}}/t_{\text{crop}}$ )	RP (kt/year)	SRR (%)	CU (%)	AR (kt/year)
Cocoa	227.83					
Shell		1.5	314.75	—	50	170.87
Coconut	*694.86					
Husk		0.49	340.48	—	10	306.43
Shell		0.39	270.99	—	10	243.90
Coffee	2,643.6					
Husk		1.32	3,489.60	—	50	1,744.8
Banana	6,923.9					
Pruning		0.8	5,539.12	—	50	2,769.6
Mango	*115.50					
Seed		0.07	8.09	—	50	4.05
Apple	*173.5					
Pomace		0.30	52.05	—	50	26.03
Maize	56,688.7					
Cob		0.33	18,707.3	40	60	2,993.2
Husk		0.22	12,471.5	40	60	1,995.4
Stover		1.96	111,109.9	40	60	17,777.6
Soybean	64,194.4					
Straw		1.53	98,217.4	30	25	22,098.9
Sorghum	1,861.00					
Stalk		1.4	2,605.4	30	50	390.80
Sugarcane	625,452.7					
Top/leaves		0.20	125,090.5	30	25	28,145.4
Bagasse		0.26	162,617.7		90	16,261.8
Cassava	24,743.0					
Stalk		0.13	3,216.6	30	25	723.73
Wheat	5,130.8					
Straw		1.28	6,567.5	40	50	1,313.5
Rice	12,181.0					
Husk		0.25	3,045.2		75	761.3
Straw		1.33	16,200.7	40	25	4,860.2
Bean	3,194.5					
Straw		1.7	5,430.7	40	50	1,086.1
Cotton	3,818.0					
Hull		0.26	992.7		50	496.3
Stalk		3.4	12,981.4	40	25	3,894.4
Pineapple	*648.9					
Peel		0.12	77.9	—	50	38.9
Tomato	*1,265.4					
Pomace		0.01	12.7	—	50	6.3
Potato	*349.5					
Skin		0.04	13.98	—	50	6.99

Figure 3.3 summarizes the information discussed so far about the availability of residues and the average percentage of cellulose. Evaluating only these two parameters, it can be observed the

greater relevance of sugarcane top/leaves, soybean straw, maize stover, sugarcane bagasse and rice straw, which accounted for about 82% of the total production of available residues. The remaining residues, despite having higher percentages of cellulose, present less significant AR values when compared to the others. It is worth highlight the relevance of sugarcane crop, which contributes alone with 41% of the total residues.

By comparison, the estimates obtained in this study resemble others identified in literature, especially when taken into consideration the total production of residues and not only the portion available [22, 44, 60]. For instance, Forster-Carneiro et al. [22] also highlight the sugarcane as the crop with the largest production of residues (estimated at 157 million tons), and stressed a possible increase in the generation of agroindustrial residues around 25.2% by 2020.

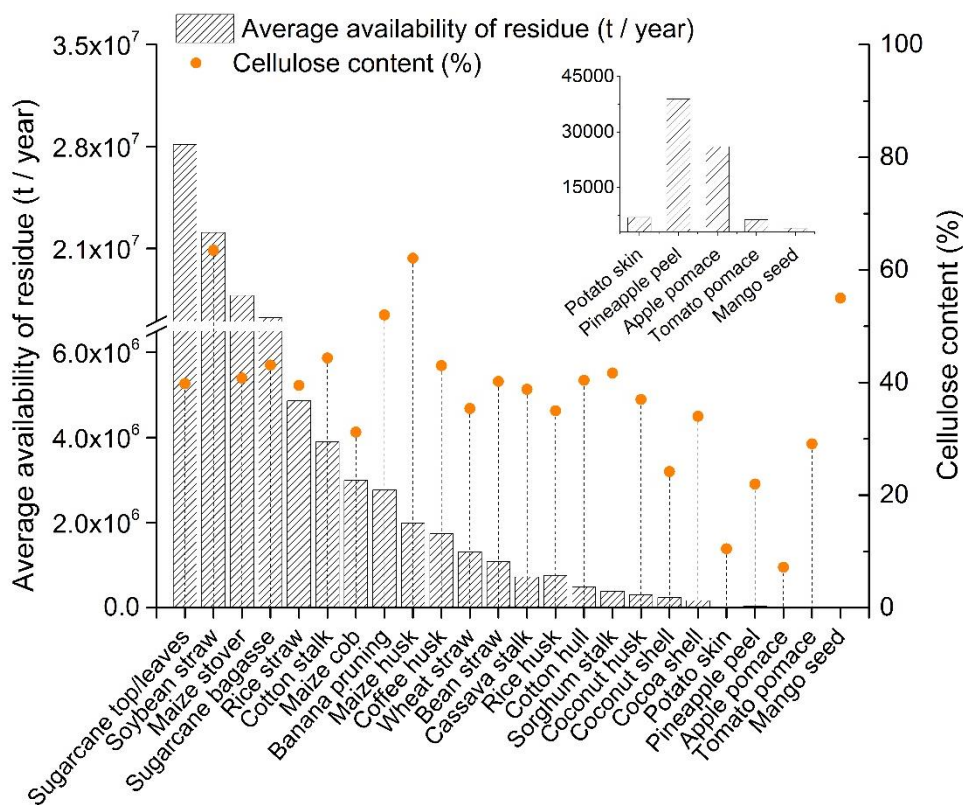


Figure 3-3. Availability and cellulose content of the major agroindustrial residues identified.

Assessing the annual variability of AR for the whole historical series (Figure 3.4) it is possible to notice a marked increase of residues generation throughout the years. For instance, from 2005 to 2014 the availability of residues increased 40%. It is estimated that 134 million tons of residues were available in Brazil in 2014. These estimates are consistent with current developments in the global agricultural sector. Only in the last three decades the Brazilian agricultural production more

than doubled in volume. The sector has contributed significantly to the country's trade balance, mainly as a foreign currency collector due to export activity. Driven by continuous productivity improvements, and the implementation of stimulus and investment policies in research and development as well, the outlook for 2024 is that the sector continues to grow [115].

In line with the expected increase of agricultural productivity is the large generation of residues (Figure 3.4), which still have marginal economic use [22]. Taking as reference the average availability of residues from 2004 to 2014, and the years in which have been verified the lowest and highest residues generation, positive and negative variations ranging from -25.7 and +24.04% were found. Moreover, it is possible to predict an increase of agroindustrial residues generation, considering that, since 2005, the availability of residues has shown positive growth rate, with average annual fluctuation of about + 5.43%.

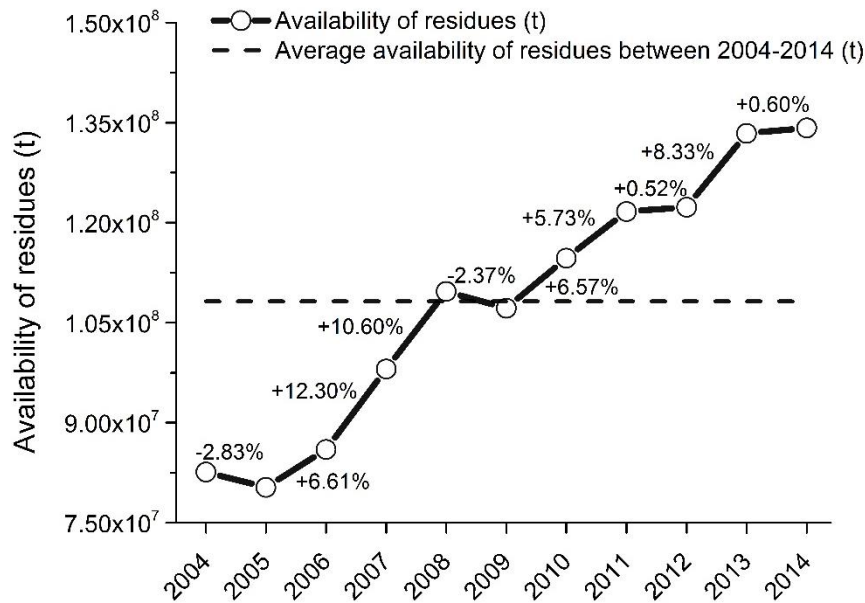


Figure 3-4. Annual evolution of availability of residues in Brazil.

### 3.3.4. Suitability of Agroindustrial Residues

The ranking of residues with greater potential to be used as raw material (Figure 3.5) was obtained from the substitution of calculated parameters  $AR_i$ ,  $CC_i$  e  $R_{C/Li}$  (Table 3.6) in equation 3. It could be noticed that, mainly the parameters  $AR$  e  $R_{C/L}$  had a significant influence on the residues ranking. The low lignin content associated with pineapple peel resulted in a normalized cellulose-to-lignin ratio much higher than of other residues (Table 3.3 and 3.6), which contributed

significantly to the final value of suitability. The same is true for sugarcane top/leaves and soybean straw, in response to their great availability.

Table 3.6. Availability of residues, Cellulose content and cellulose-to-lignin ratio normalized values.

Residue	Normalized available residue (AR <sub>i</sub> )	Normalized cellulose content (CC <sub>i</sub> )	Normalized cellulose-to-lignin ratio (R <sub>CLi</sub> )
Cocoa shell	0.105	0.551	0.353
Coconut husk	0.110	0.576	0.195
Coffee husk	0.156	0.672	0.610
Maize cob	0.196	0.484	0.302
Maize husk	0.164	0.977	0.550
Maize stover	0.668	0.637	0.277
Sugarcane bagasse	0.620	0.674	0.269
Cassava stalk	0.123	0.605	0.440
Rice husk	0.124	0.544	0.239
Rice straw	0.255	0.616	0.348
Bean straw	0.135	0.628	0.318
Cotton hull	0.116	0.694	0.378
Cotton stalk	0.224	0.631	0.285
Banana pruning	0.188	0.816	0.426
Mango seed	0.100	0.864	0.328
Apple pomace	0.101	0.100	0.100
Soybean straw	0.807	1.000	0.827
Sorghum stalk	0.112	0.652	0.326
Sugarcane top/leaves	1.000	0.621	0.267
Wheat straw	0.142	0.551	0.281
Pineapple peel	0.101	0.336	1.000
Tomato pomace	0.100	0.450	0.123
Potato skin	0.100	0.153	0.364

Among the major agroindustrial residues identified, those with greater potential to be used as raw material are soybean straw, sugarcane top/leaves, maize husk, maize stover and sugarcane bagasse. The lowest suitability values were assigned to apple pomace, potato skin and tomato pomace (Figure 3.5). A close relationship between the suitability of residues and the productivity of crops was identified, since the most suitable residues are originated from the most productivity crops. Additionally, in the production and manufacturing cycle of agricultural products, the largest parcel of residues is generated during the harvest phase. However, some residues coming from



processing industries excel as potential feedstock for cellulose-based materials manufacturing, namely sugarcane bagasse, mango seed, coffee husk and pineapple peel.

Residues with intermediate or low value of suitability may also be applied to the application concerned. However, in such situations, the feasibility of using these residues should be assessed, since the improvement and optimizing of treatments or pretreatments techniques must be carried out. For instance, besides to affect the efficiency of pretreatment steps, the presence of substantial amounts of non-cellulosic components may negatively influence their biodegradability, crystallinity, density, tensile strength, modulus and moisture of fibers and end products [11, 116, 117].

It is worth mentioning that the use of agricultural residues as polymer feedstock requires to encompass a number of issues besides the availability and chemical composition. The temporal variability of generation, technological alternatives available for valorization, perception and social impact on different farmers' category and logistical issues should also be taken into account. For instance, in Brazil, about 63% of sugarcane production takes place in the southeast region, hence, the largest share of sugarcane residues will be available in that region.

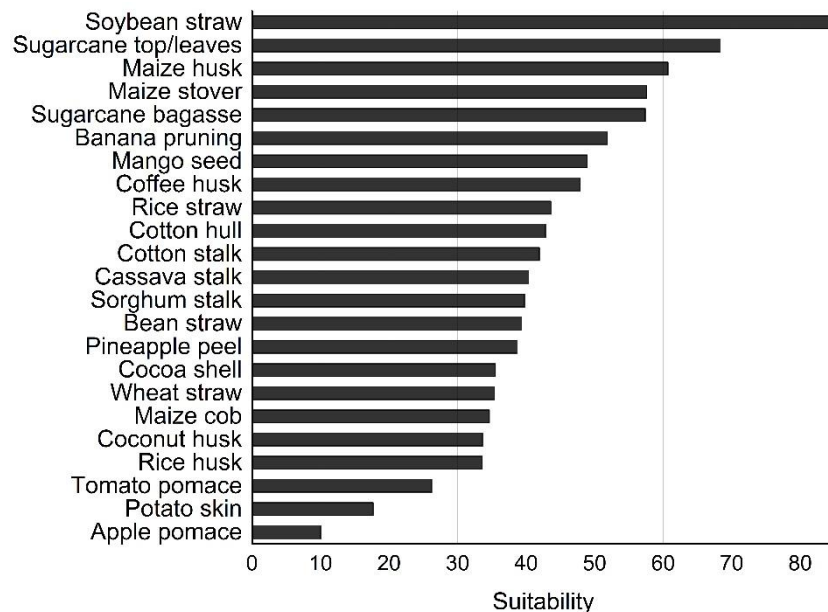


Figure 3-5. Suitability of agroresidues for cellulose-based materials production.

Several agroindustrial residues highlighted herein have already been reported as source for nanocellulose production, namely mango seed [110], soy hulls [118], cotton stalk [119], sugarcane bagasse [120], oil palm empty fruit bunch pulp [121], corncob [122] and wheat straw [123]. Ongoing studies in this field are focused mainly on the use of nanocrystalline cellulose (NCC)

and microfibrillated cellulose (MFC) as fillers to nanocomposites, aiming the improvement of packaging and films properties [124–126].

Other newly applications and trends on cellulose-based materials are focused on the functionalization of natural lignocellulosic fibers, to produce polymeric composites [127–129] and biosorbents [130, 131], and NCC and MFC for assembling well-defined nanomaterials with unique properties [14, 119, 126, 132]. Additionally, is worth mentioning the development of regenerated cellulose, which is manufactured through the dissolution of cellulose, followed by its shaping and subsequent regeneration [13], and the conversion of lignocellulosic biomass into chemical building blocks through the biorefinery concept approach [133, 134].

### **3.4. Conclusion**

In this study, a methodology to select agroindustrial residues suitable for cellulose-based materials production has been conducted based on the agricultural sector of Brazil. The chemical composition and availability of residues were taken into account. The availability of residues was estimated at about 108 million tons/year, on average. Moreover, it is likely that residues generation keeps growing, once, since 2005 the availability of residues has shown positive growth rate. However, the spatial and temporal variability related to residues generation should be considered when planning valorizations routes.

A number of residues highlighted herein present potential to be used as feedstock to produce cellulose-based materials. Among the most suitable residues are the soybean straw, sugarcane top/leaves, maize husk and stover and sugarcane bagasse. Triggered by the search for sustainable process and products, over the next decades these residues tend to be increasingly seen and used as a potential resource. Notwithstanding, besides to present acceptable physical performance, the viability of using the new developed products will be defined by environmental and economic aspects associated with their production, use and post use destination chains, which must be assess by life and cost cycle analysis.

### **Acknowledgements**

This work was supported by the Brazilian National Council for Scientific and Technological Development (Grant number 201940/2015-9).

## References

1. EuBP: Biopalstics Facts and Figures. (2016)
2. Avio, C.G., Gorbi, S., Regoli, F.: Plastics and microplastics in the oceans: From emerging pollutants to emerged threat. *Mar. Environ. Res.* 128, 2–11 (2017). doi:10.1016/j.marenvres.2016.05.012
3. Hervy, M., Evangelisti, S., Lettieri, P., Lee, K.Y.: Life cycle assessment of nanocellulose-reinforced advanced fibre composites. *Compos. Sci. Technol.* 118, 154–162 (2015). doi:10.1016/j.compscitech.2015.08.024
4. ABRELPE: Panorama of solid waste in Brazil 2015. (2015)
5. Shah, A.A., Hasan, F., Hameed, A., Ahmed, S.: Biological degradation of plastics: A comprehensive review. *Biotechnol. Adv.* 26, 246–265 (2008). doi:10.1016/j.biotechadv.2007.12.005
6. Webb, H.K., Arnott, J., Crawford, R.J., Ivanova, E.P.: Plastic degradation and its environmental implications with special reference to poly(ethylene terephthalate). *Polymers (Basel)*. 5, 1–18 (2013). doi:10.3390/polym5010001
7. Andrady A. L.: Persistence of Plastic Litter in the Oceans. In: Bergmann, M., Gutow, L., and Klages, M. (eds.) *Marine Anthropogenic Litter*. pp. 57–72. Springer Berlin Heidelberg (2015)
8. Eriksen, M., Lebreton, L.C.M., Carson, H.S., Thiel, M., Moore, C.J., Borrorro, J.C., Galgani, F., Ryan, P.G., Reisser, J.: Plastic Pollution in the World's Oceans: More than 5 Trillion Plastic Pieces Weighing over 250,000 Tons Afloat at Sea. *PLoS One*. 9, 1–15 (2014). doi:10.1371/journal.pone.0111913
9. Singh, M., Kaushik, A., Ahuja, D.: Surface functionalization of nanofibrillated cellulose extracted from wheat straw: Effect of process parameters. *Carbohydr. Polym.* 150, 48–56 (2016). doi:10.1016/j.carbpol.2016.04.109
10. Lee, H. V, Hamid, S.B. a, Zain, S.K.: Conversion of Lignocellulosic Biomass to Nanocellulose : Structure and Chemical Process Conversion of Lignocellulosic Biomass to Nanocellulose : *Sci. World J.* 2014, 1–14 (2014). doi:10.1155/2014/631013
11. Reddy, N., Yang, Y.: Biofibers from agricultural byproducts for industrial applications. *Trends Biotechnol.* 23, 22–27 (2005). doi:10.1016/j.tibtech.2004.11.002

12. Yue, Y., Han, J., Han, G., Aita, G.M., Wu, Q.: Cellulose fibers isolated from energycane bagasse using alkaline and sodium chlorite treatments: Structural, chemical and thermal properties. *Ind. Crops Prod.* 76, 355–363 (2015). doi:10.1016/j.indcrop.2015.07.006
13. Wang, S., Lu, A., Zhang, L.: Recent advances in regenerated cellulose materials. *Prog. Polym. Sci.* 53, 169–206 (2016). doi:10.1016/j.progpolymsci.2015.07.003
14. Grishkewich, N., Mohammed, N., Tang, J., Tam, K.C.: Recent advances in the application of cellulose nanocrystals. *Curr. Opin. Colloid Interface Sci.* 29, 32–45 (2017). doi:10.1016/j.cocis.2017.01.005
15. Klemm, D., Heublein, B., Fink, H.P., Bohn, A.: Cellulose: Fascinating biopolymer and sustainable raw material. *Angew. Chemie - Int. Ed.* 44, 3358–3393 (2005). doi:10.1002/anie.200460587
16. Habibi, Y., Lucia, L.A., Rojas, O.J.: Cellulose nanocrystals: Chemistry, self-assembly, and applications. *Chem. Rev.* 110, 3479–3500 (2010). doi:10.1021/cr900339w
17. Ojeda, T.: Polymers and the environment. In: F., Y. (ed.) *Polymer Science*. pp. 1–34. InTech (2013)
18. Li, Q., Jiang, X., He, Y., Li, L., Xian, M., Yang, J.: Evaluation of the biocompatible ionic liquid 1-methyl-3-methylimidazolium dimethylphosphite pretreatment of corn cob for improved saccharification. *Appl. Microbiol. Biotechnol.* 87, 117–126 (2010). doi:10.1007/s00253-010-2484-8
19. Mondal, S.: Preparation, properties and applications of nanocellulosic materials. *Carbohydr. Polym.* 163, 301–316 (2017). doi:10.1016/j.carbpol.2016.12.050
20. Ullah, K., Kumar Sharma, V., Dhingra, S., Braccio, G., Ahmad, M., Sofia, S.: Assessing the lignocellulosic biomass resources potential in developing countries: A critical review. *Renew. Sustain. Energy Rev.* 51, 682–698 (2015). doi:10.1016/j.rser.2015.06.044
21. Schneider, V.E., Peresin, D., Trentin, A.C., Bortolin, T.A., Sambuichi, R.H.R.: *Caderno de diagnósticos: Resíduos Agrosilvopastoris I.* (2011)
22. Forster-Carneiro, T., Berni, M.D., Dorileo, I.L., Rostagno, M.A.: Biorefinery study of availability of agriculture residues and wastes for integrated biorefineries in Brazil. *Resour. Conserv. Recycl.* 77, 78–88 (2013). doi:10.1016/j.resconrec.2013.05.007
23. IBGE - Brazilian institute of geography and statistics: No Title, <https://sidra.ibge.gov.br/pesquisa/lspa/tabelas>

24. FAO - Food and Agricultural Organization: Natural resources module - biomass potential assesment, <http://www.fao.org/energy/bioenergy/befs/assessment/befs-ra/natural-resources/en/>
25. Jiang, D., Zhuang, D., Fu, J., Huang, Y., Wen, K.: Bioenergy potential from crop residues in China: Availability and distribution. *Renew. Sustain. Energy Rev.* 16, 1377–1382 (2012). doi:10.1016/j.rser.2011.12.012
26. Panoutsou, C., Labalette, F.: Cereals straw for bioenergy and competitive uses. *Proc. Cereal. Straw Resour. Bioenergy Eur. Union, Pamplona, Pamplona.* 18–19 (2006)
27. Koopmans, A., Koppejan, J.: Agricultural and forest residues - Generation, utilization and availability. *Reg. Consult. Mod. Appl. Biomass Energy.* 6–10 (1997). doi:10.1016/S0251-1088(83)90310-8
28. Rosal, A., Rodriguez, A., Gonzalez, Z. and Jimenez, L.: Use of banana tree residues as pulp for paper and combustible. *Int. J. Phys. Sci.* 7, 2406–2413 (2012). doi:10.5897/IJPS11.1661
29. Schieber, a, Stintzing, F., Carle, R.: By-products of plant food processing as a source of functional compounds—recent developments. *Trends Food Sci. Technol.* 12, 401–413 (2001). doi:10.1016/S0924-2244(02)00012-2
30. Arapoglou, D., Varzakas, T., Vlyssides, A., Israilides, C.: Ethanol production from potato peel waste (PPW). *Waste Manag.* 30, 1898–1902 (2010). doi:10.1016/j.wasman.2010.04.017
31. Dhillon, G.S., Kaur, S., Brar, S.K.: Perspective of apple processing wastes as low-cost substrates for bioproduction of high value products: A review. *Renew. Sustain. Energy Rev.* 27, 789–805 (2013). doi:10.1016/j.rser.2013.06.046
32. Jiang, F., Hsieh, Y. Lo: Cellulose nanocrystal isolation from tomato peels and assembled nanofibers. *Carbohydr. Polym.* 122, 60–68 (2015). doi:10.1016/j.carbpol.2014.12.064
33. del Campo, I., Alegria, I., Zazpe, M., Echeverría, M., Echeverría, I.: Diluted acid hydrolysis pretreatment of agri-food wastes for bioethanol production. *Ind. Crops Prod.* 24, 214–221 (2006). doi:10.1016/j.indcrop.2006.06.014
34. Ayala-Zavala, J.F., Rosas-Domínguez, C., Vega-Vega, V., González-Aguilar, G.A.: Antioxidant enrichment and antimicrobial protection of fresh-cut fruits using their own byproducts: Looking for integral exploitation. *J. Food Sci.* 75, (2010). doi:10.1111/j.1750-3841.2010.01792.x
35. Okpala, L.C., Gibson-Umeh, G.I.: Physicochemical Properties of Mango Seed Flour. *Niger. Food J.* 31, 23–27 (2013). doi:10.1016/S0189-7241(15)30052-7

36. Kareem, S., Akpan, I., Alebiowu, O.: Production of citric acid by *Aspergillus niger* using pineapple waste. *Mal J Microbiol.* 6, 161–165 (2010)
37. Scarlat, N., Martinov, M., Dallemand, J.F.: Assessment of the availability of agricultural crop residues in the European Union: Potential and limitations for bioenergy use. *Waste Manag.* 30, 1889–1897 (2010). doi:10.1016/j.wasman.2010.04.016
38. Lindstrom, M.J.: Effects of residue harvesting on water runoff, soil erosion and nutrient loss. *Agric. Ecosyst. Environ.* 16, 103–112 (1986). doi:https://doi.org/10.1016/0167-8809(86)90097-6
39. Nikolaou, A., Remrova, M., Jeliakov, I.: Biomass availability in Europe. *EU Energy.* 1–80 (2003)
40. Wilhelm, W.W., Johnson, J.M.F., Hatfield, J.L., Voorhees, W.B., Linden, D.R.: Crop and Soil Productivity Response to Corn Residue Removal: A Literature Review. *Agron. J.* 96, 1–17 (2004). doi:10.2134/agronj2004.0001
41. Kludze, H., Deen, B., Weersink, A., van Acker, R., Janovicek, K., De Laporte, A., McDonald, I.: Estimating sustainable crop residue removal rates and costs based on soil organic matter dynamics and rotational complexity. *Biomass and Bioenergy.* 56, 607–618 (2013). doi:10.1016/j.biombioe.2013.05.036
42. SoCo Project Team, SoCo, P.T.: Addressing soil degradation in EU agriculture: relevant processes, practices and policies. (2009)
43. Karkee, M., McNaull, R.P., Birrell, S.J., Steward, B.L.: Estimation of Optimal Biomass Removal Rate Based on Tolerable Soil Erosion for Single-Pass Crop Grain and Biomass Harvesting System. *Trans. Asabe.* 55, 107–115 (2012)
44. Tolmasquim M. T. et al: Inventário Energético de Resíduos Rurais. EPE, Resur. tecnológicos. 1–47 (2014)
45. Koubaissy, B., Toufaily, J., Cheikh, S., Hassan, M., Hamieh, T.: Valorization of agricultural waste into activated carbons and its adsorption characteristics for heavy metals. *Open Eng.* 4, (2014). doi:10.2478/s13531-013-0148-z
46. Zhang, P., Dong, S.J., Ma, H.H., Zhang, B.X., Wang, Y.F., Hu, X.M.: Fractionation of corn stover into cellulose, hemicellulose and lignin using a series of ionic liquids. *Ind. Crops Prod.* 76, 688–696 (2015). doi:10.1016/j.indcrop.2015.07.037

47. Mtui, G.Y.S.: Recent advances in pretreatment of lignocellulosic wastes and production of value added products. *African J. Biotechnol.* Vol. 8, 1398–1415 (2009). doi:10.1073/pnas.1014862107/-/DCSupplemental.www.pnas.org/cgi/
48. Cuenca, M.A.G., Resende, J.M., Saggin Júnior, O.J. et al.: Mercado brasileiro do coco: situação atual e perspectivas. In: Aragão, W.M. (ed.) *Coco: pós póscolheita*. pp. 11–18. Embrapa Informação Tecnológica, Brasília, DF (2002)
49. Ferraz, M.S.: Perspectivas de mercado - Produção e Consumo de manga. In: *I Simpósio de manga do Vale do São Francisco*. p. 12 (2005)
50. Treichel Michelle, et al.: *Anuário Brasileiro da Fruticultura*. Editora Gazeta Santa Cruz, Santa Cruz do Sul (2016)
51. Treichel Michelle, et al.: *Brazilian tomato Yearbook 2016*. Editora Gazeta Santa Cruz, Santa Cruz do Sul (2016)
52. HF Brasil: Procuram-se agroindústrias, <http://migre.me/wKQ8N>, (2011)
53. Bernardo, B. K., et al.: *Brazilian Apple Yearbook 2016*. Editora Gazeta Santa Cruz, Santa Cruz do Sul (2016)
54. Müller, I., et al.: *Brazilian Cocoa yearbook 2012*. Editora Gazeta Santa Cruz, Santa Cruz do Sul (2012)
55. Kist, B.B., dos Santos, C.E., Carvalho, C., Reetz, E.G., Müller, I., Beling, R.R.: *Brazilian Coffee Yearbook 2015*. Editora Gazeta Santa Cruz, Santa Cruz do Sul (2015)
56. Roozen, A.: Availability of sustainable lignocellulosic biomass residues in Brazil for export to the EU, (2015)
57. Ferreira-Leitao, V., Gottschalk, L.M.F., Ferrara, M.A., Nepomuceno, A.L., Molinari, H.B.C., Bon, E.P.S.: Biomass residues in Brazil: Availability and potential uses. *Waste and Biomass Valorization*. 1, 65–76 (2010). doi:10.1007/s12649-010-9008-8
58. Torres, G.A., Renato, L., Tarifa, M.: *Aproveitamento de Resíduos Agrícolas*. (2012)
59. Brum, S.S., Oliveira, L.C. a. De, Bianchi, M.L., Guerreiro, M.C., Oliveira, L.K. De, Carvalho, K.T.G.: Síntese de acetato de celulose a partir da palha de feijão utilizando N-bromossuccinimida (NBS) como catalisador. *Polímeros*. 22, 0–0 (2012). doi:10.1590/S0104-14282012005000061
60. Carvalho, F.C. De: Disponibilidade De Resíduos Agroindustriais E Do Beneficiamento De Produtos Agrícolas. *Informações Econômicas*. 22, 31–46 (1992)
61. CitrusBR: *Brazilian orange juice: en route to sustainability*. (2012)

62. Mello, L.M.R., Silva, G.A.: Disponibilidade e Características de Resíduos Provenientes da Agroindústria de Processamento de Uva do Rio Grande do Sul. Embrapa Comun. Técnico 155. Fevereiro, 1–6 (2014)
63. Mattos, A.L.A., Rosa, M.D.F., Crisóstomo, L.A., Bezerra, F.C., Correia, D.: Beneficiamento da casca de coco verde. Embrapa Agroindústria Trop. Fortaleza. 37 (2011)
64. Fontenele, R.E.S.: Cultura do coco no Brasil: Caracterização do mercado atual e perspectivas futuras. XII Congr. da SOBER. 1–20 (2005)
65. Idoeta, P.A.: Indústria do coco cresce, mas alto desperdício gera desafio tecnológico, [http://www.bbc.com/portuguese/noticias/2014/02/140207\\_coco\\_reciclagem\\_abre\\_pai](http://www.bbc.com/portuguese/noticias/2014/02/140207_coco_reciclagem_abre_pai)
66. Azevêdo, J.A. V., Filho, S.C. V., Pina, D.S., Detmann, E., Valadares, F.R.D., Pereira, L.G.R., Souza, N.K.P., Silva, L.F.C.: Intake, total digestibility, microbial protein production and the nitrogen balance in diets with fruit by-products for ruminants. Rev. Bras. Zootec. 40, 1052–1060 (2011)
67. Pereira, L.G.R., Aragão, A.L.S., Santos, R.D., Azevêdo, J.A.G., Neves, A.L.A., Ferreira, A.L., Chizzotti, M.L.: Com Farelo De Manga. Arq. Bras. Med. Veterinária e Zootec. 65, 675–680 (2013)
68. García Herrera, P., Sánchez-Mata, M.C., Cámara, M.: Nutritional characterization of tomato fiber as a useful ingredient for food industry. Innov. Food Sci. Emerg. Technol. 11, 707–711 (2010). doi:10.1016/j.ifset.2010.07.005
69. Mirabella, N., Castellani, V., Sala, S.: Current options for the valorization of food manufacturing waste: A review. J. Clean. Prod. 65, 28–41 (2014). doi:10.1016/j.jclepro.2013.10.051
70. Kehili, M., Schmidt, L.M., Reynolds, W., Zammel, A., Zetzl, C., Smirnova, I., Allouche, N., Sayadi, S.: Biorefinery cascade processing for creating added value on tomato industrial by-products from Tunisia. Biotechnol. Biofuels. 9, 261 (2016). doi:10.1186/s13068-016-0676-x
71. Nelson, M.L.: Utilization and application of wet potato processing coproducts for finishing cattle. J. Anim. Sci. 88, (2010). doi:10.2527/jas.2009-2502
72. Paganini, C., Nogueira, A., Silva, N.C., Wosiacki, G.: Utilization of apple pomace for ethanol production and food fiber obtainment. Ciência e agrotecnologia. 29, 1231–1238 (2005)
73. Daud, Z., Kassim, A.S.M., Aripin, A.M., Awang, H., Hatta, M.Z.M.: Chemical Composition and Morphological of Cocoa Pod Husks and Cassava Peels for Pulp and Paper Production. Aust. J. Basic Appl. Sci. 7, 406–411 (2013)
74. Araújo, D.J.C., Machado, A. V., Vilarinho, M.C.L.G.: Suitability of agroindustrial residues for cellulose-based materials production. In: Vilarinho, C., Castro, F., and Russo, M. (eds.) Wastes:



solutions, treatments and opportunities. p. 452. CRC Press, Taylor & Francis Group, Boca Raton (2017)

75. Kumar, P., Barrett, D.M., Delwiche, M.J., Stroeve, P.: Methods for pretreatment of lignocellulosic biomass for efficient hydrolysis and biofuel production. *Ind. Eng. Chem. Res.* 48, 3713–3729 (2009)

76. Brandt, A., Gräsvik, J., Hallett, J.P., Welton, T.: Deconstruction of lignocellulosic biomass with ionic liquids. *Green Chem.* 15, 550–583 (2013). doi:10.1039/c2gc36364j

77. Choonut, A., Saejong, M., Sangkharak, K.: The production of ethanol and hydrogen from pineapple peel by *Saccharomyces cerevisiae* and *Enterobacter aerogenes*. *Energy Procedia.* 52, 242–249 (2014). doi:10.1016/j.egypro.2014.07.075

78. Silanikove, N., Levanon, D.: Cotton straw: Composition, variability and effect of anaerobic preservation. *Biomass.* 9, 101–112 (1986). doi:10.1016/0144-4565(86)90114-9

79. R.H.Balasubramanya, Shaikh, A.J.: Utilization of cottonseed by-products. , Coimbatore (2007)

80. Prasad Reddy, J., Rhim, J.W.: Isolation and characterization of cellulose nanocrystals from garlic skin. *Mater. Lett.* 129, 20–23 (2014). doi:10.1016/j.matlet.2014.05.019

81. Wang, B., Li, D.: Strong and optically transparent biocomposites reinforced with cellulose nanofibers isolated from peanut shell. *Compos. Part A Appl. Sci. Manuf.* 79, 1–7 (2015). doi:10.1016/j.compositesa.2015.08.029

82. Kim, J.W., Kim, K.S., Lee, J.S., Park, S.M., Cho, H.Y., Park, J.C., Kim, J.S.: Two-stage pretreatment of rice straw using aqueous ammonia and dilute acid. *Bioresour. Technol.* 102, 8992–8999 (2011). doi:10.1016/j.biortech.2011.06.068

83. Chaker, A., Mutjé, P., Vilar, M.R., Boufi, S.: Agriculture crop residues as a source for the production of nanofibrillated cellulose with low energy demand. *Cellulose.* 21, 4247–4259 (2014). doi:10.1007/s10570-014-0454-5

84. Johar, N., Ahmad, I., Dufresne, A.: Extraction, preparation and characterization of cellulose fibres and nanocrystals from rice husk. *Ind. Crops Prod.* 37, 93–99 (2012). doi:10.1016/j.indcrop.2011.12.016

85. Rowell, R.M., Han, J.S., Rowell, J.S.: Characterization and Factors Effecting Fiber Properties. *Nat. Polym. an Agrofibers Compos.* 115–134 (2000)

86. Önal, E.P., Uzun, B.B., Pütün, A.E.: Steam pyrolysis of an industrial waste for bio-oil production. *Fuel Process. Technol.* 92, 879–885 (2011). doi:10.1016/j.fuproc.2010.12.006

87. Szczerbowski, D., Pitarelo, A.P., Zandoná Filho, A., Ramos, L.P.: Sugarcane biomass for biorefineries: Comparative composition of carbohydrate and non-carbohydrate components of bagasse and straw. *Carbohydr. Polym.* 114, 95–101 (2014). doi:10.1016/j.carbpol.2014.07.052
88. Rhim, J.W., Reddy, J.P., Luo, X.: Isolation of cellulose nanocrystals from onion skin and their utilization for the preparation of agar-based bio-nanocomposites films. *Cellulose.* 22, 407–420 (2015). doi:10.1007/s10570-014-0517-7
89. Sosulski, F.W., Wu, K.K.: High-fiber breads containing field pea hulls, wheat, corn, and wild oat brans. *Cereal Chem.* 65, 186–191 (1988)
90. Kopania, E., Wietecha, J., Ciechańska, D.: Studies on isolation of cellulose fibres from waste plant biomass. *Fibres Text. East. Eur.* 96, 167–172 (2012)
91. Abraham, E., Deepa, B., Pothan, L.A., Jacob, M., Thomas, S., Cvelbar, U., Anandjiwala, R.: Extraction of nanocellulose fibrils from lignocellulosic fibres: A novel approach. *Carbohydr. Polym.* 86, 1468–1475 (2011). doi:10.1016/j.carbpol.2011.06.034
92. Chen, W., Yu, H., Liu, Y., Hai, Y., Zhang, M., Chen, P.: Isolation and characterization of cellulose nanofibers from four plant cellulose fibers using a chemical-ultrasonic process. *Cellulose.* 18, 433–442 (2011). doi:10.1007/s10570-011-9497-z
93. Castaño P., H., Reales A., J.G., Zapata M., J.: Enzymatic hydrolysis of cassava stalk pretreated with the alkaline method. *Agron. Colomb.* 33, 238–243 (2015). doi:10.15446/agron.colomb.v33n2.50115
94. Ma, Z., Pan, G., Xu, H., Huang, Y., Yang, Y.: Cellulosic fibers with high aspect ratio from cornhusks via controlled swelling and alkaline penetration. *Carbohydr. Polym.* 124, 50–56 (2015). doi:10.1016/j.carbpol.2015.02.008
95. Silvério, H.A., Flauzino Neto, W.P., Dantas, N.O., Pasquini, D.: Extraction and characterization of cellulose nanocrystals from corncob for application as reinforcing agent in nanocomposites. *Ind. Crops Prod.* 44, 427–436 (2013). doi:10.1016/j.indcrop.2012.10.014
96. Mohanty, A.K., M., M., Drzal, L.T.: *Natural fibres, biopolymers and biocomposites.* USA: Taylor & Francis Group, Boca Raton (2005)
97. Saha, P., Chowdhury, S., Roy, D., Adhikari, B., Kim, J.K., Thomas, S.: A brief review on the chemical modifications of lignocellulosic fibers for durable engineering composites. *Polym. Bull.* 73, 587–620 (2015). doi:10.1007/s00289-015-1489-y
98. Reddy, N., Yang, Y.: Natural cellulose fibers from soybean straw. *Bioresour. Technol.* 100, 3593–3598 (2009). doi:10.1016/j.biortech.2008.09.063

99. Theerarattananoon, K., Xu, F., Wilson, J., Staggenborg, S., Mckinney, L., Vadlani, P., Pei, Z., Wang, D.: Effects of the pelleting conditions on chemical composition and sugar yield of corn stover, big bluestem, wheat straw, and sorghum stalk pellets. *Bioprocess Biosyst. Eng.* 35, 615–623 (2012). doi:10.1007/s00449-011-0642-8
100. Font, R., Moltó, J., Gálvez, A., Rey, M.D.: Kinetic study of the pyrolysis and combustion of tomato plant. *J. Anal. Appl. Pyrolysis.* 85, 268–275 (2009). doi:10.1016/j.jaap.2008.11.026
101. Chiou, B. Sen, Valenzuela-Medina, D., Bilbao-Sainz, C., Klamczynski, A.K., Avena-Bustillos, R.J., Milczarek, R.R., Du, W.X., Glenn, G.M., Orts, W.J.: Torrefaction of pomaces and nut shells. *Bioresour. Technol.* 177, 58–65 (2015). doi:10.1016/j.biortech.2014.11.071
102. Fu, D., Mazza, G., Tamaki, Y.: Lignin extraction from straw by ionic liquids and enzymatic hydrolysis of the cellulosic residues. *J. Agric. Food Chem.* 58, 2915–2922 (2010). doi:10.1021/jf903616y
103. Vlyssides, A.G., Loizides, M., Karlis, P.K.: Integrated strategic approach for reusing olive oil extraction by-products. *J. Clean. Prod.* 12, 603–611 (2004). doi:10.1016/S0959-6526(03)00078-7
104. Zuluaga, R., Putaux, J.L., Cruz, J., Vélez, J., Mondragon, I., Gañán, P.: Cellulose microfibrils from banana rachis: Effect of alkaline treatments on structural and morphological features. *Carbohydr. Polym.* 76, 51–59 (2009). doi:10.1016/j.carbpol.2008.09.024
105. Preethi, P., Balakrishna, M.G.: Physical and Chemical Properties of Banana Fibre Extracted from Commercial Banana Cultivars Grown in Tamilnadu State. *Agrotechnology.* 01, 10–12 (2013). doi:10.4172/2168-9881.S11-008
106. Murthy, P.S., Madhava Naidu, M.: Sustainable management of coffee industry by-products and value addition - A review. *Resour. Conserv. Recycl.* 66, 45–58 (2012). doi:10.1016/j.resconrec.2012.06.005
107. Rosa, M.F., Medeiros, E.S., Malmonge, J.A., Gregorski, K.S., Wood, D.F., Mattoso, L.H.C., Glenn, G., Orts, W.J., Imam, S.H.: Cellulose nanowhiskers from coconut husk fibers: Effect of preparation conditions on their thermal and morphological behavior. *Carbohydr. Polym.* 81, 83–92 (2010). doi:10.1016/j.carbpol.2010.01.059
108. Marín, F.R., Soler-Rivas, C., Benavente-García, O., Castillo, J., Pérez-Alvarez, J.A.: By-products from different citrus processes as a source of customized functional fibres. *Food Chem.* 100, 736–741 (2007). doi:10.1016/j.foodchem.2005.04.040

109. Dhillon, G.S., Kaur, S., Brar, S.K., Verma, M.: Potential of apple pomace as a solid substrate for fungal cellulase and hemicellulase bioproduction through solid-state fermentation. *Ind. Crops Prod.* 38, 6–13 (2012). doi:10.1016/j.indcrop.2011.12.036
110. Henrique, M.A., Silvério, H.A., Flauzino Neto, W.P., Pasquini, D.: Valorization of an agro-industrial waste, mango seed, by the extraction and characterization of its cellulose nanocrystals. *J. Environ. Manage.* 121, 202–209 (2013). doi:10.1016/j.jenvman.2013.02.054
111. Lani, N.S., Ngadi, N., Johari, A., Jusoh, M.: Isolation, Characterization and Application of a Cellulose-degrading Strain *Neurospora crassa* S1 from Oil Palm Empty Fruit Bunch. *Microb. Cell Fact.* 13, 1–8 (2014). doi:10.1155/2014/702538
112. Aguedo, M., Kohnen, S., Rabetafika, N., Vanden Bossche, S., Sterckx, J., Blecker, C., Beauve, C., Paquot, M.: Composition of by-products from cooked fruit processing and potential use in food products. *J. Food Compos. Anal.* 27, 61–69 (2012). doi:10.1016/j.jfca.2012.04.005
113. Rahman, M.M., Khan, M.A.: Surface treatment of coir (*Cocos nucifera*) fibers and its influence on the fibers' physico-mechanical properties. *Compos. Sci. Technol.* 67, 2369–2376 (2007). doi:10.1016/j.compscitech.2007.01.009
114. Rodrigues, B.V.M., Ramires, E.C., Santos, R.P.O., Frollini, E.: Ultrathin and nanofibers via room temperature electrospinning from trifluoroacetic acid solutions of untreated lignocellulosic sisal fiber or sisal pulp. *J. Appl. Polym. Sci.* 132, 1–8 (2015). doi:10.1002/app.41826
115. OCDE/FAO: Brazilian agriculture: prospects and challenges. (2015)
116. Sánchez, C.: Lignocellulosic residues: Biodegradation and bioconversion by fungi. *Biotechnol. Adv.* 27, 185–194 (2009). doi:10.1016/j.biotechadv.2008.11.001
117. Abdulkhani, A., Hojati Marvast, E., Ashori, A., Karimi, A.N.: Effects of dissolution of some lignocellulosic materials with ionic liquids as green solvents on mechanical and physical properties of composite films. *Carbohydr. Polym.* 95, 57–63 (2013). doi:10.1016/j.carbpol.2013.02.040
118. Flauzino Neto, W.P., Silvério, H.A., Dantas, N.O., Pasquini, D.: Extraction and characterization of cellulose nanocrystals from agro-industrial residue - Soy hulls. *Ind. Crops Prod.* 42, 480–488 (2013). doi:10.1016/j.indcrop.2012.06.041
119. Rahbar Shamskar, K., Heidari, H., Rashidi, A.: Preparation and evaluation of nanocrystalline cellulose aerogels from raw cotton and cotton stalk. *Ind. Crops Prod.* 93, 203–211 (2016). doi:10.1016/j.indcrop.2016.01.044

120. Wulandari, W.T., Rochliadi, A., Arcana, I.M.: Nanocellulose prepared by acid hydrolysis of isolated cellulose from sugarcane bagasse. *IOP Conf. Ser. Mater. Sci. Eng.* 107, 12045 (2016). doi:10.1088/1757-899X/107/1/012045
121. Zianor Azrina, Z.A., Beg, M.D.H., Rosli, M.Y., Ramli, R., Junadi, N., Alam, A.K.M.M.: Spherical nanocrystalline cellulose (NCC) from oil palm empty fruit bunch pulp via ultrasound assisted hydrolysis. *Carbohydr. Polym.* 162, 115–120 (2017). doi:10.1016/j.carbpol.2017.01.035
122. Ditzel, F.I., Prestes, E., Carvalho, B.M., Demiate, I.M., Pinheiro, L.A.: Nanocrystalline cellulose extracted from pine wood and corncob. *Carbohydr. Polym.* 157, 1577–1585 (2017). doi:10.1016/j.carbpol.2016.11.036
123. Barbash, V.A., Yaschenko, O. V., Shniruk, O.M.: Preparation and Properties of Nanocellulose from Organosolv Straw Pulp. *Nanoscale Res. Lett.* 12, 241 (2017). doi:10.1186/s11671-017-2001-4
124. Brinchi, L., Cotana, F., Fortunati, E., Kenny, J.M.: Production of nanocrystalline cellulose from lignocellulosic biomass: Technology and applications. *Carbohydr. Polym.* 94, 154–169 (2013). doi:10.1016/j.carbpol.2013.01.033
125. Dufresne, A.: Nanocellulose: A new ageless bionanomaterial. *Mater. Today.* 16, 220–227 (2013). doi:10.1016/j.mattod.2013.06.004
126. Julkapli, N.M., Bagheri, S.: Progress on nanocrystalline cellulose biocomposites. *React. Funct. Polym.* 112, 9–21 (2017). doi:10.1016/j.reactfunctpolym.2016.12.013
127. Asgher, M., Ahmad, Z., Iqbal, H.M.N.: Bacterial cellulose-assisted de-lignified wheat straw-PVA based bio-composites with novel characteristics. *Carbohydr. Polym.* 161, 244–252 (2017). doi:10.1016/j.carbpol.2017.01.032
128. Yan, L., Kasal, B., Huang, L.: A review of recent research on the use of cellulosic fibres, their fibre fabric reinforced cementitious, geo-polymer and polymer composites in civil engineering. *Compos. Part B Eng.* 92, 94–132 (2016). doi:10.1016/j.compositesb.2016.02.002
129. Gurunathan, T., Mohanty, S., Nayak, S.K.: A review of the recent developments in biocomposites based on natural fibres and their application perspectives. *Compos. Part A Appl. Sci. Manuf.* 77, 1–25 (2015). doi:10.1016/j.compositesa.2015.06.007
130. Kumar, R., Sharma, R.K., Singh, A.P.: Cellulose based grafted biosorbents - Journey from lignocellulose biomass to toxic metal ions sorption applications - A review. *J. Mol. Liq.* 232, 62–93 (2017). doi:10.1016/j.molliq.2017.02.050

131. Hokkanen, S., Bhatnagar, A., Sillanpää, M.: A review on modification methods to cellulose-based adsorbents to improve adsorption capacity. *Water Res.* 91, 156–173 (2016). doi:10.1016/j.watres.2016.01.008
132. Sazali, N., Salleh, W.N.W., Ismail, A.F.: Carbon tubular membranes from nanocrystalline cellulose blended with P84 co-polyimide for H<sub>2</sub> and He separation. *Int. J. Hydrogen Energy.* 42, 9952–9957 (2017). doi:10.1016/j.ijhydene.2017.01.128
133. Harmsen, P.F., Hackmann, M.M., Bos, H.L.: Green building blocks for bio-based plastics. *Biofuels, Bioprod. Biorefining.* 8, 306–324 (2014). doi:10.1002/bbb
134. Özdenkçi, K., De Blasio, C., Muddassar, H.R., Melin, K., Oinas, P., Koskinen, J., Sarwar, G., Järvinen, M.: A novel biorefinery integration concept for lignocellulosic biomass. *Energy Convers. Manag.* (2017). doi:10.1016/j.enconman.2017.04.034

Chapter 4. Effect of combined dilute-alkaline and green pretreatments on corncob fractionation: pretreated biomass characterization and regenerated cellulose film production

*Published in Industrial Crops and Products, 2019, 141, 111785*

---

**David Jefferson Cardoso Araújo<sup>1</sup>, Maria Cândida Lobo Guerra Vilarinho<sup>2</sup>,  
Ana Vera Machado<sup>3</sup>**

<sup>1</sup>Institute for Polymers and Composites/I3N and Centre for Waste Valorization, University of Minho, Guimarães, Portugal.

<sup>2</sup>Mechanical Engineering and Resources Sustainability Centre, University of Minho, Guimarães, Portugal.

<sup>3</sup>Institute for Polymers and Composites/i3N, University of Minho, Guimarães, Portugal.

\*Corresponding author: David Jefferson Cardoso Araújo (david\_bct@hotmail.com)

## Abstract

Pretreatment is an essential step prior to the effective valorization of lignocellulosic biomass. However, depending on the pretreatment method, it can be costly and originate potential environmental threats. In this study, green pretreatments, namely Liquid Hot Water and 1-butyl-3-methylimidazolium chloride, as well as low concentrated sodium hydroxide solution, were applied individually and in combination to pretreat corncob, and their effects on physicochemical properties of fibers were analyzed. The pretreated samples were dissolved in ionic liquid and attempts to prepare regenerated cellulose films have been made. While NaOH was efficient to removal lignin, LHW presented higher solubilization hemicellulose. By combining these treatments, the biomass was fractionated in a complementary way, and a solid enrich-cellulose fraction with high thermal stability and crystallinity was obtained. The BmimCl did not significantly change the chemical composition of biomass and, independent of the treatment applied in combination, samples were regenerated as amorphous cellulose coexisting with lesser amount of cellulose crystalline I. This structural conversion was also confirmed through thermogravimetric analysis, from which a decrease in thermal stability was verified. This latter property was markedly affected by the presence of hemicellulose remained after some pretreatments. The obtained results indicate that each pretreatment performed can meet different application requirements. The LHW-NaOH pretreated sample was the only one suitable to produce regenerated films, which exhibited good mechanical properties to be used in value-added applications, such as packaging.

**Keywords:** lignocellulosic biomass; green pretreatments; regenerated film; cellulose; crystallinity; thermal stability.

## 4.1. Introduction

The depletion of fossil resources, as well as the social and environmental impacts associated with its extraction and production chain, have fostered, in recent years, the search for unconventional and renewable substitute raw materials. Among the available sources, lignocellulosic biomass has been extensively studied and has shown potential to be applied as a starting substrate to produce value-added materials, such as biofuels and biopolymers [1–4]. Its abundant availability and accessibility make the LCB a source of easy acquisition and low cost, but still underexploited [5]. For instance, Corncob is an agroindustrial residue widely generated and



little valued. To date, corncobs are used on a limited basis for bedding, animal feed, oil sorbent and polishing agent [5, 6]. In Brazil it is estimated an average generation of more than 18000 kilotons per year, of which 2990 kilotons would be available [5].

LCB is essentially composed of natural biopolymers (cellulose, hemicellulose and lignin) and its main sources include agroindustrial residues, forest residues and municipal and industrial waste [7]. The main drawback regarding the valorization of LCB deals with the presence of covalent crosslinks between cellulose and hemicellulose with lignin in the cell wall of plants, which leads to its recalcitrant property. Hence, in order to disrupt this complex structural arrangement, pretreatments are usually performed prior to its effective use and valorization.

The application of pretreatment techniques basically promotes the disruption and fractionation of LCB components, which opens the material structure and facilitates the performance of subsequent processes [8, 9]. When it turns to added value cellulose-based biopolymeric materials production, the application of pretreatments aiming the selective delignification of biomass to obtain a solid cellulose enriched fraction is of crucial importance. Otherwise, the presence of substantial amounts of non-cellulosic materials on fibers may negatively influence their structure and properties [10–12].

Basically, the pretreatments methods can be classified into four categories, namely physical, chemical, physicochemical and biological. Some of the existing and applicable methods make use of harsh chemicals and severe treatment conditions [13]. However, as the use of cellulose extracted from renewable raw materials is mainly motivated by its environmentally-friendly concept, it does not make sense to adopt non-sustainable processing techniques. Therefore, more recent studies within this scope have been aimed at optimizing the so-called green pretreatment technologies in order to develop less costly and environmentally harmful processes [13–16]. In addition, since the performance and efficiency of each pretreatment varies widely according to its reaction mechanisms and the chemical and structural characteristic of biomass, the optimization of a single pretreatment is not always the universal choice for a specific purpose [13, 17]. Thus, to overcome possible drawbacks associated with single operations, such as technological problems, high-energy consumption and long reaction times, combined processes have been extensively applied. Generally, their application can significantly improve the synergistic aspects involved in the treatment of biomass, which can lead, for example, to better performance of delignification [16, 17].

Liquid hot water and room temperatures ionic liquids in response to their fractionation efficiency and eco-friendly aspect, are among the main green pretreatment methods applied to fractionate biomass. Regarding the conventional techniques, NaOH pretreatment is the most widely chemical pretreatment used, mainly because of its simplified application and excellent delignification capacity. NaOH solutions essentially cause the cleavage of intermolecular  $\alpha$ - and  $\beta$ -aryl ether linkages between hemicellulose and lignin, leading to a swelling of the biomass pores, disruption of the lignin structure and an increase of available surface area [17–20]. This alkaline treatment is one of the preferred pretreatment technologies since it is carried out under mild conditions, does not present physical hazard (explosive, combustible and oxidizing), does not have sufficient volatility to constitute an inhalation danger, besides being non-carcinogenic, non-persistent and non-bioaccumulative [21–23]. In addition, the direct contact with NaOH solutions should be prevented only for concentrations higher than 2% (in water), due to its corrosive effects [24]. The main downsides related to this pretreatment deals with the processing time and the black liquor generated. These problems can be partially mitigated by using the NaOH technique in combination with other treatments, which ultimately demands low concentrated solutions and reduced processing times [25]. Notwithstanding, it is worth to emphasize that the black liquor has yet to be treated even after dilute-alkaline treatment, and its economically and environmentally feasibility must be taken into account when planning large scale plants.

Liquid Hot Water is a physicochemical or hydrothermal method that uses only water at reasonably milder conditions compared to other pretreatments. During the process, water penetrates into the biomass structure and substantially hydrolyze hemicelluloses (up to 80%) and partially removes lignin [13, 18, 26–28]. The chemical effect in the LHW occurs as an autohydrolysis process since the organic acids released from polysaccharides auto-catalyze the hydrolysis of hemicellulose and lignin. The main advantages of this method comprise low environmental impact, low cost and the no need of chemicals or catalysts. Ionic Liquids are salts with low melting point ( $< 100$  °C) composed by organic cations and organic or inorganic anions. The application of ionic liquids in chemical reactions is considered a green method due to its characteristics, namely thermal stability, inflammability, low volatility and recyclability [29–31]. Ionic liquids constituted by imidazolium cations, such as 1-allyl-3-methylimidazolium and 1-butyl-3-methylimidazolium chloride, are the most applied to biomass fractionation and cellulose dissolution [31]. In this process, firstly the ionic liquid anions are able to form hydrogen bonds with hydroxyl groups of biomass, leading to its structural disruption and dissolution. Subsequently, the

cellulose fraction can be recovered as a regenerated product by addition of organic solvents. The successful dissolution of lignocellulosic biomass in BmimCl was demonstrated by Fort et al. [32], Kilpeläinen et al. [33] and Pang et al. [34].

Within the scope of cellulose-based materials produced from LCB, regenerated cellulose films synthesized from green and non-derivatizing solvents (such as ionic liquids) have drawn increasing attention as they possess excellent physical and chemical properties, and also because the dissolution and regeneration techniques are simple, sustainable, versatile and easy for industrialization [35]. Regenerated films prepared from others LCB through dissolution in IL have shown remarkable mechanical properties, besides transparency and non-toxicity, which gives them great potential applications [36–39]. However, the production of regenerated cellulose films requires cellulose-enriched samples with a very small percentage of other constituents (such as lignin and hemicellulose). In order to achieve this, standard methods of pulping and bleaching as pretreatments are still commonly used, which goes against the environmental sustainability imputed by the resources and techniques (dissolution and regeneration) applied.

The aim of this work is to investigate the effect of combined pretreatments, including green and dilute-alkaline techniques, on physicochemical properties of corncob fibers and prepare regenerated cellulose films from pretreated samples using BmimCl as a solvent. Combined pretreatments including chemical and physicochemical methods, namely dilute sodium hydroxide, Liquid Hot Water and Ionic Liquid, were selected based on their complementary characteristics, and to the best of our knowledge, some combinations set in this paper have not yet been addressed for the treatment of corncob, namely LHW-dilute NaOH and LHW-BmimCl. In literature, studies performed in the scope of corncob fractionation by applying combined pretreatments can be found, whilst not exhaustive [40–45]. It should be emphasized that the combined treatments proposed are designed as two and three-stage pretreatments. Besides being scalable and non-conflicting, this arrangement may avoid drawbacks such as the generation of sugar degradation by-products in certain combinations, as verified by Imman et al. [45] and Yang et al. [47] when NaOH was used as a catalyst in LHW treatment. The characterization of the physicochemical changes on pretreated samples and regenerated films was accomplished by compositional, morphological, X-Ray diffraction and Fourier transform infrared spectroscopy analysis, as well as by thermal characterization. Dynamic mechanical analysis of the regenerated cellulose films was also performed.

## 4.2. Materials and methods

### 4.2.1. Materials

Corncob was obtained from local agricultural cooperatives from the North of Portugal. The corncob residue was firstly ground and sieved to particles sizes from 0.25 to 0.5 mm and stored in sealed plastic bags at room temperature. Cellulose sheets (cellulose pulp), provided by a local factory, were torn into small fragments and dried at 60 °C for 24 h. Ionic liquid 1-butyl-3-methylimidazolium chloride was purchased from Sigma-Aldrich (98%), Germany, and used as received. Sodium hydroxide (pellets) was acquired from Fisher Chemicals.

### 4.2.2. Liquid Hot Water treatment

Pretreatment was performed in a stainless steel cylindrical reactor (10 cm internal diameter and 24 cm internal height) with an approximate volume of 2 L. Feedstock loading rate of 10% (residue weight / distilled water volume) was pretreated at 190 °C, 0.79 MPa, for 30 min (after the heat-up time) under constant mechanical stirring. After the reactor was cooled by means of a coupled cooling system. The insoluble solid was collected, thoroughly washed with deionized water and dried at 60 °C for further treatments and analysis (this sample was named as LWH-CC). The choice of the experimental conditions was based on the calculation of the severity factor ( $\log(R_0)$ ), which can be used as an indicator of the effects of destruction, disaggregation and depolymerization of biomass. The severity factor was calculated according to Equation (1)[27], that associate the residence time (t, min), the holding temperature (T, °C) and an empirical parameter (14.75) related to activation energy and temperature.

$$\log(R_0) = \log \left[ \exp \left( \frac{T-100}{14.75} \right) t \right] \quad (1)$$

### 4.2.3. Alkali treatment of corncob

Dried corncob and liquid hot water treated corncob (LHW - CC) were soaked in NaOH with 2 wt.% concentration at 90 °C for 1.5 h at a 1/30 solid/liquid ratio (w/w) under magnetic stirring. The alkali treated corncob (NaOH-CC) and LHW-CC (NaOH-LHW-CC) were then filtered and washed several times with deionized water until colorless. The resulting material was dried at 60 °C for further treatments and characterization.

#### 4.2.4. Ionic liquid treatment and regeneration of treated biomass

Prior to biomass dissolution, BmimCl was poured into a 100 mL beaker and thoroughly stirred at 100 °C for 20 min in order to evaporate any residual moiety. After that, raw corncob, LHW-CC, NaOH-CC, NaOH-LHW-CC and cellulose pulp (CP) samples were dispersed, individually, in the ionic liquid at a 4% solid/liquid (w/w) ratio and treated at about 130 °C under magnetic stirring for 5 h, 2 h, 1.5 h, 1.5 h and 0.5 h, respectively. The previously pretreated samples were kept under treatment in the ionic liquid until complete dissolution and a homogeneous solution was obtained. Particularly to the raw corncob residue, the treatment was undertaken under different dissolution times, ranging from 1 to 5 hours, in order to verify the optimal treatment condition. However, even after 5 hours of treatment the raw corncob did not dissolve completely.

After the treatment, the temperature was set to about 60 °C and a mixture of acetone and ethanol, composed as a molar ratio X (acetone): Y (ethanol): Z (ionic liquid) with X = 3.5, Y = 1 and Z = 1, was added into the solution containing IL and biomass and stirred vigorously to precipitate the regenerated cellulosic biomass. The solid material precipitated was separated by vacuum filtration, washed 3 – 4 times with distilled water to remove residual ionic liquid and dried in an oven at 60 °C for further treatments and analysis. The resulting BmimCl treated samples are referred to as IL-CC, IL-LHW-CC, IL-NaOH-CC and IL-NaOH-LHW-CC. A schematic arrangement of pretreatments performed is presented in Figure 4.1.

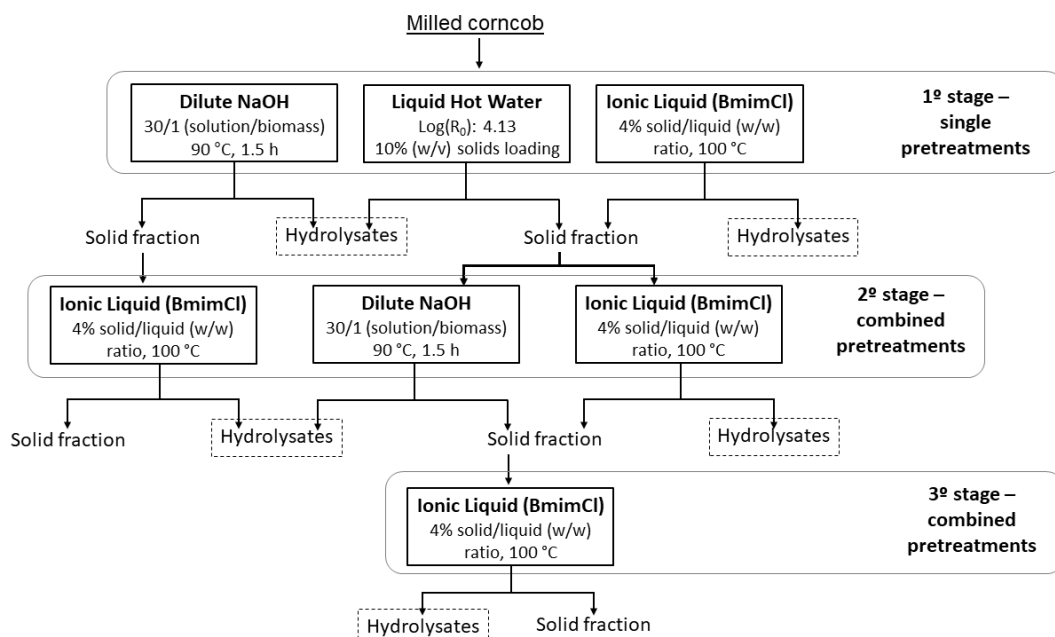


Figure 4-1. Schematic representation of pretreatments performed.

## 4.2.5. Characterization of untreated and treated corncob

### 4.2.5.1 Thermogravimetric analysis and Differential scanning calorimetry (DSC)

Thermogravimetry analyses and DSC of untreated and treated corncob were performed simultaneously on TA Instruments SDT 2960 model. The sample weight was in the range of 3-5 mg and heated from 30 to 700 °C at a rate of 10°C/min, under purified argon to prevent thermo-oxidative degradation.

### 4.2.5.2 Chemical composition of untreated and treated biomass

The chemical composition of all samples was determined by deconvolution of the derivative curves obtained from the thermogravimetry analysis [48–51]. The decomposition processes of the three pseudo-components presented in the lignocellulosic biomass (cellulose, hemicellulose and lignin) were modeled by a Gaussian distribution. For this, a multi-peaks method was used to determine the Gaussian distribution model using the Levenberg–Marquardt algorithm (the modeled equation, as well as graphs and parameters are available in the Appendix A). The percentage of each component was assumed to correspond to the integrated area above each single deconvoluted reaction curve.

### 4.2.5.3. Fourier transform infrared spectroscopy (FTIR)

FTIR spectra of cellulose, as well as treated and untreated biomass samples, were recorded on a Jasco FT/IR-4100 spectrometer. The ground and dried samples were pelletized with KBr and the spectra were obtained in the wavelength range 400 – 4000 cm<sup>-1</sup> at a resolution of 4 cm<sup>-1</sup>.

### 4.2.5.4. X-Ray Diffraction (XRD) analysis

The X-ray diffractograms patterns of all samples were obtained at room temperature using a diffractometer Bruker D8 Discover, operated with Cu-K $\alpha$  radiation (wavelength of 0.154 nm) at a power of 40 mA and accelerating voltage of 40 kV. Diffraction intensities were scanned in the range of  $2\theta = 5 - 50^\circ$  with a scanning rate of 0.05°/second. The crystallinity index (CrI) of samples was determined by the Segal method [52] according to the following Equation (2).

$$\text{CrI} = \left( \frac{I_{002} - I_{AM}}{I_{002}} \right) \times 100 \quad (2)$$

CrI express the relative degree of crystallinity,  $I_{002}$  is the maximum intensity of the 002 lattice diffraction, found between the scattering angles of  $2\theta = 22^\circ$  and  $23^\circ$ , and  $I_{AM}$  is the minimum intensity, positioned between the 002 and 101 diffraction peaks (typically between  $2\theta = 18^\circ$  and  $19^\circ$ ). It is assumed that the  $I_{AM}$  have little crystalline contribution, comprising only the amorphous contribution, while the  $I_{002}$  represents both crystalline and amorphous regions.

#### 4.2.5.5. Morphological analysis

The surface morphologies of untreated and treated samples were examined by scanning electron microscopy (SEM) using a FEI Nova 200. Samples were previously sputter coated with gold.

#### 4.2.6. Preparation of regenerated cellulose film

To produce the cellulose films, a 4% (wt.) solution was prepared by dissolving 0.2 g of the extracted cellulose in 5 g of BmimCl under magnetic stirring at  $120^\circ\text{C}$  for 1.5 h. After completely dissolved, the regenerated film was made by solution casting on a glass plate using an alloy spreader, followed by soaking in 70 ml of deionized water. After 1h the deionized water was replaced and left for another hour. Then, the regenerated cellulose film was dried at room temperature for 24 h in vacuum desiccator.

#### 4.2.7. Dynamic mechanical analysis

Dynamic mechanical analysis was performed on a PerkinElmer DMA 800 using a dual-cantilever bending mode in order to obtain the storage modulus ( $E'$ ), the loss modulus ( $E''$ ) and the damping capacity ( $\tan \delta$ ), the latter calculated as the ratio of the loss to the storage modulus. Regenerated films with  $20/4/0.015$  mm of dimensions, approximately, were analyzed under temperature ranging from  $40 - 250^\circ\text{C}$ , heating rate of  $5^\circ\text{C}/\text{min}$ , preload 1N,  $10\ \mu\text{m}$  of displacement amplitude and 1 Hz of frequency. Dynamic Young's modulus ( $E^*$ ) was also determined by using equation 3 [53].

$$E^* = \sqrt{(E')^2 + (E'')^2} \quad (3)$$

## 4.3. Results and discussion

### 4.3.1. Compositional analysis

The chemical composition of untreated and treated corncob is presented in Table 4.1, and images of all samples are presented in Figure 4.2. Depending on the treatment type, considerable physical changes, namely color and texture, are noticeable. These changes are mainly due to the removal or not of color-conferring constituents (such as lignin), chemical transformations or changes in crystalline structure.

The corncob showed a content of cellulose, hemicellulose and lignin similar to previous studies [6, 54]. It is important to remark that corncob presents also other constituents, such as ash (generally present in percentages around  $2.88\% \pm 0.11$ ) and extractives (generally present in percentages around 2.1%) [55–57], which are not accounted in Table 4.1 because the compositional analysis method applied does not have enough sensitivity to estimate them.

The dissolution (and subsequent regeneration) of corncob in IL did not change significantly its final composition. As it can be seen, the treatment with ionic liquid was only able to remove a small fraction of hemicellulose. However, the physical appearance of the corncob after this treatment changed and seemed to be smoothed, probably due to a structural transformation of cellulose. As expected, the treatment with LHW effectively solubilized hemicellulose (around 90% of the original content), leading to a final product rich in cellulose and lignin. Other authors have also reported 80-100% of hemicellulose hydrolysis after LHW treatment of lignocellulosic biomass [27, 28, 58–60]. This result also indicates that LHW treatment is not effective in lignin removal, which is in agreement with other published works [27, 61]. It's worth mentioning that, under the treatment conditions chosen, the severity (severity factor,  $\log R_0$ ) of the reaction ( $\log R_0 = 4.13$ ) results in high levels of hemicellulose solubilization, as well as low cellulose depolymerization [27, 28, 62, 63]. Under this treatment condition, the generation of hydronium ions by ionization of water is known to increase, leading to an effective dissolution of primary products related to hemicellulose constitution (e.g. xylan and acetyl groups) and their subsequent decomposition into oligomers and organic acids, such as acetic acid. This latter auto-catalyze the polysaccharides breakdown into soluble fractions and results in higher hydrolysis efficiency [27, 63]. As a result of the LHW treatment, substantial morphological changes have been taken on biomass (as will be also shown in section 4.3.4 Scanning electron microscopy), which are usually associated with an increase in available surface area and porosity [61, 63, 64]. In contrast, the alkali treatment removed mainly the lignin fraction. A lignin content reduction by 50% resulted in a mass loss at around half of the



original weight of the untreated corncob on a dry basis. Moreover, by removing lignin, the alkali treatment partially disrupts the linkages between the lignin and hemicellulose, and consequently solubilizes hemicellulose (its reduction can be noticed in Table 4.1).

Regarding the combined pretreatments, even after the prior changes and weakening of corncob structure reached through the LHW treatment, the subsequent dissolution in BmimCl only removed a small amount of the remaining lignin. Conversely, the regenerated product presents a smooth and homogenized morphology, as well as a film-like aspect (Figure 4.2), which proves that, by removing hemicellulose, the LHW treatment increased the accessibility of cellulose and favored its dissolution in BmimCl. Minor effects on chemical composition have also been noticed by combining NaOH and IL treatments (Table 4.1). In line with other studies, these results demonstrate the low capacity of the BmimCl in fractionating the biomass [65, 66]. On the opposite, remarkable changes were verified by combining LHW with alkali treatment. This can be explained by the solubilization of most hemicellulose during the LHW treatment, the disruption of the lignin-hemicellulose complexes and a decrease in  $\beta$ -O-4 linkages of lignin (the most abundant substructure in this component) also took place, which makes the lignin more accessible [61, 64]. Consequently, the cleavage of ester, ether and carbon-to-carbon bonds between lignin-cellulose, lignin components (e.g. syringyl and guaiacyl monolignols) and the remaining lignin-hemicellulose complexes was easier during the alkaline treatment, leading to the breaking of lignin into small molecules and their dissolution. The broken of lignin structure and its decoupling with carbohydrates are confirmed and easily identified by FTIR analysis (Figure 4.3). Their complementary and selective effects of LHW and NaOH treatments on fractionating the biomass contributed positively to obtain a solid cellulose-enriched final product (84.73%), with reasonably low amounts of hemicellulose (reduced by 90%) and lignin (reduced by 34.5%). This result is comparable to the ones archived by established laboratory methods for delignification in which, besides alkaline, acidic and oxidative reagents are used. Little improvements have been made to the fractionation process by combining LHW, NaOH and IL treatments. However, the dried regenerated material was semitransparent and had a plastic film-like appearance (Figure 4.2g), completely different from the starting material (Figure 4.2f). This physical characteristic suggests a decrease in the CrI of the sample in response to an amorphous conversion, as it will be, indeed, confirmed and explored in detail in the following analysis.

Table 4.1. Chemical composition of untreated and pretreated corncob.

Sample	Content (%)			Mass recovery (%)
	Cellulose	Hemicellulose	Lignin	
Corn cob	36.35	47.32	16.32	-
IL-CC	39.28	43.70	17.02	90
LHW-CC	78.34	3.95	17.70	59.5
NaOH-CC	64.12	27.88	8.0	46
LHW-IL-CC	80.96	4.02	15.01	56.52
NaOH-IL-CC	67.19	25	7.81	43.2
LHW-NaOH-CC	84.73	4.58	10.68	37.68
LHW-NaOH-IL-CC	86.10	3.53	10.35	36.7



Figure 4-2. Photographs of (a) corncob, (b) ground corncob, (c) ionic liquid treated corncob, (d) LHW treated corncob, (e) NaOH treated corncob, (f) LHW-NaOH treated corncob, (g) LHW-NaOH-IL treated corncob, (h) NaOH-IL treated corncob and (i) LHW-IL treated corncob.


### 4.3.2. Fourier-transformed Infrared spectroscopy

FTIR spectra of untreated and treated corncob are shown in Figure 4.3. The broad band observed at 3000-3700  $\text{cm}^{-1}$  is assigned to different OH stretching of cellulose and hemicellulose [67, 68]. The peak absorption at 1640  $\text{cm}^{-1}$ , typical of absorbed water in biomass, was also verified in all samples analyzed [69]. From Figure 4.3, well defined common bands typical of functional groups in cellulose were identified at 3000-3700  $\text{cm}^{-1}$  (O-H stretching), 2919  $\text{cm}^{-1}$  (C-H stretching vibration), 1420  $\text{cm}^{-1}$  ( $\text{CH}_2$  banding vibration), 1374  $\text{cm}^{-1}$  (C-H asymmetric deformation), 1318  $\text{cm}^{-1}$  ( $\text{CH}_2$  wagging), 1164  $\text{cm}^{-1}$  (asymmetric C-O-C stretching), 1114  $\text{cm}^{-1}$  (C-OH skeletal vibration), 1059  $\text{cm}^{-1}$  (C-O-C pyranose ring skeletal vibration) and 897  $\text{cm}^{-1}$  (C-H deformation vibration, characteristic of the  $\beta$ -glycosidic linkages between glucose monomers) [37, 67, 69–71]. As it can be seen in Figure 4.3a and 4.3b, all typical bands of cellulose can be easily identified in the spectrum after NaOH and LHW-NaOH treatments. Besides, notable bands at around 1730 (acetyl group in hemicellulose), 1250  $\text{cm}^{-1}$  (C-O stretching in the aryl-ether group of lignin and acetyl groups in

hemicellulose), 1598 and 1513 (in response to aromatic ring stretch ascribed to lignin), are notice mainly in the raw corncob spectrum (Figure 4.3a), which were attributed to the presence of hemicellulose and lignin [37, 67]. The intensity of these bands has become significantly reduced after LHW-NaOH and NaOH treated corncob, which evidences their better capacity to partially fractionate and remove non-cellulosic components of corncob.

Less noticeable chemical changes were observed on the spectra after other treatments, such as LHW and IL (Figure 4.3a), mainly due to the high content of lignin remaining in the biomass after treated. However, the appearance of peaks at 1420 and 1114  $\text{cm}^{-1}$  (in the LHW treated sample) and the more pronounced peak at 1059  $\text{cm}^{-1}$  in both treatments, compared to those in raw corncob, suggest a higher cellulose content. Table 4.2 shows the main absorption bands and the respective group of cellulose, as well as treated and untreated biomass samples.

Table 4.2. FTIR absorbance bands and the respective functional groups in cellulose pulp, untreated and treated corncob.

Wavenumber ( $\text{cm}^{-1}$ )	Chemical group	assignment	Reference
3000-3700	O-H	O-H stretching of cellulose and hemicellulose	[67, 68]
2919	C-H	C-H stretching in cellulose-rich material	[70]
1730	C=O	C=O stretching of acetyl group in Hemicellulose and aldehyde in lignin	[37, 67]
1640	O-H	O-H bending vibration of absorbed water molecules	[37, 72]
1598 and 1513		Aromatic ring (Ar) stretch ascribed to lignin	[70, 73]
1420	$\text{CH}_2$	$\text{CH}_2$ banding vibration in cellulose	[37]
1374	C-H	C-H asymmetric deformation in cellulose	[37]
1318	$\text{CH}_2$	$\text{CH}_2$ Wagging in cellulose	[37]
1250	C-O	C-O stretching in the aryl group of lignin and acetyl groups of hemicellulose	[74]
1164	C-O-C	Asymmetric C-O-C stretching ascribed to cellulose	[69, 71]
1114	C-OH	C-OH skeletal vibration in cellulose	[71]
1059	C-O-C	C-O-C pyranose ring skeletal vibration ascribed to cellulose	[71, 72]
897	C-H	C-H deformation of cellulose	[69–71]

FTIR spectra can also be applied to investigate changes in cellulose crystalline structure. In the cell wall of plants, cellulose mainly contains cellulose crystalline I, but, depending on the type of processing and treatment to which it is submitted, this primary structure can be transformed into other allomorphic forms, such as amorphous cellulose and cellulose crystalline II [37, 75–77]. Variations in the absorption bands around 1425, 1370, 1157, 1108 and 898  $\text{cm}^{-1}$ , typical of cellulose I, can be used as an indication of crystalline structural transformations [37, 68, 69]. From the cellulose pulp spectrum in Figure 4.3, it is possible to assume that characteristic bands at 1420, 1114 and 897  $\text{cm}^{-1}$  correspond to cellulose crystalline I. Among the treatments performed, those involving the dissolution of cellulosic biomass with ionic liquid significantly decreased the intensity of bands at 1420 and 1114  $\text{cm}^{-1}$ , while the absorption intensity band at 897  $\text{cm}^{-1}$  increased after LHW-IL treatment and kept unchanged after NaOH-IL and LHW-NaOH-IL treatments. Moreover, from ionic liquid combined treatments spectrum, it is visible that the peaks assigned to O-H stretching vibrations (3000-3700  $\text{cm}^{-1}$ ) became sharper, probably due to the scission of intra- and intermolecular hydrogen bonds [78]. The FTIR spectra of BmimCl treated samples seems to be typical of amorphous cellulose, although they also resemble cellulose crystalline II [37, 78]. These crystalline structural changes will be clearly elucidated with the XRD analysis, which will confirm that the combined IL treatments result mainly in amorphous cellulose.

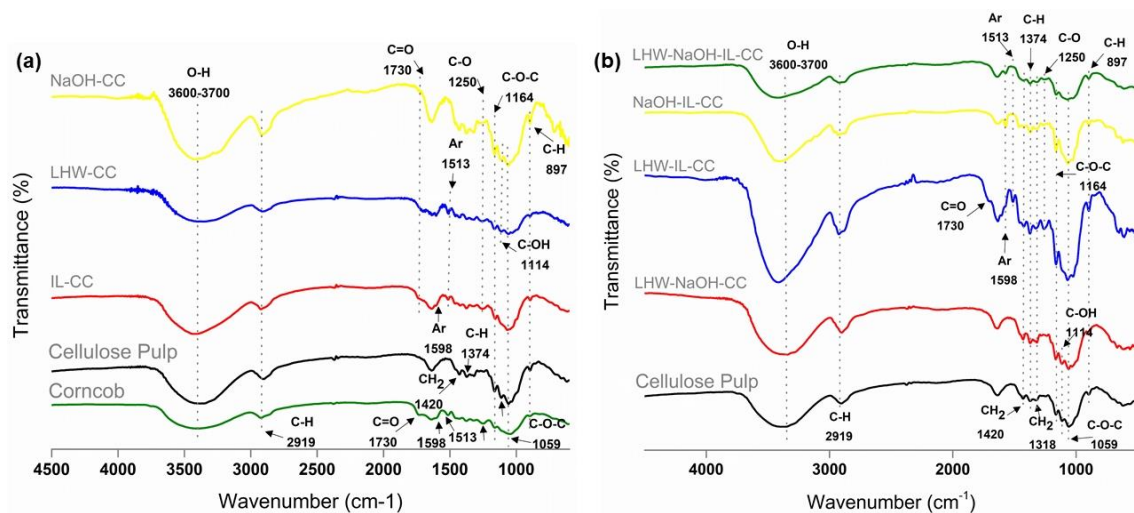


Figure 4-3. FTIR spectra of (a) cellulose pulp, corncob and single pretreatments and (b) combined pretreatments. Abbreviation Ar in graphs means aromatic ring.

### 4.4.3. X-ray Diffraction Analysis

X-ray diffractograms of cellulose pulp, corncob and all treated samples are shown in Figure 4.4. Diffractograms of cellulose pulp and samples treated with LHW, NaOH and LHW-NaOH present three major peaks, typical of cellulose crystalline I. The main peak position varies with sample analyzed from  $2\theta = 22.2^\circ$  to  $2\theta = 22.6^\circ$ . This peak is indicative of the distance between hydrogen-bonded sheets in cellulose crystalline I. The second peak, viewed as a wide peak at lower  $2\theta$  values, is known to be correlated to allomorphs of cellulose crystalline I, and varies from  $15.5^\circ$  to  $16^\circ$ . The third is depicted as a small peak at  $34.7^\circ$  and arises from ordering along the fiber direction [78–82]. The CrI of samples was determined by the Segal method [52] as specified in section 4.2.5.4 of the materials and methods. This method provides a faster and useful measurement for comparing the relative differences of CrI among samples. In the literature several different techniques are reported to measure CrI, and depending on the chosen method the CrI can vary significantly [80]. The obtained CrI values of cellulose pulp (CrI = 70), corncob (CrI = 30) and samples treated with LHW (CrI = 50), NaOH (CrI = 63) and LHW-NaOH (CrI = 67) are shown in Figure 4.4a and 4.4b. The high CrI of samples treated with LHW, NaOH and LHW-NaOH, in comparison to the corncob, can be related to the removal of non-cellulosic components. Despite the high cellulose content in LHW-CC sample, it still presents a reasonable percentage of lignin (Table 4.1), which is closely associated with cellulose microfibrils and directly affects the crystallinity. It can also be observed that LHW-NaOH treated sample presented CrI value very close to the cellulose pulp, and from the high-intensity peak at  $34.7^\circ$  is possible to deduce that this sample has a greater ordering of fibers.

Samples subjected to combined treatments with ionic liquid (Figure 4.4b) gave diffractograms that clearly support the previous results obtained by FTIR. In general, a strong reduction of peaks around  $2\theta = 22^\circ$  and  $23^\circ$  and  $2\theta = 15^\circ$  is observed, as well as the appearance of a single broad peak extending from  $15^\circ$  to  $22.5^\circ$ , which are characteristic of amorphous cellulose [78, 80]. In fact, throughout the dissolution of cellulosic biomass in BmimCl, initially the cations and anions of the IL come into contact with the hydrogen bonds C2-O and C6-O of cellulose, forming new H-bonds and making the surface chains swelling, followed by the gradually peeled of its chains and the breaking of C3-O hydrogen bonds, which result in the partial or complete dissolution of cellulose [83]. As a result of the hydrogen bond network disruption, the cellulose is not allowed to recrystallize during the fast regeneration process and settles as an amorphous form [82, 84, 85].

Similar results were reported in several studies [37, 65, 86]. Amorphous structures were also obtained by [85] independent time dissolution in BmimCl and the regeneration medium.

Especially for the NaOH-IL-CC regenerated sample, three distinct diffracted peaks appeared at  $2\theta = 12.2^\circ$ ,  $19.9^\circ$  and  $22^\circ$  (Figure 4.4b). The emerging of these peaks, along with the spectra shape, might suggest a possible conversion from cellulose crystalline I to II [37, 87], but actually these features result from the conversion of cellulose crystalline I to amorphous cellulose and the high amount of hemicellulose embedded in this sample. As a consequence of this amorphous conversion after IL treatment, the crystalline peaks identified in the NaOH pretreated samples were reduced and the diffracted peaks related to hemicellulose, typically located around  $2\theta = 12.4^\circ$  and  $2\theta = 19.1^\circ$  [88], were emphasized, given rise to the concerned diffractogram shown in Figure 4.4b. In addition, the high content of hemicellulose in this sample seems to have a negative effect on cellulose dissolution, since the peak at  $2\theta = 34.7^\circ$  associated with the cellulose crystalline I can be notice in the NaOH-IL-CC spectra. Therefore, it is possible to assume that, besides the high hemicellulose content, the NaOH-IL combined treatment results in a cellulosic biomass sample composed mainly by amorphous cellulose and lesser amounts of cellulose crystalline I. This result is also supported by the low temperature of maximum rate of weight loss related to this sample (Figure 4.6b) verified through thermogravimetric analysis.

Regarding the raw corncob, there were no significant changes between the patterns of untreated and only IL-treated, except for a decrease in the intensity of curve related to the IL-CC (Figure 4.4a). Therefore, from the obtained results it is possible verifying that, independent of the pretreatment applied prior to dissolution in BmimCl, amorphous cellulose is the dominant structure in the regenerated samples.

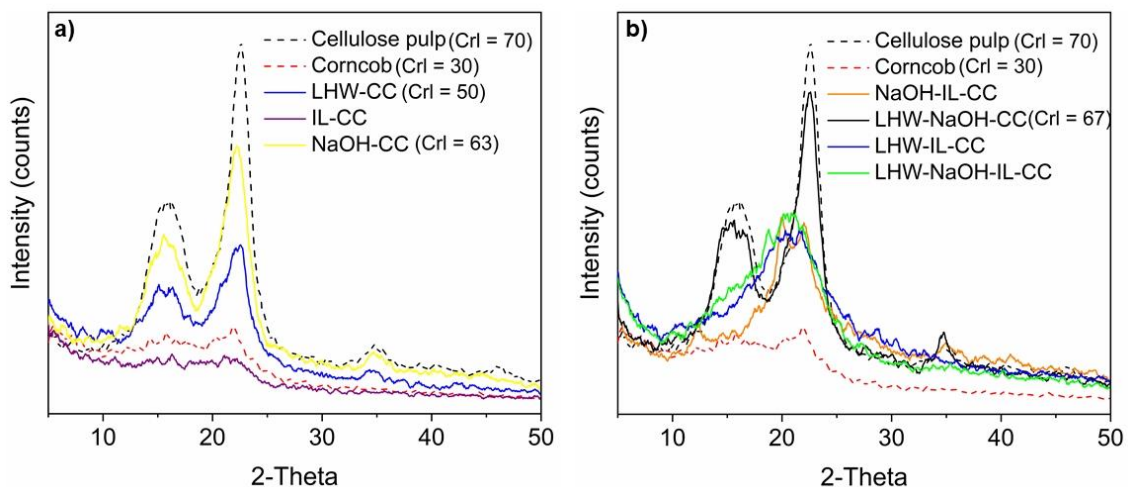


Figure 4.4. X-ray diffractograms of (a) cellulose pulp, corncob and single pretreatments and (b) combined pretreatments.

#### 4.3.4. Scanning electron microscopy

SEM study of samples (Figure 4.5) shows that untreated corncob has a rigid, porous and irregular morphology assembled into compact layers with different surface textures. Corncob is made up of different components, namely the beeswing, coarse chaff and woody ring, which confers stiffness, and the pith, the innermost part of the cob, with a consistency similar to foam plastic [89]. Each component has different morphology, constitution (regarding the content of cellulose, hemicellulose, lignin and waxes), and consequently different physicochemical features, which may play an important role in the characteristics of the material obtained after the pretreatments. From Figure 4.5e it is clear that the morphology of BmimCl treated corncob remained relatively unchanged (no defibrillation process can be seen), only smoothing and homogenization of the surface were observed. After the treatment with LHW considerable morphological changes became evident. The defibrillation process, resulting mainly from the removal of hemicellulose, partly collapsed the cell wall of corncob, leading to an increase in available surface area and porosity. Imman et al. [64] showed that, under the same severity factor, the LHW treatment could duplicate the available surface area of corncob. However, due to the large amount of residual lignin remaining in biomass, the cellulose fibers have kept still arranged together in large bundles. Contrarily, the treatment with NaOH could dissolve bulk and inter-fibrillar lignin, leading to the disruption and disaggregation of biomass fibers.

As a result of the combined LHW-NaOH treatment, more uniform fiber distribution and a remarkable disaggregation are noticed (Figure 4.5d). By promoting the initial defibrillation of the biomass, the previous treatment conducted with LHW increased the accessibility to the complex lignin-cellulose matrix and enhanced the performance of the alkaline treatment. In general, cellulosic fibers with different shapes, sizes and rough surface topography were obtained at the end of the treatment (probably due to the mix of components that make up the corncob). Except for the average diameter of the longer fibers, the characteristics of LHW-NaOH-CC extracted fibers hardly resemble the cellulose pulp fibers (Figure 4.5d and 4.5i). This can be simply explained by the different morphology inherent to the corresponding plant sources and the effect of different background processing/treatments applied to both samples.

Regarding the combined treatments with BmimCl (Figure 4.5f, g and h), the obtained regenerated material had no fibrous aspect and a smooth and uniform surface. Similar regenerated products were also observed by Geng and Henderson [65], Abdulkhani et al. [10] and Reddy et al.

[37], who performed the dissolution of other cellulosic biomass with ionic liquids and obtained regenerated materials with a flat surface.

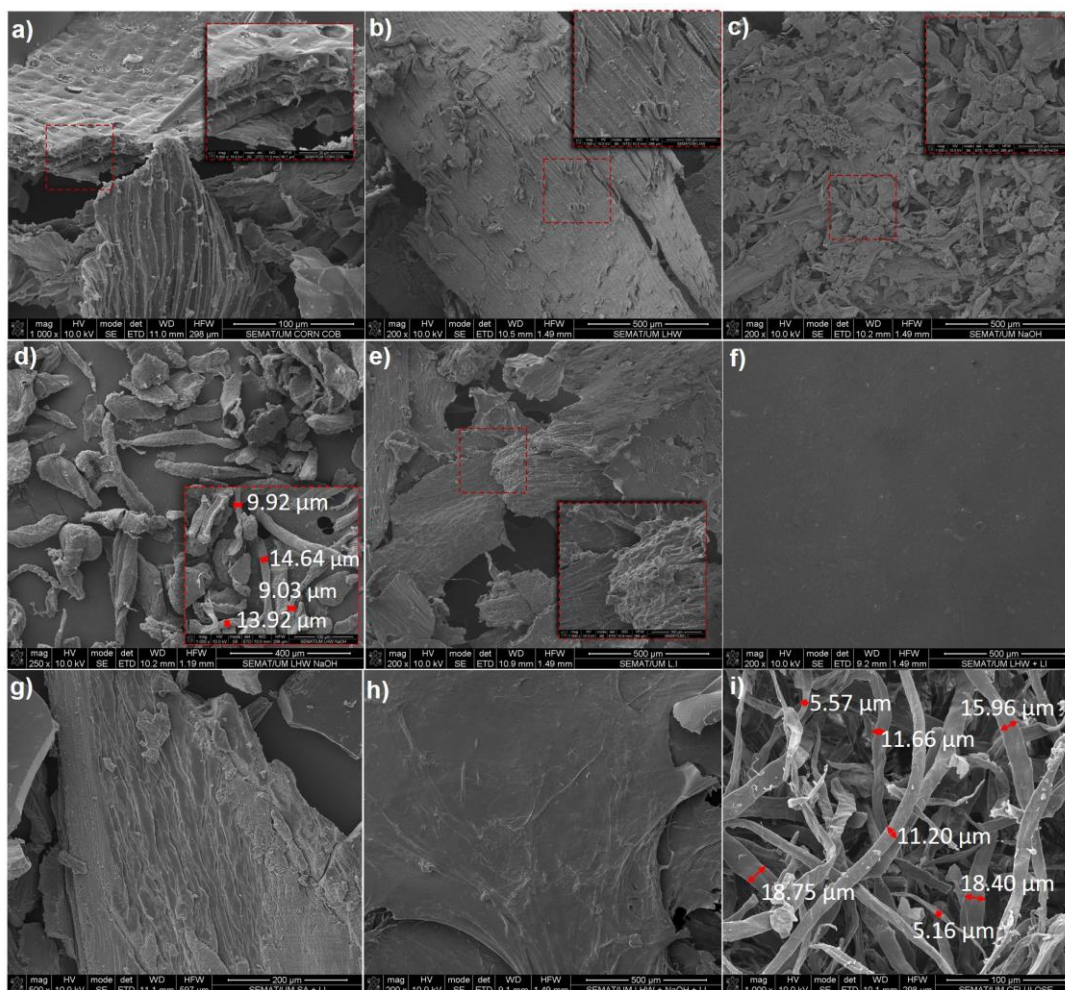


Figure 4-5. SEM micrographs of (a) untreated corncob, (b) LHW-CC, (c) NaOH-CC, (d) LHW-NaOH-CC, (e) IL-CC, (f) LHW-IL-CC, (g) NaOH-IL-CC, (h) LHW-NaOH-IL-CC and (i) Cellulose Pulp.

#### 4.3.5. Thermogravimetric properties

The thermal properties of all samples were investigated by TG and DSC, as illustrated in Figure 4.6. The temperature at which the degradation processes start ( $T_{\text{onset}}$ , °C), the temperature of maximum rate of weight loss ( $T_{\text{max}}$ , °C), the weight loss (%) /WL) and the enthalpy of melting ( $\Delta H$ , J/g) for all samples are presented in Table 3. Herein,  $T_{\text{onset}}$  will be considered as the temperature at which the process of decomposition starts, excluding the initial mass loss that was due to water evaporation. When it turns to lignocellulosic biomass,  $T_{\text{onset}}$  corresponds to the temperature at which low molar mass substances start to degrade, such as hemicellulose and possibly some lignin. Along with the  $T_{\text{max}}$ ,  $T_{\text{onset}}$  will be used to evaluate the thermal stability conferred to the lignocellulosic



fibers of corncob after pretreatments. Besides, data regarding the thermal process in Table 4.3 are discretized into two phases, that arise, in some samples, as an effect of the chemical composition or physicochemical changes after the pretreatments.

Table 4.3. Thermogravimetric results for cellulose pulp, untreated and treated corncob samples.

Sample	T <sub>onset</sub> (°C)	Phase I		Phase II		Enthalpy (J/g)
		Tmax (°C)	WL (%)	Tmax (°C)	WL (%)	
Cellulose pulp	275	357	72.8			101.6
Corncob	240	301	38	342	30.65	2.5
IL	247	282	37.5	356	34	2.1
LHW	294	351	75.17			233.3
NaOH	275	351	72.2			43
LHW+IL	241	313	60.6	348	8.6	n.d.
LHW+NaOH	294	363	75.45			104.5
LHW+NaOH+IL	252	300	70.47	348	2.9	56.6
NaOH+IL	238	277	64.7			38.8

From the thermograms exhibited in Figure 4.6, it is noticeable that the pretreatments performed had a remarkable effect over the thermal decomposition process. A small weight loss at lower temperatures (< 150 °C) due to water evaporation or low molecular weight compounds is observed in all curves. Two other distinct peaks characteristic of hemicellulose and cellulose decomposition are observed at temperatures between 200 and 400 °C. Due to the wide temperature degradation range of lignin (200-600 °C), it overlaps partially with cellulose and hemicellulose thermal decomposition curves and, consequently, does not present maximum weight loss rate [19, 77]. In general, with exception of combined treatments with ionic liquid, all the pretreatments increased the thermal stability of fibers compared to the corncob raw fibers.

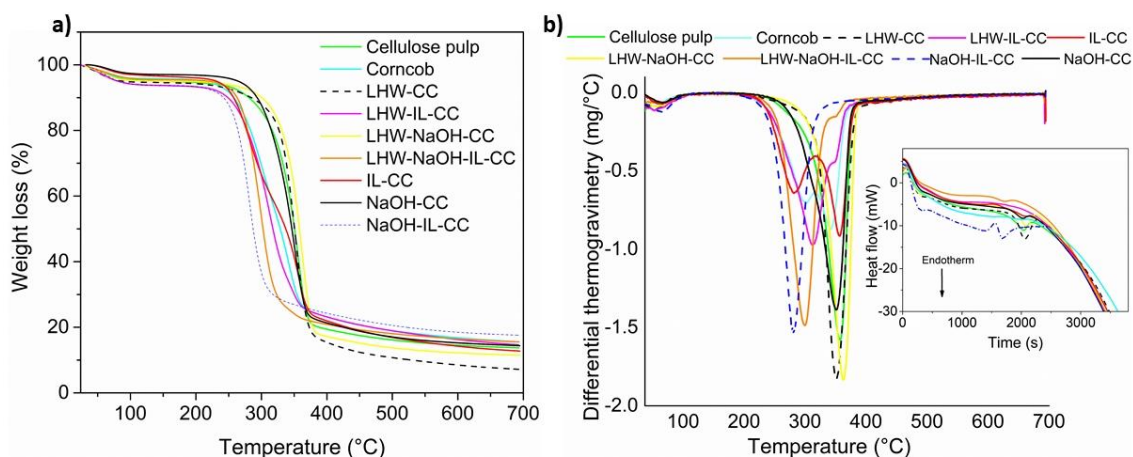


Figure 4-6. (a) TGA, (b) DTG and DSC (inset plot in the graph 5b) curves of the cellulose pulp, untreated and treated corncob.

The thermal profiles related to LHW-CC and NaOH-CC pretreated samples present single step with a narrow temperature range. In comparison to the cellulose pulp curve, the LHW-CC profile has a slightly lower  $T_{max}$  derived mainly from its rather high content of lignin. However, its  $T_{onset}$  increased significantly in comparison to the corncob profile as a result of the effective hemicellulose solubilization during the LHW treatment. Similar  $T_{max}$  value is also displayed by the NaOH treated sample, but due to the high content of hemicellulose embedded in this sample, it presents a broad curve base.

Degradation reactions observed in the curve associated to LHW-NaOH pretreated sample occurred in a single step and in a narrow temperature range, similar to the cellulose pulp curve, which decomposes in a narrow range between 275 and 400 °C (Figure 4.6a). The results evidence that this pretreatment had the best performance in terms of hemicellulose and lignin removal, resulting in a product composed mainly of cellulose, as evidenced by the other analysis performed. Compared to the single pretreatments, the combination between LHW and dilute NaOH solution resulted in a narrower and stable degradation curve, with higher  $T_{max}$ . By removing the amorphous hemicellulose and the aromatic rings of lignin, the thermal stability of fibers was increased in response to the high crystallinity of the remaining cellulose chains. The final product obtained after the coupled treatment of LWH-NaOH ( $T_{onset}$  of 294 °C and  $T_{max}$  of 363 °C) presented higher thermal stability than the cellulose pulp ( $T_{onset}$  of 275 °C and  $T_{max}$  of 357 °C), which might be probably related to the different biological sources of cellulose.

In contrast, despite the increased thermal stability of the crude substrate after ionic liquid treatment, this study suggests that the BmimCl presents reduced performance on the fractionation

of lignocellulosic biomass, which is in agreement with other studies [66], [90], [91] and [65]. As shown in Figure 6, the IL-CC degradation profile can be discretized into two phases and presents two weight loss regions between 200 and 400 °C (Figure 4.6 and Table 4.3). The first peak, with corresponding  $T_{max}$  of 282 °C, is related to hemicellulose degradation, while the second assigns to the cellulose degradation, with corresponding  $T_{max}$  of 356 °C. Few changes are verified when compared to the raw corncob profile. Moreover, when applied in combination with other treatments, the ionic liquid decreased the thermal stability of fibers and displaced  $T_{max}$  to lower values. Such effects can be attributed to the conversion of the native cellulose (cellulose crystalline I) to an amorphous structure, which is in agreement with the results obtained in the other analysis. The IL treatment gave rise to a second phase identified by a shoulder-like around 350 °C in the differential thermogravimetry profiles. This temperature is typical of cellulose decomposition and thus confirms the coexistence of cellulose crystalline I. The application of previous treatments on corncob decreased its recalcitrant property and provided the direct interaction of the ionic liquid with the cellulose, which, in turn, causes the rupture of more intermolecular and intramolecular hydrogen bonds of original cellulose during the dissolution process. The same was not observed in the direct treatment of the corncob with ionic liquid, since the cellulose dissolution was hindered by the dense packaging of hemicellulose and lignin and the high viscosity of the ionic liquid, limiting its performance to components more easily hydrolyzable. Particularly for the NaOH-IL sample, the lowest  $T_{max}$  value verified is greatly attributed to the high amount of hemicellulose remained after the treatments, which presents maximum rate of weight loss around 300 °C.

From DSC results in Figure 4.6 (inset plot in graph 4.6b), all samples presented endothermic peaks consistent with  $T_{max}$  from DTG, which are attributed to the depolymerization of cellulosic and non-cellulosic components. DSC results indicated that the melting enthalpy of the treated samples with IL was drastically reduced compared to the native cellulose and other treatments (Table 4.3), which can be associated to both a decrease of hydrogen bonds and crystallinity of cellulose [92, 93]. Thus, all the results demonstrate that the treatment with IL converted the native cellulose mostly to an amorphous and less thermally stable structure, which corroborates with XRD analysis.

#### **4.3.6. Dynamic mechanical analysis and chemical characterization of regenerated film**

Through dissolution with IL and regeneration in deionized water, attempts to produce regenerated films from the previously pretreated samples were made. However, the only sample

suitable to produce films resulted from the LHW-NaOH combined treatment. Due to the remaining reasonably amounts of lignin and hemicellulose in other samples the obtained films were very brittle films and impossible to be analyzed via DMA. The suitability of samples to produce regenerated films supports the previous chemical characterization discussions, from which the superior fractionation capacity of the LHW-NaOH combined treatment was revealed.

Briefly, the regenerated cellulose film presents a uniform and dense smooth surface (Figure 4.7c and d), as well as chemical characteristics similar to that of LHW-NaOH-IL pretreated sample (regenerated as a gel), as can be seen by comparing figures 4.3, 4.4 and 4.7b. Both samples also presented similar thermal properties (not shown). Therefore, it is clear that the different regeneration techniques and anti-solvents applied did not change the chemical structure or influence the formation of crystalline phases, but only resulted in different regenerated shapes. Thus, the regenerated film prepared from the LHW-NaOH-IL combined treatment sample is not included in the following discussions.

Figure 4.7a shows the viscoelastic properties of the produced regenerated film,  $E'$  and  $E''$  drop as the temperature increases. The transparency of the film (Figure 4.7d) is also indicative of its amorphous state, since this property is related to the unpackaging of cellulose chains. The operating range of the regenerated film was limited by the glass transition temperature ( $T_g$ ), which was found as 120 °C, approximately, and determined through the peak of  $\tan \delta$  curve. Similar  $T_g$  values of other regenerated cellulose films were reported by Yeng et al. [94] and loelovich [95]. From this temperature, the physical properties of the film may change greatly, which end up compromising its performance depending on the intended application. Moreover, from approximately 75 °C the loss modulus drops markedly, and the mechanical deformation applied begins to be converted into internal friction and nonelastic deformation.

As a new material for potential applications it is important to determine the storage modulus and the dynamic Young's modulus, as they quantify the material's stiffness. Taking as reference the values at 40 °C,  $E'$  and  $E^*$  are 3.04 GPa and 3.06 GPa, respectively. These values are higher than regenerated films produced from cotton linter pulp – 2.54-5 GPa [96, 97], Polylactic acid (PLA) – 2 GPa [98], PLA/bamboo fabric laminate – 1.75 GPa [99], microcrystalline cellulose – 2.57 GPa [100] and bleached hardwood kraft pulp – 1.5 GPa [101]. The results presented suggest that the regenerated cellulose, produced herein via a sustainable processing from corncob residues, could be potentially used in value-added applications, such as packaging.

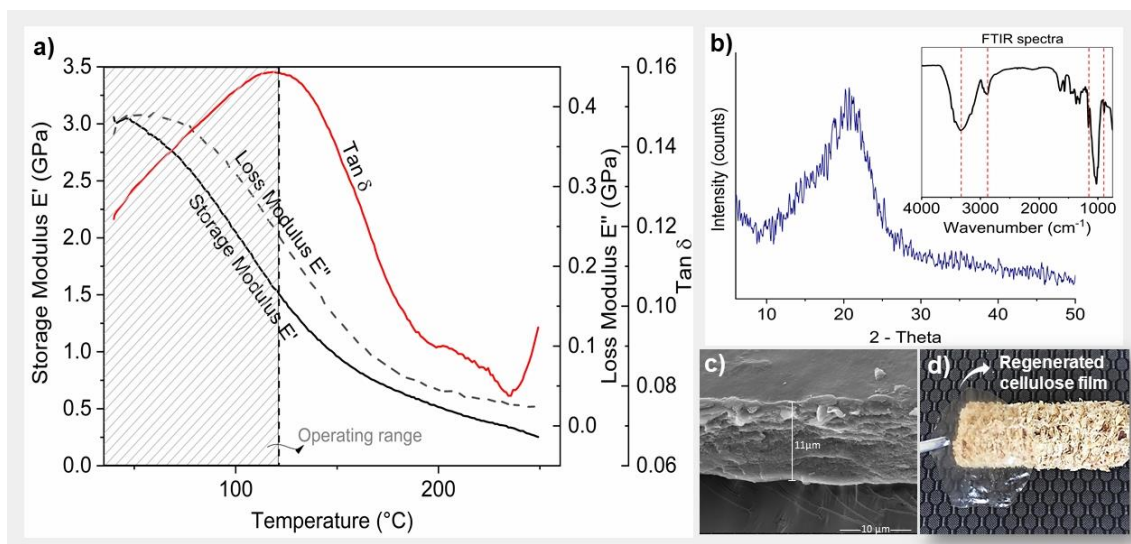


Figure 4-7. (a) Dynamic mechanical analysis, (b) X-ray diffraction and FTIR spectra (inset graph in figure 7b) and (c) SEM cross section of (d) regenerated cellulose film produced from LHW-NaOH pretreated corncob.

#### 4.4. Conclusions

In this study, corncob was pretreated by performing individual and combined green pretreatments, namely liquid hot water and ionic liquid (BmimCl), as well as dilute NaOH solution, and attempts to produce regenerated cellulose films were carried out through dissolution of pretreated samples in BmimCl. The results confirmed the low fractionation capacity of BmimCl and the complementary effects of LHW (which efficiently removed hemicellulose) and NaOH (efficient in lignin removal). The disruption of hemicellulose and the subsequent weakening of the biomass structure resulting from the LHW treatment increased the accessibility of lignin. Therefore, the combined LHW-NaOH pretreatment was very efficient at removing the non-cellulosic components from corncob and leads to a solid enrich-cellulose fraction with high crystallinity and thermal stability. The results also revealed that, regardless of the pretreatment applied prior to dissolution in BmimCl, the regenerated samples were constituted mainly by amorphous structure.

This work shows the efficient application of some combined green and conventional treatments, with results comparable with those obtained by established laboratory methods for delignification. The results also revealed that, suitability of biomass to different types of valorization can be optimized by pretreatments combination. Moreover, the high stable and crystalline cellulose obtained after LHW-NaOH combine treatment gave rise to a regenerated film with outstanding viscoelastic properties, suitable for packaging applications. The sequential process design involving combined green pretreatments and ionic liquid dissolution to produce regenerated cellulose films can be seen as a sustainable approach, but it is still challenging in terms of costs and scalability.

Nevertheless, the development of life cycle and costs assessment can give more insights on the feasibility, design and optimization of this production method.

## Acknowledgements

This work was supported by the Brazilian National Council for Scientific and Technological Development (Grant number 201940/2015-9).

## Reference

1. Reddy, J.P., Rhim, J.W.: Isolation and characterization of cellulose nanocrystals from garlic skin. *Mater. Lett.* 129, 20–23 (2014). <https://doi.org/10.1016/j.matlet.2014.05.019>
2. Ravindran, R., Jaiswal, A.K.: A comprehensive review on pre-treatment strategy for lignocellulosic food industry waste: Challenges and opportunities. *Bioresour. Technol.* 199, 92–102 (2016). <https://doi.org/10.1016/j.biortech.2015.07.106>
3. Zhou, Z., Lei, F., Li, P., Jiang, J.: Lignocellulosic biomass to biofuels and biochemicals: A comprehensive review with a focus on ethanol organosolv pretreatment technology. *Biotechnol. Bioeng.* 115, 2683–2702 (2018). <https://doi.org/10.1002/bit.26788>
4. Brodin, M., Vallejos, M., Tanase, M., Cristina, M., Chinga-carrasco, G.: Lignocellulosics as sustainable resources for production of bioplastics e A review. *J. Clean. Prod.* 162, 646–664 (2017). <https://doi.org/10.1016/j.jclepro.2017.05.209>
5. Araújo, D.J.C., Machado, A. V., Vilarinho, M.C.L.G.: Availability and Suitability of Agroindustrial Residues as Feedstock for Cellulose-Based Materials: Brazil Case Study. *Waste and Biomass Valorization.* 16 (2018). <https://doi.org/10.1007/s12649-018-02910>
6. Silvério, H.A., Flauzino Neto, W.P., Dantas, N.O., Pasquini, D.: Extraction and characterization of cellulose nanocrystals from corncob for application as reinforcing agent in nanocomposites. *Ind. Crops Prod.* 44, 427–436 (2013). <https://doi.org/10.1016/j.indcrop.2012.10.014>
7. Ullah, K., Kumar Sharma, V., Dhingra, S., Braccio, G., Ahmad, M., Sofia, S.: Assessing the lignocellulosic biomass resources potential in developing countries: A critical review. *Renew. Sustain. Energy Rev.* 51, 682–698 (2015). <https://doi.org/10.1016/j.rser.2015.06.044>
8. Bhutto, A.W., Qureshi, K., Harijan, K., Abro, R., Abbas, T., Bazmi, A.A., Karim, S., Yu, G.: Insight into progress in pre-treatment of lignocellulosic biomass. *Energy.* 122, 724–745 (2017). <https://doi.org/10.1016/j.energy.2017.01.005>

9. Seidl, P.R., Goulart, A.K.: Pretreatment processes for lignocellulosic biomass conversion to biofuels and bioproducts. *Curr. Opin. Green Sustain. Chem.* 2, 48–53 (2016). <https://doi.org/10.1016/j.cogsc.2016.09.003>
10. Abdulkhani, A., Hojati Marvast, E., Ashori, A., Karimi, A.N.: Effects of dissolution of some lignocellulosic materials with ionic liquids as green solvents on mechanical and physical properties of composite films. *Carbohydr. Polym.* 95, 57–63 (2013). <https://doi.org/10.1016/j.carbpol.2013.02.040>
11. Sánchez, C.: Lignocellulosic residues: Biodegradation and bioconversion by fungi. *Biotechnol. Adv.* 27, 185–194 (2009). <https://doi.org/10.1016/j.biotechadv.2008.11.001>
12. Reddy, N., Yang, Y.: Biofibers from agricultural byproducts for industrial applications. *Trends Biotechnol.* 23, 22–27 (2005). <https://doi.org/10.1016/j.tibtech.2004.11.002>
13. Capolupo, L., Faraco, V.: Green methods of lignocellulose pretreatment for biorefinery development. *Appl. Microbiol. Biotechnol.* 100, 9451–9467 (2016). <https://doi.org/10.1007/s00253-016-7884-y>
14. Singh, R., Krishna, B.B., Kumar, J., Bhaskar, T.: Opportunities for utilization of non-conventional energy sources for biomass pretreatment. *Bioresour. Technol.* 199, 398–407 (2016). <https://doi.org/10.1016/j.biortech.2015.08.117>
15. Daza Serna, L. V., Orrego Alzate, C.E., Cardona Alzate, C.A.: Supercritical fluids as a green technology for the pretreatment of lignocellulosic biomass. *Bioresour. Technol.* 199, 113–120 (2016). <https://doi.org/10.1016/j.biortech.2015.09.078>
16. Zhang, Q., Hu, J., Lee, D.J.: Pretreatment of biomass using ionic liquids: Research updates. *Renew. Energy.* 111, 77–84 (2017). <https://doi.org/10.1016/j.renene.2017.03.093>
17. Chen, H., Liu, J., Chang, X., Chen, D., Xue, Y., Liu, P., Lin, H., Han, S.: A review on the pretreatment of lignocellulose for high-value chemicals. *Fuel Process. Technol.* 160, 196–206 (2017). <https://doi.org/10.1016/j.fuproc.2016.12.007>
18. Rabemanolontsoa, H., Saka, S.: Various pretreatments of lignocellulosics. *Bioresour. Technol.* 199, 83–91 (2016). <https://doi.org/10.1016/j.biortech.2015.08.029>
19. Yue, Y., Han, J., Han, G., Aita, G.M., Wu, Q.: Cellulose fibers isolated from energycane bagasse using alkaline and sodium chlorite treatments: Structural, chemical and thermal properties. *Ind. Crops Prod.* 76, 355–363 (2015). <https://doi.org/10.1016/j.indcrop.2015.07.006>

20. Sun, Y., Cheng, J.: Hydrolysis of lignocellulosic materials for ethanol production : a review q. *Bioresour. Technol.* 83, 1–11 (2002). [https://doi.org/10.1016/S0960-8524\(01\)00212-7](https://doi.org/10.1016/S0960-8524(01)00212-7)
21. Wan, C., Zhou, Y., Li, Y.: Bioresource Technology Liquid hot water and alkaline pretreatment of soybean straw for improving cellulose digestibility. *Bioresour. Technol.* 102, 6254–6259 (2011). <https://doi.org/10.1016/j.biortech.2011.02.075>
22. Government of Canada: Environmental emergency planning: sodium hydroxide risk evaluation, <https://www.canada.ca/en/environment-climate-change/services/environmental-emergencies-program/regulations/sodium-hydroxide-risk-evaluation.html>
23. Kim, J.S., Lee, Y.Y., Kim, T.H.: A review on alkaline pretreatment technology for bioconversion of lignocellulosic biomass. *Bioresour. Technol.* 199, 42–48 (2016). <https://doi.org/10.1016/j.biortech.2015.08.085>
24. Hellenic Petroleum: Global Product Strategy ( GPS ) Safety Summary - caustic soda. (2013)
25. Chen, Y., Stevens, M.A., Zhu, Y., Holmes, J., Xu, H.: Understanding of alkaline pretreatment parameters for corn stover enzymatic saccharification. *Biotechnol. Biofuels.* 6, 1 (2013). <https://doi.org/10.1186/1754-6834-6-8>
26. Agbor, V.B., Cicek, N., Sparling, R., Berlin, A., Levin, D.B.: Biomass pretreatment: Fundamentals toward application. *Biotechnol. Adv.* 29, 675–685 (2011). <https://doi.org/10.1016/j.biotechadv.2011.05.005>
27. Michelin, M., Teixeira, J.A.: Liquid hot water pretreatment of multi feedstocks and enzymatic hydrolysis of solids obtained thereof. *Bioresour. Technol.* 216, 862–869 (2016). <https://doi.org/10.1016/j.biortech.2016.06.018>
28. Sabanci, K., Buyukkileci, A.O.: Bioresource Technology Comparison of liquid hot water, very dilute acid and alkali treatments for enhancing enzymatic digestibility of hazelnut tree pruning residues. *Bioresour. Technol.* 261, 158–165 (2018). <https://doi.org/10.1016/j.biortech.2018.03.136>
29. Lopes, J., Bermejo, M., Martín, Á., Cocero, M.: Ionic Liquid as Reaction Media for the Production of Cellulose-Derived Polymers from Cellulosic Biomass. *ChemEngineering.* 1, 10 (2017). <https://doi.org/10.3390/chemengineering1020010>
30. Farrán, A., Cai, C., Sandoval, M., Xu, Y., Liu, J., Hernáiz, M.J., Linhardt, R.J.: Green Solvents in Carbohydrate Chemistry: From Raw Materials to Fine Chemicals. *Chem. Rev.* 115, 6811–6853 (2015). <https://doi.org/10.1021/cr500719h>



31. Brandt, A., Gräsvik, J., Hallett, J.P., Welton, T.: Deconstruction of lignocellulosic biomass with ionic liquids. *Green Chem.* 15, 550–583 (2013). <https://doi.org/10.1039/c2gc36364j>
32. Fort, D.A., Remsing, R.C., Swatloski, R.P., Moyna, P., Rogers, R.D.: Can ionic liquids dissolve wood? Processing and analysis of lignocellulosic materials with 1- n -butyl-3-methylimidazolium chloride. *R. Soc. Chem.* 63–69 (2007). <https://doi.org/10.1039/b607614a>
33. Kilpeläinen, I.L.K., Xie, H.A.X., King, A.L.K., Ranstrom, M.A.R.I.G., Eikkinen, S.A.M.I.H., Rgyropoulos, D.I.S.A.: Dissolution of Wood in Ionic Liquids. *J. Agric. Food Chem.* 9142–9148 (2007)
34. Pang, Z., Dong, C., Pan, X.: Enhanced deconstruction and dissolution of lignocellulosic biomass in ionic liquid at high water content by lithium chloride. *Cellulose.* 23, 323–338 (2016). <https://doi.org/10.1007/s10570-015-0832-7>
35. Wang, S., Lu, A., Zhang, L.: Recent advances in regenerated cellulose materials. *Prog. Polym. Sci.* 53, 169–206 (2016). <https://doi.org/10.1016/j.progpolymsci.2015.07.003>
36. Zhang, K., Xiao, H., Su, Y., Wu, Y., Cui, Y., Li, M.: Mechanical and Physical Properties of Regenerated Biomass Composite Films from Lignocellulosic Materials in Ionic Liquid. 14, 2584–2595 (2019)
37. Reddy, K.O., Maheswari, C.U., Dhlamini, M.S., Mothudi, B.M., Zhang, J., Zhang, J., Nagarajan, R., Rajulu, A.V.: Preparation and characterization of regenerated cellulose films using borassus fruit fibers and an ionic liquid. *Carbohydr. Polym.* 160, 203–211 (2017). <https://doi.org/10.1016/j.carbpol.2016.12.051>
38. Nor Amalini, A., Melina Cheah, M.Y., Wan Rosli, W.D., Hayati, S., Mohamad Haafiz, M.K.: Fabrication and characterization of regenerated cellulose films obtained from oil palm empty fruit bunch. *AIP Conf. Proc.* 1901, (2017). <https://doi.org/10.1063/1.5010529>
39. Pang, J., Wu, M., Zhang, Q., Tan, X., Xu, F., Zhang, X., Sun, R.: Comparison of physical properties of regenerated cellulose films fabricated with different cellulose feedstocks in ionic liquid. *Carbohydr. Polym.* 121, 71–78 (2015). <https://doi.org/10.1016/j.carbpol.2014.11.067>
40. Xie, N.A.N., Jiang, N., Zhang, M., Al., E.: Cellulose chemistry and technology effect of different pretreatment methods of corncob on bioethanol production and enzyme recovery. *Cellul. Chem. Technol.* 48, 313–319 (2014)
41. Luo, W., Wang, J., Liu, X., Li, H., Pan, H., Gu, Q., Yu, X.: Bioresource Technology A facile and efficient pretreatment of corncob for bioproduction of butanol. *Bioresour. Technol.* 140, 86–89 (2013). <https://doi.org/10.1016/j.biortech.2013.04.063>

42. Kawee-Ai, A., Srisuwun, A., Tantiwa, N., Nontaman, W., Boonchuay, P., Kuntiya, A., Chaiyaso, T., Seesuriyachan, P.: Eco-friendly processing in enzymatic xylooligosaccharides production from corncob: Influence of pretreatment with sonocatalytic-synergistic Fenton reaction and its antioxidant potentials. *Ultrason. Sonochem.* 31, 184–192 (2016). <https://doi.org/10.1016/j.ultsonch.2015.12.018>
43. Upajak, S., Laosiripojana, N., Champreda, V., Kreethachart, T., Thonburi, T., Author, C.: Effect of combination of liquid hot water system and hydrogen peroxide pretreatment on enzymatic. *Int. J. GEOMATE.* 15, 31–38 (2018)
44. Michelin, M., Ruiz, H.A., Lourdes, M. De, Polizeli, T.M., Teixeira, J.A.: Bioresource Technology Multi-step approach to add value to corncob: Production of biomass- degrading enzymes, lignin and fermentable sugars. *Bioresour. Technol.* 247, 582–590 (2018). <https://doi.org/10.1016/j.biortech.2017.09.128>
45. Thangavelu, K., Desikan, R., Taran, O.P., Uthandi, S.: Biotechnology for Biofuels Delignification of corncob via combined hydrodynamic cavitation and enzymatic pretreatment: process optimization by response surface methodology. *Biotechnol. Biofuels.* 1–13 (2018). <https://doi.org/10.1186/s13068-018-1204-y>
46. Imman, S., Arnthong, J., Burapatana, V., Champreda, V.: Influence of alkaline catalyst addition on compressed liquid hot water pretreatment of rice straw. *Chem. Eng. J.* 278, 85–91 (2015). <https://doi.org/10.1016/j.cej.2014.12.032>
47. Yang, H., Shi, Z., Xu, G., Qin, Y., Deng, J., Yang, J.: Bioresource Technology Bioethanol production from bamboo with alkali-catalyzed liquid hot water pretreatment. *Bioresour. Technol.* 274, 261–266 (2019). <https://doi.org/10.1016/j.biortech.2018.11.088>
48. Teng, H., Lin, H.C., Ho, J.A.: Thermogravimetric Analysis on Global Mass Loss Kinetics of Rice Hull Pyrolysis. *Ind. Eng. Chem. Res.* 36, 3974–3977 (1997). <https://doi.org/10.1021/ie970017z>
49. Carrier, M., Loppinet-Serani, A., Denux, D., Lasnier, J.-M., Ham-Pichavant, F., Cansell, F., Aymonier, C.: Thermogravimetric analysis as a new method to determine the lignocellulosic composition of biomass. *Biomass and Bioenergy.* 35, 298–307 (2011). <https://doi.org/10.1016/j.biombioe.2010.08.067>
50. Saldarriaga, J.F., Aguado, R., Pablos, A., Amutio, M., Olazar, M., Bilbao, J.: Fast characterization of biomass fuels by thermogravimetric analysis (TGA). *Fuel.* 140, 744–751 (2015). <https://doi.org/10.1016/j.fuel.2014.10.024>

51. Chen, T., Li, L., Zhao, R., Wu, J.: Pyrolysis kinetic analysis of the three pseudocomponents of biomass–cellulose, hemicellulose and lignin: Sinusoidally modulated temperature method. *J. Therm. Anal. Calorim.* 128, 1825–1832 (2016). <https://doi.org/10.1007/s10973-016-6040-3>
52. Segal, L., Creely, J.J., Martin Jr, A.E., Conrad, C.M.: An Empirical Method for Estimating the Degree of Crystallinity of Native Cellulose Using the X-Ray Diffractometer. *Têxtil Res. J.* 29, 786–794 (1959). <https://doi.org/10.1177/004051755902901003>
53. Menard, K.P.: *Dynamic mechanical analysis - a practical introduction*. CRC Press LLC, New York (1999)
54. Lee, H. V, Hamid, S.B. a, Zain, S.K.: Conversion of Lignocellulosic Biomass to Nanocellulose: Structure and Chemical Process Conversion of Lignocellulosic Biomass to Nanocellulose : *Sci. World J.* 2014, 1–14 (2014). <https://doi.org/10.1155/2014/631013>
55. Nabarlantz, D., Farriol, X., Montané, D.: Kinetic Modeling of the Autohydrolysis of Lignocellulosic Biomass for the Production of Hemicellulose-Derived Oligosaccharides. *Ind. Eng. Chem. Res.* 43, 4124–4131 (2004). <https://doi.org/10.1021/ie034238i>
56. Pointner, M., Kuttner, P., Obrlik, T., Jäger, A., Kahr, H.: Composition of corncobs as a substrate for fermentation of biofuels. *Agron. Res.* 12, 391–396 (2014)
57. Silva, J.C. da, Oliveira, R.C. de, Neto, A. da S., Pimentel, V.C., Santos, A. de A. dos: Extraction, Addition and Characterization of Hemicelluloses from Corn Cobs to Development of Paper Properties. *Procedia Mater. Sci.* 8, 793–801 (2015). <https://doi.org/10.1016/j.mspro.2015.04.137>
58. Liu, C., Li, B., Du, H., Lv, D., Zhang, Y., Yu, G., Mu, X., Peng, H.: Properties of nanocellulose isolated from corncob residue using sulfuric acid, formic acid, oxidative and mechanical methods. *Carbohydr. Polym.* 151, 716–724 (2016). <https://doi.org/10.1016/j.carbpol.2016.06.025>
59. Yu, Q., Zhuang, X., Lv, S., He, M., Zhang, Y., Yuan, Z., Qi, W., Wang, Q., Wang, W., Tan, X.: Bioresource Technology Liquid hot water pretreatment of sugarcane bagasse and its comparison with chemical pretreatment methods for the sugar recovery and structural changes. *Bioresour. Technol.* 129, 592–598 (2013). <https://doi.org/10.1016/j.biortech.2012.11.099>
60. Mtui, G.Y.S.: Recent advances in pretreatment of lignocellulosic wastes and production of value-added products. *African J. Biotechnol.* Vol. 8, 1398–1415 (2009). <https://doi.org/10.1073/pnas.1014862107/-/DCSupplemental.www.pnas.org/cgi/>

61. Li, M., Cao, S., Meng, X., Studer, M., Wyman, C.E., Ragauskas, A.J., Pu, Y.: The effect of liquid hot water pretreatment on the chemical-structural alteration and the reduced recalcitrance in poplar. *Biotechnol. Biofuels.* 10, 1–13 (2017). <https://doi.org/10.1186/s13068-017-0926-6>
62. Overend, R.P., Chornet, E., Gascoigne, J.A.: Fractionation of Lignocellulosics by Steam-Aqueous Pretreatments [and Discussion]. *Philos. Trans. R. Soc. A Math. Phys. Eng. Sci.* 321, 523–536 (1987). <https://doi.org/10.1098/rsta.1987.0029>
63. Imman, S., Arnthong, J., Burapatana, V., Laosiripojana, N., Champreda, V.: Autohydrolysis of tropical agricultural residues by compressed liquid hot water pretreatment. *Appl. Biochem. Biotechnol.* 170, 1982–1995 (2013). <https://doi.org/10.1007/s12010-013-0320-1>
64. Imman, S., Laosiripojana, N., Champreda, V.: Effects of Liquid Hot Water Pretreatment on Enzymatic Hydrolysis and Physicochemical Changes of Corncobs. *Appl. Biochem. Biotechnol.* 1–12 (2018). <https://doi.org/10.1007/s12010-017-2541-1>
65. Geng, X., Henderson, W.A.: Pretreatment of corn stover by combining ionic liquid dissolution with alkali extraction. *Biotechnol. Bioeng.* 109, 84–91 (2012). <https://doi.org/10.1002/bit.23281>
66. Mahmood, H., Moniruzzaman, M., Yusup, S., Akil, H.M.: Pretreatment of oil palm biomass with ionic liquids: A new approach for fabrication of green composite board. *J. Clean. Prod.* 126, 677–685 (2016). <https://doi.org/10.1016/j.jclepro.2016.02.138>
67. Ma, Z., Pan, G., Xu, H., Huang, Y., Yang, Y.: Cellulosic fibers with high aspect ratio from cornhusks via controlled swelling and alkaline penetration. *Carbohydr. Polym.* 124, 50–56 (2015). <https://doi.org/10.1016/j.carbpol.2015.02.008>
68. Rhim, J.W., Reddy, J.P., Luo, X.: Isolation of cellulose nanocrystals from onion skin and their utilization for the preparation of agar-based bio-nanocomposites films. *Cellulose.* 22, 407–420 (2015). <https://doi.org/10.1007/s10570-014-0517-7>
69. Poletto, M., Pistor, V., Zattera, A.J.: Structural Characteristics and Thermal Properties of Native Cellulose. *Cellul. – Fundam. Asp.* 45–68 (2013). <https://doi.org/10.5772/50452>
70. Ang, T.N., Ngoh, G.C., Seak, A., Chua, M., Lee, M.G.: Elucidation of the effect of ionic liquid pretreatment on rice husk via structural analyses. *Biotechnol. Biofuels.* 5, 1–10 (2012)
71. Wang, F., Li, S., Sun, Y., Han, H., Zhang, B.: Ionic liquids as efficient pretreatment solvents for lignocellulosic biomass. *R. Soc. Chem.* 7, 47990–47998 (2017). <https://doi.org/10.1039/c7ra08110c>

72. Wulandari, W.T., Rochiliadi, A., Arcana, I.M.: Nanocellulose prepared by acid hydrolysis of isolated cellulose from sugarcane bagasse. *Mater. Sci. Eng.* 1–8 (2016). <https://doi.org/10.1088/1757-899X/107/1/012045>
73. Kristensen, J.B., Thygesen, L.G., Felby, C., Jørgensen, H., Elder, T.: Biotechnology for Biofuels Cell-wall structural changes in wheat straw pretreated for bioethanol production. *Biotechnol. Biofuels.* 9, 1–9 (2008). <https://doi.org/10.1186/1754-6834-1-5>
74. Yu, L., Lin, J., Tian, F., Al., E.: Cellulose nanofibrils generated from jute fibers with tunable polymorphs and crystallinity. *J. Mater. Chem. A.* 6402–6411 (2014). <https://doi.org/10.1039/c4ta00004h>
75. Heinze, T.: Cellulose Chemistry and Properties: Fibers, Nanocelluloses and Advanced Materials. In: Rojas, O.J. (ed.) *Advances in Polymer Science* 271. p. 341. Springer International Publishing Switzerland (2016)
76. Cheng, G., Varanasi, P., Arora, R., Stavila, V., Simmons, B.A.: Impact of Ionic Liquid Pretreatment Conditions on Cellulose Crystalline Structure Using 1 - Ethyl-3-methylimidazolium Acetate. *J. Phys. Chem.* 10049–10054 (2012). <https://doi.org/10.1021/jp304538v>
77. Zhang, J., Feng, L., Wang, D., Zhang, R., Liu, G., Cheng, G.: Thermogravimetric analysis of lignocellulosic biomass with ionic liquid pretreatment. *Bioresour. Technol.* 153, 379–382 (2014). <https://doi.org/10.1016/j.biortech.2013.12.004>
78. Ciolacu, D., Ciolacu, F., Popa, V.I.: Amorphous Cellulose – Structure and Characterization. *Cellul. Chem. Technol.* 45, 13–21 (2011). <https://doi.org/10.1163/156856198X00740>
79. Ahvenainen, P., Kontro, I., Svedström, K.: Comparison of sample crystallinity determination methods by X-ray diffraction for challenging cellulose I materials. *Cellulose.* 23, 1073–1086 (2016). <https://doi.org/10.1007/s10570-016-0881-6>
80. Park, S., Baker, J.O., Himmel, M.E., Parilla, P.A., Johnson, D.K.: Cellulose crystallinity index: Measurement techniques and their impact on interpreting cellulase performance. *Biotechnol. Biofuels.* 3, (2010). <https://doi.org/10.1186/1754-6834-3-10>
81. Thygesen, A., Oddershede, J., Lilholt, H., Thomsen, A.B., Ståhl, K.: On the determination of crystallinity and cellulose content in plant fibres. *Cellulose.* 12, 563–576 (2005). <https://doi.org/10.1007/s10570-005-9001-8>
82. Cheng, G., Varanasi, P., Li, C., Liu, H., Melnichenko, Y.B., Simmons, B.A., Kent, M.S., Singh, S.: Transition of Cellulose Crystalline Structure and Surface Morphology of Biomass as a

Function of Ionic Liquid Pretreatment and Its Relation to Enzymatic Hydrolysis. *Biomacromolecules*. 12, 933–941 (2011). <https://doi.org/10.1021/bm101240z>

83. Li, Y., Wang, J., Liu, X., Zhang, S.: Towards a molecular understanding of cellulose dissolution in ionic liquids: anion/cation effect, synergistic mechanism and physicochemical aspects. *Chem. Sci.* 9, 4027–4043 (2018). <https://doi.org/10.1039/C7SC05392D>

84. Gupta, K.M., Jiang, J.: Cellulose dissolution and regeneration in ionic liquids: A computational perspective. *Chem. Eng. Sci.* 121, 180–189 (2015). <https://doi.org/10.1016/j.ces.2014.07.025>

85. Dadi, A.P., Varanasi, S., Schall, C.A.: Enhancement of Cellulose Saccharification Kinetics Using an Ionic Liquid Pretreatment Step. *Biotechnol. Bioeng.* 95, 904–910 (2006). <https://doi.org/10.1002/bit>

86. Singh, S., Varanasi, P., Singh, P., Adams, P.D., Auer, M., Simmons, B.A.: Understanding the impact of ionic liquid pretreatment on cellulose and lignin via thermochemical analysis. *Biomass and Bioenergy*. 54, 276–283 (2013). <https://doi.org/10.1016/j.biombioe.2013.02.035>

87. Ciolacu, D., Valentin, I.P.: ON THE THERMAL DEGRADATION OF CELLULOSE ALLOMORPHS. *Cellul. Chem. Technol.* 40, 445–449 (2006)

88. Zhang, X.Q., Chen, M.J., Wang, H.H., Wen, X.X., Liu, C.F., Sun, R.C.: Ionic Liquid as Green Solvent for Ring-Opening Graft Polymerization of  $\epsilon$ -Caprolactone onto Hemicelluloses. In: Handy, S. (ed.) *Ionic Liquids: Current State of the Art*. p. 13. IntechOpen (2016)

89. Matsushima, J., Dowe, T.W., Arthaud, V.H.: Evaluation of Ground Corncobs and Corncob Components as Nutritive Materials in Rations for Beef Cattle. *Historical Res. Bull. Nebraska Agric. Exp. Stn.* 1913–1993 (1957)

90. Gräsvik, J., Winstrand, S., Normark, M., Jönsson, L.J., Mikkola, J.P.: Evaluation of four ionic liquids for pretreatment of lignocellulosic biomass. *BMC Biotechnol.* 14, 1–11 (2014). <https://doi.org/10.1186/1472-6750-14-34>

91. Swatloski, R.P., Spear, S.K., Holbrey, J.D., Rogers, R.D.: Dissolution of cellulose with ionic liquids. *J. Am. Chem. Soc.* 124, 4974–4975 (2002). <https://doi.org/ja025790m> [pii]

92. Wan Daud, W.R., Djuned, F.M.: Cellulose acetate from oil palm empty fruit bunch via a one-step heterogeneous acetylation. *Carbohydr. Polym.* 132, 252–260 (2015). <https://doi.org/10.1016/j.carbpol.2015.06.011>

93. Filho, G.R., Da Cruz, S.F., Pasquini, D., Cerqueira, D.A., Prado, V.D.S., De Assunção, R.M.N.: Water flux through cellulose triacetate films produced from heterogeneous acetylation of

- sugar cane bagasse. *J. Memb. Sci.* 177, 225–231 (2000). [https://doi.org/10.1016/S0376-7388\(00\)00469-5](https://doi.org/10.1016/S0376-7388(00)00469-5)
94. Yeng, L.C., Wahit, M.U., Othman, N.: Thermal and flexural properties of regenerated cellulose (RC)/poly (3- hydroxybutyrate)(PHB)biocomposites. *J. Teknol.* 75, 107–112 (2015). <https://doi.org/10.11113/jt.v75.5338>
95. loelovich, M.: Isophase Transitions of Cellulose – A Short Review. *Athens J. Sci.* 3, 309–322 (2016). <https://doi.org/10.30958/ajs.3-4-4>
96. Ashok, B., Reddy, K.O., Madhukar, K., Cai, J., Zhang, L., Rajulu, A.V.: Properties of cellulose/Thespesia lampas short fibers bio-composite films. *Carbohydr. Polym.* 127, 110–115 (2015). <https://doi.org/10.1016/j.carbpol.2015.03.054>
97. Qi, H., Chang, C., Zhang, L.: Properties and applications of biodegradable transparent and photoluminescent cellulose films prepared via a green process. *Green Chem.* 11, 177–184 (2009). <https://doi.org/10.1039/b814721c>
98. Kamthai, S., Magaraphan, R.: Thermal and mechanical properties of polylactic acid (PLA) and bagasse carboxymethyl cellulose (CMC B) composite by adding isosorbide diesters. *AIP Conf. Proc.* 1664, (2015). <https://doi.org/10.1063/1.4918424>
99. Porras, A., Maranon, A.: Development and characterization of a laminate composite material from polylactic acid (PLA) and woven bamboo fabric. *Compos. Part B Eng.* 43, 2782–2788 (2012). <https://doi.org/10.1016/j.compositesb.2012.04.039>
100. Duchemin, B.J.C., Newman, R.H., Staiger, M.P.: Structure-property relationship of all-cellulose composites. *Compos. Sci. Technol.* 69, 1225–1230 (2009). <https://doi.org/10.1016/j.compscitech.2009.02.027>
101. Zhang, X., Xiao, N., Wang, H., Liu, C., Pan, X.: Preparation and characterization of regenerated cellulose film from a solution in lithium bromide molten salt hydrate. *Polymers (Basel)*. 8, (2018). <https://doi.org/10.3390/polym10060614>

Chapter 5. Green synthesis of cellulose acetate from  
corn cob: physicochemical properties and assessment of  
environmental impacts

*Submitted to Journal of Cleaner Production*

---

**David Araújo<sup>1,2\*</sup>, M. Cidália R. Castro<sup>1</sup>, Aline Figueiredo<sup>3</sup>, Maria  
Vilarinho<sup>2,4</sup> Ana Machado<sup>1</sup>**

<sup>1</sup>Institute for Polymers and Composites/i3N, University of Minho, Guimarães, Portugal.

<sup>2</sup>Centre for Waste Valorization, University of Minho, Guimarães, Portugal

<sup>3</sup>Department of Sanitary and Environmental Engineering, Federal University of Maranhão,  
Maranhão, Brazil.

<sup>4</sup>Mechanical Engineering and Resources Sustainability Centre, University of Minho, Guimarães,  
Portugal.

\*Corresponding author: David Jefferson Cardoso Araújo (david\_bct@hotmail.com)



**Abstract**

The widespread availability and chemical constitution of agroindustrial residues have stood them out as a promising source of natural chemicals and polymers, such as cellulose. However, to date, green alternative synthesis routes developed to turn the agroindustrial residues into value-added products lack environmental performance regarding the quantification of impacts. In this work a promising green pretreatment and acetylation techniques to obtaining cellulose acetate from corncob were applied. Physicochemical characterization techniques were carried out to investigate the effectivity of pretreatment, as well as the properties of synthesized CA. The results revealed successful cellulose extraction and acetylation. CA synthesized by the green and standard acetylation methods presented degree of substitutions of 2.68 and 2.89, and yield of 60% and 40%, respectively. The dynamic Young's modulus and the storage modulus of the produced film were found to be 1.88 GPa and 1.89 GPa, respectively, and its operating range was limited to 140 °C. The environmental performance of the green approach was modeled via life cycle assessment and compared with a conventional approach. The life cycle assessment shows that the green approach is more advantageous than the conventional approach. The less use of chemicals throughout the pretreatment and acetylation steps of the green approach was critical to achieving environmental benefits. Results also indicate that the acetylation processes were the main contributors to environmental impacts, and the primary consumption of dichloromethane in the purification step significantly influences this negative outlook. Environmental savings for human toxicity and stratospheric ozone depletion could reach 27% and 90%, respectively, if DCM was recycled and used in subsequent cycles of acetylation. In addition, sensitivity analysis shows that the high yield obtained by the green acetylation was crucial to lowering environmental impacts.

**Keywords:** lignocellulosic biomass; agroindustrial residues; pretreatment; cellulose acetylation; life cycle assessment.

## 5.1. Introduction

The use of lignocellulosic residues as feedstock for bio-based applications has been increasing as a promising alternative for the functioning of modern industrial societies [1–3]. Their attractiveness as a capable sustainable source of biomaterials comes mainly from their low-cost, availability and chemical composition. An unending stream of lignocellulosic residue is derived from agricultural activities. For instance, in countries where prevails an agriculture-based economy, such as Brazil, United States, China and Africa, the annual availability of lignocellulosic residues achieves remarkable values. It is estimated that in Brazil an average of 108 million tonnes/year of agricultural residues are generated [4]. Although some industrial valorization techniques have already been implemented in this country, such as the production of second-generation ethanol and composites, the use of these residues is still very low, and they are usually inserted in the market as waste without added value, which eventually integrate the current paths of the linear waste management systems. In a recent publication, Araújo et al. [4] provided the availability of various crop and industry processing residues in Brazil, and highlighted, among others, the high generation of corncob, soybean straw, sugarcane top/leaves and rice straw. For instance, the generation of corncob is estimated to be approximately 18.700 kt/year, which is still used on a limited basis.

The agroindustrial residues are mainly composed by cellulose (50%), hemicellulose (20-40%) and lignin (10-40%) [5]. Cellulose is a basic structural component of plants and the most abundant renewable resource in nature. It is a high molecular weight homopolymer generated from repeating D-glucopyranose ring units linked by  $\beta$ -1,4-glycosidic bonds (cellobiose unit). Each glucose monomers within the cellulose chain present three hydroxyl groups positioned in the plane of the ring, which have a great influence on properties [6]. Due to the intra and intermolecular interactions of the hydroxyl groups presented in the cellobiose unit, the cellulose molecules crystallize in a horizontal plane and in parallel chains, forming microfibril packages. The elementary fibers that make up the microfibril packaging are basically organized into high order crystalline parts interspersed by amorphous regions. As a consequence of its structural organization, cellulose presents some properties that limit its application (e.g. lack of antimicrobial properties, high hydrophilicity and low dimensional stability high melting temperature). To overcome these drawbacks, cellulose is generally modified into derivatives. Due to its broad range of applications and easy processability, the modification of cellulosic biomass into cellulose acetate has been the most commonly explored approach. In 2015 the global cellulose acetate production reached the

astonishing value of 4.82 billion tones and the trend is upward [7]. While at large scale (industrial) cellulose acetate is synthesized primary from wood and cotton pulp via the acetic acid route (standard route), at experimental level (bench tests) the use of agroindustrial residues and environmentally friendly synthesis routes have been increasingly reported [8–13]. These alternative synthesis routes are mainly focused on replacing the sulfuric and acetic acids, used respectively as catalyst and reaction media in the standard acetylation, by eco-friendly reagents, such as iodine as catalyst in the presence of acetic anhydride [10, 12], phosphotungstic acid as catalyst [14], room temperature ionic liquid [13, 15] and solid superacid  $\text{SO}_2^4/\text{ZrO}_2$  [16]. However, despite the environmental benefits resulting from the application of these substituent reagents, the aforementioned studies almost unanimously made use of harsh chemicals and processing, such as the conventional alkali and bleaching pretreatment, to isolate the cellulose from the biomass. Since cellulosic fibers do not occur as an isolated component in the agroindustrial residues, instead they are bounded with other non-cellulosic materials which can negatively affect their physicochemical properties, as well as the modification and dissolution processes [8, 17, 18]. Thus, it is essential to apply fractionation techniques to extract the cellulose content prior to acetylation.

The fractionation techniques, also named as pretreatment methods, can be classified into four categories, namely physical, chemical, physicochemical and biological [5]. Currently, the pretreatment step is considered one of the main bottlenecks to the cost-effective valorization of agroindustrial residues. Its application may demand, besides high energy and material consumption, the use of harsh chemicals, which implies the production of excessive wastes. These led to the development of new approaches based on the “Green Chemistry” concept, among which it is worth to mention liquid hot water, steam explosion, organosolv and fine-tuned green solvents (deep eutectic solvent, ionic liquid and supercritical fluids) [19–22]. Recently, great attention has also been focused on combining pretreatments, as reported by Araújo et al. [23] and Sun et al. [24].

Although some studies have reported the application of less impacting pretreatments and acetylation techniques to synthesized cellulose acetate from lignocellulosic biomass [9, 14], for the best of our knowledge, there are no reports addressing the environmental performance modeling of these techniques. Therefore, life cycle assessment has been progressively used to analyze the environmental viability of bio-based products. Moreover, this analysis tool has proven to be reliable for the evaluation of environmental sustainability of products and methodologies within the

framework of lignocellulosic biomass valorization [25–27]. Hence, the purpose of this work is to use potential environmentally-friendly pretreatment and acetylation techniques to synthesize cellulose acetate from corncob and calculate the environmental impacts related to the applied process. The pretreatment method applied is described in a recent publication of Araújo et al. [23], who used a combined LHW-dilute NaOH solution treatment to pretreat biomass and obtained cellulose-enriched final samples with great yield. The acetylation step was based on the solvent-free method as suggested by Das et al. [10], since remarkable yields were obtained from the acetylation of rice husk. The environmental impact associated with this synthesis route was determined through life cycle assessment and compared with those associated with the conventional route, composed of alkali-bleaching pretreatment and acetic acid process acetylation. The specific objectives of this work are: (1) synthesize cellulose acetate by means of green and conventional approaches; (2) investigate the physical-chemical properties of both synthesized samples in order to assess their quality and suitability to be compared via LCA; (3) develop thin films from the cellulose acetate synthesized by the green approach to prove its potential application as a value-added product; (4) evaluate the environmental impacts resulting from the green approach in comparison to the current conventional approach to synthesize cellulose acetate.

## **5.2. Materials and methods**

### **5.2.1. Materials**

Corn cob was obtained from local agricultural cooperatives from the North of Portugal. The corn cob residue was firstly ground and sieved to particles sizes from 0.25 to 0.5 mm and stored in sealed plastic bags at room temperature. Cellulose sheets (cellulose pulp), provided by a local factory, were torn into small fragments and fibers and dried at 60 °C for 24 h. Cellulose acetate (Mn-50.000 by GPC) and Sodium hydroxide (NaOH) pellets were acquired from Sigma-Aldrich. Acetic anhydride (>99%) and sodium thiosulfate (Na<sub>2</sub>S<sub>2</sub>O<sub>3</sub>) (98.50%) were purchased from Acros Organics. Iodine (99.80%), acetic acid glacial (99.88%), sulfuric acid (H<sub>2</sub>SO<sub>4</sub>) (>95%), ethanol (99.80%), methanol (99.99%), dichloromethane (DCM) (99.88%) and dimethyl sulfoxide (99.99%) were purchased from Fisher Chemical. All the reactants were used without further purification.

### **5.2.2. Isolation of cellulose from corncob**

Cellulose extraction from dried milled corncob was carried out by applying a combined green pretreatment previously reported [23]. Briefly, a two-step process was performed by combining a

first stage-liquid hot water, followed by dilute NaOH solution treatment. The LHW was performed in a stainless steel cylindrical reactor with an approximate volume of 2 L and feedstock loading rate of 10% (residue weight / distilled water volume). The pretreatment was carried out at 190 °C, 0.79 MPa, for 30 min under constant mechanical stirring. After the insoluble solid was collected, thoroughly washed with deionized water and dried at 60 °C. Then, the dried liquid hot water-treated corncob (LHW - CC) was soaked in 2 wt% NaOH at 90 °C for 1.5 h at a 1/30 solid/liquid ratio (w/w) under magnetic stirring. The alkali treated LHW-CC (NaOH-LHW-CC) was then filtered and washed several times with deionized water until colorless. The resulting material was dried at 60 °C and stored in a sealed plastic bag.

### 5.2.3 Synthesis of cellulose acetate

Two different acetylation methodologies were carried out, one proposed herein, referred to as a green acetylation, which is based on the method described by Das et al. [10] with some modifications, and another one mentioned as standard acetylation (acetic acid process), which is a commonly used technique and presents similarities (at the level of chemical components used) with the methods applied at industrial level. Regarding the green acetylation, basically, 0.4 g of cellulose extracted from corncob was taken into a 100 mL round bottom flask, and 20 mL of acetic anhydride and 0.6 g of iodine were added. The mixture was heated to 80 °C and left reacting for 5 hours with stirring. After that, the solution was allowed to cool at room temperature and treated with 10 mL saturated solution of sodium thiosulfate with stirring, in order to reduce the iodine to iodide. Then, 60 mL of ethanol was added to the mixture and stirred for 60 min. The product was filtered and thoroughly washed with 75% (v/v) ethanol and distilled water to remove the unreacted acetic acid and byproducts. The solid material obtained was dried at 60 °C in an oven under vacuum and further dissolved in dichloromethane and filtered. Cellulose acetate was formed as a film inside the flask after evaporating the filtrate, which was easily removed without any additional treatment and dried at 60 °C in a vacuum oven overnight.

The standard acetylation applied is based on methods described by Jo et al. [28], Coletti et al. [29], Bello et al. [30] and Cao et al. [9], and was carried out, initially, by reacting the extracted cellulose at different cellulose:reagents ratio (w/w) with acetic acid (1:31.5), acetic anhydride (1:14) and sulfuric acid (1:0.08) in a 100 mL round bottom flask. The mixture was heated to 40 °C and magnetically stirred for 3 h. After that, the reaction was allowed to cool to room temperature, filtered and the filtrate was collected in a large beaker. Then, methanol was added,

and the mixture was stirred overnight at room temperature. Further, the solution was filtrated, and the cellulose acetate was collected in a paper filter and placed in Petri dishes evaporating dishes to evaporate and dry at 60 °C in a vacuum oven overnight. The obtained dried cellulose acetate was dissolved in dichloromethane, filtered and collected as a film after evaporating the filtrate. Then, it was dried at 60 °C in a vacuum oven overnight.

#### 5.2.4. Chemical characterization

FTIR spectra of pretreated corncob, cellulose pulp and cellulose acetate samples were recorded on a Jasco FT/IR-4100 spectrometer, in the wavelength range of 400 – 4000 cm<sup>-1</sup> and at a resolution of 4 cm<sup>-1</sup>, using the attenuated total reflection technique. Thermogravimetry analyses of untreated corncob extracted cellulose, cellulose pulp and CA samples were performed on TA Instruments SDT 2960 model. The sample weight was in the range of 5-10 mg and heated from 30 to 700 °C at a rate of 10°C/min, under purified argon to prevent thermo-oxidative degradation. The <sup>1</sup>H NMR spectroscopy using a Bruker Avance III, 400 MHz, and deuterated dimethyl sulfoxide as solvent. The spectra were internally referenced to the residual proton tetramethylsilane (TMS, δ = 0.00 ppm) and the chemical shifts (δ) are reported as part per million (ppm). Based on Biswas et al. [31], the average number of hydroxyl groups replaced by acetyl groups was determined from HNMR results and used for calculating the degree of substitution (DS) of synthesized CA samples. The DS was calculated by dividing 1/3 of the three methyl proton absorbance peak area of acetyl group, in the range of 1.5-2.2, by 1/7 of the seven anhydrocellulose absorbance peak area, in the range of 3.5-5.2 ppm (Equation 1).

$$DS = \frac{7 \times \int_{1.5}^{2.2} f(x) dx}{3 \times \int_{3.5}^{5.2} f(x) dx} \quad (1)$$

#### 5.2.5. Chemical composition of untreated and treated biomass

The chemical composition of the untreated and treated corncob was determined by deconvolution of the derivative curves obtained from the thermogravimetry analysis [23, 32–35]. Briefly, the decomposition processes of the three pseudo-components presented in the lignocellulosic biomass (cellulose, hemicellulose and lignin) were modeled by a Gaussian distribution and the percentage of each component was assumed to correspond to the integrated area above each single deconvoluted reaction curve (the modeled equation, as well as graphs and parameters are available in the Appendix A).

### 5.2.6. Cellulose acetate film preparation

Cellulose acetate films were prepared by the casting method. Initially, 50 mg of CA synthesized by the green approach was mixed with 6 g of DCM and stirred for 5 h at 35 °C. After that, the mixture was sonicated for 10 min in order to remove air bubbles. Then, the solution was poured on a Teflon dish with 4 cm of diameter and placed in the vacuum oven at 40 °C to allow the solvent to evaporate.

### 5.2.7. Morphological analysis

The surface morphologies of untreated and treated samples were observed by scanning electron microscopy (SEM) using a FEI Nova 200. Samples were previously sputter coated with gold.

### 5.2.8. Dynamic mechanical analysis

A Perkin Elmer DMA 800 Instrument was used at a dual-cantilever bending mode and at a constant frequency in order to obtain the storage modulus ( $E'$ ), the loss modulus ( $E''$ ) and the damping capacity ( $\tan \delta$ ), the later calculated as the ratio of the loss to the storage modulus [36]. CA Films with the size of 20/5.7/0.04 mm, approximately, were analyzed under temperature ranging from 40 – 160°C, heating rate of 5 °C/min, preload 1N, 10  $\mu$ m of displacement amplitude and 1 Hz of frequency. Dynamic Young's modulus ( $E^*$ ) was also determined by using Equation 2 [36].

$$E^* = \sqrt{(E')^2 + (E'')^2} \quad (2)$$

### 5.2.9. Life cycle assessment

#### 5.2.9.1. Goal and scope

LCA performed in this study aims to compare the environmental impact associated with two methods used to synthesize CA from corncob. The concerned methods are distinguished by their processing design; while one takes into account strategies under the green chemistry, the other employs the use of conventional techniques. Both product systems contemplate the production of materials and energy, as well as pollutants emission, accounted at the level of laboratory scale when recorded as primary data. Corncob production and process such as transport and wastewater treatment are not considered in this study. Transportation of residues and chemicals are also not considered since processing plants, in this scope of this manufacturing purpose, are still at the

laboratory stage, and consequently their locations have not yet been defined. Notwithstanding, in a scenario projected to facilitate and make feasible logistic issues, these industrial plants would be installed in proximity to companies that generate such wastes, and thus the transportation of residues at least could be disregarded. The functional unit adopted was the synthesis of 10 g of cellulose acetate. The comparison between product systems' LCA results in terms of the same FU was validated through the physical-chemical characterization performed previously.

#### 5.2.9.2. Modelling approach

LCA modeling was performed using the Open Life Cycle Assessment software (openLCA), developed by the GreenDelta and suitable to conducting sustainability assessment of products, process and services [37]. This study followed the guidelines specified in ISO14044 [38], and based on elucidations about LCI framework modelling presented in the International Reference Life Cycle Data System (ILCD) Handbook [39], it is considered an attributional LCA, with similarities, in scope, with studies presented by Arvidsson et al. [26] and Walser et al. [40]. As mentioned before, the cultivation, harvesting and processing of maize are not included within the system boundary as corncob is a by-product of maize with no market value, often disposed of or burned in the harvest field. Moreover, despite the potential application of the synthesized CA as a polymeric film (further presented in the subtopic 5.2.5), their processing and applicability have not been technically and economically defined yet, and therefore, the end-of-life of the material, as a commercial product, is also not included in the boundary system. Consequently, a gate-to-gate perspective is assigned to this study. As emphasized by Arvidsson et al. [26], this kind of perspective is particularly important for materials that might have many subsequent applications, of which some have not yet been developed.

#### 5.2.9.3. Scenarios description and life cycle inventory data

Two scenarios were modeled and assessed as shown in Figure 5.1. The one indicated as "Green Approach" (left branch in Figure 5.1) includes corncob milling, the combined LHW-Dilute NaOH pretreatment, green acetylation based on Das et al. [10], washing, drying and the respective inputs (water, electricity and chemicals) and outputs. The other mentioned as "Conventional Approach" (right branch in Figure 5.1), was modeled as a referential scenario since it encompasses the corncob milling, pretreatment and acetylation techniques conventionally applied. The detailed description of the combined LHW-Dilute NaOH pretreatment, the green acetylation and the



standard acetylation have already been presented in previous topics of materials and methods. When it comes to the conventional pretreatment (alkali and bleaching), it was not experimentally performed, but rather modeled according to Silvério et al. [41], Boonsombuti et al. [42] and Rosa et al. [43]. Succinctly, the milled dried corncob was treated with a sodium hydroxide aqueous solution of 2% (w/w) for 2h at 100 °C under magnetic stirring, and then filtered and washed with distilled water. After washing, the alkaline treatment was repeated, and the resulting material was dried overnight at 60°C in an oven. After this treatment, the fibers were bleached with a solution made up of equal parts (v:v) of acetate buffer (27g NaOH and 75 ml glacial acetic acid, dilute to 1 L of distilled water) and aqueous chlorite (1.7 wt% NaClO<sub>2</sub> in water). This treatment was performed at 80 °C for 6h. The bleached fibers were filtered, washed with distilled water and dried at 60 °C overnight. After the alkali-bleaching treatment, it was estimated a yield of 40%.

The inventory data related to all process here modeled was sourced from previously publications, life cycle assessment studies and Ecoinvent (version 3.3), as well as calculated experimentally. Inputs or process highlighted with an asterisk in the product system flow chart do not exist in Ecoinvent database, therefore they had to be modeled as individual process in Open LCA, based on background data from previously published studies. All assumptions made, as well as input and output associated with processes in both product systems, are described in detail in Appendix B.

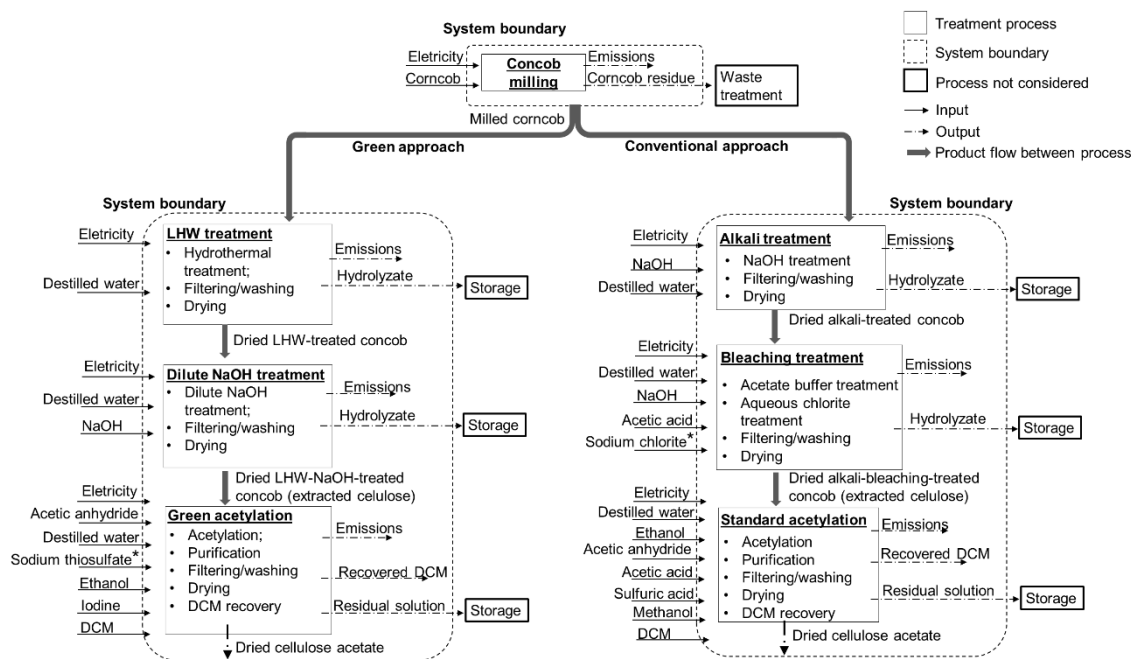


Figure 5-1. Flow chart of product systems: Left branch – modeled green approach scenario; right branch – modeled conventional approach scenario. Inputs highlighted with an asterisk do not exist in Ecoinvent database and had to be modeled in OpenLCA.

## 5.2.9.4 Impact categories

LCA impact categories, recommended under the International Reference Life Cycle Data System [39], relevant to the work, as already reported in similar studies and in accordance with the ISO 14044 [38], were used. The chosen categories, shown in Table 5.1, are segmented into non-toxicity, toxicity and resource related impact categories. In the absence of normalization references for Brazil, it was used global normalization references provided by Sala et al. [44], for the reference year of 2010. This limitation does not compromise the results (normalized impacts) since, at laboratory activity level, many chemical reagents are produced and supplied by foreigner companies. Moreover, in the absence of regional normalized factors it is preferable to use global factors, as some impact methods (such as CML 2002 and Usetox) present a global scope for the application of their impact categories. By using global values, it is also avoided an imbalance in normalization resulting from comparison with activities of different populations [45].

Table 5.1. Environmental impact categories and normalization references used. CFC: Chlorofluorocarbon, kBq: Kilobecquerel, NMVO: Non-Methane Volatile Organic Compounds; CTU: Comparative Toxicity Unit, e: Ecotoxicity, h: Human.

Impact category	Abbreviation	Method	Normalization reference	Unit
<i>Non-toxicity related impact categories</i>				
Global Warming Potential	GWP	IPCC 2013	8400	kg CO <sub>2</sub> -eq/person
Stratospheric Ozone Depletion	ODP	CML 2001 [46]	2.34x10 <sup>-2</sup>	kg CFC11-eq/person
Ionizing Radiation – Human Health	IR	ILCD 2016 [47]	4.220	kBq-U-235-eq/person
Photochemical Ozone Formation	POF	ReCiPe (H) [48]	40.6	kg-NMVO-eq/person
Freshwater Eutrophication	FE	ReCiPe (H) [48]	0.734	Kg P-eq/person
Marine Eutrophication	ME	ReCiPe (H) [48]	28.3	Kg N-eq/person
Terrestrial Acidification	TA	ILCD 2016 [47]	55.5	Mol H <sup>+</sup> -eq/person
Terrestrial Eutrophication	TE	ILCD 2016 [47]	177	Mol N-eq/person
Particulate Matter	PM	Selected LCI results [49]	2.76	Kg PM <sub>2.5</sub> /person
<i>Toxicity related impact categories</i>				
Human toxicity, Cancer Effect	HTc	USEtox [50]	3.75x10 <sup>-5</sup>	CTUh/person
Human Toxicity, non-Cancer Effect	HTnc	USEtox [50]	4.75x10 <sup>-4</sup>	CTUh/person
Freshwater Ecotoxicity	ET	USEtox [50]	1.18x10 <sup>-6</sup>	CTUe/person
<i>Resource impact categories</i>				
Depletion of Abiotic Resources - Fossil	Rf	Cumulative Exergy Demand [49]	6.54x10 <sup>6</sup>	MJ-eq/person

## 5.2.9.5. Sensitivity analysis

The sensitivity of the assessments' approaches was performed via scenario analysis. It was first modeled a scenario named as “intermediate approach” in order to assess the effect of changing the alkali-bleaching pretreatment at the conventional approach by the combined green

pretreatment. On impact categories, this change allows comparing the Influence of the two main processes (pretreatment and acetylation) on both product systems.

Moreover, taking into account the different acetylation yields reported in literature as a result of the application of the standard acetylation [10, 11, 30], improvements over the concerned technique, represented as a percentual increase in weight gain, were assumed. For this, all the process and parameters regarding the green pretreatment were kept unchanged and percentual increments of 10%, 20% and 30% were added upon the yield obtained experimentally for the standard acetylation (in the scope of the conventional approach). These changes gave rise to three scenarios with results presented as impact increment (in percentage) taking as baseline reference the green approach scenario. Through this, it is possible to assess the environmental viability of performing the green approach in face of possible variations in the standard acetylation yield.

## **5.3. Results**

### **5.3.1. Effect of combined pretreatment on corncob fractionation – compositional analysis**

The determined chemical composition of untreated corncob presented hemicellulose (47.32%), lignin (16.32%) and cellulose (36.35%) fractions similar to others in literature [41, 51]. Remarkable changes on chemical composition of corncob were verified after the combined pretreatment. The LHW caused the hydrolyze of hemicellulose and effectively solubilized around 90% of its original content, leading to a final product rich in cellulose and lignin. High levels of hemicellulose solubilization (over 90%) were also reported by Sbanci and Buyukkileci [52] and Michelin and Teixeira [53] in response to LHW treatment of lignocellulosic biomass. In the wake of this treatment, the dilute NaOH solution caused mainly the disruption of the lignin structure through the cleavage of intermolecular  $\alpha$ - and  $\beta$ -aryl ether linkages. The complementary effects of these pretreatments on fractionating the biomass contributed positively to obtain a solid cellulose-enriched final product (84.73%), with reasonably low amounts of hemicellulose (reduced by 90%) and lignin (reduced by 34.5%). This combined process converted the milled corncob into a fine, light gray and fluffy powder.

### **5.3.2. Cellulose acetate syntheses – degree of substitution and yield**

The acetylation methods performed in this study differ from each other since the chemical reagents used and the reactions mechanisms are dissimilar. Briefly, the green acetylation runs as

heterogeneous process in which, firstly, the iodine activates the carbonyl carbon of the acetic anhydride in the presence of an alcoholic group. Then, the acetic anhydride reacts with hydroxyl groups of cellulose and the esterification takes place, leading to the generation of acetic acid as a byproduct [10, 31]. Conversely, the standard acetylation occurs as a homogeneous process, set in through sulfate reaction in response to the catalytic effect of  $H_2SO_4$ , which helps to dissolve the cellulose pulp in the reaction media (acetic acid). Following, subsequent acetylation via displacement of hydroxyl with acetyl groups by acetic anhydride is triggered [54].

The applied synthesis methods gave different acetylation yields (calculated as dry weight percent gain), calculated as 60% for the green method and 40% for the standard. These results are comparable with others yields derived from the acetylation of cellulose-rich biomasses, such as rice husk (66%) [10], cotton stalk (48.5%) [30], cotton linters (54%) [55] and landscaping waste (45.6%) [9]. These indicate that the optimization of the synthesis using iodine as catalyst in the presence of acetic anhydride, proposed by Das et al. [10] for the acetylation of rice husk, also works out for the acetylation of corncob.

Figure 5.2 shows the  $^1H$  NMR spectra of CA synthesized from green (Figure 5.2a) and standard (Figure 5.2b) acetylation methods. Both spectra display typical resonances of CA chemical structures, with peaks in the region of 3.5-5.3 ppm related to the protons bonded to the seven ring protons of anhydroglucose (AGU) (indexes  $H_1$  to  $H_6$  in both graphs). The successful synthesis of CA by both methods was confirmed by the presence of peaks in the region 2.2-1.5 ppm, assigned to the methyl ( $CH_3$ ) of acetyl groups. The peak around 2.49 and 3.3 are related to the protons of DMSO and residual water, respectively. The DS of CA samples were calculated based on methodology previously described [31]. Both methodologies resulted in synthesized CA with high DS, namely 2.68 and 2.89 obtained by the green and by the standard, respectively. Cellulose acetate with DS varying from 2.5-3, synthesized from standard acetylation, or through few variations of this technique, was also obtained by Jo et al. [28], Coletti et al. [29], Candido et al. [8] and Cao et al. [9]. By varying parameters of the green acetylation method, Das et al. [10] synthesized cellulose acetate with DS ranging from 2.12 to 2.91. These results demonstrate that both methodologies originate CA with similar characteristics and in agreement with other studies.

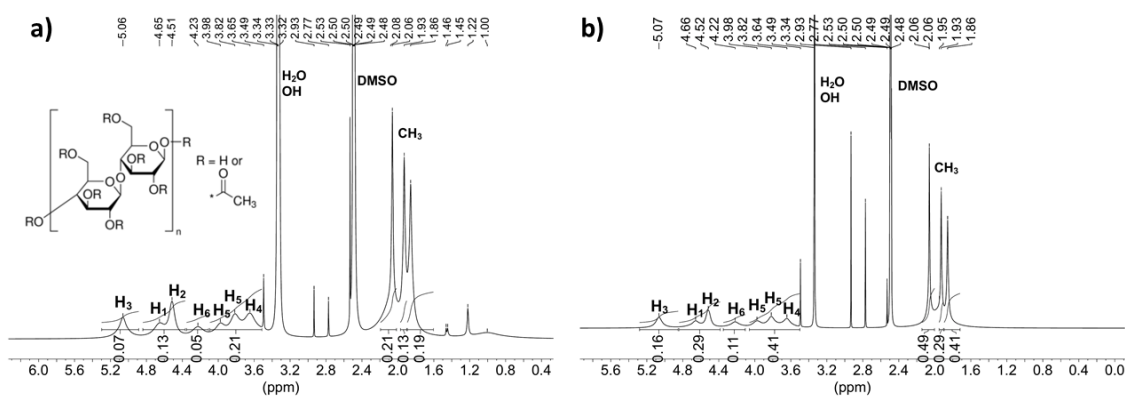


Figure 5-2. <sup>1</sup>H NMR spectra of cellulose acetate synthesized by (a) green and (b) standard acetylation methods.

### 5.3.3. Fourier Transformed Infrared analysis

The FTIR spectra of cellulose pulp, corncob extracted cellulose (through combined green pretreatment), CA commercial, as well as the CA synthesized from green and standard acetylation methods are presented in Figure 5.3. The absorbed peaks in corncob extracted cellulose around 2890 cm<sup>-1</sup> (C-H stretching in cellulose-rich material), 1431 cm<sup>-1</sup> (CH<sub>2</sub> banding vibration in cellulose), 1368 cm<sup>-1</sup> (C-H asymmetric deformation in cellulose), 1315 cm<sup>-1</sup> (CH<sub>2</sub> wagging in cellulose), 1161 (asymmetric C-O-C stretching), 1102 cm<sup>-1</sup> (C-OH skeletal vibration), 1028 cm<sup>-1</sup> (C-O-C pyranose ring skeletal vibration) and 897 cm<sup>-1</sup> (C-H deformation), typical of cellulose-rich materials [17, 56–59], confirm the effectivity of the combined green pretreatment performed in fractionating the corncob and extracting cellulose. Besides, the absence of peaks around 1598, 1513 (aromatic ring stretch ascribed to lignin) and 1250 (C-O stretching in the aryl group of lignin and acetyl group in hemicellulose), related to non-cellulosic polysaccharides [17, 57], highlight the efficiency of the pretreatment in removing lignin and hemicellulose.

The presence of absorbed peaks related to the cellulose chemical structure, along with the rising of new absorption peaks in acetylated samples, namely 1734 cm<sup>-1</sup>, 1368 cm<sup>-1</sup> and 1217 cm<sup>-1</sup> related to C=O stretching of ester group, C-H in O(C=O)-CH<sub>3</sub> and C-O stretching of acetyl groups, respectively, confirm the successful acetylation of corncob extracted cellulose. Moreover, the reduced intensity of peaks assigned to -OH stretching also provides evidence of acetylation, since it results from the substitution of -OH groups in cellulose by acetyl groups. Lately, the definitive proof of the successful synthesis of cellulose acetate by both methods is taken from the comparative analysis (peak-by-peak) between the synthesized CA samples and the CA commercial. The absence of absorption peaks around 1700 cm<sup>-1</sup> and 1760-1840 cm<sup>-1</sup> indicates that the obtained synthesized CA are free of acetic acid and unreacted acetic anhydride [10, 11, 33].

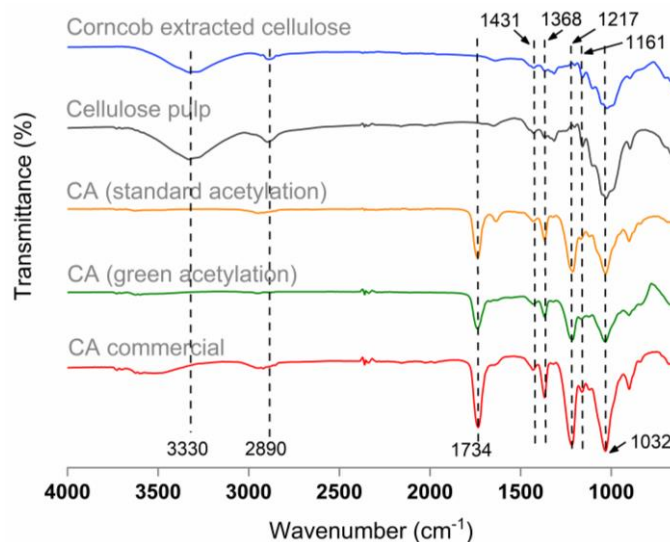


Figure 5-3. FTIR spectra of cellulose pulp, commercial CA, extracted cellulose (LHW-dilute NaOH pretreatment) and CA synthesized by green and standard acetylation.

#### 5.3.4. Thermogravimetric analysis

The TG and DTG curves of all samples are presented in Figure 5.4a and 5.4b, respectively. In general, degradation reactions observed in all curves occurred in a single step and in a narrow temperature range, allowing to infer that all samples are composed mainly by a unique component. The onset ( $T_{\text{onset}}$ ) and end ( $T_{\text{end}}$ ) temperatures of both synthesized cellulose acetate samples are identical ( $T_{\text{onset}} = 320 \text{ }^{\circ}\text{C}$ ,  $T_{\text{end}} = 366 \text{ }^{\circ}\text{C}$ ), and their maximum weight loss rate ( $T_{\text{max}}$ ) slightly differ, as shown in Figure 5.4 and Table 5.2. Taking into account the error associated with measurement, these results clearly show that, notwithstanding the different acetylation techniques applied, the thermal stability of synthesized CA samples is very similar. Furthermore,  $T_{\text{onset}}$  and  $T_{\text{max}}$  of synthesized samples are slightly higher than that of the commercial CA, probably due to their higher DS or to the origins of precursor materials. As evidenced by Cao et al. [60] and Morgado and Frolline [61], the thermal stability of CA samples increases as the DS value increases. This can be explained by the fact that, as DS increases more acetyl groups are introduced onto the C2 and C3 carbons of the anhydroglucose unit (AGU), which require more energy, when compared to the least sterically hindered group  $\text{C6COOCH}_3$ , and increase the apparent activation energy for thermal decomposition, leading to an increase in thermal stability [61].

The most remarkable changes on thermal profiles are verified when comparing the extracted cellulose profiles with the synthesized CA curves. The onset and end temperatures of the extracted cellulose ( $T_{\text{onset}} = 294 \text{ }^{\circ}\text{C}$ ,  $T_{\text{end}} = 361 \text{ }^{\circ}\text{C}$ ) are higher than those of CA obtained by both acetylation methods (Figure 5.4 and Table 5.2). Likewise, the temperature of maximum weight loss rate

related to the extracted cellulose (363 °C) is higher than that of synthesized samples (CA green acetylation – 350 °C; CA standard acetylation – 347 °C). These indicate that the thermal stability of the extracted cellulose decreased due to acetylation, which is in agreement with the literature [60, 62].

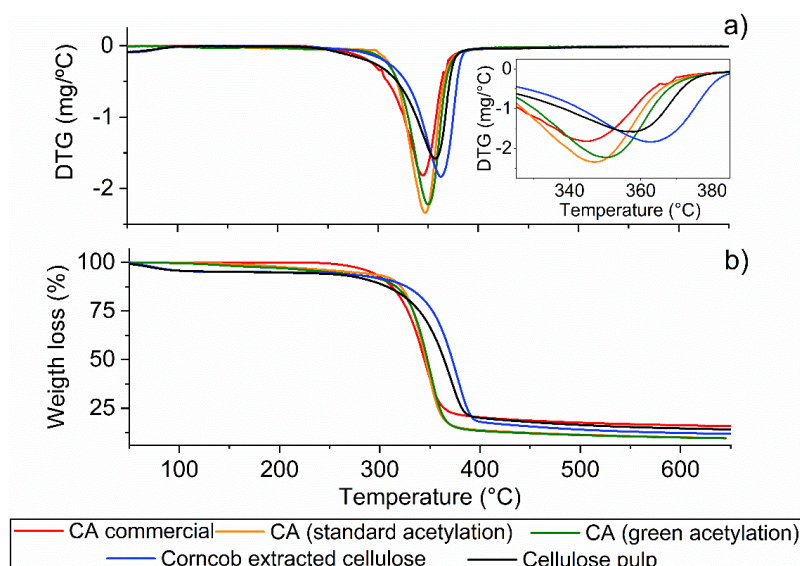


Figure 5-4. (a) TG and (b) DTG (as well as inset plot in the graph 4b of DTG ranging from 330 °C to 390 °C) curves of cellulose pulp, commercial CA, extracted cellulose (LHW-dilute NaOH pretreatment) and CA synthesized by green and standard acetylation.

Table 5.2. Thermogravimetric results for cellulose pulp, commercial CA, extracted cellulose (LHW-dilute NaOH pretreatment) and CA synthesized by green and standard acetylation.  $T_{onset}$ : onset temperature,  $T_{max}$ : temperature of maximum weight loss rate,  $T_{end}$ : end temperature.

Sample	DS	$T_{onset}$ (°C)	$T_{max}$ (°C)	$T_{end}$ (°C)
CA commercial	2.4	310	345	361
Cellulose pulp	0	327	357	383
Corncob extracted cellulose	0	242	363	392
CA (green acetylation)	2.68	320	350	366
CA (standard acetylation)	2.86	320	347	366

The thermogravimetry analysis, along with the previous chemical characterization, were performed first and foremost to investigate the properties of cellulose acetate produced from both synthesis route and assess their suitability to be compared via LCA, which was successfully confirmed. Upon reaching this target of the work, the next following two topics will be mostly dedicated to the elucidations about the potential application of the CA produced by the green approach as a film forming.

### 5.3.5. Scanning Electron Microscopy Analysis

A thin film of cellulose acetate synthesized by from the green approach was produced in order to demonstrate the potential of this material for industrial applications. SEM images of the raw corncob, LHW-NaOH pretreated corncob, as well as the cellulose acetate film surface and cross-section are presented in Figure 5.5.

As a result of the combined green pretreatment, the rigid and layered assembled structure of the corncob (Figure 5.5a) was unpacked and a remarkable disaggregation of fibers is noticed (Figure 5.5b). After the acetylation of extracted cellulose and subsequent dissolution, the quite smooth, flat and homogeneous surface of the produced film (Figure 5.5c and 5.5d) hardly assemble the disparate fibrous shapes of the extracted cellulose (Figure 5.5b). This indicates that the acetylation reaction successfully occurred, and reagents used could penetrate into the cellulose fibers. The few porous and rough surface in the cross section and film surface may be attributed to the solvent evaporation process.

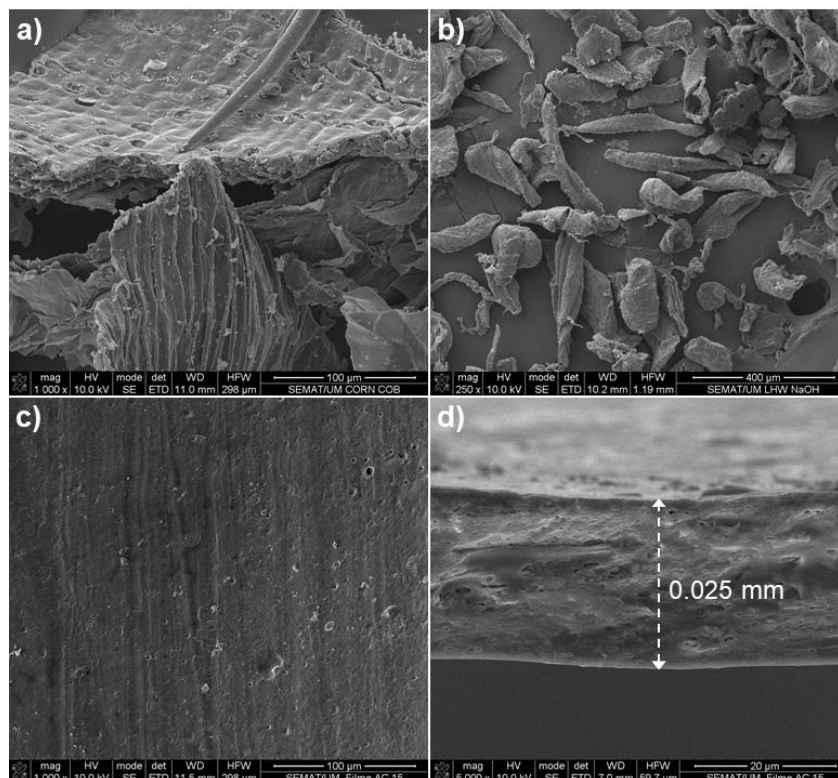


Figure 5-5. SEM micrographs of (a) untreated corncob, (b) LHW-dilute NaOH pretreated corncob, as well as the (c) surface and (d) cross-section of the cellulose acetate film.



### 5.3.6. Dynamic mechanical analysis

The viscoelastic behavior of the produced film was investigated by dynamic mechanical analysis (Figure 5.6a). The acetylation reaction, as well as the cellulose acetate film prepared, are depicted in Figure 5.6b. The viscoelastic properties of the film were characterized by the storage modulus (a measure of the material's ability to recover from deformation), the loss modulus (a measure of the material's ability to lose energy as heat) and the  $\tan \delta$  or damping (an indicator of how efficiently the material loses energy to molecular rearrangement and internal friction). The behavior of  $E'$  and  $E''$  in Figure 5.6a is typical of amorphous thermoplastics, as no defined transition zones are identified, but rather a continuous decrease along the temperature range. This can be associated to the introduction of acetyl groups onto the AGU unity, which prevent the packaging of cellulose chains and the resultant polymer becomes more amorphous and less opaque [63]. At lower temperatures, despite the presence of a secondary relaxation, the molecules are reasonably immobile and remain in an energy elastic state, which was characterized by a drop in  $E'$  of about 0.8 GPa over the temperature range 40-138 °C. This is followed by an intermediate state, the glass transition, characterized by a sharp drop in  $E'$  of about 0.8 GPa in a short temperature range 138-152 °C, and further by an entropy elastic state at elevated temperatures. For this class of material, the operating range is usually defined by the glass transition temperature, which was found to be 140 °C, approximately, using the peak of  $\tan \delta$  curve method. Similar  $T_g$  values of other cellulose acetate films were reported by de Freitas et al. [63], Bao et al. [64], Abdel-Naby et al. [65] and Számel et al. [66]. However, the  $T_g$  found may differ from others in literature since this property is intrinsically related to the DS, and higher DS leads to a lower  $T_g$ .

The  $E''$  reaches the maximum dissipated energy at 136 °C, which means that the mechanical deformation applied is converted into the maximum internal friction and nonelastic deformation. From this point until 160 °C the storage modulus drops roughly one decade. A broad secondary peak in  $E''$  is also verified at about 64 °C. In response there is a decrease in  $E'$  from 40 °C to 100 °C, probably originated from the natural mobility of chains in response to temperature rising and relaxation transitions triggered by local mobility of chains plasticized with water [67].

The storage modulus of the produced film, at 50 °C, is 1.88 GPa, which is higher than the  $E'$  value of a commercial one (1.58 GPa) with DS of 2.48, as reported by de Freitas et al. [63]. Furthermore, at a temperature close to 160 °C the cellulose acetate film produced presents a rather significant  $E'$ , with value around 178 MPa, demonstrating excellent processing conditions and high resistance. Despite the dynamic Young's modulus calculated from DMA is not exactly the

same as Young's modulus (elastic modulus) resultant from the classic stress-strain curve, they are ideally equivalent so that their comparison does not commit the interpretation of results. From literature, commercial cellulose acetate is known to have elastic modulus varying from 600-3000 MPa, depending on the DS and the average molecular weight [65]. By applying Equation 2, at 40 °C the  $E^*$  of the produced film is equivalent to 1.89 GPa, which is consistent with the previously mentioned range of values. The similar values of  $E'$  and  $E^*$  come from the prevailing elastic property of the film. Notwithstanding, at 40 °C the material runs through an increase of the atomic vibration yet, which, in turn, may decrease the stress needed to produce a given strain. Thus, these results suggest that the cellulose acetate film produced via a green approach, using corncob residue as a material source, could be potentially used in value-added applications, such as packaging.

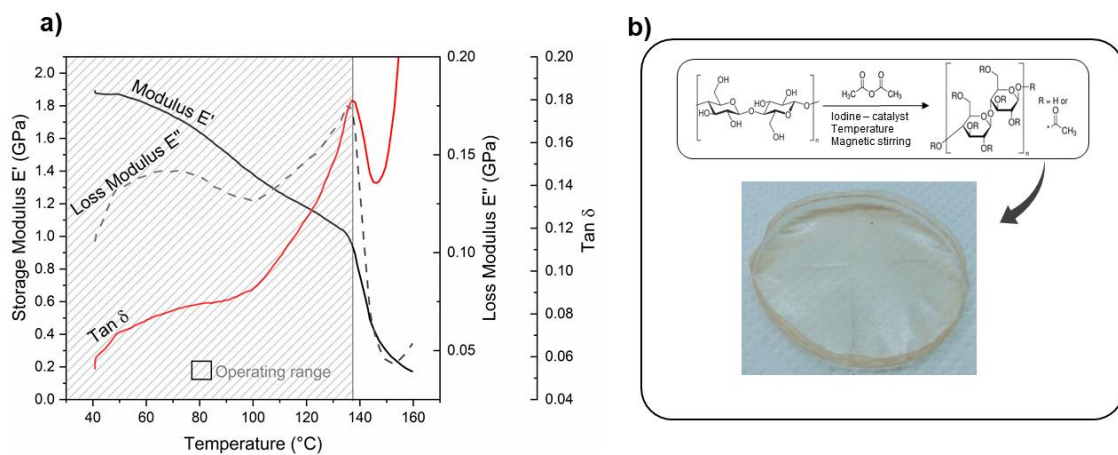


Figure 5-6. (a) Dynamic mechanical analysis of cellulose acetate film produced and (b) cellulose acetate film.

### 5.3.7. Life Cycle assessment

The overall environmental impact categories of conventional and green approaches, considering the functional unit of 10 g of synthesized cellulose acetate, are compared in Figure 5.7a. The LCA results show that, except for ET, the proposed green approach exhibited lower environmental impacts for all categories. This is the result of the lowest energy consumption and chemical throughout the green pretreatment and acetylation steps, which, in percentage terms, resonated in a reduction of impacts varying from 4% (fossil resources depletion) to 19% (ionizing radiation). The higher ET impact associated with the green approach were caused mainly by copper emissions involved in the production of acetic anhydride. In the green acetylation method this reagent is used in amount over four times greater than the amount deployed in the standard acetylation.

The acetylation processes were the main contributors to environmental impacts in both approaches, mainly due to their energy-demanding characteristic and chemicals used. The

following aspects/process were identified as having major influences on environmental impacts of conventional approach: electricity consumption (related to the standard acetylation process) > alkali and bleaching treatment (chemicals used and electricity consumption) > dichloromethane consumption (purification step) > ethanol consumption. The proportional contribution of individual processes associated with the green approach can be found in Figure 5.7b. The overall impact analysis for this approach also shows that the electricity consumption related to the acetylation process is the main contributor to environmental burdens, followed by the chemicals used throughout the acetylation (being the ethanol and acetic anhydride consumption the most prominent contributors), dichloromethane consumption in the purification step and, lastly, the combined green pretreatment. The proportional impacts of corncob milling were also accounted, but its contribution to the global impacts was too low to be evidenced in Figure 5.7b. As the precedence of aspects/process for both approaches were drawn up on the basis of an overall LCA analysis, they might slightly vary in some impact categories, though. By comparing both approaches within the order of precedence dictated by the process/aspects' contribution impacts, it is possible to verify that, not surprisingly, significant environmental savings could be achieved through the reduction on electricity and chemicals in the pretreatment stage. The effective savings provided by the green pretreatment are discussed in more detail further in the sensitivity analysis. Furthermore, it is interesting to note that the combined green pretreatment contributed more than 20% only for three impact categories, namely IR, FE and PM, (Figure 5.7b). These categories are particularly affected by impacts related to energy generation, which coherently agree with the energy-demanding characteristic of the LHW treatment. Comparatively to the combined green pretreatment, the proportional contribution of the alkali-bleaching pretreatment on each impact categories is substantially greater. For the same impact categories referred previously (IR, FE and PM) the conventional pretreatment accounted roughly for 33%, 29% and 29% respectively of their total impacts.

Besides, in previous studies Boonterm et al. [25] and Dedpakdee et al. [68] have shown that, in comparison to hydrothermal treatments, concentrate NaOH solution can lead to higher potential impacts on toxicity (HTc, HTnc and ET). Consistently with these findings, the dilute NaOH solution here applied reduced significantly impacts in the context of toxicity, and showed lower impacts on HTc, HTnc and ET than that of the LHW treatment by 43%, 42% and 43%, respectively. Moreover, within the framework of the conventional approach, the alkali-bleaching pretreatment had relevant

influence over these ecotoxicity categories and affected the impacts on HTc and ET by 20% and 26%, respectively.

It is worth mentioning that, within the acetylation process are also computed the impacts related to the recovery of dichloromethane. At the laboratory scale level its recovery was possible and can represent an overriding strategy in view of environmental gains. For instance, the primary consumption of dichloromethane leads to a significant impact share for ODP, HTc, GWP, ME and TE. Particularly for HTc and ODP, classified as some of the largest impact categories when expressed in person-equivalents (Figure 5.8), the primary dichloromethane consumption contributed roughly with 33 and 98%, respectively, in both approaches. Assuming a recovery rate of dichloromethane at about 80% (estimated experimentally in laboratory) when performing the green approach processing, the savings for HTc could reach 27%. In addition, by using recovered dichloromethane ultimately reduces atmospheric emissions of carbon dioxide and methane originated from its production, which also substantially imparts environmental negative impacts on the GWP and POF. Therefore, the recovery and recyclability of dichloromethane is an effective way to reduce the environmental footprint of subsequent acetylation cycles.

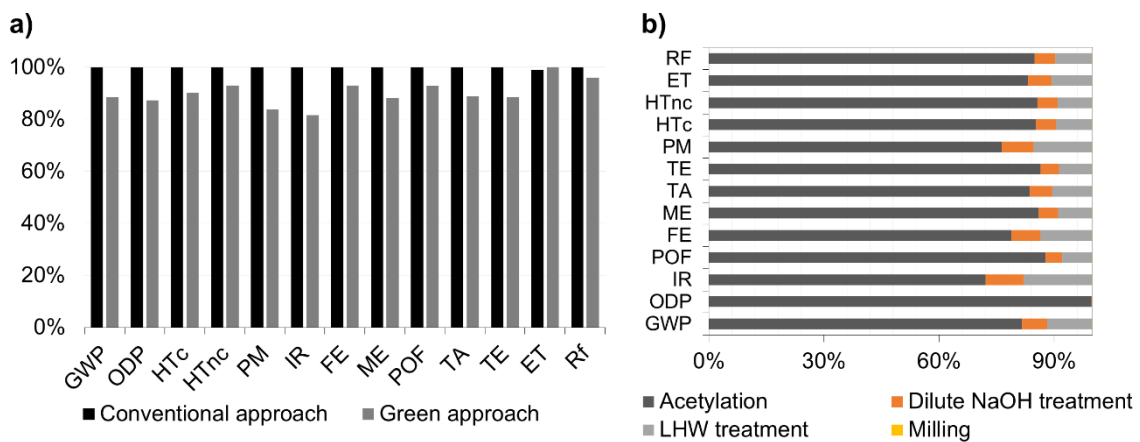


Figure 5-7. (a) Potential environmental impacts of cellulose acetate synthesized by green and conventional approaches and (b) proportional contributions of green approach processing steps on each environmental impact category.

By dividing the LCA results of each impact categories by their correspondent normalization reference, their characterized values are adjusted to a notionally common scale – person-equivalents (PE) – that means the fraction of the contribution to the concerned impact deriving from the average person in the reference geographical area. Thus, these normalized values can give information on impacts' magnitude and enable comparison of different impact categories. From Figure 5.8, it is clear that the magnitude of HTc is much higher than that of the other

categories. The main aspect enclosed to potential impacts over human toxicity (with carcinogenic effects) deals with the emission at long-term of chromium VI to groundwater, resulting from the landfilling of residual materials originated in dichloromethane and electricity production. In the conventional approach this impact is compounded by the effects associated with the pretreatment used. The large magnitude of impact also seen on freshwater eutrophication is mainly affected by the emission at long-term of phosphate resulting from the landfilling of residual material originated from fossil fuel energy production and chemicals production. Especially for the conventional approach, it is also resultant from the pretreatment step and chemicals used in the acetylation (namely acetic acid and anhydride acetic). Taking into account also the marked magnitude of HTnc, it is reasonable to infer that both processing approaches contributed the most to toxicity related impact categories. More precise information on this regard could be obtained by performing weighting, but this step is not in the scope of the study. By contrast, the lower magnitude of categories IR, ME and TE, in both approaches, are partially raised from the processing design and requirements in its core, as well as from the system boundary assumed, which ultimately limited the inputs and consequential outputs linked to the occurrence of environmental aspects with repercussion on such impacts.

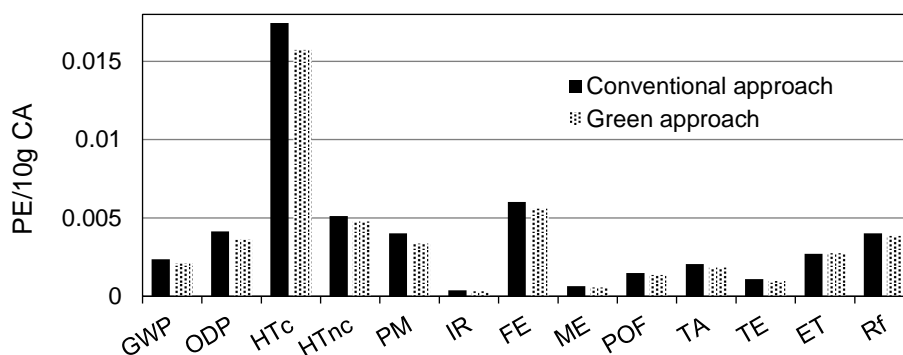


Figure 5-8. Potential impact contribution in PE/10g of cellulose acetate of the green and conventional approach.

#### 5.3.7.1. Sensitivity Analysis

A sensitivity analysis based on comparison of scenarios was conducted to investigate the specific contribution of acetylation and pretreatment process over the impact categories. For this, an additional scenario, referred to as intermediate approach, was modeled by setting up the combined green pretreatment preceding the standard acetylation. The following discussion will be carried out taking as reference the green approach impacts, since it sets a lower limit for all impact categories, except for ET. From Figure 5.9 it is noticeable that the enlargement of impacts over

ODP, TA, TE and Rf are independent of the pretreatment applied, indicating that they come almost entirely from the standard acetylation process. Conversely, the alkali-bleaching pretreatment step was the main contributor to increase the HTnc and FE impacts. For all other impact categories, the extent of impacts is almost equally provided by both process (conventional pretreatment and standard acetylation), other than for a slightly superior contribution assigned to the standard acetylation. The findings drawn from this analysis support the previous discussion and makes clear that the application of green pretreatments is an obvious way to reduce negative environmental impacts, although its gains may not extend to all impact categories. Additional savings can be achieved by reducing the use of chemicals, as afforded by the green acetylation, or through recovery of solvents. Last, but certainly not least, reducing energy consumption might be the most effective way to reduce the environmental footprint of the concerned process. However, this has been reported to be a challenge when it comes to biomass valorization [25, 26, 69], and the most obvious way to manage this bottleneck seems to be the use of integrated renewable energy sources, as suggested by Yates et al. [70].

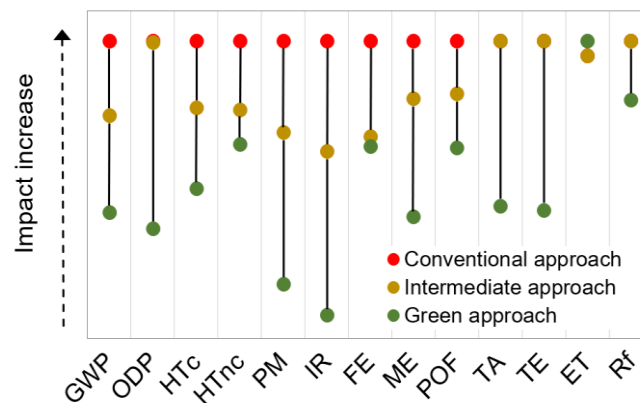


Figure 5-9. Influence of pretreatments and acetylation techniques on environmental impacts. Comparison of reference scenarios with Modeled intermediate one constituted by LHW-dilute NaOH pretreatment and acetic acid acetylation process.

The sensitivity of the LCA results regarding the overall advantages of the green approach in comparison to the conventional approach was also tested via a different perspective. As stated previously, the yield of green acetylation is 12.5% greater than that of standard acetylation. Considering that both approaches are assessed under the same functional unit, this yield gap has a direct influence on the amount of raw material (corn cob) to be processed and consequently on the number of chemicals and electricity consumed, which means that the lower the yield, the greater the need for inputs. However, the yield of the standard acetylation is susceptible to optimization by slightly changing the reaction parameters, as reported by Bello et al. [30]. Thus,

potential perspective scenarios for the conventional approach were modeled by varying its acetylation weight gain from 40% to 70%, and named as WG-40%, WG-50% and so on, as presented in Figure 5.10. By conducting this assessment is possible to ascertain to what extent the green approach (baseline scenario) remains environmentally viable in face of a possible optimization of the standard acetylation processing.

The LCA sensitivity analysis for each impact category associated with all modeled scenarios is reported in Figure 5.10. Taking as baseline scenario the green approach, by comparison, a positive impact increment indicates a negative environmental effect, while a negative impact increment indicates a positive effect. Results indicate that, although both processes have a quite similar environmental footprint in the assumption of same yield (WG-60%), the performance of the conventional approach only exhibits overall positive environmental effects for weight gains  $\geq 70\%$ . Along with the results previously discussed, this analysis clearly indicates that, in comparison to the standard acetylation synthesis, the key factors to lower the environmental impacts resulting from the green acetylation are the high yield obtained and not use acetic acid as reaction media. The attempts made in previous works to substitute the traditional catalyst  $\text{H}_2\text{SO}_4$  by eco-friendly ones, could not be deeply investigated here since, based on the FU adopted, this chemical was used in little quantity which could have masked its pollution effects.

Nevertheless, even with a weight gain of 70% the conventional approach still results in superior environmental burdens for IR and PM, and notwithstanding the prospective analysis, the green acetylation may also be subject of optimization, as shown by Das et al. [10], who successfully varied the acetylation yield as a function of the acetylation time and iodine amount. It is also important to bear in mind that environmental impacts related to the green pretreatment would probably be reduced when scaling-up this processing step, mainly due to the higher cellulosic fiber yielding produced per electricity consumed [25].

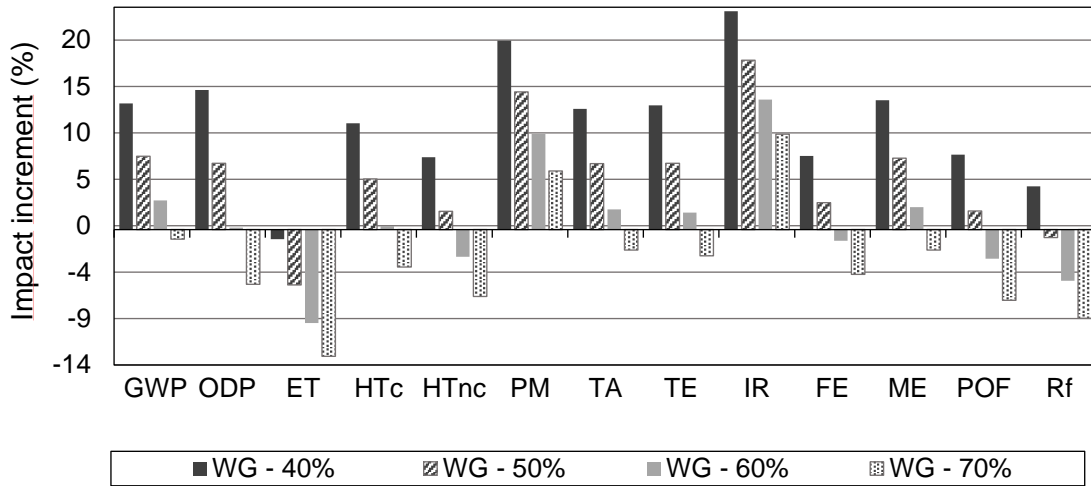


Figure 5-10. Potential impact differences in all categories due to possible changes in the acetylation yield of the conventional approach. Impact increment was calculated taking as baseline scenario the green approach. WG means weight gain.

#### 4. Conclusions

Cellulose was successfully extracted and cellulose acetate was synthesized from corncob by applying a green approach, constituted by a combined LHW-dilute NaOH pretreatment and iodine-catalyzed acetylation free of solvent. The outstanding physicochemical properties of the synthesized cellulose acetate endorse its use as a value-added product, which was proved by the preparation of a thin film with remarkable mechanical properties. The effective fractionation and cellulose extraction capacity of the pretreatment was confirmed via chemical composition analysis and backed up by the high DS (2.68) and yield (60%) obtained after the acetylation. Along with the high yield of acetylation, the less use of chemical reagents associated with the green approach were key aspects within its environmental benefits. In comparison with a current conventional approach, the environmental sustainability of the proposed green route was confirmed through life cycle assessment. Overall LCA results revealed that the proposed green approach exhibited lower environmental impacts than the conventional approach for all categories, except for ET. Moreover, in both approaches the acetylation process accounted for the main share of impacts, which was in part due to the length of the process and the consequent amount of electricity required. In general, the most obvious way to improve even more the proposed processing design relies on the use of integrated renewable energy sources and recycling of solvents, namely DCM. Although there are few studies regarding these addressed subject for comparison purpose, the data used fulfilled the requirements of the LCA and the obtained outcome is reliable.



## Acknowledgements

This work was supported by the Brazilian National Council for Scientific and Technological Development (Grant number 201940/2015-9). The authors also acknowledge the Portuguese Foundation of Science and Technology (TSSiPRO-technologies for sustainable and smart innovative products-norte-01-0145-FEDER-000015) and UID/CTM/50025/2019 for the financial support.

## Reference

1. Iqbal, N.M.H., Kamal, S.: Economical Bioconversion of Lignocellulosic Materials to Value-Added Products. *J. Biotechnol. Biomater.* 02, (2012). <https://doi.org/10.4172/2155-952x.1000e112>
2. Anwar, Z., Gulfraz, M., Irshad, M.: Agro-industrial lignocellulosic biomass a key to unlock the future bio-energy: A brief review. *J. Radiat. Res. Appl. Sci.* 7, 163–173 (2014). <https://doi.org/10.1016/j.jrras.2014.02.003>
3. Isikgor, F.H., Becer, R.: Lignocellulosic biomass: a sustainable platform for the production of bio-based chemicals and polymers. *Polym. Chem.* 6, 4497–4559 (2015). <https://doi.org/10.1039/c5py00263j>
4. Araújo, D.J.C., Machado, A. V., Vilarinho, M.C.L.G.: Availability and Suitability of Agroindustrial Residues as Feedstock for Cellulose-Based Materials: Brazil Case Study. *Waste and Biomass Valorization.* 16 (2018). <https://doi.org/10.1007/s12649-018-0291-0>
5. Hassan, S.S., Williams, G.A., Jaiswal, A.K.: Emerging technologies for the pretreatment of lignocellulosic biomass. *Bioresour. Technol.* 262, 310–318 (2018). <https://doi.org/10.1016/j.biortech.2018.04.099>
6. Klemm, D., Heublein, B., Fink, H.P., Bohn, A.: Cellulose: Fascinating biopolymer and sustainable raw material. *Angew. Chemie - Int. Ed.* 44, 3358–3393 (2005). <https://doi.org/10.1002/anie.200460587>
7. Research, Z.M.: Cellulose Acetate Market (Cellulose Acetate Tow and Cellulose Acetate Filament) for Cigarette Filters, Textile & Apparel, Photographic Films, Tapes & Labels, Extrusion & Molding and Other Applications - Global Industry Perspective, Comprehensive Analysis. (2016)
8. Candido, R.G., Godoy, G.G., Gonc, A.R.: Characterization and application of cellulose

- acetate synthesized from sugarcane bagasse. *Carbohydr. Polym. j.* 167, 280–289 (2017). <https://doi.org/10.1016/j.carbpol.2017.03.057>
9. Cao, L., Luo, G., Tsang, D.C.W., Chen, H., Zhang, S., Chen, J.: A novel process for obtaining high quality cellulose acetate from green landscaping waste. *J. Clean. Prod.* 176, 338–347 (2018). <https://doi.org/10.1016/j.jclepro.2017.12.077>
  10. Das, A.M., Ali, A.A., Hazarika, M.P.: Synthesis and characterization of cellulose acetate from rice husk: Eco-friendly condition. *Carbohydr. Polym.* 112, 342–349 (2014). <https://doi.org/10.1016/j.carbpol.2014.06.006>
  11. Wan Daud, W.R., Djuned, F.M.: Cellulose acetate from oil palm empty fruit bunch via a one step heterogeneous acetylation. *Carbohydr. Polym.* 132, 252–260 (2015). <https://doi.org/10.1016/j.carbpol.2015.06.011>
  12. Biswas, A., Shogren, R.L., Willett, J.L.: Solvent-free process to esterify polysaccharides. *Biomacromolecules.* 6, 1843–1845 (2005). <https://doi.org/10.1021/bm0501757>
  13. Cao, Y., Wu, J., Meng, T., Zhang, J., He, J., Li, H., Zhang, Y.: Acetone-soluble cellulose acetates prepared by one-step homogeneous acetylation of cornhusk cellulose in an ionic liquid 1-allyl-3-methylimidazolium chloride (AmimCl). *Carbohydr. Polym.* 69, 665–672 (2007). <https://doi.org/10.1016/j.carbpol.2007.02.001>
  14. Fan, G., Wang, M., Liao, C., Fang, T., Li, J., Zhou, R.: Isolation of cellulose from rice straw and its conversion into cellulose acetate catalyzed by phosphotungstic acid. *Carbohydr. Polym.* 94, 71–76 (2013). <https://doi.org/10.1016/j.carbpol.2013.01.073>
  15. Wu, J., Zhang, J., Zhang, H., He, J., Ren, Q., Guo, M.: Homogeneous acetylation of cellulose in a new ionic liquid. *Biomacromolecules.* 5, 266–268 (2004). <https://doi.org/10.1021/bm034398d>
  16. Yan, L., Li, W., Qi, Z., Liu, S.: Solvent-free synthesis of cellulose acetate by solid superacid catalysis. *J. Polym. Res.* 13, 375–378 (2006). <https://doi.org/10.1007/s10965-006-9054-x>
  17. Reddy, K.O., Maheswari, C.U., Dhlamini, M.S., Mothudi, B.M., Zhang, J., Zhang, J., Nagarajan, R., Rajulu, A.V.: Preparation and characterization of regenerated cellulose films using borassus fruit fibers and an ionic liquid. *Carbohydr. Polym.* 160, 203–211 (2017). <https://doi.org/10.1016/j.carbpol.2016.12.051>
  18. Abdulkhani, A., Hojati Marvast, E., Ashori, A., Karimi, A.N.: Effects of dissolution of some lignocellulosic materials with ionic liquids as green solvents on mechanical and physical

- properties of composite films. *Carbohydr. Polym.* 95, 57–63 (2013). <https://doi.org/10.1016/j.carbpol.2013.02.040>
19. Farrán, A., Cai, C., Sandoval, M., Xu, Y., Liu, J., Hernáiz, M.J., Linhardt, R.J.: Green Solvents in Carbohydrate Chemistry: From Raw Materials to Fine Chemicals. *Chem. Rev.* 115, 6811–6853 (2015). <https://doi.org/10.1021/cr500719h>
  20. Bhutto, A.W., Qureshi, K., Harijan, K., Abro, R., Abbas, T., Bazmi, A.A., Karim, S., Yu, G.: Insight into progress in pre-treatment of lignocellulosic biomass. *Energy.* 122, 724–745 (2017). <https://doi.org/10.1016/j.energy.2017.01.005>
  21. Mamilla, J.L.K., Novak, U., Grilc, M., Likozar, B.: Biomass and Bioenergy Natural deep eutectic solvents ( DES ) for fractionation of waste lignocellulosic biomass and its cascade conversion to value-added bio-based chemicals. *Biomass Bioenergy J.* 120, 417–425 (2019). <https://doi.org/10.1016/j.biombioe.2018.12.002>
  22. Yoo, C.G., Pu, Y., Ragauskas, A.J.: ScienceDirect Ionic liquids : Promising green solvents for lignocellulosic biomass utilization. *Curr. Opin. Green Sustain. Chem.* 5, 5–11 (2017). <https://doi.org/10.1016/j.cogsc.2017.03.003>
  23. Araújo, D., Vilarinho, M., Machado, A.: Effect of combined green pretreatments on corncob fractionation: pretreated biomass characterization and regenerated cellulose film production. *Ind. Crops Prod.* (2019)
  24. Sun, S., Sun, S., Cao, X., Sun, R.: Bioresource Technology The role of pretreatment in improving the enzymatic hydrolysis of lignocellulosic materials. *Bioresour. Technol.* 199, 49–58 (2016). <https://doi.org/10.1016/j.biortech.2015.08.061>
  25. Boonterm, M., Sunyadeth, S., Dedpakdee, S., Athichalinthorn, P., Patcharaphun, S., Mungkung, R., Techapiesancharoenkij, R.: Characterization and comparison of cellulose fiber extraction from rice straw by chemical treatment and thermal steam explosion. *J. Clean. Prod.* 134, 592–599 (2016). <https://doi.org/10.1016/j.jclepro.2015.09.084>
  26. Arvidsson, R., Nguyen, D., Svanström, M.: Life cycle assessment of cellulose nanofibrils production by mechanical treatment and two different pretreatment processes. *Environ. Sci. Technol.* 49, 6881–6890 (2015). <https://doi.org/10.1021/acs.est.5b00888>
  27. Benavente, V., Fullana, A., Berge, N.D.: Life cycle analysis of hydrothermal carbonization of olive mill waste: Comparison with current management approaches. *J. Clean. Prod.* 142, 2637–2648 (2017). <https://doi.org/10.1016/j.jclepro.2016.11.013>
  28. Jo, J.S., Jung, J.Y., Byun, J.H., Lim, B.K., Yang, J.K.: Preparation of cellulose acetate

- produced from lignocellulosic biomass. *J. Korean wood Sci. Technol.* 44, 241–252 (2016)
29. Coletti, A., Valerio, A., Vismara, E.: *Posidonia oceanica* as a renewable lignocellulosic biomass for the synthesis of cellulose acetate and glycidyl methacrylate grafted cellulose. *Materials (Basel)*. 6, 2043–2058 (2013). <https://doi.org/10.3390/ma6052043>
  30. Bello, A., Tijjani, M., Olufemi, B.O., Mukhtar, B.: Acetylation of Cotton Stalk for Cellulose Acetate Production. *Am. Sci. Res. J. Eng. Technol. Sci.* 15, 137–150 (2016)
  31. Biswas, A., Saha, B.C., Lawton, J.W., Shogren, R.L., Willett, J.L.: Process for obtaining cellulose acetate from agricultural by-products. *Carbohydr. Polym.* 64, 134–137 (2006). <https://doi.org/10.1016/j.carbpol.2005.11.002>
  32. Carrier, M., Loppinet-Serani, A., Denux, D., Lasnier, J.-M., Ham-Pichavant, F., Cansell, F., Aymonier, C.: Thermogravimetric analysis as a new method to determine the lignocellulosic composition of biomass. *Biomass and Bioenergy*. 35, 298–307 (2011). <https://doi.org/10.1016/j.biombioe.2010.08.067>
  33. Chen, T., Li, L., Zhao, R., Wu, J.: Pyrolysis kinetic analysis of the three pseudocomponents of biomass–cellulose, hemicellulose and lignin: Sinusoidally modulated temperature method. *J. Therm. Anal. Calorim.* 128, 1825–1832 (2016). <https://doi.org/10.1007/s10973-016-6040-3>
  34. Saldarriaga, J.F., Aguado, R., Pablos, A., Amutio, M., Olazar, M., Bilbao, J.: Fast characterization of biomass fuels by thermogravimetric analysis (TGA). *Fuel*. 140, 744–751 (2015). <https://doi.org/10.1016/j.fuel.2014.10.024>
  35. Teng, H., Lin, H.C., Ho, J.A.: Thermogravimetric Analysis on Global Mass Loss Kinetics of Rice Hull Pyrolysis. *Ind. Eng. Chem. Res.* 36, 3974–3977 (1997). <https://doi.org/10.1021/ie970017z>
  36. Menard, K.P.: *Dynamic mechanical analysis - a practical introduction*. CRC Press LLC, New York (1999)
  37. Noi, C.D., Ciroth, A., Srocka, M.: *OPENLCA 1.7 - Comprehensive user manual*. , Berlin (2017)
  38. ISO: *Environmental Management – Life Cycle Assessment – Requirements and Guidelines – ISO 14044*. , rue de Stassart, 36, B-1050 Brussels (2006)
  39. European Commission: *ILCD handbook*. (2011)
  40. Walser, T., Demou, E., Lang, D.J., Hellweg, S.: Prospective environmental life cycle assessment of nanosilver T-shirts. *Environ. Sci. Technol.* 45, 4570–4578 (2011).

- <https://doi.org/10.1021/es2001248>
41. Silvério, H.A., Flauzino Neto, W.P., Dantas, N.O., Pasquini, D.: Extraction and characterization of cellulose nanocrystals from corncob for application as reinforcing agent in nanocomposites. *Ind. Crops Prod.* 44, 427–436 (2013). <https://doi.org/10.1016/j.indcrop.2012.10.014>
  42. Boonsombuti, A., Luengnaruemitchai, A., Wongkasemjit, S.: Enhancement of enzymatic hydrolysis of corncob by microwave-assisted alkali pretreatment and its effect in morphology. *Cellulose*. 20, 1957–1966 (2013). <https://doi.org/10.1007/s10570-013-9958-7>
  43. Rosa, M.F., Medeiros, E.S., Malmonge, J.A., Gregorski, K.S., Wood, D.F., Mattoso, L.H.C., Glenn, G., Orts, W.J., Imam, S.H.: Cellulose nanowhiskers from coconut husk fibers: Effect of preparation conditions on their thermal and morphological behavior. *Carbohydr. Polym.* 81, 83–92 (2010). <https://doi.org/10.1016/j.carbpol.2010.01.059>
  44. Sala, S., Crenna, E., Secchi, M., Pant, R.: Global normalisation factors for the Environmental Footprint and Life Cycle Assessment. *JRC Tech. Rep.* (2017). <https://doi.org/10.2760/88930>
  45. Stranddorf, K., Heidi, Leif, H., Schmidt, A.: Impact categories, normalisation and weighting in LCA: Updated on selected EDIP97-data. *Environ. News, Danish Environ. Prot. Agency, Copenhagen*. 78, 90 (2005). [https://doi.org/Environmental project nr. 995](https://doi.org/Environmental%20project%20nr.%20995)
  46. Guinée, J.B., Gorrée, M., Heijungs, R., Huppes, G., Kleijn, R., Koning, A. de, Oers, L. van, Wegener Sleeswijk, A. Suh, S., Udo de Haes, H.A. Bruijn, H. de, Duin, R. van, Huijbregts, M.A.J.: Handbook on life cycle assessment. Operational guide to the ISO standards. I: LCA in perspective. IIa: Guide. IIb: Operational annex. III: Scientific background. Kluwer Academic Publishers, Dordrecht, (2002)
  47. European Commission: Characterisation factors of the ILCD Recommended Life Cycle Impact Assessment methods: database and supporting information. Publications Office of the European Union, Luxembourg (2012)
  48. Goedkoop, M.J., Heijungs, R., Huijbregts, M.A.J., Schryver, A. De, Struijs, J., van Zelm, R.: A life cycle impact assessment method which comprises harmonised category indicators at the midpoint and the endpoint level. (2013)
  49. Hischer, R., Weidema, B., Althaus, H.-J., Bauer, C., Doka, G., Dones, R., Hellweg, S.F.R., Humbert, S., Jungbluth, N., Köllner, T., Loerincik, Y., Margni, M., Nemecek, T.:

- Implementation of Life Cycle Impact Assessment Methods. Ecoinvent report N ° 3, v 2.2. , Dübendorf (2010)
50. Rosenbaum, R.K., Bachmann, T.M., Gold, L.S., Huijbregts, M.A.J., Jolliet, O., Juraske, R., Koehler, A., Larsen, H.F., MacLeod, M., Margni, M., McKone, T.E., Payet, J., Schuhmacher, M., Van De Meent, D., Hauschild, M.Z.: USEtox - The UNEP-SETAC toxicity model: Recommended characterisation factors for human toxicity and freshwater ecotoxicity in life cycle impact assessment. *Int. J. Life Cycle Assess.* 13, 532–546 (2008). <https://doi.org/10.1007/s11367-008-0038-4>
  51. Lee, H. V, Hamid, S.B. a, Zain, S.K.: Conversion of Lignocellulosic Biomass to Nanocellulose : Structure and Chemical Process Conversion of Lignocellulosic Biomass to Nanocellulose : *Sci. World J.* 2014, 1–14 (2014). <https://doi.org/10.1155/2014/631013>
  52. Sabanci, K., Buyukkileci, A.O.: Bioresource Technology Comparison of liquid hot water , very dilute acid and alkali treatments for enhancing enzymatic digestibility of hazelnut tree pruning residues. *Bioresour. Technol.* 261, 158–165 (2018). <https://doi.org/10.1016/j.biortech.2018.03.136>
  53. Michelin, M., Teixeira, J.A.: Liquid hot water pretreatment of multi feedstocks and enzymatic hydrolysis of solids obtained thereof. *Bioresour. Technol.* 216, 862–869 (2016). <https://doi.org/10.1016/j.biortech.2016.06.018>
  54. Luo, W., Wang, J., Liu, X., Li, H., Pan, H., Gu, Q., Yu, X.: Bioresource Technology A facile and efficient pretreatment of corncob for bioproduction of butanol. *Bioresour. Technol.* 140, 86–89 (2013). <https://doi.org/10.1016/j.biortech.2013.04.063>
  55. Mostafa, N.A., Tayeb, A.M.: Production of biodegradable plastic from agricultural wastes. *Arab. J. Chem.* 11, 546–553 (2018). <https://doi.org/10.1016/j.arabjc.2015.04.008>
  56. Ang, T.N., Ngoh, G.C., Seak, A., Chua, M., Lee, M.G.: Elucidation of the effect of ionic liquid pretreatment on rice husk via structural analyses. *Biotechnol. Biofuels.* 5, 1–10 (2012)
  57. Ma, Z., Pan, G., Xu, H., Huang, Y., Yang, Y.: Cellulosic fibers with high aspect ratio from cornhusks via controlled swelling and alkaline penetration. *Carbohydr. Polym.* 124, 50–56 (2015). <https://doi.org/10.1016/j.carbpol.2015.02.008>
  58. Poletto, M., Pistor, V., Zattera, A.J.: Structural Characteristics and Thermal Properties of Native Cellulose. *Cellul. – Fundam. Asp.* 45–68 (2013). <https://doi.org/10.5772/50452>
  59. Wang, F., Li, S., Sun, Y., Han, H., Zhang, B.: Ionic liquids as e ffi cient pretreatment solvents for lignocellulosic biomass. *R. Soc. Chem.* 7, 47990–47998 (2017).

- <https://doi.org/10.1039/c7ra08110c>
60. Cao, Y., Zhang, J., He, J., Li, H., Zhang, Y.: Homogeneous acetylation of cellulose at relatively high concentrations in an ionic liquid. *Chinese J. Chem. Eng.* 18, 515–522 (2010). [https://doi.org/10.1016/S1004-9541\(10\)60252-2](https://doi.org/10.1016/S1004-9541(10)60252-2)
  61. Morgado, D.L., Frollini, E.: Thermal decomposition of mercerized linter cellulose and its acetates obtained from a homogeneous reaction. *Polímeros.* 21, 111–117 (2011). <https://doi.org/10.1590/s0104-14282011005000025>
  62. Yang, Y., Song, L., Peng, C., Liu, E., Xie, H.: Activating cellulose via its reversible reaction with CO<sub>2</sub> in the presence of 1,8-diazabicyclo[5.4.0]undec-7-ene for the efficient synthesis of cellulose acetate. *Green Chem.* 17, 2758–2763 (2015). <https://doi.org/10.1039/c5gc00115c>
  63. de Freitas, R.R.M., Senna, A.M., Botaro, V.R.: Influence of degree of substitution on thermal dynamic mechanical and physicochemical properties of cellulose acetate. *Ind. Crops Prod.* 109, 452–458 (2017). <https://doi.org/10.1016/j.indcrop.2017.08.062>
  64. Bao, C., Long, D.R., Vergelat, C.: Miscibility and dynamical properties of cellulose acetate/plasticizer systems. *Carbohydr. Polym.* 116, 95–112 (2015)
  65. Abdel-naby, A.S., Al-ghamdi, A.A.: Original Research Article Chemical modification of Cellulose Acetate by Diallylamine. *Int.J.Curr.Microbiol.App.Sci.* 3, 10–24 (2014)
  66. Számel, G., Klébert, S., Sajó, I., Pukánszky, B.: Thermal analysis of cellulose acetate modified with caprolactone. *J. Therm. Anal. Calorim.* 91, 715–722 (2008)
  67. Startsev, O. V., Makhonkov, A., Erofeev, V., Gudojnikov, S.: Impact of moisture content on dynamic mechanical properties and transition temperatures of wood. *Wood Mater. Sci. Eng.* 12, 55–62 (2017). <https://doi.org/10.1080/17480272.2015.1020566>
  68. Dedpakdee, S., Mungkung, R., Techapiesanchaenkit, R.: Life Cycle Assessment of Natural Fiber-Based Insulator Corrugated Paper Box to Identify Eco-Design Strategies. In: 6th International Conference on Environmental Science and Technology. pp. 19–23 (2015)
  69. Prasad, A., Sotenko, M., Blenkinsopp, T., Coles, S.R.: Life cycle assessment of lignocellulosic biomass pretreatment methods in biofuel production. *Int. J. Life Cycle Assess.* 21, 44–50 (2016). <https://doi.org/10.1007/s11367-015-0985-5>
  70. Yates, M.R., Barlow, C.Y.: Life cycle assessments of biodegradable, commercial biopolymers - A critical review. *Resour. Conserv. Recycl.* 78, 54–66 (2013). <https://doi.org/10.1016/j.resconrec.2013.06.010>





Chapter 6. A novel eco-friendly synthesis processing to  
produce cellulose acetate/ TiO<sub>2</sub>/MgO bionanocomposite  
films

*Submitted to International journal of environment, agriculture and biotechnology*

---

**David Araújo<sup>1,2\*</sup>, Caroline Moura<sup>3</sup>, M. Cidália R. Castro<sup>1</sup>, Filipe Samuel<sup>4</sup>,  
Maria Vilarinho<sup>2,4</sup>, Ana Machado<sup>1</sup>**

<sup>1</sup>Institute for Polymers and Composites/i3N, University of Minho, Guimarães, Portugal.

<sup>2</sup>Centre for Waste Valorization, University of Minho, Guimarães, Portugal.

<sup>3</sup>CMEMS-UMinho, University of Minho, Guimarães, Portugal.

<sup>4</sup>Mechanical Engineering and Resources Sustainability Centre, University of Minho, Guimarães,  
Portugal.

\*Corresponding author: David Jefferson Cardoso Araújo (david\_bct@hotmail.com)

## Abstract

This study aimed at developing a novel approach to produce a bionanocomposite film by applying green raw materials and eco-friendly processing techniques. Cellulose acetate emerged from agroindustrial residue was used as matrix and metal oxide nanofillers were produced by the pulsed laser ablation in liquid (PLAL) of bare titanium and magnesium targets. Green pretreatment and derivatization techniques were performed to extract and acetylate cellulose, respectively. Subsequently, the synthesized cellulose acetate was directed dissolved in the nanoparticles' colloidal suspension, and the nanocomposite film was produced via solvent casting method. Physicochemical characterization techniques were undertaken to investigate the effectivity of the nanoparticles synthesis, biomass pretreatment, acetylation, as well as the biofilm properties. Viscoelastic properties of the film were also assessed via dynamic mechanical analysis. A solid enrich-cellulose fraction could be obtained after the applied pretreatment, which reflected in the successful high-yield acetylation synthesis. Metal oxides nanoparticles with relatively large sizes could be easily and rapidly synthesized through PLAL. Formation of the metal oxidized phases, as well as their embedment into the film, were clearly identified by UV-vis spectrometry, energy dispersive X-ray spectroscopy and X-ray diffraction. In comparison to the neat cellulose acetate film, the introduction of nanoparticles increased the porous structures of the nanocomposite, which in turn decreased its stiffness, by making it more flexible. Besides, the glass transition temperature ( $T_g$ ) of the composite film increased significantly, possibly due to the restrictive effects of the  $TiO_2/MgO$  nanoparticles on the segmental mobility of the cellulose acetate chains. By increasing the  $T_g$ , the operating range of the material was also extended, which is an especially important property within industrial processing requirements. Thus, the present work shows a facile and effective eco-friendly approach to produce bio-based nanocomposite films with potential active properties.

**Keywords:** bio-based polymer; nanocomposite; ecofriendly techniques; lignocellulosic biomass; agroindustrial residues; cellulose acetate; pulsed laser ablation.

## 6.1. Introduction

For more than 60 years the global production of plastics has shown an upward trend, reaching an astonishing value of 348 million tonnes in 2017 [1]. From this total, the polyolefins accounted for more than 50%, which were mostly aimed at the production of single used packaging. Besides

being petroleum-based dependents, these synthetic plastics are nonbiodegradable and can threaten the environment through accumulation in landfills, oceans and other biocompartments. In the past few decades, advances in chemical processing and biotechnology have allowed the production of commercially viable bio-based and biodegradable polymers, such as polylactic acid, polyhydroxyalcanoates (PHA), starch blends and bio-based PET and polyolefins [2, 3]. However, although the production capacity of these bio-based alternatives has shown a positive growth rate over the last years, they are still expensive in comparison to the synthetic polymers (mainly because of the low crude oil price) and may compete with food production as they emerge from first-generation feedstock.

Alternatively, increasing interest has been devoted to developing packaging made of biodegradable polymers from second-generation renewable resources, namely lignocellulosic residues. Lignocellulosic biomass is the most economical and abundantly renewable source of biopolymers on earth. Annually, huge amounts of lignocellulose are available as non-edible agroindustrial residues in the form of stalk, stover, branches, leaves, straw, bagasse, husk and pellets, which are mainly composed by cellulose (50%), hemicellulose (20-40%) and lignin (10-40%) [4, 5]. The valorization of these residues, besides not generating competition with food production, can still prevent their insertion into the conventional solid waste disposal paths and may promote the circular economy.

Highlighted as one of the world's largest producers of agricultural commodities, Brazil also generates fair amounts of agroindustrial residues. For instance, the country is the third-largest producer of corn and, consequently, it is estimated that impressive amounts of residues in the form of corncob (18700 ktons), husk (12470 ktons) and stover (111109 ktons) are also generated annually [5]. Corncob is the central part of the ear of maize, chemically constituted mainly by cellulose and hemicellulose [6]. Cellulose, the most abundant organic compound on earth, is a high molecular weight homopolymer generated from repeating D-glucopyranose ring units linked by  $\beta$ -1,4-glycosidic bonds (cellobiose unit). Many studies have already reported the potential application of cellulose extracted from agroindustrial residues for the development of biodegradable food packaging, e.g. Silvério et al. [7] – corncob, Reddy et al. [8] - Borassus fruit fibers, Vanitjinda et al. [9]– sugarcane bagasse, Zhang et al. [10] - corn husk and Otoni et al. [11] – carrot processing waste. Notwithstanding, because of the intra and intermolecular interactions of the hydroxyl groups present in the cellobiose unit, the cellulose molecules crystallize in a horizontal plane and in parallel chains, forming microfibril packages, which leads to some properties that

limits its application, namely lack of antimicrobial properties, high hydrophilicity, poor solubility in common solvents and low dimensional stability and thermoplasticity. To overcome these drawbacks and widen its manufacturing potential into value-added materials, the cellulose is usually processed into derivatives. Among the existent derivatizing techniques, the esterification of cellulose into cellulose acetate is the most commonly applied approach. In addition to its physical-chemical properties, cellulose acetate is biodegradable, and therefore it is an excellent choice for film applications as food packaging [12].

The development of cost-effective and sustainable methods to produce cellulose-based food packaging from residues is still challenging and the most innovative products available in the market are still based on high-quality cellulose from wood pulp or cotton. Furthermore, in addition to performing its essential function (i.e., to ensure the food safety and quality, as well as prevent environmental degradation) throughout the food distribution and storage chain, the development of new bio-based materials for packaging still have to meet market and consumers requirements, which currently are turned towards materials with eco-friendly and active properties [13–15].

Recently, nanotechnology has received enormous attention from researches to develop active bio-based hybrid materials with antimicrobial properties. Among the most focused nanoparticles applied for antibacterial purposes are the metals and metal oxides, such as Ag, TiO<sub>2</sub>, CuO, ZnO and MgO [14, 16, 17]. Nevertheless, as an emerging application and research field, there are concerns related to the migration of nanoparticles to food and their toxicity [14]. In this regard, the inorganic metal oxides TiO<sub>2</sub> and MgO are of particular interest because they are safe for human beings, in addition to be stable under harsh processing conditions [18, 19]. On top of that, the use of TiO<sub>2</sub> and MgO as additive in food is allowed and regulated by food safety authorities, such as Food and Drug Administration (USA) and the European Food Safety Authority.

The use of magnesium oxide and hydroxide (Mg(OH)<sub>2</sub>) nanoparticles have attracted a great deal of interest because of their properties, including nontoxicity, antibacterial activity and thermal stability [19, 20]. TiO<sub>2</sub> is among the most explored nanomaterials in active food packaging, and it is also considered a promising alternative since it can enhance photo-degradability and exhibit antimicrobial and ethylene photodegradation activity when exposed to UV light [14, 21–23]. Among the possible multifunctionalities imparted by these nanomaterials, their complementary antimicrobial effect is of particular interest since antimicrobial packaging is one of the most pursued properties of active packaging technologies [24]. While the individual antimicrobial effect of TiO<sub>2</sub> nanoparticles as a component of polymeric packaging are well documented [21, 23, 25, 26], the

assessment of MgO nanoparticles [16] and their combined application [27] are limited. Synthesis methods in the scope of the wet chemical routes (such as solvothermal, precipitation and sol-gel) are the main approaches used to obtaining metal oxide nanoparticles. They can involve different precursors (e.g.  $\text{Ti}(\text{OCH}(\text{CH}_3)_2)_4$ ,  $\text{Ti}(\text{OBU})_4$ , thiobenzoate complex with Ti,  $\text{MgCl}_2$ ,  $\text{MgSO}_4$  and alkoxides metals), solvent medium (e.g. Lauryl alcohol + hexane, toluene, ethanol, benzyl alcohol, NaOH, sorbitol and urea) and surfactants (e.g. PEG, SDS, oleic acid and ammonia) [20, 28–32]. Although wet chemical approaches are generally scalable and low cost, the use of some chemical agents, as well as the possibility of longer reaction times and high temperature and pressure processing, can lead to negative environment effects and biological toxicity [33, 34]. Besides, chemical synthesis routes are usually complicated by impurities from precursors and incomplete conversion into uniform particles [33]. A promising, well-established and environmentally friendly physical synthesis route to produce metal oxide nanoparticles, which may efficiently overcome some of the problems arising from chemical routes, is the pulsed laser ablation in liquid. In this method, a target material immersed in a liquid medium is irradiated by an ultra-short laser pulse, which causes the removal of material from target and formation of nanoparticles through nucleation and growth [35, 36]. The production of high-purity metal oxide nanoparticles with well-defined properties have been addressed by several reports [33, 37–41].

To date, there are few reports on the use of second-generation renewable sources along with environmentally friendly processing routes to produce potential active food packaging. Therefore, the present study aimed to develop cellulose acetate/ $\text{TiO}_2$ /MgO bio-based composite film by means of a novel route, comprised of simple and environmentally friendly processing steps (from cellulose extraction to film preparation/formation). The processing steps encompass: (i) the performance of a combine liquid hot water-dilute sodium hydroxide pretreatment (LHW-dilute NaOH) to extract cellulose from corncob; (ii) a solvent-free cellulose esterification to produce cellulose acetate and; (iii) bionanocomposite film production through the direct dissolution of the synthesized cellulose acetate in a  $\text{TiO}_2$ /MgO colloidal solution prepared by PLAL, followed solvent casting.

Nanoparticles characterization was accomplished by scanning electron microscopy (STEM), energy dispersive X-ray spectroscopy (EDS) and ultraviolet-visible spectroscopy (UV-vis), while essential properties of the developed  $\text{TiO}_2$ /MgO biofilm were investigated by Fourier transform infrared spectroscopy, X-Ray diffraction, SEM, EDS, thermal characterization and dynamic mechanical analysis.

## 6.2. Materials and methods

### 6.2.1. Materials

Corncob was obtained from local agricultural cooperatives from the North of Portugal. The corncob residue was firstly ground and sieved to particles sizes from 0.25 to 0.5 mm and stored in sealed plastic bags at room temperature. Cellulose acetate (Mn-50.000 by GPC) and Sodium hydroxide pellets were acquired from Sigma-Aldrich. Acetic anhydride (>99%) and sodium thiosulfate (98.50%) were purchased from Acros Organics. Iodine (99.80%), acetic acid glacial (99.88%), sulfuric acid (>95%), ethanol (99.80%), methanol (99.99%), dichloromethane (99.88%) and dimethyl sulfoxide (99.99%) were purchase from Fisher Chemical. All the reactants were used without further purification.

### 6.2.2. Isolation of cellulose from corncob

Cellulose extraction from dried milled corncob was carried out by applying a combined green pretreatment previously reported by our research group [42]. Firstly, LHW treatment with a feedstock loading rate of 10% (residue weight / distilled water volume) was pretreated at 190 °C, 0.79 MPa, for 30 min (after the heat-up time) under constant mechanical stirring. After the required time, the reactor was cooled and the insoluble solid was collected and thoroughly washed with deionized water and dried at 60 °C. The dried liquid hot water-treated corncob (LHW - CC) was then soaked in 2 wt% NaOH at 90 °C for 1.5 h at a 1/30 solid/liquid ratio (w/w) under magnetic stirring. The alkali-treated LHW-CC (NaOH-LHW-CC) was filtered and washed with deionized water until colorless. The resulting material was dried at 60 °C and stored in a sealed plastic bag.

### 6.2.3. Synthesis of cellulose acetate

Cellulose acetate was synthesized based on the method described by Das et al. [43] with some modifications. Basically, a mixture of 0.4 g of cellulose (extracted from corncob), 20 mL of acetic anhydride and 0.6 g of iodine was heated to 80 °C and left reacting for 5 hours. After that, the solution was allowed to cool at room temperature and treated with 10 mL saturated solution of sodium thiosulfate with stirring. Then, 60 mL of ethanol was added to the mixture and stirred for 60 min. The product was filtered and thoroughly washed with 75% (v/v) ethanol and distilled water to remove the unreacted acetic acid and byproducts. The solid material obtained was dried at 60

°C in an oven and further dissolved in dichloromethane and filtered. After evaporating the filtrate, the cellulose acetate was collected and dried at 60 °C in a vacuum oven overnight.

#### **6.2.4. Production of Nanoparticles/colloidal solution**

The synthesis of TiO<sub>2</sub> nanoparticles was performed using a 1064 nm high power Nd:YAG laser (OEM Plus, Italy) with an output power of 6W, spot size of 3 mm, pulse width ~35 ns and operated at the repetition rate of 20 kHz. The target metal plate was fixed on the bottom of a glass vessel filled with 35 ml liquid and a level of liquid/air interface above the targeted substrate of about 1.5 mm in height. Irradiation was carried out with a power of 0.3 mJ/pulse through focusing a lens with focal length of 160mm. During the ablation, the liquid was stirred to keep the ablated particles out of the beam path. Besides, the scanning of the target surface was carried out by means of a XY translation stage to ensure that ablation occurred on an unaffected area.

The experiments were performed in pure dichloromethane as ambient liquid solution regarding its suitability to dissolve the synthesized CA. Firstly, the titanium plate was irradiated by a laser beam with fluence of 4244.0 J/cm<sup>2</sup> during 1.5 h. After the required time has elapsed, the vessel containing the titanium plate and the NPs solution was taken out, and another vessel containing a magnesium plate was placed. The ablation processing was performed with unchanged conditions. It is worth mentioning that both metal targets contained a natural oxide surface layer. After the required processing time, the ablation process was interrupted, the TiO<sub>2</sub> and MgO colloidal solutions were stored for further analysis and dissolution processing.

#### **6.2.5. Cellulose acetate/TiO<sub>2</sub>/MgO nanocomposite film preparation**

After the ablation process is over, both colloidal solutions were mixed and the synthesized cellulose acetate was added into the solution containing DCM/metal oxides nanoparticles. This solution was kept under stirring for 4h at 35 °C. A schematic representation of the proposed process is depicted in Figure 6.1. Succeeding complete dissolution, the mixture was sonicated for 10 min, in order to remove air bubbles, poured on a Teflon dish with 4 cm of diameter and placed in the vacuum oven overnight to allow the solvent to evaporate. The bionanocomposite films produced were stored in sealed plastic bags for further analysis.

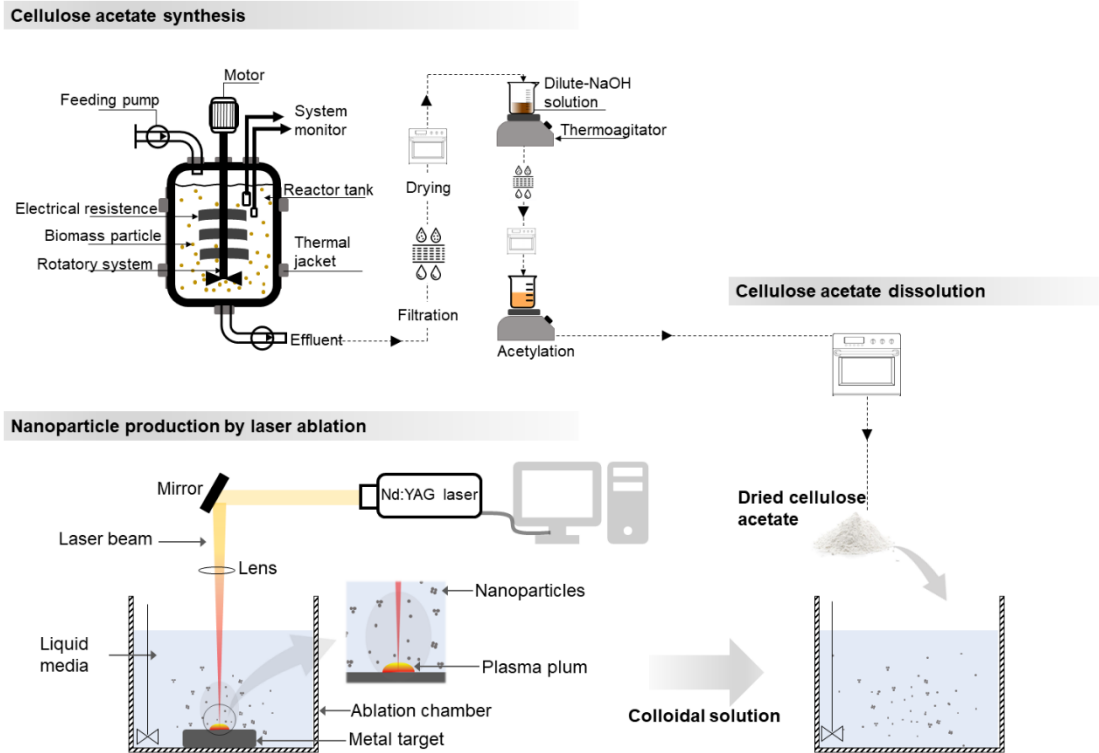


Figure 6-1. Schematic representation of the eco-friendly approach to produce bionanocomposite films.

## 6.2.6. Material characterization

### 6.2.6.1. Nanoparticles characterization

TiO<sub>2</sub> and MgO colloidal suspensions were characterized by optical absorbance spectroscopy and scanning electron with transmission electron detection (STEM). Optical absorption spectra of the mixed colloidal suspensions were recorded in the range from 225 to 800 nm of wavelength by using an UV–vis absorption spectrophotometer Model 2501 PC, Shimadzu. Observation of colloidal particles was performed by STEM (FEI Nova 200 Nano SEM) operated at 20 Kv. For STEM characterization, samples were prepared by adding droplets of the colloidal solutions on carbon-coated copper grids.

### 6.2.6.2. Chemical composition of untreated and treated corncob

The chemical composition of untreated and treated corncob was determined by deconvolution of the derivative curves obtained from the thermogravimetry analysis [44–48]. Briefly, the decomposition processes of the three pseudo-components presented in the lignocellulosic biomass (cellulose, hemicellulose and lignin) were modeled by a Gaussian distribution, and the percentage of each component was assumed to correspond to the integrated area above each single



deconvoluted reaction curve (the modeled equation, as well as graphs and parameters are available in the Appendix A).

#### 6.2.6.3. Fourier transform infrared spectroscopy (FTIR)

FTIR spectra of raw corncob, pretreated corncob and cellulose acetate samples were recorded on a Jasco FT/IR-4100 spectrometer, in the wavelength range of 400 – 4000  $\text{cm}^{-1}$  and at a resolution of 4  $\text{cm}^{-1}$ , using the attenuated total reflection technique.

#### 6.2.6.4. X-ray diffraction analysis

The X-ray diffractograms patterns of all samples were obtained at room temperature using a diffractometer Bruker D8 Discover, operated with Cu-K $\alpha$  radiation (wavelength of 0.154 nm) at a power of 40 mA and accelerating voltage of 40 kV. Diffraction intensities were scanned in the range of  $2\theta = 5 - 50^\circ$  with a scanning rate of 0.04 $^\circ$ /second.

#### 6.2.6.5. $^1\text{H}$ NMR spectra

The  $^1\text{H}$ NMR spectroscopy was performed in a Bruker Avance III, 400 MHz, and deuterated dimethyl sulfoxide was used as solvent. The spectra were internally referenced to the residual proton tetramethylsilane (TMS,  $\delta = 0.00$  ppm) and the chemical shifts ( $\delta$ ) are reported as part per million (ppm). Based on Biswas et al. [49], the degree of substitution of acetyl groups was calculated by dividing 1/3 of the three methyl proton absorbance peak area of acetyl group, in the range of 1.5-2.2, by 1/7 of the seven anhydrocellulose absorbance peak area, in the range of 3.5-5.2 ppm.

#### 6.2.6.6. Morphological analysis of the films

The surface and cross-section morphologies of untreated and treated samples were examined by scanning electron microscopy (SEM) using a FEI Nova 200 equipped with energy-dispersive X-ray (EDS) analyzer. For SEM analysis, samples were previously sputter coated with gold.

#### 6.2.6.7. Thermogravimetry analysis

Thermogravimetry analyses of untreated corncob, extracted cellulose and CA samples were performed on TA Instruments SDT 2960 model. The sample weight was in the range of 3-5 mg and heated from 30 to 700  $^\circ\text{C}$  at a rate of 10 $^\circ\text{C}/\text{min}$ , under purified argon to prevent thermo-oxidative degradation.

### **6.2.7. Dynamic mechanical analysis of the bionanocomposite film**

Dynamic mechanical analysis was performed on a PerkinElmer DMA 800 using a dual-cantilever bending mode at a constant frequency. The viscoelastic properties were characterized based on the storage modulus ( $E'$ ), the loss modulus ( $E''$ ) and the damping capacity ( $\tan \delta$ ), the later calculated as the ratio of the loss to the storage modulus. CA Films with 20/5.7/0.04 mm of dimensions, approximately, were analyzed under temperature ranging from 40 – 160°C, heating rate of 5 °C/min, preload 1N, 10  $\mu\text{m}$  of displacement amplitude and 1 Hz of frequency.

## **6.3. Results**

### **6.3.1. Cellulose extraction from corncob**

In substitution of the conventional cellulose extraction technique typically applied for this purpose (namely alkali-bleaching treatment), a less polluting combined pretreatment reported by Araújo et al. [44], performed as a two-stage LHW/dilute-NaOH process, was applied. The removal of non-cellulosic constituents was visually stressed by physical changes after each stage of the pretreatment, which converted the corncob into a fine, light gray and fluffy powder. The LHW treatment effectively solubilized around 90% of the initial hemicellulose content. In turn, the dilute-alkali treatment selectively removed a great share of lignin (leading to a lignin reduction by 50%). By partially disrupting the lignin-hemicellulose complex, the dilute-NaOH treatment could also remove hemicellulose, but at a lower proportion. Consequently, in comparison to the chemical composition of raw corncob (cellulose – 36.35%, hemicellulose – 47.32% and lignin – 16.32), the pretreated sample had a higher cellulose content (84.73%) while the hemicellulose (4.58%) and lignin (10.68%) content were lower.

### **6.3.2. Cellulose acetate synthesis**

The extracted cellulose was acetylated by a free-solvent iodine-catalyzed method, reported by Das et al. [43] as an eco-friendly technique. Under the experimental conditions applied, an acetylation yield (calculated as dry weight percent gain) of 60% was obtained. Similar yields have already been reported in response to the acetylation of other cellulose-enrich lignocellulosic biomasses [43, 50]. Through  $^1\text{H}$  NMR spectrum, the degree of substitution of the three hydroxyl groups in the glucose monomer was calculated as 2.68.

### 6.3.3. Characterization of nanoparticles

The morphology and size distribution of MgO/TiO<sub>2</sub> nanoparticles were assessed by STEM. Figure 6.2a and 6.2b revealed that, under the same ablation parameters, MgO and TiO<sub>2</sub> particles were produced with different morphology and size. After the Mg ablation, the solution became turbid with a milky appearance and significant particle agglomeration occurred even during the ablation process. The observed MgO particles have irregular shapes (with some resembling platelet-like and spherical shapes) and formed clusters of agglomerates. Because of their morphology, the size distribution was calculated taking into account the largest length of the particles, which gave rise to a mix of nanoparticles and microparticles with sizes ranging from 59 to 313 nm. The largest length was taken into account since large nanoparticles size can impair certain applications and properties of the nanoparticles. The related histogram (Figure 6.3d) shows a unimodal, skewed right pattern, with 50% of particles not exceeding 175 nm and an average size around 155 nm. PLAL synthesized MgO particles with similar shapes were also obtained by Somanathan et al. [51] and Liang et al. [52]. The gray shades seen on images suggest that the organic solvent medium was decomposed or altered due to laser heating and this contributed to the poor visibility of particles. Furthermore, based on the difference of weight, the ablated Mg mass was calculated as 1.8 mg, leading to a solution with concentration of 0.15 mg/ml.

Besides the use of oxidized target materials, the formation of oxidized nanoparticles also takes place during the ablation process. During PLAL, the laser pulse delivery energy to the target through multiphoton absorption and direct photoionization, causing the detachment of high ionized species and the formation of a plasma-plume. As this plasma-plume expands and quenches, the ablated species interact with the solution and oxidized phases of the bulk material are formed. In addition, energy is released to the surrounding liquid and a cavitation bubble rises as effect. Subsequently, this cavitation expands and collapses, leading to nanomaterials nucleation and growth and finally the release of nanoparticles to the liquid medium [35]. It is worth mentioning that all this process occurs in a fraction of seconds, of the order of 10<sup>-4</sup> s [35]. Although the solvent used is not the most suitable medium for the formation of oxidized phases, very short liquid depth (measured from the target surface) was used to provide natural aeration with the upper air atmosphere. As both target materials (Ti and Mg) are very reactive, oxidation is expected to occur under the experimental setup. The formation of oxidized phases will be further confirmed through X-ray diffraction analysis.

The large particles produced after laser ablation are probably originated from the ejection of melted drops. Despite material detachment occur in a region almost coincident with the laser

spot, the energy density at the border of the laser beam is lower than that of the central. As a response, the heating temperature in this surrounding area only melts the target, and large nanoparticles in the form of melted drops can be blown away by the shockwave generated during plasma plume formation and cavitation bubble collapsing [53].

The formation of titanium dioxide, as well as the production of large particles evidenced in Figure 6.2a, follow the same synthesis mechanisms applied to the MgO. Based on the difference of weight, the ablated mass of TiO<sub>2</sub> was calculated as 2.8 mg, leading to a solution with concentration of 0.224 mg/ml. Through PLAL, TiO<sub>2</sub> is formed as well-defined spherical nanoparticles and diameters ranging from 15 to 330 nm. The related histogram (Figure 6.2c) shows a skewed right and unimodal pattern, with 50% of nanoparticles not exceeding 33 nm and an average size around 71.8 nm. Similar histogram pattern distribution and NPs size have recently been reported by Zimbone et al. [38], Zuñiga-Ibarra et al. [54], Singh et al. [37] and Aziz et al. [55]. In contrast to the MgO NPs, during ablation the solution color changes to a metallic gray and the produced TiO<sub>2</sub> NPs did not significantly cluster.

The presence of both nanoparticles (MgO and TiO<sub>2</sub>) in the mixed colloidal solution can be detected via the UV-vis spectroscopy analysis presented in Figure 6.2e. The UV-vis spectrum exhibited a characteristic absorption band with a single plasmon absorption peak located in the low UV-region at 242 nm. The maximum absorption band verified, as well as the absorption edge around 400 nm, are typical of both nanoparticles [39, 54–61]. The presence of MgO and TiO<sub>2</sub> in the scope of the UV-vis spectroscopy can also be verified through the analysis of the band gap parameter. The band gap can be defined as the distance between the valence band (VB) of electrons and the conduction band (CB), and represents the minimum energy that is required to excite an electron up to a state in the conduction band so that it becomes free [62]. This parameter is crucial in many applications of TiO<sub>2</sub> nanoparticles as it largely influences their photocatalytic activity [54, 63]. The optical band gap ( $E_g$ ) can be obtained via the Tauc method [64], which relates optical absorption strength with the photon energy and the band gap. Through this method, the optical band gap can be calculated by plotting  $\alpha h\nu^{(2/n)}$  versus  $h\nu$  (Tauc plots), where  $h$  is the Planck's constant,  $\nu$  is the frequency of light,  $\alpha$  is the absorption coefficient and the exponent  $n$  is related to the electronic of the band gap (here denoted as indirect allowed transitions). The linear trend given by the Tauc plots is modeled as the tangent of the curve and extrapolated to the point where  $\alpha h\nu^{(2/n)}$  is zero, which gives the  $E_g$ . From the inset graph in Figure 6.2e, the band gap of the mixed colloidal solution was estimated as 3.24 eV, which is higher than that of bare TiO<sub>2</sub> (close to

3.1 eV) and lower than that of bare MgO, that requires excitation energy in the range of 8-9 eV [65, 66]. In Ye et al. [61] the introduction of MgO as additive in TiO<sub>2</sub> films also caused the enlargement of the band gap. Therefore, the band gap value confirms that both nanoparticles were successfully synthesized and are present in the mixed colloidal suspension.

Although the enlarged band gap may impair the properties of TiO<sub>2</sub> under the visible light spectrum, when combined with TiO<sub>2</sub> the MgO NPs can act as electron trap and barrier for recombination, enhancing its photocatalytic activity [66]. When TiO<sub>2</sub> is exposed to UV radiation, particles absorb light leading to band gap extinction and consequent charge separation of electrons and holes into the CB and VB, respectively. However, a large proportion of charge carriers (e<sup>-</sup> / h<sup>+</sup> pairs) recombine quickly at the surface and interior of particles, dissipating the absorbed energy. This issue stands out one of the main drawbacks related to the photocatalytic property of TiO<sub>2</sub>, since the electrons and holes, that work as electrons donors and acceptors, respectively, in reduction and oxidation reactions, are responsible for the generation of reactive oxygen species [62, 63]. In the scope of active packaging applications, these reactive radicals are recognized to effectively kill some microorganisms and enhance biodegradation of biodegradable polymers [67, 68]. Therefore, the improvement of the photocatalytic properties of TiO<sub>2</sub> NPs is imperative depend on the application, namely in active packaging. In this regard, MgO may play an important role when applied in combination with TiO<sub>2</sub> NPs since its microcrystalline structure contains a high density of defects with anion vacancies and cations vacancies sites. The anion vacancies are capable of trapping the excited electrons produced by photo-irradiation of TiO<sub>2</sub>, while the holes remain on the TiO<sub>2</sub>, as evidenced in Bandara et al. [66]. Consequently, photogenerated negative and positive charges are widely separated and recombination can be suppressed [61, 66].

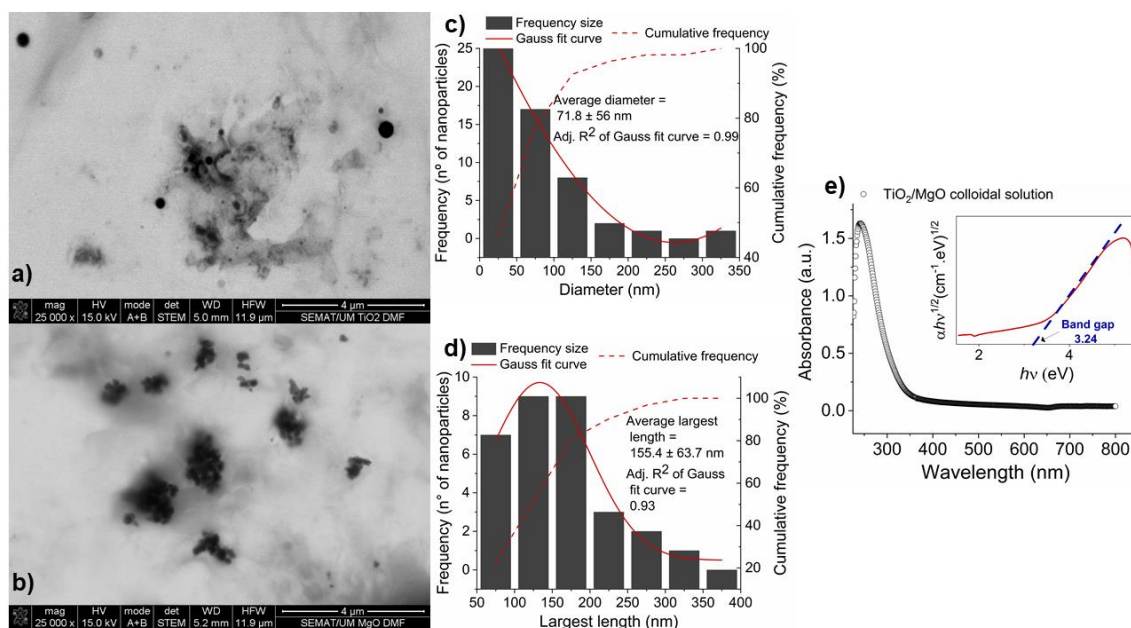


Figure 6-2. Nanoparticles characterization. (a) SEM image of TiO<sub>2</sub> NPs, (b) SEM image of MgO, (c) NPs distribution histogram of TiO<sub>2</sub>, (d) NPs distribution histogram of MgO and (e) UV-vis spectra of colloidal TiO<sub>2</sub>/MgO ablated nanoparticles in DCM (the inset graph shows the Tauc plot for  $\alpha h\nu^{1/2}$  versus  $h\nu$  and the respective band gap).

### 6.3.4. Fourier-transformed infrared spectroscopy

FTIR spectra were performed to verify the effectivity of the pretreatment and chemical modification applied, as well as possible chemical interactions between the CA matrix and TiO<sub>2</sub>/MgO nanoparticles fillers (Figure 6.3). Absorbed peaks in extracted cellulose profile around 2890 cm<sup>-1</sup> (C-H stretching in cellulose-rich material), 1431 cm<sup>-1</sup> (CH<sub>2</sub> banding vibration in cellulose), 1368 cm<sup>-1</sup> (C-H asymmetric deformation in cellulose), 1315 cm<sup>-1</sup> (CH<sub>2</sub> wagging in cellulose), 1161 (asymmetric C-O-C stretching), 1102 cm<sup>-1</sup> (C-OH skeletal vibration), 1028 cm<sup>-1</sup> (C-O-C pyranose ring skeletal vibration) and 897 cm<sup>-1</sup> (C-H deformation), typical of cellulose-rich materials [8, 69–72], confirm the successful performance of the pretreatment applied to extract cellulose from corncob.

Regarding the acetylation procedure, the rising of new absorption peaks in the acetylated samples spectra, namely at 1734 cm<sup>-1</sup>, 1368 cm<sup>-1</sup> and 1217 cm<sup>-1</sup> related to C=O stretching of ester group, C-H in O-(C=O)-CH<sub>3</sub> and C-O stretching of acetyl groups, respectively, confirm that the chemical modification was undoubtedly accomplished [43, 73]. Additional evidence of the acetylation is provided by the reduced intensity of peaks assigned to -OH stretching and through comparisons with the CA commercial spectra.

When it comes to the CA/MgO/TiO<sub>2</sub> nanocomposite film spectra, the absence of significant new peaks indicates that the nanoparticle fillers are only physically mixed into the CA matrix. No chemical interaction between the polymeric matrix and metal oxide nanoparticles has also been

verified by Swaroop et al. [16] and Ahmed et al. [74]. Notwithstanding, the rise of a broad peak from 3750 to 3100  $\text{cm}^{-1}$  is possibly associated with the OH stretching vibrations of MgO surface-adsorbed water molecules [75]. Peaks in the region of 2920-2850 can be attributed to asymmetrical stretching vibrations of hydrocarbon methyl groups from residual dichloromethane [76]. Although the FTIR analysis is not conclusive about the successful synthesis and embedment of MgO/TiO<sub>2</sub> nanoparticles into CA films, these issues will be, indeed, confirmed and explored in detail in the following X-ray diffractogram and EDS analysis.

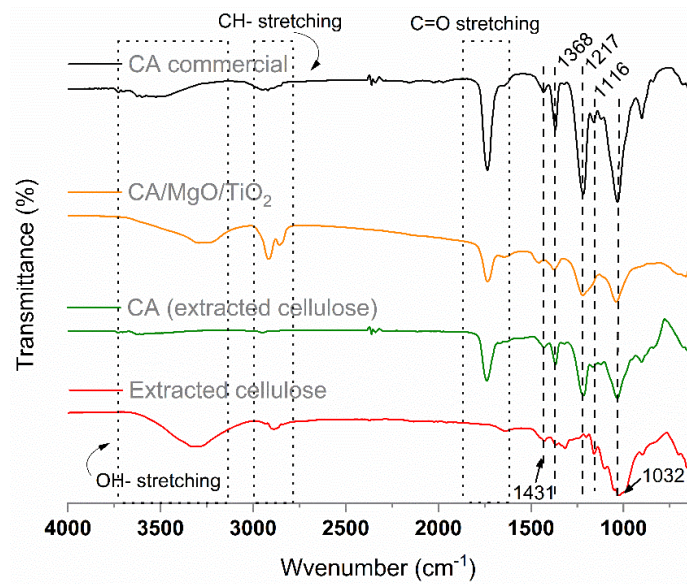


Figure 6-3. FTIR spectra of the extracted cellulose (LHW-dilute NaOH pretreatment), commercial CA, synthesized CA and CA/MgO/TiO<sub>2</sub> bionanocomposite film.

### 6.3.5. X-ray diffraction analysis

The diffractograms of the synthesized CA and the nanocomposite films are presented in Figure 6.4b. No sharp peaks are observed in the synthesized CA film profile, indicating that the produced film has reduced crystallinity. The appearance of a broad peak ranging from  $2\theta = 13^\circ$  to  $2\theta = 17^\circ$  can be assigned to the introduction of acetyl groups in the cellulosic fibers and the consequent enlargement of spaces between layers in the crystal facets [77, 78]. This feature indicates that occurred a change from crystalline to an amorphous structure during the esterification. The rise of another distinct peak around  $2\theta = 8^\circ$  is also typical of cellulose acetylation and refers to a disorder in the crystalline structure of the cellulose. The disorder is associated with an increase in the interfibrillar distance due to the insertion of acetate groups, as well as with the breakdown of microfibrillar structures, as depicted in Figure 6.4a.

The prepared nanocomposite film also demonstrates the same peaks corresponding to amorphous CA, in addition to the rise of new peaks around  $2\theta = 37.5^\circ$  and  $43^\circ$ , typical of MgO NPs [16, 79]. Additional peaks at  $2\theta = 19.3^\circ$  and  $2\theta = 34.2^\circ$  and  $47.7^\circ$  may also disclose the coexistence of  $\text{Mg}(\text{OH})_2$  and pure Mg nanoparticles, respectively [39, 41]. The defined peak at  $2\theta = 23^\circ$  and  $27.5^\circ$  indicates that rutile was the most prominent phase of  $\text{TiO}_2$  produced, which was also evidenced by other authors who conducted  $\text{TiO}_2$  NPs synthesis through PLAL [37, 54]. However, typical peaks related to anatase  $\text{TiO}_2$  ( $2\theta = 25^\circ$ ,  $31.3^\circ$  and  $47.7^\circ$ ) have been also clearly detected [53, 79]. In general, the XRD patterns related to  $\text{TiO}_2$  and MgO nanoparticles show sharp peaks, suggesting that they consist of an array of crystalline grains, but low intensities, which is probably because the prepared materials are not presented in high concentrations. These findings support the successful synthesis of the metal oxides by PLAL, as well as the effective preparation of nanocomposite films through direct dissolution of the synthesized CA in the  $\text{TiO}_2/\text{MgO}/\text{DCM}$  colloidal solution, followed by solvent casting.

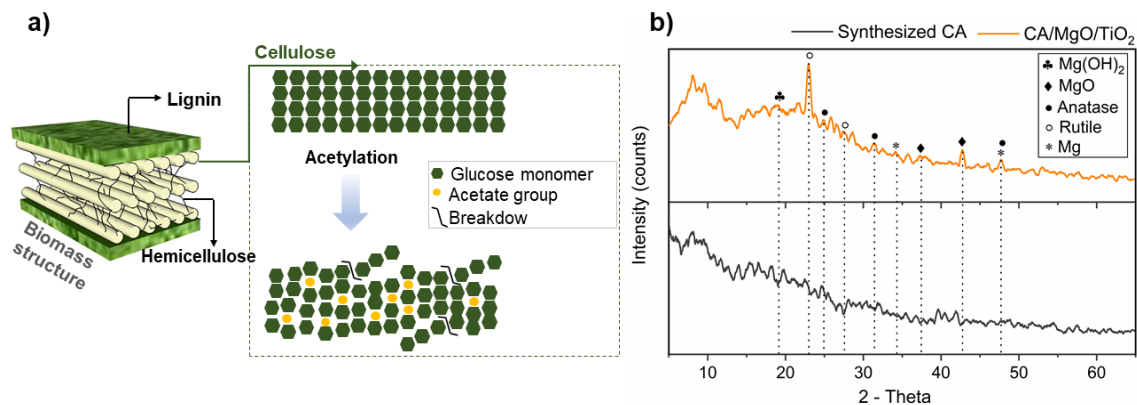


Figure 6-4. (a) Schematic representation of disorder caused in the cellulose structure due to acetate groups insertion and (b) XRD diffractograms of the synthesized CA and  $\text{CA}/\text{MgO}/\text{TiO}_2$  films.

### 6.3.6. Scanning electron microscopy of the films

The surface morphology and cross-section of the synthesized CA and  $\text{CA}/\text{MgO}/\text{TiO}_2$  films are presented, respectively, in Figures 6.5 (a and b) and Figure 6.5 (d and e). In general, surface investigation of the films revealed the occurrence of some roughness patterns and holes. The rough surface and the few porous structures verified in the cross-section relative to the synthesized CA may be attributed to the solvent evaporation processes, the casting surface or some undissolved remaining material. Notwithstanding, the quite smooth, flat and homogeneous surface of the produced synthesized CA film, with no fiber-like structure typical of the start cellulosic material,



denotes the successful acetylation procedure. This also highlights the effectivity of the combined pretreatment applied, which, by removing a great share of recalcitrant components, allowed the penetration of the acetylation reagents into the cellulose fibers.

By introducing the  $\text{TiO}_2$  and  $\text{MgO}$  nanoparticles into the CA film, the porous size and porosity increased. This was expected to happen since the CA/acetone ratio in the casting solution of both films was kept the same. Besides, the agglomeration of metal oxide nanoparticles during film formation can give rise to microporous structures [80]. At high filler loading,  $\text{MgO}$  and  $\text{TiO}_2$  tend to agglomerate in order to minimize their surface energy, and this effect has been reported to cause micro-cracks inside polymeric matrices [80, 81]. From surface and cross-section SEM images, it is evident that no physical defects are present on the  $\text{CA/MgO/TiO}_2$  film, suggesting that the concentration of nanoparticles used was not able to cause structural defects in the film.

Although the nanoparticles are not visible in Figures 6.5d and 6.5e, possibly due to limitation of the SEM equipment or to their perfect embedment/immobilization inside the film, their presence (detected as Ti and Mg elements in Figure 6.6f) was confirmed by EDS analysis. Additional EDS analysis (not shown) confirmed uniform dispersion of nanoparticles throughout the film. Elemental composition of the synthesized CA film is also illustrated in Figure 6.5c, and confirms that the high content of carbon (C) and oxygen (O) comes from the cellulose acetate, and the presence residual elements (Na, Cl and S) are originated from previous treatments.

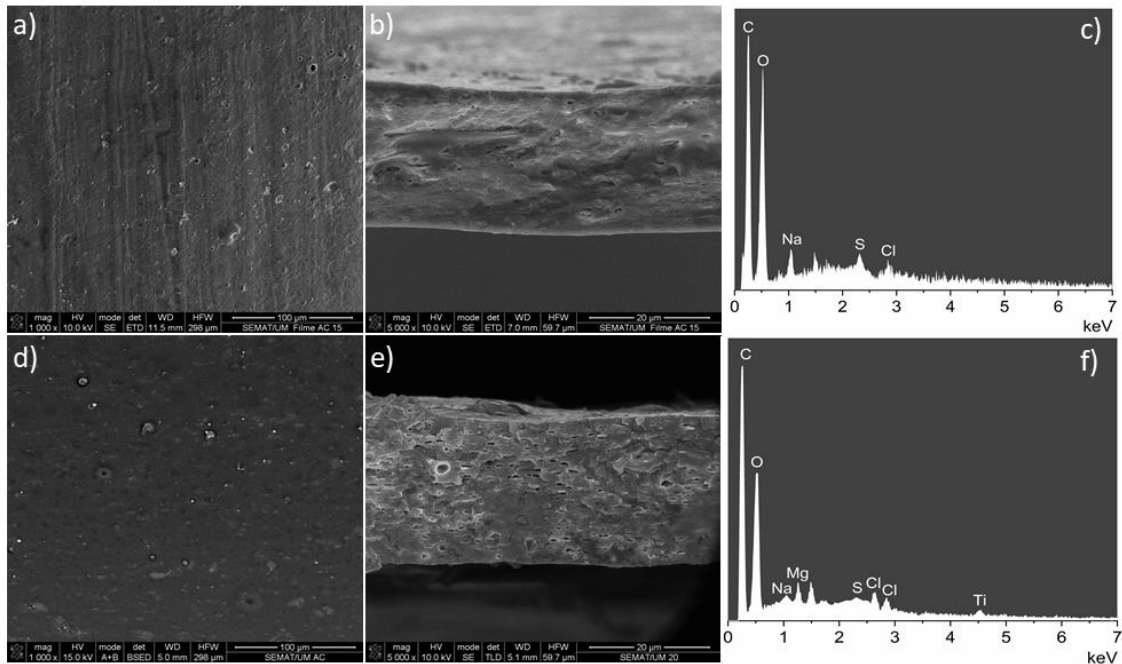


Figure 6-5. SEM micrographs and EDS analysis of the produced films: (a), (b), (c) refer to synthesized CA surface, cross-section and EDS analysis, respectively, and (d), (e), (f) refer to CA/TiO<sub>2</sub>/MgO surface, cross section and EDS, respectively.

### 6.3.7. Thermogravimetry analysis of films

Thermal stability of synthesized CA and CA/TiO<sub>2</sub>/MgO films was determined using thermogravimetry analysis technique as shown in Figure 6.6. Degradation reactions observed in the synthesized CA curve occurred in a single step and in a narrow temperature range ( $T_{\text{onset}} = 320$ ;  $T_{\text{end}} = 366$ ). Regarding the CA/TiO<sub>2</sub>/MgO film, two main weight loss zones are clearly identified in the DTG thermal profile. The distinguished initial weight loss of about 8.6 % in the temperature range of 140 – 202 °C can be related to an isolated thermal degradation of polymer chains due to the formation of a new crystalline phase favored by the introduction of TiO<sub>2</sub>, as reported by Valentim et al. [82] and Mohr et al. [68]. The latter authors concluded that TiO<sub>2</sub> NPs act as nucleation agents for new crystalline phases on PLA with lower melting temperatures. Mohr et al. [68] also suggested that TiO<sub>2</sub> can increase the amorphous phase due to molecular disorganization leading to reduced visible radiation transmission. Overall, in comparison to the neat CA, the nanocomposite film started to degrade early. Indeed, the photoactivity/catalytic effect related to metal oxides, including TiO<sub>2</sub> and MgO, can make the polymer matrix degrade more easily and therefore decrease its degradation temperature [83, 84]. Other authors have also reported reduction on  $T_{\text{onset}}$  after incorporating TiO<sub>2</sub>, MgO and other metal oxides NPs into polymeric matrices [16, 81, 85]. For instance, in Restrepo et al. [84] the introduction of zinc oxide nanoparticles (5 % at weight basis) into polylactic acid (PLA) caused a reduction up to 117 °C on  $T_{\text{onset}}$ . Despite this, the temperature of maximum rate of weight loss ( $T_{\text{max}} - 350$  °C) and the temperature at which the degradation processes of the CA/TiO<sub>2</sub>/MgO film ends ( $T_{\text{end}}$ ) were maintained the same as the neat synthesized CA. After incorporating TiO<sub>2</sub> nanoparticles into a PLA matrix, Sangiorgi et al. [83] verified this same thermal pattern. A similar result was also verified by Das & Gebru [86] when TiO<sub>2</sub> NPs were embedded into CA to prepare hybrid membranes, and by Mohr et al. [68]. At 600 °C the weight loss of the CA/TiO<sub>2</sub>/MgO (89.23%) film was slightly higher than that of the neat CA (80.14 %). In response, a higher residual mass, partly related to the NPs contribution, was also recorded.

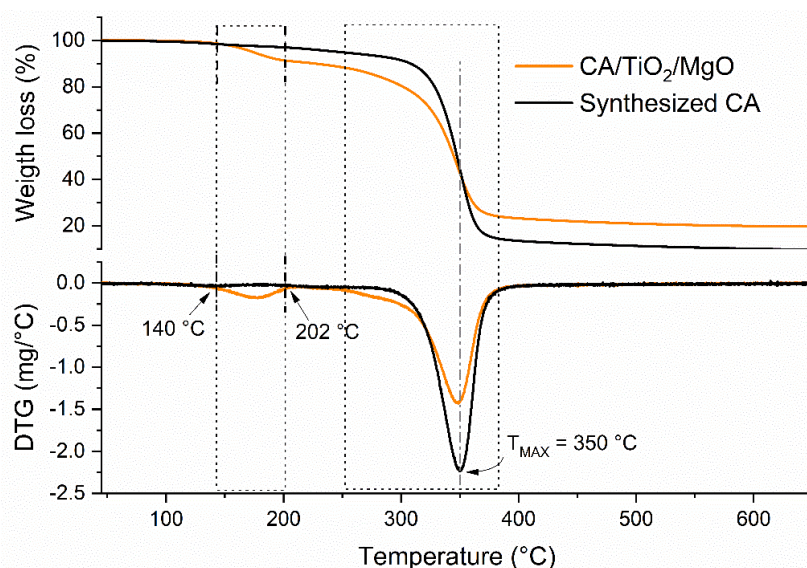


Figure 6-6. TG (upper graph) and DTG (lower graph) curves of the synthesized CA and CA/TiO<sub>2</sub>/MgO films.

### 6.3.8. Dynamic mechanical analysis

The viscoelastic behavior of both films was characterized by the storage modulus  $E'$  (a measure of the material's ability to recover from deformation), the loss modulus  $E''$  (a measure of the material's ability to lose energy as heat) and the  $\tan \delta$  or damping (an indicator of how efficiently the material loses energy to molecular rearrangement and internal friction), as illustrated in Figure 6.7a and 6.7b. The storage modulus profiles of both films show a pattern typical of amorphous polymers, which is related to the introduction of acetyl groups onto the AGU unity of cellulose fibers and the consequent unpacking of chains. By comparing the viscoelastic properties of the films, it is clear that, after the embedment of nanoparticles, a reduction in the  $E'$  of about three times took place (Figure 6.7b). Based on the SEM images, this was expected since the neat CA film showed to have a denser structure, which translated into high stiffness when it comes to mechanical properties. In contrast, the enlarged porous structures brought by the embedment of TiO<sub>2</sub>/MgO NPs into the CA matrix reduced stiffness and made the nanocomposite more flexible, which is supported by the higher  $\tan \delta$  values. Another possible cause for this issue lies with the agglomeration of particles during film formation. Agglomeration leads to domains that are rich in the nanofillers and poor in the polymer, which ultimately can act as stress concentrating centers in a way that, if the inter-particle attractions are weak, they may play a large role in the storage and loss of applied mechanical energy [80, 87]. On the other hand, aggregation has been reported as an improving factor of photocatalytic activity for colloidal suspensions with mixed-phase anatase-rutile TiO<sub>2</sub> nanoparticles, since the migration of electrons across a phase junction was beneficial

for charge separation [38]. The decrease in elastic modulus of polymeric matrices provided by the introduction of metal oxide nanoparticles has already been reported by other authors [81, 85, 88]. Mohr et al. [68] associated the elastic modulus reduction of a PLA/TiO<sub>2</sub> nanocomposite with the formation of new crystalline forms that act as defects, handicapping the mechanical performance of the film. In general, from the literature it is possible to conclude that mechanical properties may change in function of the nanoparticle's concentration, type and dimension, as well as surround environmental conditions [16, 80, 81, 88].

Furthermore, in both films the storage modulus decreases when temperature increases due to increased segmental mobility of chains. However, a distinguished small plateau in the range of 60-75 °C is verified in the E' profile of the nanocomposite film (Figure 6.7b). This can be attributed to the reinforcement effect provided by the NPs, or to the formation of a small neck, observed exclusively in the concerned sample (inset image highlighted in Figure 6.7b). Within this neck, the chain axes become aligned parallel to the elongation direction, which leads to localized strengthening. In comparison to the neat CA film, the nanocomposite film also exhibited a less significant drop in E' over the entire temperature range, which can be related to mechanical restrictions introduced by the NPs. Besides, the nanocomposite had a broader transition instead of a steep drop-off in the E', indicating the presence and influence of embedded nanoparticles.

The broadening of the loss modulus curve of the nanocomposite film may also reflect a compositional gradient or a molecular mobility gradient [89]. Distinctly, a sharp peak is observed in the E'' of the neat CA film curve preceding its drop around 136 °C. A broad secondary peak in E'' of the neat CA film is also verified at about 64 °C. In response there is a decrease in E' from 40 °C to 100 °C, probably originated from the natural mobility of chains in response to temperature rising and relaxation transitions triggered by local mobility of chains plasticized with water [90].

By applying the peak of Tan  $\delta$  curve method to obtain the glass transition temperature ( $T_g$ ), it is noticeable that the incorporation nanoparticles increased significantly the  $T_g$  of the nanocomposite film ( $T_g = 176$  °C). This trend is in line with the E' and E'', which once more indicates that, near the nanoparticles, the cellulose acetate chains have their mobility affected. The  $T_g$  value of the pure synthesized CA film was found to be similar to other cellulose acetate films reported in literature [91–94]. The glass transition temperature is an important parameter to be defined since it determines the operating range of the material, which was extended in the nanocomposite film.

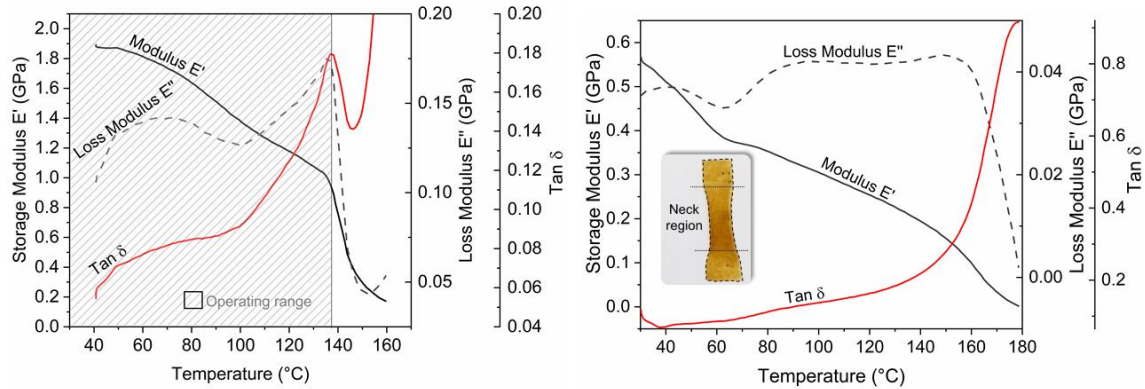


Figure 6-7. Dynamic mechanical analysis of the (a) synthesized CA and (b) CA/TiO<sub>2</sub>/MgO film.

## 6.4. Conclusions

This study was focused on presenting an eco-friendly processing route to produce bio-based nanocomposites with potential to be applied as active packaging. By applying a green two-stage combined pretreatment, non-cellulosic components of corncob could be removed, which greatly favored the synthesis of cellulose acetate with remarkable yield. Parallel to that, colloidal suspensions of TiO<sub>2</sub> and MgO were effortlessly produced through PLA in DCM. The mixed colloidal suspensions could be promptly used to dissolve the synthesized CA, which was further turned into a film via the solvent casting method. The FTIR analysis did not present any response regarding the metal oxides, suggesting that there was no chemical interaction between the CA matrix and nanofillers. The formation of crystalline oxidized phases of the metals, as well as their presence in the mixed colloidal suspension and embedment into the CA matrix, could be confirmed through UV-vis spectroscopy, XRD and EDS, attesting the suitability of the proposed processing. The thermal stability of the CA matrix was not significantly affected after the introduction of nanoparticles, but its onset temperature was lowered as expected. Conversely, the stiffness of the CA matrix was reduced due to the increase of porous structures, which leads to flexible nanocomposites. By restricting chain mobility of the cellulose acetate, the metal oxide nanoparticles could also extend the operating range of the bionanocomposite. Overall, in addition to the eco-friendly aspect, the versatility and scalability of the applied techniques, as well as the low cost of raw-materials used, also underpin the technical feasibility of the presented synthesis processing. Changes in cellulose acetate and nanoparticle properties can be easily accomplished by tailoring their synthesis methodologies, and their effects on nanocomposite film properties can be studied in the future. Furthermore, the active properties of the produced nanocomposite (namely biodegradability and antimicrobial properties) can be assessed and validated in the forthcoming activities.

## Acknowledgements

This work was supported by the Brazilian National Council for Scientific and Technological Development (Grant number 201940/2015-9). The authors also acknowledge the Portuguese Foundation of Science and Technology (TSSiPRO-technologies for sustainable and smart innovative products-norte-01-0145-FEDER-000015) and UID/CTM/50025/2019 for the financial support.

## References

1. Statista: Global plastic production from 1950 to 2017 (in million metric tons), <https://www.statista.com/statistics/282732/global-production-of-plastics-since-1950/>
2. Baltus, W., Beckmann, J., Carrez, D., Carus, M.: Market study on Bio-based Polymers in the World Capacities, Production and Applications: Status Quo and Trends towards 2020. Huerth (2013)
3. Meraldo, A.: Introduction to Bio-Based Polymers. In: John R. Wagner, J. (ed.) Multilayer Flexible Packaging. William Andrew (2016)
4. Hassan, S.S., Williams, G.A., Jaiswal, A.K.: Emerging technologies for the pretreatment of lignocellulosic biomass. *Bioresour. Technol.* 262, 310–318 (2018). <https://doi.org/10.1016/j.biortech.2018.04.099>
5. Araújo, D.J.C., Machado, A. V., Vilarinho, M.C.L.G.: Availability and Suitability of Agroindustrial Residues as Feedstock for Cellulose-Based Materials: Brazil Case Study. *Waste and Biomass Valorization*. 16 (2018). <https://doi.org/10.1007/s12649-018-0291-0>
6. Lee, H. V, Hamid, S.B. a, Zain, S.K.: Conversion of Lignocellulosic Biomass to Nanocellulose: Structure and Chemical Process Conversion of Lignocellulosic Biomass to Nanocellulose: *Sci. World J.* 2014, 1–14 (2014). <https://doi.org/10.1155/2014/631013>
7. Silvério, H.A., Flauzino Neto, W.P., Dantas, N.O., Pasquini, D.: Extraction and characterization of cellulose nanocrystals from corncob for application as reinforcing agent in nanocomposites. *Ind. Crops Prod.* 44, 427–436 (2013). <https://doi.org/10.1016/j.indcrop.2012.10.014>
8. Reddy, K.O., Maheswari, C.U., Dhlamini, M.S., Mothudi, B.M., Zhang, J., Zhang, J., Nagarajan, R., Rajulu, A.V.: Preparation and characterization of regenerated cellulose films using

- borassus fruit fibers and an ionic liquid. *Carbohydr. Polym.* 160, 203–211 (2017). <https://doi.org/10.1016/j.carbpol.2016.12.051>
9. Vanitjinda, G., Nimchua, T., Sukyai, P.: Effect of xylanase-assisted pretreatment on the properties of cellulose and regenerated cellulose films from sugarcane bagasse. *Int. J. Biol. Macromol.* 122, 503–516 (2019). <https://doi.org/10.1016/j.ijbiomac.2018.10.191>
  10. Zhang, J., Luo, N., Xia, G., Yu, J.: Directly Converting Agricultural Straw into All-Biomass Nanocomposite Films Reinforced with Additional in Situ-Retained Cellulose Nanocrystals. *ACS Sustain. Chem. Eng.* 5, 5127–5133 (2017). <https://doi.org/10.1021/acssuschemeng.7b00488>
  11. Otoni, C.G., Lodi, B.D., Lorevice, M. V, Leitão, R.C., Ferreira, M.D., Moura, M.R. De, Mattoso, L.H.C.: Industrial Crops & Products Optimized and scaled-up production of cellulose-reinforced biodegradable composite films made up of carrot processing waste. *Ind. Crop. Prod.* 121, 66–72 (2018). <https://doi.org/10.1016/j.indcrop.2018.05.003>
  12. Puls, J., Wilson, S.A., Ho, D.: Degradation of Cellulose Acetate-Based Materials : A Review. *J Polym Env.* 19, 152–165 (2011). <https://doi.org/10.1007/s10924-010-0258-0>
  13. Goshal, G.: Recent Trends in Active, Smart, and Intelligent Packaging for Food Products. In: Grumezescu, A. and Holban, A.-M. (eds.) *Food Packaging and Preservation*. pp. 343–374. Academic Press (2018)
  14. Huang, Y., Mei, L., Chen, X., Wang, Q.: Recent Developments in Food Packaging Based on Nanomaterials. *Nanomaterials.* 8, 1–29 (2018). <https://doi.org/10.3390/nano8100830>
  15. Araújo, D.J.C., Vilarinho, M.C.L.G., Machado, A. V.: Agroindustrial residues as cellulose source for food packaging applications. In: Virarinho, M.C.L.G. and Al., E. (eds.) *Wastes: solutions, treatments and opportunities*. pp. 217–223. Taylor & Francis, London (2019)
  16. Swaroop, C., Shukla, M.: International Journal of Biological Macromolecules Nano-magnesium oxide reinforced polylactic acid bio films for food packaging applications. *Int. J. Biol. Macromol.* 113, 729–736 (2018). <https://doi.org/10.1016/j.ijbiomac.2018.02.156>
  17. Youssef, A.M., El-sayed, S.M.: Bionanocomposites materials for food packaging applications: Concepts and future outlook. *Carbohydr. Polym.* 193, 19–27 (2018). <https://doi.org/10.1016/j.carbpol.2018.03.088>
  18. Tang, Z.X., Lv, B.F.: MgO nanoparticles as antibacterial agent: Preparation and activity. *Brazilian J. Chem. Eng.* 31, 591–601 (2014). <https://doi.org/10.1590/0104-6632.20140313s00002813>

19. Nguyen, N.Y.T., Grelling, N., Wetteland, C.L., Rosario, R., Liu, H.: Antimicrobial Activities and Mechanisms of Magnesium Oxide Nanoparticles (nMgO) against Pathogenic Bacteria, Yeasts, and Biofilms. *Sci. Rep.* 8, 1–23 (2018). <https://doi.org/10.1038/s41598-018-34567-5>
20. Pilarska, A.A., Klapiszewski, Ł.: Recent development in the synthesis, modification and application of Mg (OH) 2 and MgO: A review. *Powder Technol.* 319, 373–407 (2017). <https://doi.org/10.1016/j.powtec.2017.07.009>
21. Kaewklin, P., Siripatrawan, U., Suwanagul, A., Suk, Y.: Active packaging from chitosan-titanium dioxide nanocomposite film for prolonging storage life of tomato fruit. *Int. J. Biol. Macromol.* 112, 523–529 (2018). <https://doi.org/10.1016/j.ijbiomac.2018.01.124>
22. Bodaghi, H., Mostofi, Y., Oromiehie, A., Zamani, Z., Ghanbarzadeh, B., Costa, C., Conte, A., Del Nobile, M.A.: Evaluation of the photocatalytic antimicrobial effects of a TiO<sub>2</sub> nanocomposite food packaging film by in vitro and in vivo tests. *LWT - Food Sci. Technol.* 50, 702–706 (2013). <https://doi.org/10.1016/j.lwt.2012.07.027>
23. Baek, N., Kim, Y.T., Marcy, J.E., Duncan, S.E., O’Keefe, S.F.: Physical properties of nanocomposite polylactic acid films prepared with oleic acid modified titanium dioxide. *Food Package. Shelf Life.* 17, 30–38 (2018). <https://doi.org/10.1016/j.fpsl.2018.05.004>
24. Dobrucka, R., Ankiel, M.: Possible applications of metal nanoparticles in antimicrobial food packaging. 1–7 (2018). <https://doi.org/10.1111/jfs.12617>
25. Xie, J., Hung, Y.: UV-A activated TiO<sub>2</sub> embedded biodegradable polymer film for antimicrobial food packaging application. *LWT - Food Sci. Technol.* 96, 307–314 (2018). <https://doi.org/10.1016/j.lwt.2018.05.050>
26. Siripatrawan, U., Kaewklin, P.: Fabrication and characterization of chitosan-titanium dioxide nanocomposite film as ethylene scavenging and antimicrobial active food packaging. *Food Hydrocoll.* 84, 125–134 (2018). <https://doi.org/10.1016/j.foodhyd.2018.04.049>
27. Anaya-Esparza, L.M., Montalvo-González, E., González-Silva, N., Méndez-Robles, M.D., Romero-Toledo, R., Yahia, E.M., Pérez-Larios, A.: Synthesis and characterization of TiO<sub>2</sub>-ZnO-MgO mixed oxide and their antibacterial activity. *Materials (Basel)*. 12, (2019). <https://doi.org/10.3390/ma12050698>
28. Nikam, A. V., Prasad, B.L.V., Kulkarni, A.A.: Wet chemical synthesis of metal oxide nanoparticles: A review. *Cryst. Eng. Comm.* 20, 5091–5107 (2018). <https://doi.org/10.1039/C8CE00487K>



29. Dar, M.I., Chandiran, A.K., Grätzel, M., Nazeeruddin, M.K., Shivashankar, S.A.: Controlled synthesis of TiO<sub>2</sub> nanoparticles and nanospheres using a microwave assisted approach for their application in dye-sensitized solar cells. *J. Mater. Chem. A*, 2, 1662–1667 (2014). <https://doi.org/10.1039/c3ta14130f>
30. Kim, C.S., Moon, B.K., Park, J.H., Choi, B.C., Seo, H.J.: Solvothermal synthesis of nanocrystalline TiO<sub>2</sub> in toluene with surfactant. *J. Cryst. Growth*, 257, 309–315 (2003). [https://doi.org/10.1016/S0022-0248\(03\)01468-4](https://doi.org/10.1016/S0022-0248(03)01468-4)
31. Yu, J.C., Xu, A., Zhang, L., Song, R., Wu, L.: Synthesis and characterization of porous magnesium hydroxide and oxide nanoplates. *J. Phys. Chem. B*, 108, 64–70 (2004). <https://doi.org/10.1021/jp035340w>
32. Pilarska, A., Paukszta, D., Ciesielczyk, F., Jesionowski, T.: Physico-chemical and dispersive characterization of magnesium oxides precipitated from the Mg(NO<sub>3</sub>)<sub>2</sub> and MgSO<sub>4</sub> solutions. *Polish J. Chem. Technol.* 12, 52–56 (2010). <https://doi.org/10.2478/v10026-010-0018-x>
33. Wagener, P., Jakobi, J., Rehbock, C., Chakravadhanula, V.S.K., Thede, C., Wiedwald, U., Bartsch, M., Kienle, L., Barcikowski, S.: Solvent-surface interactions control the phase structure in laser-generated iron-gold core-shell nanoparticles. *Sci. Rep.* 6, 1–12 (2016). <https://doi.org/10.1038/srep23352>
34. Sarwar, M.S., Niazi, M.B.K., Jahan, Z., Ahmad, T., Hussain, A.: Preparation and characterization of PVA / nanocellulose / Ag nanocomposite films for antimicrobial food packaging. *Carbohydr. Polym.* 184, 453–464 (2018). <https://doi.org/10.1016/j.carbpol.2017.12.068>
35. Amendola, V., Meneghetti, M.: What controls the composition and the structure of nano-materials generated by laser ablation in liquid solution? *Phys. Chem. Chem. Phys.* 15, 3027–3046 (2013). <https://doi.org/10.1039/c2cp42895d>
36. Reich, S., Schönfeld, P., Wagener, P., Letzel, A., Ibrahimkuty, S., Gökce, B., Barcikowski, S., Menzel, A., Rolo, S., Plech, A.: Pulsed laser ablation in liquids: Impact of the bubble dynamics on particle formation. *J. Colloid Interface Sci.* 489, 106–113 (2017). <https://doi.org/10.1016/j.jcis.2016.08.030>
37. Singh, A., Vihinen, J., Frankberg, E., Hyvärinen, L., Honkanen, M., Levänen, E.: Pulsed Laser Ablation-Induced Green Synthesis of TiO<sub>2</sub> Nanoparticles and Application of Novel Small Angle X-Ray Scattering Technique for Nanoparticle Size and Size Distribution Analysis. *Nanoscale Res. Lett.* 11, 1–9 (2016). <https://doi.org/10.1186/s11671-016-1608-1>

38. Zimbone, M., Buccheri, M.A., Cacciato, G., Sanz, R., Rappazzo, G., Boninelli, S., Reitano, R., Romano, L., Privitera, V., Grimaldi, M.G.: Photocatalytic and antibacterial activity of TiO<sub>2</sub> nanoparticles obtained by laser ablation in water. *Appl. Catal. B Environ.* 165, 487–494 (2015). <https://doi.org/10.1016/j.apcatb.2014.10.031>
39. Phuoc, T.X., Howard, B.H., Martello, D. V, Soong, Y., Chyu, M.K.: Synthesis of Mg (OH) 2 , MgO , and Mg nanoparticles using laser ablation of magnesium in water and solvents. *Opt. Lasers Eng.* 46, 829–834 (2008). <https://doi.org/10.1016/j.optlaseng.2008.05.018>
40. Hsieh, H.F., Chen, Y.H., Wang, C.F.: A magnesium hydroxide preconcentration/matrix reduction method for the analysis of rare earth elements in water samples using laser ablation inductively coupled plasma mass spectrometry. *Talanta.* 85, 983–990 (2011). <https://doi.org/10.1016/j.talanta.2011.05.011>
41. Niu, K.Y., Yang, J., Sun, J., Du, X.W.: One-step synthesis of MgO hollow nanospheres with blue emission. *Nanotechnology.* 21, (2010). <https://doi.org/10.1088/0957-4484/21/29/295604>
42. Araújo, D.J.C., Vilarinho, M.C.L.G., Machado, A.: Effect of combined dilute-alkaline and green pretreatments on corncob fractionation: Pretreated biomass characterization and regenerated cellulose film production. *Ind. Crops Prod.* 141, 111785 (2019). <https://doi.org/10.1016/j.indcrop.2019.111785>
43. Das, A.M., Ali, A.A., Hazarika, M.P.: Synthesis and characterization of cellulose acetate from rice husk: Eco-friendly condition. *Carbohydr. Polym.* 112, 342–349 (2014). <https://doi.org/10.1016/j.carbpol.2014.06.006>
44. Araújo, D., Vilarinho, M., Machado, A.: Effect of combined green pretreatments on corncob fractionation: pretreated biomass characterization and regenerated cellulose film production. *Ind. Crops Prod.* (2019)
45. Carrier, M., Loppinet-Serani, A., Denux, D., Lasnier, J.-M., Ham-Pichavant, F., Cansell, F., Aymonier, C.: Thermogravimetric analysis as a new method to determine the lignocellulosic composition of biomass. *Biomass and Bioenergy.* 35, 298–307 (2011). <https://doi.org/10.1016/j.biombioe.2010.08.067>
46. Chen, T., Li, L., Zhao, R., Wu, J.: Pyrolysis kinetic analysis of the three pseudocomponents of biomass–cellulose, hemicellulose and lignin: Sinusoidally modulated temperature method. *J. Therm. Anal. Calorim.* 128, 1825–1832 (2016). <https://doi.org/10.1007/s10973-016-6040-3>

47. Saldarriaga, J.F., Aguado, R., Pablos, A., Amutio, M., Olazar, M., Bilbao, J.: Fast characterization of biomass fuels by thermogravimetric analysis (TGA). *Fuel*. 140, 744–751 (2015). <https://doi.org/10.1016/j.fuel.2014.10.024>
48. Teng, H., Lin, H.C., Ho, J.A.: Thermogravimetric Analysis on Global Mass Loss Kinetics of Rice Hull Pyrolysis. *Ind. Eng. Chem. Res.* 36, 3974–3977 (1997). <https://doi.org/10.1021/ie970017z>
49. Biswas, A., Saha, B.C., Lawton, J.W., Shogren, R.L., Willett, J.L.: Process for obtaining cellulose acetate from agricultural by-products. *Carbohydr. Polym.* 64, 134–137 (2006). <https://doi.org/10.1016/j.carbpol.2005.11.002>
50. Mostafa, N.A., Tayeb, A.M.: Production of biodegradable plastic from agricultural wastes. *Arab. J. Chem.* 11, 546–553 (2018). <https://doi.org/10.1016/j.arabjc.2015.04.008>
51. Somanathan, T., Krishna, V.M., Saravanan, V., Kumar, R., Kumar, R.: MgO nanoparticles for effective uptake and release of doxorubicin drug: PH sensitive controlled drug release. *J. Nanosci. Nanotechnol.* 16, 9421–9431 (2016). <https://doi.org/10.1166/jnn.2016.12164>
52. Liang, C., Sasaki, T., Shimizu, Y., Koshizaki, N.: Pulsed-laser ablation of Mg in liquids: Surfactant-directing nanoparticle assembly for magnesium hydroxide nanostructures. *Chem. Phys. Lett.* 389, 58–63 (2004). <https://doi.org/10.1016/j.cplett.2004.03.056>
53. Zhou, R., Lin, S., Zong, H., Huang, T., Li, F., Pan, J., Cui, J.: Continuous Synthesis of Ag / TiO<sub>2</sub> Nanoparticles with Enhanced Photocatalytic Activity by Pulsed Laser Ablation. *J. Nanomater.* 2017, 10 (2017)
54. Zuñiga-Ibarra, V.A., Shaji, S., Krishnan, B., Johny, J., Sharma Kanakillam, S., Avellaneda, D.A., Martinez, J.A.A., Roy, T.K.D., Ramos-Delgado, N.A.: Synthesis and characterization of black TiO<sub>2</sub> nanoparticles by pulsed laser irradiation in liquid. *Appl. Surf. Sci.* 483, 156–164 (2019). <https://doi.org/10.1016/j.apsusc.2019.03.302>
55. Aziz, W.J., Ali, S.Q., Jassim, N.Z.: Production TiO<sub>2</sub> Nanoparticles Using Laser Ablation in Ethanol. *Silicon*. 10, 2101–2107 (2018). <https://doi.org/10.1007/s12633-017-9730-y>
56. Zhang, Y.X., Jia, Y.: Synthesis of MgO/TiO<sub>2</sub>/Ag composites with good adsorption combined with photodegradation properties. *Mater. Sci. Eng. B Solid-State Mater. Adv. Technol.* 228, 123–131 (2018). <https://doi.org/10.1016/j.mseb.2017.11.024>
57. Mathew, S., Kumar Prasad, A., Benoy, T., Rakesh, P.P., Hari, M., Libish, T.M., Radhakrishnan, P., Nampoori, V.P.N., Vallabhan, C.P.G.: UV-visible photoluminescence of TiO<sub>2</sub>

- nanoparticles prepared by hydrothermal method. *J. Fluoresc.* 22, 1563–1569 (2012). <https://doi.org/10.1007/s10895-012-1096-3>
58. Liu, Z., Yin, Z., Cox, C., Bosman, M., Qian, X., Li, N., Zhao, H., Du, Y., Li, J., Nocera, D.G.: Room temperature stable CO<sub>x</sub>-free H<sub>2</sub> production from methanol with magnesium oxide nanophotocatalysts. *Sci. Adv.* 2, (2016). <https://doi.org/10.1126/sciadv.1501425>
59. Adnan, S., Al-dahan, Z.T., Ghadhban, E.: Titanium Dioxide Nanoparticles Synthesis by Pulsed Laser Ablation. *Int. J. Eng. Sci.* 8, 28–32 (2019). <https://doi.org/10.9790/1813-0801012832>
60. Heydary, V., Navaei-Nigjeh, M., Rahimifard, M., Mohammadirad, A., Baeeri, M., Abdollahi, M.: Biochemical and molecular evidences on the protection by magnesium oxide nanoparticles of chlorpyrifos-induced apoptosis in human lymphocytes. *J. Res. Med. Sci.* 20, 1021–1031 (2015). <https://doi.org/10.4103/1735-1995.172811>
61. Ye, C., Pan, S.S., Teng, X.M., Li, G.H.: Optical properties of MgO-TiO<sub>2</sub> amorphous composite films. *J. Appl. Phys.* 102, (2007). <https://doi.org/10.1063/1.2752118>
62. Kang, X., Liu, S., Dai, Z., He, Y., Song, X., Tan, Z.: Titanium dioxide: From engineering to applications. (2019)
63. Higashimoto, S.: Titanium-dioxide-based visible-light-sensitive photocatalysis: Mechanistic insight and applications. *Catalysts.* 9, (2019). <https://doi.org/10.3390/catal9020201>
64. Tauc, J.: Optical properties and electronic structure of amorphous Ge and Si. *Mater. Res. Bull.* 3, 37–46 (1968)
65. Zhang, B., Cao, S., Du, M., Ye, X., Wang, Y., Ye, J.: Titanium dioxide (TiO<sub>2</sub>) mesocrystals: Synthesis, growth mechanisms and photocatalytic properties. *Catalysts.* 9, (2019). <https://doi.org/10.3390/catal9010091>
66. Bandara, J., Hadapangoda, C.C., Jayasekera, W.G.: TiO<sub>2</sub>/MgO composite photocatalyst: The role of MgO in photoinduced charge carrier separation. *Appl. Catal. B Environ.* 50, 83–88 (2004). <https://doi.org/10.1016/j.apcatb.2003.12.021>
67. Gold, K., Slay, B., Knackstedt, M., Gaharwar, A.K.: Antimicrobial Activity of Metal and Metal-Oxide Based Nanoparticles. *Adv. Ther.* 1700033, 1–15 (2018). <https://doi.org/10.1002/adtp.201700033>
68. Mohr, L.C., Capelezzo, A.P., Baretta, C.R.D.M., Martins, M.A.P.M., Fiori, M.A., Mello, J.M.M.: Titanium dioxide nanoparticles applied as ultraviolet radiation blocker in the polylactic acid

- bidegradable polymer. *Polym. Test.* 77, 105867 (2019).  
<https://doi.org/10.1016/j.polymertesting.2019.04.014>
69. Ang, T.N., Ngoh, G.C., Seak, A., Chua, M., Lee, M.G.: Elucidation of the effect of ionic liquid pretreatment on rice husk via structural analyses. *Biotechnol. Biofuels.* 5, 1–10 (2012)
70. Ma, Z., Pan, G., Xu, H., Huang, Y., Yang, Y.: Cellulosic fibers with high aspect ratio from cornhusks via controlled swelling and alkaline penetration. *Carbohydr. Polym.* 124, 50–56 (2015).  
<https://doi.org/10.1016/j.carbpol.2015.02.008>
71. Poletto, M., Pistor, V., Zattera, A.J.: Structural Characteristics and Thermal Properties of Native Cellulose. *Cellul. – Fundam. Asp.* 45–68 (2013). <https://doi.org/10.5772/50452>
72. Wang, F., Li, S., Sun, Y., Han, H., Zhang, B.: Ionic liquids as efficient pretreatment solvents for lignocellulosic biomass. *R. Soc. Chem.* 7, 47990–47998 (2017).  
<https://doi.org/10.1039/c7ra08110c>
73. Chen, J., Xu, J., Wang, K., Cao, X., Sun, R.: Cellulose acetate fibers prepared from different raw materials with rapid synthesis method. *Carbohydr. Polym.* 137, 685–692 (2016).  
<https://doi.org/10.1016/j.carbpol.2015.11.034>
74. Ahmed, J., Arfat, Y.A., Castro-Aguirre, E., Auras, R.: Mechanical, structural and thermal properties of Ag–Cu and ZnO reinforced polylactide nanocomposite films. *Int. J. Biol. Macromol.* 86, 885–892 (2016)
75. Ansari, A., Ali, A., Asif, M., Shamsuzzaman: Microwave-assisted MgO NP catalyzed one-pot multicomponent synthesis of polysubstituted steroidal pyridines. *New J. Chem.* 42, 184–197 (2018)
76. Wang, N., Lim, L.-T.: Physicochemical Changes of Coffee Beans During Roasting. *J. Agric. Food Chem.* 60, 5446–5453 (2012)
77. Wan Daud, W.R., Djuned, F.M.: Cellulose acetate from oil palm empty fruit bunch via a one step heterogeneous acetylation. *Carbohydr. Polym.* 132, 252–260 (2015).  
<https://doi.org/10.1016/j.carbpol.2015.06.011>
78. Fan, X., Liu, Z.W., Lu, J., Liu, Z.T.: Cellulose triacetate optical film preparation from ramie fiber. *Ind. Eng. Chem. Res.* 48, 6212–6215 (2009). <https://doi.org/10.1021/ie801703x>
79. Sathish Kumar, K., Rohit Narayanan, K.R., Siddarth, S., Pavan Kumar, R., Badri Narayan, R., Goutham, R., Samynaathan, V.: Synthesis of MgO/TiO<sub>2</sub> Nanocomposite and Its Application in Photocatalytic Dye Degradation. *Int. J. Chem. React. Eng.* 16, 1–14 (2018).  
<https://doi.org/10.1515/ijcre-2017-0136>

80. Shirkevad, S., Moslehifard, E.: Effect of TiO<sub>2</sub> nanoparticles on tensile strength of dental acrylic resins. *J. Dent. Res. Dent. Clin. Dent. Prospects.* 8, 197–203 (2014). <https://doi.org/10.5681/joddd.2014.036>
81. Zeng, J., Liu, S., Cai, J., Zhang, L.: TiO<sub>2</sub> immobilized in cellulose matrix for photocatalytic degradation of phenol under weak UV light irradiation. *J. Phys. Chem.* 114, 7806–7811 (2010)
82. Valentim, A.C.S., Tavares, M.I.B., da Silva, E.O.: Effect of adding TiO<sub>2</sub> to ethylene vinyl acetate on the latter's thermal properties and crystallinity. *Quim. Nov.* 37, 255–259 (2014)
83. Sangiorgi, A., Gonzalez, Z., Ferrandez-Montero, A., Yus, J., Sanchez-Herencia, A.J., Galassi, C., Sanson, A., Ferrari, B.: 3D printing of photocatalytic filters using a biopolymer to immobilize TiO<sub>2</sub> nanoparticles. *J. Electrochem. Soc.* 166, H3239–H3248 (2019). <https://doi.org/10.1149/2.0341905jes>
84. Restrepo, I., Benito, N., Medinam, C., Mangalaraja, R. V., Flores, P., Rodriguez-Llamazares, S.: Development and characterization of polyvinyl alcohol stabilized polylactic acid/ZnO nanocomposites. *Mater. Res. Express.* 0–22 (2017). <https://doi.org/https://doi.org/10.1088/2053-1591/aa8b8d> Manuscript
85. Glass, S., Trinklein, B., Abel, B., Schulze, A.: TiO<sub>2</sub> as photosensitizer and photoinitiator for synthesis of photoactive TiO<sub>2</sub>-PEGDA hydrogel without organic photoinitiator. *Front. Chem.* 6, 1–9 (2018). <https://doi.org/10.3389/fchem.2018.00340>
86. Das, C., Gebru, K.A.: Cellulose Acetate Modified Titanium Dioxide (TiO<sub>2</sub>) Nanoparticles Electrospun Composite Membranes: Fabrication and Characterization. *J. Inst. Eng. Ser. E.* 12 (2016). <https://doi.org/10.1007/s40034-017-0104-1>
87. Crosby, A.J., Lee, J.Y.: Polymer nanocomposites: The “nano” effect on mechanical properties. *Polym. Rev.* 47, 217–229 (2007). <https://doi.org/10.1080/15583720701271278>
88. Goudarzi, V., Shahabi-Ghahfarrokhi, I., Babaei-Ghazvini, A.: Preparation of ecofriendly UV-protective food packaging material by starch/TiO<sub>2</sub> bio-nanocomposite: Characterization. *Int. J. Biol. Macromol.* 95, 306–313 (2017). <https://doi.org/10.1016/j.ijbiomac.2016.11.065>
89. Spadetti, C., Da Silva Filho, E.A., De Sena, G.L., De Melo, C.V.P.: Propriedades térmicas e mecânicas dos compósitos de Polipropileno pós-consumo reforçados com fibras de cellulose. *Polimeros.* 27, 84–90 (2017). <https://doi.org/10.1590/0104-1428.2320>
90. Startsev, O. V., Makhonkov, A., Erofeev, V., Gudojnikov, S.: Impact of moisture content on dynamic mechanical properties and transition temperatures of wood. *Wood Mater. Sci. Eng.* 12, 55–62 (2017). <https://doi.org/10.1080/17480272.2015.1020566>

91. de Freitas, R.R.M., Senna, A.M., Botaro, V.R.: Influence of degree of substitution on thermal dynamic mechanical and physicochemical properties of cellulose acetate. *Ind. Crops Prod.* 109, 452–458 (2017). <https://doi.org/10.1016/j.indcrop.2017.08.062>
92. Bao, C., Long, D.R., Vergelät, C.: Miscibility and dynamical properties of cellulose acetate/plasticizer systems. *Carbohydr. Polym.* 116, 95–112 (2015)
93. Abdel-naby, A.S., Al-ghamdi, A.A.: Original Research Article Chemical modification of Cellulose Acetate by Diallylamine. *Int.J.Curr.Microbiol.App.Sci.* 3, 10–24 (2014)
94. Számel, G., Klébert, S., Sajó, I., Pukánszky, B.: Thermal analysis of cellulose acetate modified with caprolactone. *J. Therm. Anal. Calorim.* 91, 715–722 (2008)

## Chapter 7. Conclusion and Future Work

---

This chapter presents the general conclusions of this PhD project, the suggestions for future works and the further contributions of this thesis.

---



## 7.1 General conclusions

The current thesis has looked into the application of eco-friendly techniques to turn agroindustrial residues into cellulose-based bioplastics. Following the selection of a suitable agroindustrial residue, the outstanding extraction of cellulose by means a combined green pretreatment was the pivot achievement for the successful valorization of the biomass. The processing of cellulose to produce value-added biomaterials/nanocomposites was carried out by performing innovative and environmentally sustainable synthesis routes, including ionic liquid dissolution/regeneration, solvent-free acetylation and laser ablation in liquids.

**Chapter III** presented a diagnosis study assisted by the implementation of a linear model in addressing the identification of suitable agroindustrial residues in Brazil. The study revealed the huge availability of residues and its expected growth in the next years. Apart from the prompt availability, these residues represent an alternative low-cost source of raw-material as there is still no market demand for them. The linear suitability model indicates plenty of agroindustrial residues with the potential to be applied in the manufacturing of cellulose-based products, although some issues have to be tackled to ensure their maximum valorization, mainly regarding the observed spatio-temporal variability. The use of versatile processing techniques, that can be tailored to meet possible changes on processing design, including the treatment of residues with different physicochemical characteristics, may partially overcome this drawback.

Supported by the above-mentioned study, corncob was selected as a potential source of cellulose. In **Chapter IV** different green pretreatments technologies, namely ionic liquid, liquid hot water (LHW), dilute-NaOH, as well as their combined application, were performed and assessed regarding their potential effects on the physicochemical properties of the corncob. The results revealed that, depending on the pretreatment technology, different physicochemical changes may occur, whether at the chemical composition or crystalline structure. The treatment with ionic liquid (BmimCl) did not significantly change the chemical composition of the corncob, but in turn modified its crystalline structure to an amorphous phase. LHW and dilute-NaOH were highly efficient to extract hemicellulose and lignin, respectively, while maintained unchanged the crystalline structure. Among the combined pretreatments performed, LHW-dilute NaOH achieved remarkable delignification efficiency under mild conditions. By selectively removing non-cellulosic components, the recalcitrance of the biomass was significantly decreased in response of disruption of the inter- and intramolecular bonds. The obtained cellulose-enrich sample was suitable to produce a bioplastic film with notable mechanical properties.

For the concerned application, the combined LHW-dilute NaOH pretreatment has proved to be the most promising approach, as a high cellulose fraction was obtained and no changes on the crystallinity of the raw biomass have been set. Besides, it allowed the selective fractionation of hemicellulose and lignin in different stages. This is a crucial requirement for the economic viability of biomass valorization into cellulose-based products. Therefore, this pretreatment design was applied as the first processing step of subsequent treatments undertaken in this work. In **Chapter V**, the extracted cellulose was synthesized into cellulose acetate – a polymeric product with a wide range of applications and recognized biodegradable property. In line with the bias of the current thesis, a solvent-free eco-friendly acetylation technique was performed. The high yield obtained after acetylation, along with the less use of chemicals, endorsed the effectivity of the applied technique, which in turn had a positive contribution in reducing environmental impacts.

The synthesized CA was also applied to produce a bionanocomposite in **Chapter VI**. Nanocomposites based on bio-based matrices reinforced by metal oxide nanofillers are an emerged type of material in the field of active packaging. However, the development of sustainable processing technologies, whether to produce the matrices or the nanofillers, has become imperative. Therefore, in the concerned chapter, TiO<sub>2</sub> and MgO were directly synthesized via pulsed laser ablation in a solvent media suitable to dissolve the cellulose acetate. The proposed technique has shown to be versatile, easy-to-manage, clean and suitable to produce and embed the nanoparticles into the bio-based matrix. Considering that the bionanocomposite produced features good physicochemical properties and possible active antimicrobial/biodegradable activity, the proposed synthesis route appears to be a promising approach for developing novel active packaging components.

Overall, this thesis shows that agroindustrial residues may be a promising source of raw material to produce value-added polymeric materials. In addition to prevent environmental impacts related to unsuitable disposal of biomass and avoid the consumption of fossil resources, the emergence of these new bio-based products can also create new market niches and foster the circular economy. On top of that, besides to be highly effective for the concerned application, the proposed eco-friendly techniques can meet the main objectives of green chemistry. Notwithstanding, when applied as an integrated processing, some issues must be taken into account in order to ensure techno-economic feasibility, notably with regards to the valorization of the non-cellulosic components selectively extracted in the pretreatment step. It is also worth

mentioning that some of the techniques used have received increasing acceptance for large scale applications, namely LHW and laser technology, but this is still a challenging prospect.

## **7.2 Suggestions for future works**

Based on the developed work and results obtained, some suggestions of complementary and prospective investigations may include:

- The processing of other agroindustrial residues, preferentially with higher cellulose contents, and assessment of the proposed combined LHW-dilute NaOH pretreatment with regard to the fractionation of a mix of residues;
- The valorization of the other lignocellulose components, namely hemicellulose and lignin, extracted during the pretreatment step;
- Development of new approaches for the synthesis of metal oxides by means of laser ablation technology;
- Assessment of the antimicrobial and biodegradability activity, as well as barrier properties, of the produced bionanocomposite in order to prove the active properties provided by the embedment of  $\text{TiO}_2/\text{MgO}$  nanoparticles;
- Study of migration of nanoparticles from the produced bionanocomposite.
- Modeling of other life cycle assessment scenarios, taking into account the valorization of the non-cellulosic components, the laser ablation step, as well as the assumption of possible end-of-life technologies.

## Appendix A

---

This appendix presents the additional information regarding the methods and data used to determine the chemical compositions of untreated and pretreated corncob.

---

Supplementary information - Compositional analysis method and related data of untreated and pretreated samples

It is important to keep in mind that, in order to respect the typical thermal behavior of the concerned substances (cellulose, hemicellulose and lignin), when necessary some parameters were kept fixed. Therefore, the selection of the best fit modeling curves was based mainly on the Adj. R-square, the F value and the regular residual graph.

**Adj. R-square:** The Adj. R-square is a modified version of R-square, which is adjusted for the number of predictors in the fitted line. Thus, it can be used to compare the fitted lines with different numbers of predictors. If the number of predictors is greater than 1, Adj.-square is always smaller than R-square.

**F value:** is a ratio of two mean squares, which can be computed by dividing the mean square of fitted model by the mean square of error. It is a test statistic for a test of whether the fitted model differs significantly from the model  $y=\text{constant}$ , which is a flat line with slope being equal to zero. It can be inferred that the more this ratio deviates from 1, the stronger the evidence for the fitted model differing significantly from the model  $y=\text{constant}$ .

**Regular residual curve:** was used to assess the modelled fit curve quality.

- **Corncob compositional analysis** – deconvolution parameters and statistic:

**Table 1.** Deconvolution parameters. Where **y0** is the initialization parameter, **xc** curve center, **w** curve width and **A** curve area.

Parameters		Value	Standard error
Hemicellulose peak 1	y0	-0.01832	3.42E-04
Hemicellulose peak 1	xc	268.3016	0.12606
Hemicellulose peak 1	w	32.98282	0.26402
Hemicellulose peak 1	A	-9.58108	0
Hemicellulose peak 1	sigma	16.49141	0.13201
Hemicellulose peak 1	FWHM	38.83431	0.31086
Hemicellulose peak 1	Height	-0.23178	0.00186
Hemicellulose peak 2	y0	-0.01832	3.42E-04
Hemicellulose peak 2	xc	301.7857	0
Hemicellulose peak 2	w	32.31568	0.11413
Hemicellulose peak 2	A	-24.3289	0
Hemicellulose peak 2	sigma	16.15784	0.05706
Hemicellulose peak 2	FWHM	38.0488	0.13437
Hemicellulose peak 2	Height	-0.60069	0.00212
Cellulose	y0	-0.01832	3.42E-04
Cellulose	xc	340.5019	0
Cellulose	w	26.84495	0.07827
Cellulose	A	-26.0462	0.10211

Cellulose	sigma	13.42247	0.03913
Cellulose	FWHM	31.60751	0.09215
Cellulose	Height	-0.77414	0.00213
Lignin	y0	-0.01832	3.42E-04
Lignin	xc	340.5019	0
Lignin	w	173.7918	3.49218
Lignin	A	-11.6974	0
Lignin	sigma	86.89589	1.74609
Lignin	FWHM	204.6242	4.11172
Lignin	Height	-0.0537	0.00108

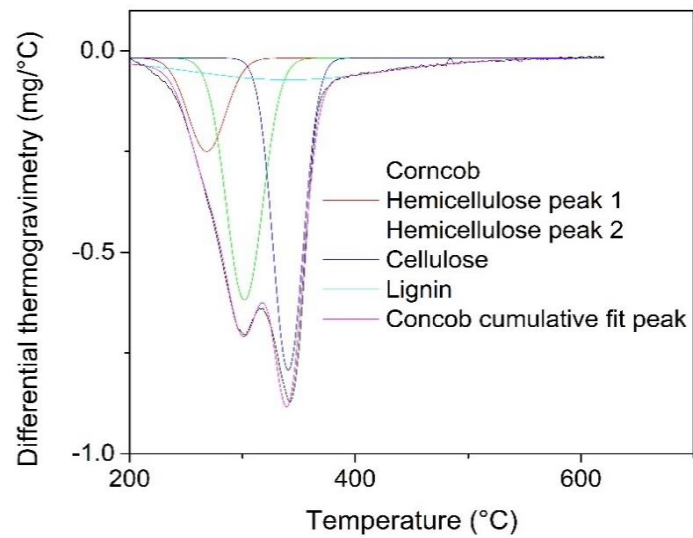
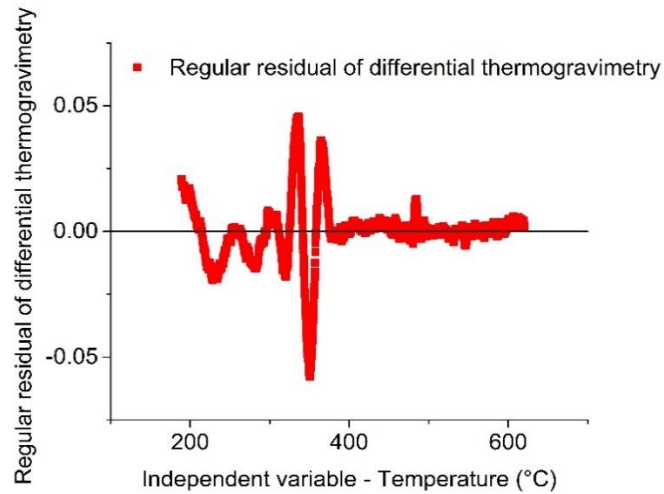


Figure 1. Corncob deconvoluted differential thermogravimetric curve

**Table 2.** Statistics and ANOVA

<b>Statistics</b>				
Number of Points				1806
Degrees of Freedom				1799
Reduced Chi-Sqr				1.57E-04
Residual Sum of Squares				0.28315
Adj. R-Square				0.99759
<b>ANOVA</b>				
	DF	Sum of Squares	Mean Square	F Value
Regression	7	177.81273	25.40182	161392.5
Residual	1799	0.28315	1.57E-04	
Uncorrected Total	1806	178.09588		
Corrected Total	1805	117.73283		



**Figure 2.** Regular residual from differential thermogravimetric of corncob.

**Adjusted model equation** - corncob cumulative fit peak (Equation 1).

$$y = y_0 + \left\{ \frac{A}{(w \times \sqrt{\pi/2})} \times e^{\left[ -2 \times \frac{(x-x_c)^2}{w^2} \right]} \right\} \quad (1)$$

- **LHW-treated corncob compositional analysis** - deconvolution parameters and statistic

**Table 3.** Deconvolution parameters. Where  $y_0$  is the initialization parameter,  $x_c$  curve center,  $w$  curve width and  $A$  curve area.

Parameters		Value	Standard Error
Hemicellulose	$y_0$	-0.0311	9.50E-04
Hemicellulose	$x_c$	300.7745	0
Hemicellulose	$A$	-2.93221	0
Hemicellulose	$w$	60.83908	0
Cellulose	$y_0$	-0.0311	9.50E-04
Cellulose	$x_c$	350.9776	0
Cellulose	$A$	-58.098	0.39646
Cellulose	$w$	32.48151	0.1636
Lignin	$y_0$	-0.0311	9.50E-04
Lignin	$x_c$	350.7821	0
Lignin	$A$	-13.1306	0.61305
Lignin	$w$	100.7608	0

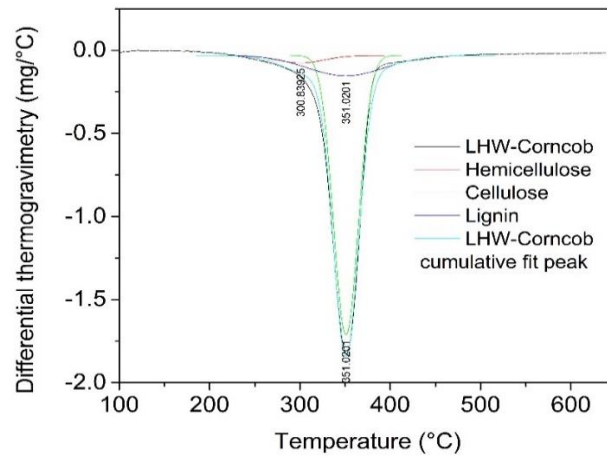


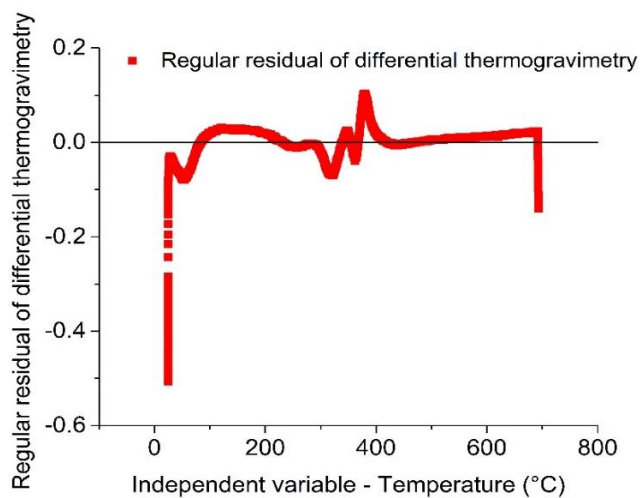
**Figure 3.** LHW-treated corncob deconvoluted differential thermogravimetric curve

**Table 4.** Statistics and ANOVA

<b>Statistics</b>				
Number of Points				2869
Degrees of Freedom				2865
Reduced Chi-Sqr				0.00192
Residual Sum of Squares				5.51418
Adj. R-Square				0.98325

<b>ANOVA</b>	<b>DF</b>	<b>Sum of Squares</b>	<b>Mean Square</b>	<b>F Value</b>
Regression	4	379.6543	94.91357	49314.18
Residual	2865	5.51418	0.00192	
Uncorrected Total	2869	385.16848		
Corrected Total	2868	329.52425		



**Figure 4.** Regular residual from differential thermogravimetric of LHW-treated corncob.

**Adjusted model equation** – LHW-treated corncob cumulative fit peak (Equation 2)



$$y=y_0+\left[\frac{A}{w\times\sqrt{\pi/4\times\ln(2)}}\right]\times e^{\left\{-4\times\ln(2)\times\left[\frac{(x-x_c)^2}{w^2}\right]\right\}} \quad (2)$$

- **LHW-IL-treated corncob compositional analysis** - deconvolution parameters and statistic

**Table 5.** deconvolution parameters. Where  $y_0$  is the initialization parameter,  $x_c$  curve center,  $w$  curve width and  $A$  curve area.

Parameters		Value	Standard Error
Hemicellulose	$y_0$	-0.02383	8.73E-04
Hemicellulose	$x_c$	265	0
Hemicellulose	$w$	21	0
Hemicellulose	$A$	-2.875	0
Hemicellulose	$\sigma$	10.5	0
Hemicellulose	FWHM	24.72561	0
Hemicellulose	Height	-0.10923	0
Cellulose 1	$y_0$	-0.02383	8.73E-04
Cellulose 1	$x_c$	309.2415	0.14612
Cellulose 1	$w$	48	0
Cellulose 1	$A$	-53	0
Cellulose 1	$\sigma$	24	0
Cellulose 1	FWHM	56.51568	0
Cellulose 1	Height	-0.881	0
Cellulose 2	$y_0$	-0.02383	8.73E-04
Cellulose 2	$x_c$	355	0
Cellulose 2	$w$	17.5	0
Cellulose 2	$A$	-4.859	0
Cellulose 2	$\sigma$	8.75	0
Cellulose 2	FWHM	20.60468	0
Cellulose 2	Height	-0.22154	0
Lignin	$y_0$	-0.02383	8.73E-04
Lignin	$x_c$	288.4015	4.19703
Lignin	$w$	155.255	0
Lignin	$A$	-10.73	0
Lignin	$\sigma$	77.6275	0
Lignin	FWHM	182.7988	0
Lignin	Height	-0.05514	0

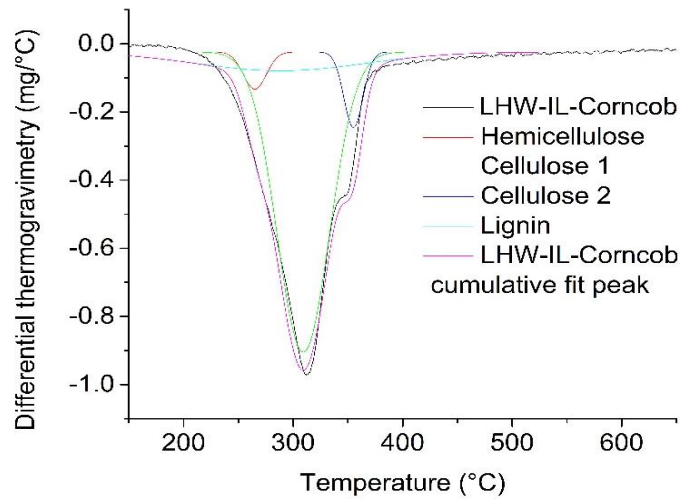


**Figure 5.** LHW-IL-treated corncob deconvoluted differential thermogravimetric curve.

**Table 6.** Statistics and ANOVA

<b>Statistics</b>				
Number of Points				2867
Degrees of Freedom				2864
Reduced Chi-Sqr				0.00218
Residual Sum of Squares				6.25735
Adj. R-Square				0.95485
<b>ANOVA</b>				
	DF	Sum of Squares	Mean Square	F Value
Regression	3	179.43908	59.81303	27376.51
Residual	2864	6.25735	0.00218	
Uncorrected Total	2867	185.69643		
Corrected Total	2866	138.68612		

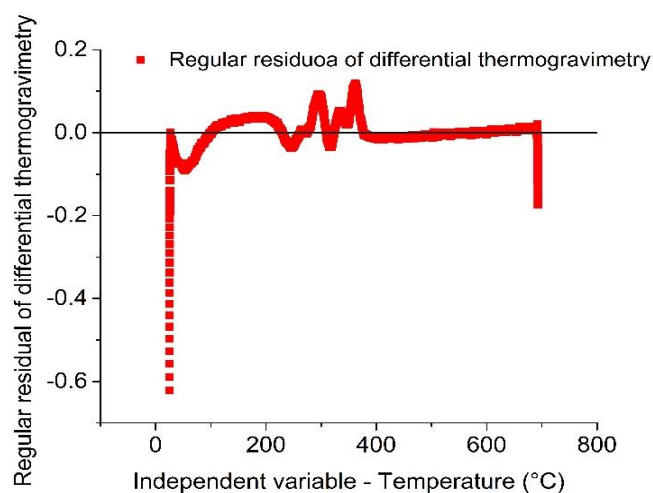


**Figure 6.** Regular residual from differential thermogravimetric of LHW-IL-treated corncob.

**Adjusted model equation** – LHW-IL-treated corncob cumulative fit peak (Equation 3)

$$y = y_0 + \left\{ \frac{A}{(w \times \sqrt{\pi/2})} \times e^{\left[-2 \times \frac{(x-x_c)^2}{w^2}\right]} \right\} \quad (3)$$

- **LHW-NaOH treated corncob compositional analysis** - deconvolution parameters and statistic

**Table 7.** deconvolution parameters. Where  $y_0$  is the initialization parameter,  $x_c$  curve center,  $w$  curve width and  $A$  curve area.

	<b>Parameters</b>	Value	Standard Error
Hemicellulose	$y_0$	-0.03872	0.0014
Hemicellulose	$x_c$	328	0
Hemicellulose	$w$	15	0
Hemicellulose	$A$	-3	0
Hemicellulose	$\sigma$	7.5	0
Hemicellulose	FWHM	17.66115	0
Hemicellulose	Height	-0.15958	0
Cellulose	$y_0$	-0.03872	0.0014
Cellulose	$x_c$	358.2	0
Cellulose	$w$	25	0
Cellulose	$A$	-55.5	0
Cellulose	$\sigma$	12.5	0
Cellulose	FWHM	29.43525	0
Cellulose	Height	-1.7713	0
Lignin	$y_0$	-0.03872	0.0014
Lignin	$x_c$	318	0
Lignin	$w$	38	0
Lignin	$A$	-7	0
Lignin	$\sigma$	19	0
Lignin	FWHM	44.74158	0
Lignin	Height	-0.14698	0

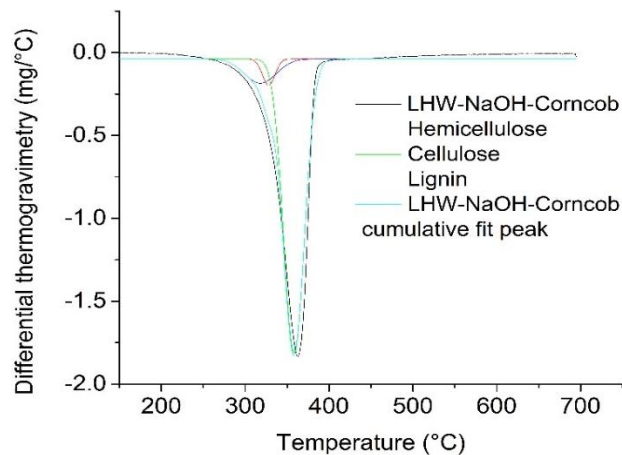


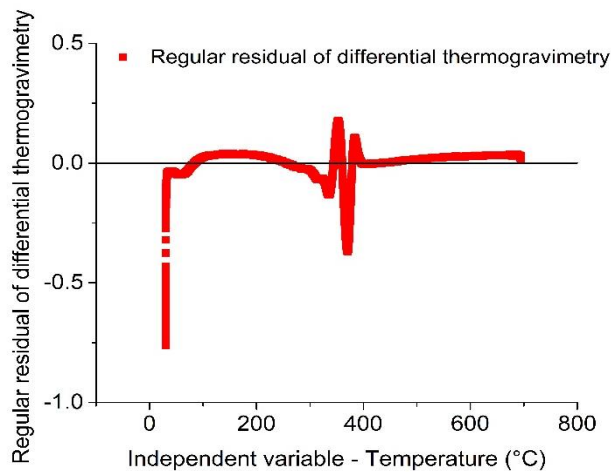
**Figure 7.** LHW-NaOH-treated corncob deconvoluted differential thermogravimetric curve.

**Table 8.** Statistics and ANOVA

<b>Statistics</b>				
Number of Points				2862
Degrees of Freedom				2861
Reduced Chi-Sqr				0.00558
Residual Sum of Squares				15.96532
Adj. R-Square				0.95209

<b>ANOVA</b>	DF	Sum of Squares	Mean Square	F Value
Regression	1	369.61839	369.61839	66235.95
Residual	2861	15.96532	0.00558	
Uncorrected Total	2862	385.58371		
Corrected Total	2861	333.22655		

**Figure 8.** Regular residual from differential thermogravimetric of LHW-NaOH-treated corncob.

**Adjusted model equation** LHW-NaOH-treated corncob cumulative fit peak (Equation 4)

$$y = y_0 + \left\{ \frac{A}{(w \times \sqrt{\pi/2})} \times e \left[ -2 \times \frac{(x-x_c)^2}{w^2} \right] \right\} \quad (4)$$

- **LHW-NaOH-IL treated corncob compositional analysis** - deconvolution parameters and statistic

**Table 9.** Deconvolution parameters. Where  $y_0$  is the initialization parameter,  $x_c$  curve center,  $w$  curve width and  $A$  curve area.

	Parameters	Value	Standard Error
Hemicellulose	$y_0$	-0.0142	8.02E-04
Hemicellulose	$x_c$	258.2081	0
Hemicellulose	$A$	-2.72845	0
Hemicellulose	$w$	40.12654	0

Cellulose peak 1	y0	-0.0142	8.02E-04
Cellulose peak 1	xc	296.5643	0
Cellulose peak 1	A	-65.1565	0
Cellulose peak 1	w	43.12656	0
Cellulose peak 2	y0	-0.0142	8.02E-04
Cellulose peak 2	xc	353.1305	0
Cellulose peak 2	A	-1.34377	0
Cellulose peak 2	w	18.12654	0
Lignin	y0	-0.0142	8.02E-04
Lignin	xc	330.6556	0
Lignin	A	-8.00355	0
Lignin	w	150.1266	0

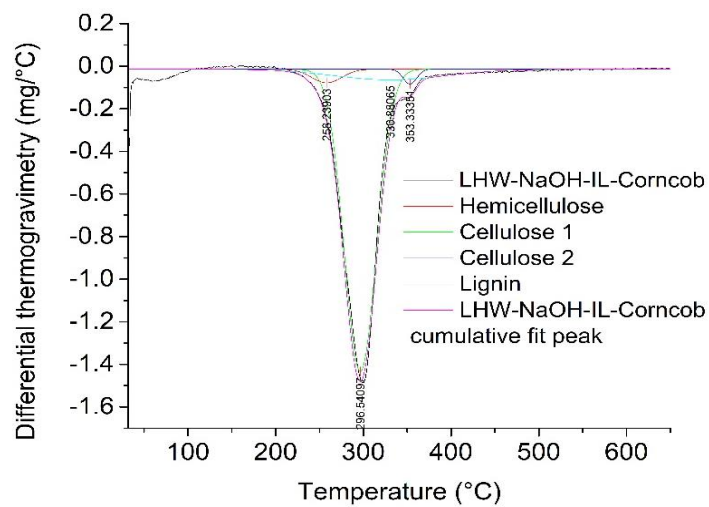


**Figure 9.** LHW-NaOH-IL-treated corncob deconvoluted differential thermogravimetric curve.

**Table 10.** Statistics and ANOVA

<b>Statistics</b>				
Number of Points				2860
Degrees of Freedom				2859
Reduced Chi-Sqr				0.00184
Residual Sum of Squares				5.25825
Adj. R-Square				0.97925
<b>ANOVA</b>				
	DF	Sum of Squares	Mean Square	F Value
Regression	1	295.10028	295.10028	160451.2
Residual	2859	5.25825	0.00184	
Uncorrected Total	2860	300.35853		
Corrected Total	2859	253.39564		

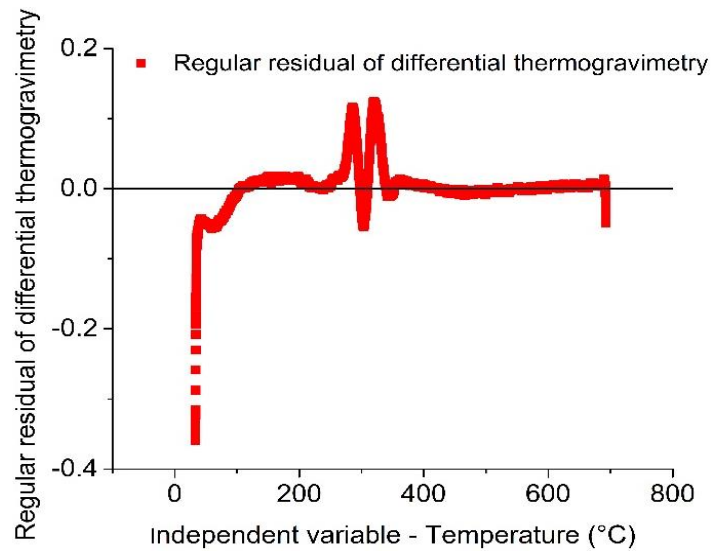


**Figure 10.** Regular residual from differential thermogravimetric of LHW-NaOH-IL-treated corncob.

**Adjusted model equation** LHW-NaOH-IL-treated corncob cumulative fit peak (Equation 5).

$$y=y_0 + \left[ \frac{A}{w \times \sqrt{\pi/4 \times \ln(2)}} \right] \times e^{\left\{ -4 \times \ln(2) \times \left[ \frac{(x-x_c)^2}{w^2} \right] \right\}} \quad (5)$$

- **NaOH-treated corncob compositional analysis** - deconvolution parameters and statistic.

**Table 11.** Deconvolution parameters. Where  $y_0$  is the initialization parameter,  $x_c$  curve center,  $w$  curve width and  $A$  curve area.

Parameters		Value	Standard Error
Hemicellulose peak 1	$y_0$	-0.02426	0.00151
Hemicellulose peak 1	$x_c$	284	0
Hemicellulose peak 1	$w$	27	0
Hemicellulose peak 1	$A$	-3	0
Hemicellulose peak 1	$\sigma$	13.5	0
Hemicellulose peak 1	FWHM	31.79007	0
Hemicellulose peak 1	Height	-0.08865	0
Hemicellulose peak 2	$y_0$	-0.02426	0.00151
Hemicellulose peak 2	$x_c$	314.5	0
Hemicellulose peak 2	$w$	28	0
Hemicellulose peak 2	$A$	-17	0
Hemicellulose peak 2	$\sigma$	14	0
Hemicellulose peak 2	FWHM	32.96748	0
Hemicellulose peak 2	Height	-0.48443	0
Cellulose	$y_0$	-0.02426	0.00151
Cellulose	$x_c$	348	0
Cellulose	$w$	28	0
Cellulose	$A$	-46	0
Cellulose	$\sigma$	14	0
Cellulose	FWHM	32.96748	0

Cellulose	Height	-1.31081	0
Lignin	y0	-0.02426	0.00151
Lignin	xc	385	0
Lignin	w	150	0
Lignin	A	-5.74	0
Lignin	sigma	75	0
Lignin	FWHM	176.6115	0
Lignin	Height	-0.03053	0

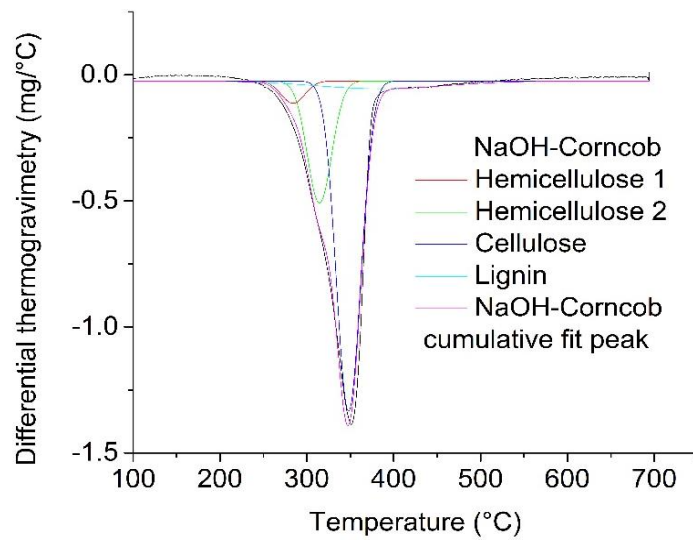


**Figure 11.** NaOH-treated corncob deconvoluted differential thermogravimetric curve.

**Table 12.** Statistics and ANOVA

<b>Statistics</b>				
Number of Points				2859
Degrees of Freedom				2858
Reduced Chi-Sqr				0.00648
Residual Sum of Squares				18.51896
Adj. R-Square				0.9261
<b>ANOVA</b>				
	DF	Sum of Squares	Mean Square	F Value
Regression	1	280.42404	280.42404	43277.37
Residual	2858	18.51896	0.00648	
Uncorrected Total	2859	298.943		
Corrected Total	2858	250.58362		

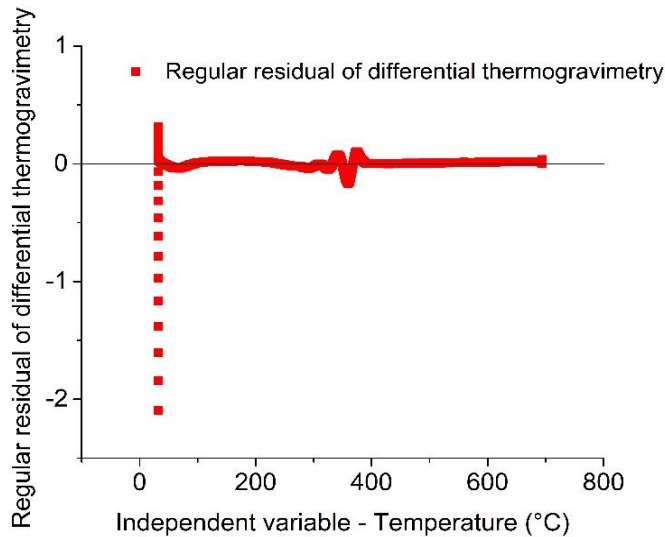


**Figure 12.** Regular residual from differential thermogravimetric of LHW-NaOH-IL-treated corncob.

**Adjusted model equation** – NaOH-treated corncob cumulative fit peak (Equation 6)

$$y = y_0 + \left\{ \frac{A}{(w \times \sqrt{\pi/2})} \times e^{\left[ -2 \times \frac{(x-x_c)^2}{w^2} \right]} \right\} \quad (6)$$

- **IL-treated corncob compositional analysis** - deconvolution parameters and statistic.

**Table 13.** Deconvolution parameters. Where  $y_0$  is the initialization parameter,  $x_c$  curve center,  $w$  curve width and  $A$  curve area.

Parameters		Value	Standard Error
Hemicellulose peak 1	$y_0$	-0.0168	4.90E-04
Hemicellulose peak 1	$x_c$	237.8476	0
Hemicellulose peak 1	$w$	16.8874	0
Hemicellulose peak 1	$A$	-0.25829	0
Hemicellulose peak 1	$\sigma$	8.4437	0
Hemicellulose peak 1	FWHM	19.8834	0
Hemicellulose peak 1	Height	-0.0122	0
Hemicellulose peak 2	$y_0$	-0.0168	4.90E-04
Hemicellulose peak 2	$x_c$	281	0
Hemicellulose peak 2	$w$	43.16918	0.19918
Hemicellulose peak 2	$A$	-33.1181	0.13856
Hemicellulose peak 2	$\sigma$	21.58459	0.09959
Hemicellulose peak 2	FWHM	50.82783	0.23452
Hemicellulose peak 2	Height	-0.61211	0.00231
Lignin peak 1	$y_0$	-0.0168	4.90E-04
Lignin peak 1	$x_c$	322	0
Lignin peak 1	$w$	27	0
Lignin peak 1	$A$	-7	0
Lignin peak 1	$\sigma$	13.5	0
Lignin peak 1	FWHM	31.79007	0
Lignin peak 1	Height	-0.20686	0
Cellulose	$y_0$	-0.0168	4.90E-04



Cellulose	xc	353.9608	0.05454
Cellulose	w	27.87115	0.08778
Cellulose	A	-30	0
Cellulose	sigma	13.93557	0.04389
Cellulose	FWHM	32.81577	0.10335
Cellulose	Height	-0.85883	0.0027
Lignin peak 2	y0	-0.0168	4.90E-04
Lignin peak 2	xc	400	0
Lignin peak 2	w	110	0
Lignin peak 2	A	-6	0
Lignin peak 2	sigma	55	0
Lignin peak 2	FWHM	129.5151	0
Lignin peak 2	Height	-0.04352	0

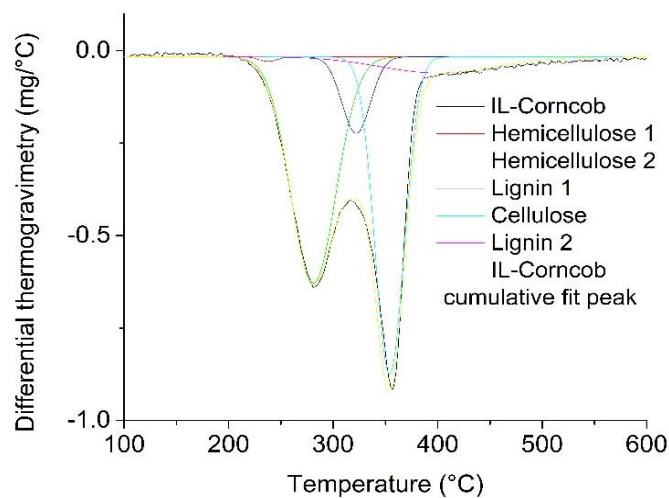


**Figure 13.** IL-treated corncob deconvoluted differential thermogravimetric curve.

**Table 14.** Statistics and ANOVA.

<b>Statistics</b>				
Number of Points				2817
Degrees of Freedom				2812
Reduced Chi-Sqr				5.57E-04
Residual Sum of Squares				1.56576
Adj. R-Square				0.98757
<b>ANOVA</b>				
	DF	Sum of Squares	Mean Square	F Value
Regression	5	172.9983	34.59966	62138.49
Residual	2812	1.56576	5.57E-04	
Uncorrected Total	2817	174.56407		
Corrected Total	2816	126.19144		

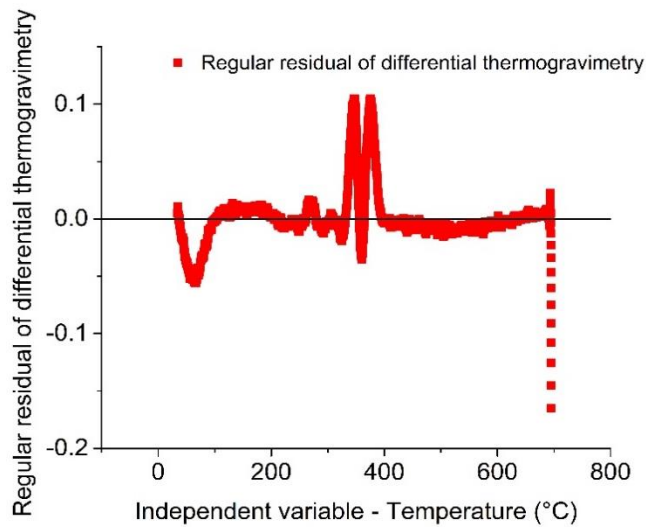


**Figure 14.** Regular residual from differential thermogravimetric of IL-treated corncob.

**Adjusted model equation** – IL-treated corncob cumulative fit peak (Equation 7).

$$y = y_0 + \left\{ \frac{A}{(w \times \sqrt{\pi/2})} \times e^{\left[ -2 \times \frac{(x-x_c)^2}{w^2} \right]} \right\} \quad (7)$$

- **NaOH-IL-treated corncob compositional analysis** - deconvolution parameters and statistic.

**Table 15.** Deconvolution parameters. Where  $y_0$  is the initialization parameter,  $x_c$  curve center,  $w$  curve width and  $A$  curve area.

Parameters		Value	Standard Error
Hemicellulose peak 1	$y_0$	-0.04048	0.00333
Hemicellulose peak 1	$x_c$	239.9392	3.76466
Hemicellulose peak 1	$w$	25	0
Hemicellulose peak 1	$A$	-3	0
Hemicellulose peak 1	$\sigma$	12.5	0
Hemicellulose peak 1	FWHM	29.43525	0
Hemicellulose peak 1	Height	-0.09575	0
Hemicellulose peak 2	$y_0$	-0.04048	0.00333
Hemicellulose peak 2	$x_c$	277.8687	5.77703
Hemicellulose peak 2	$w$	28	0
Hemicellulose peak 2	$A$	-13	0
Hemicellulose peak 2	$\sigma$	14	0
Hemicellulose peak 2	FWHM	32.96748	0
Hemicellulose peak 2	Height	-0.37045	0
Cellulose	$y_0$	-0.04048	0.00333
Cellulose	$x_c$	277.8688	2.15564
Cellulose	$w$	32	0
Cellulose	$A$	-43	0
Cellulose	$\sigma$	16	0
Cellulose	FWHM	37.67712	0
Cellulose	Height	-1.07216	0

Lignin	y0	-0.04048	0.00333
Lignin	xc	300	0
Lignin	w	120	0
Lignin	A	-5	0
Lignin	sigma	60	0
Lignin	FWHM	141.2892	0
Lignin	Height	-0.03325	0

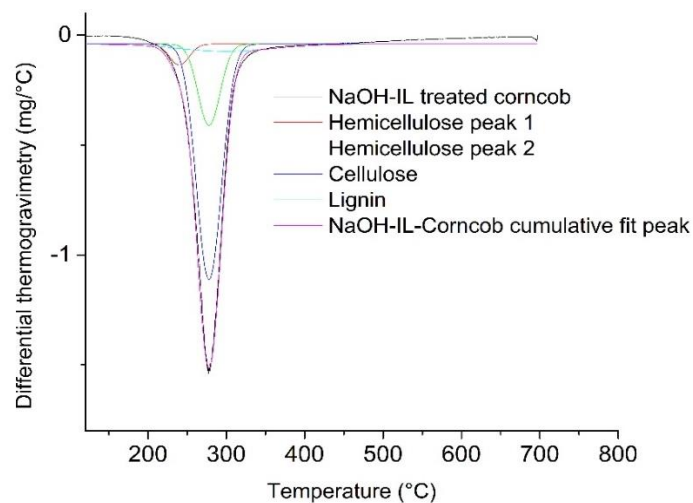


**Figure 15.** NaOH-IL-treated corncob deconvoluted differential thermogravimetric curve.

**Table 16.** Statistics and ANOVA.

<b>Statistics</b>				
Number of Points				2859
Degrees of Freedom				2855
Reduced Chi-Sqr				0.03176
Residual Sum of Squares				90.66297
Adj. R-Square				0.71065
<b>ANOVA</b>				
	DF	Sum of Squares	Mean Square	F Value
Regression	4	274.96236	68.74059	2164.6588
Residual	2855	90.66297	0.03176	
Uncorrected Total	2859	365.62533		
Corrected Total	2858	313.66171		

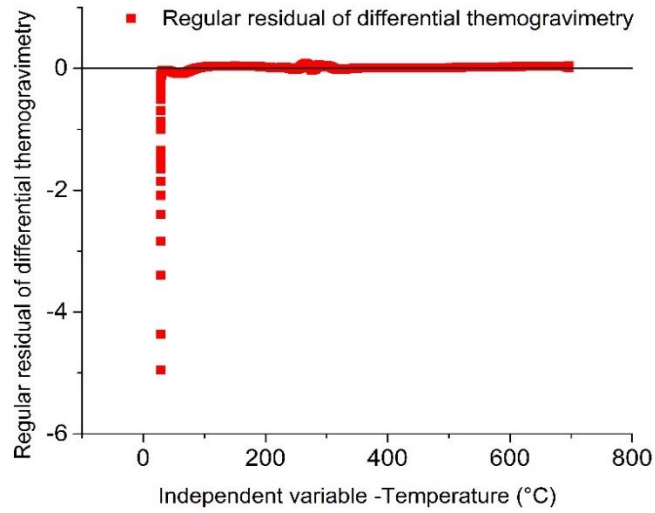


**Figure 16.** Regular residual from differential thermogravimetric of NaOH-IL-treated corncob.

**Adjusted model equation** – IL-treated corncob cumulative fit peak (Equation 8).

$$y = y_0 + \left\{ \frac{A}{(w \times \sqrt{\pi/2})} \times e^{\left[ -2 \times \frac{(x-x_c)^2}{w^2} \right]} \right\} \quad (8)$$

## Appendix B

---

This appendix presents additional information regarding the life cycle inventory used to implement the life cycle assessment model.

---

**Supplementary information** - Life cycle Inventory and additional Information.**Table 1.** Processes used in the life cycle assessment obtained from Ecoinvent 3.3.

Process	Process name in the Ecoinvent 3.3
Electricity production and distribution	Electricity voltage transformation from high to medium/electricity medium voltage/ Cutoff, U -BR
Production of NaOH	Sodium hydroxide, without water, in 50% solution state, Cutoff, U -RER
Production of NaClO <sub>2</sub> <sup>a</sup>	Chlorite dioxide, Cutoff, U - RER
	Hydrogen peroxide, without water, in 50% solution state, Cutoff, U - RER
	Sodium hydroxide, without water, in 50% solution state, Cutoff, U -RER
Production of H <sub>2</sub> SO <sub>4</sub>	Sulfuric acid, Cutoff, U - RER
Production of CH <sub>3</sub> COOH	Acetic acid, without water, in 98% solution state, Cutoff, U -RER
Production of Ac <sub>2</sub> O	Acetic anhydride, Cutoff, U -RER
Production of CH <sub>3</sub> OH	Methanol, Cutoff, U -RER
Production of C <sub>2</sub> H <sub>5</sub> OH	Ethanol, without water, in 99.7% solution state, from ethylene, Cutoff, U -RER
Production of iodine	Iodine, Cutoff, U -RER
Production of sodium thiosulfate <sup>b</sup>	Sodium sulfite, Cutoff, U -RER
	Sulfur, Cutoff, U -GLO
Production of deionized water	Water, deionized, from tap water, at user, Cutoff, U -RoW
Production of CH <sub>2</sub> Cl <sub>2</sub>	Dichloromethane, Cutoff, U -RER

<sup>a</sup>Sodium chlorite production process does not exist in the Ecoinvent database. Thus, it was modeled in OpenLCA according to the production process proposed by Ian et al., (2007).

<sup>b</sup>Sodium thiosulfate production process does not exist in Ecoinvent database. Therefore, it was modeled in OpenLCA according to production process proposed by Ferreira (2017).

**Table 2.** Life cycle inventory for producing 10 g of cellulose acetate by means the green acetylation approach.

Green acetylation of cellulose		Materials inventory		
First stage of the treatment				
Input	Output		Amount	Unit
Dried treated corncob	Acetylated solution	Electricity	13608	kJ
Iodine		Dried pretreated corncob	6.25	g
Ethanol		Iodine	9.375	g
Sodium thiosulfate		Acetic anhydride	312.5	ml
Acetic anhydride		Sodium thiosulfate	156.25	ml
Energy		Ethanol	937.5	ml
Second stage of the treatment				
Input	Output		Amount	Unit
Acetylated solution	Dried cellulose acetate	Electricity	95775	kJ
Deionized water	Filtered/washed solution	Acetylated solution	1279.91	g
Dichloromethane	dichloromethane	Ethanol	1171.875	ml
Electricity		Deionized water	390.695	ml
		Dichloromethane	937.5	ml

**Additional information used to build the inventory:**

- The process was modeled taking into account the functional unit of 10g of cellulose acetate and a yield of 160%.
- Formulation for energy consume (E):  $E = 1000 \cdot kw \cdot t(s)$ . In which t refers to time of processing and kw the potency of the equipment.
- The recovery of 90 ml of dichloromethane took 10 min.
- The green acetylation methodology was based on Das et al. (2015).

**Table 3.** Additional information to build the inventory

Sodium thiosulfate solubility	1.667 g/cm <sup>3</sup>
Acetic anhydride density	1.08 g/cm <sup>3</sup>
Ethanol density	0.789 g/cm <sup>3</sup>
Dichloromethane density	1.33 g/cm <sup>3</sup>

**Table 4.** Life cycle inventory for producing 10 g of cellulose acetate by means the standard acetylation approach.

Standard acetylation of cellulose		Materials inventory		
First stage of the treatment				
Input	Output		Amount	Unit
Dried treated corncob	Acetylated solution	Electricity	120420	kJ
Acetic acid		Dried pretreated corncob	7.143	g
Acetic anhydride		Acetic acid	225	g
Sulfuric acid		Acetic anhydride	100	g
Methanol		Sulfuric acid	0.63	g
Electricity		Methanol	285.72	ml
Second stage of the treatment				
Input	Output		Amount	Unit
Acetylated solution	Dried cellulose acetate	Electricity	971145.5	kJ
Deionized water	Filtered/washed solution	Acetylated solution	559.07	g
Methanol	dichloromethane	Methanol	1785.75	ml
Dichloromethane		Dichloromethane	1071.45	ml
Electricity				

**Additional information used to build the inventory:**

- The process was modeled taking into account the functional unit of 10g of cellulose acetate and a yield of 140%;
- Formulation for energy consume (E):  $E = 1000 \cdot kw \cdot t(s)$ . In which t refers to time of processing and kw the potency of the equipment;
- The green acetylation methodology was based on Jo et al. (2016), Coletti et al (2013), Bello et al. (2016), Mostafa et al. (2018) and Cao et al. (2018).

**Table 5.** Impact assessment associated with LCA scenarios.

<b>Impact category</b>	<b>Model</b>	<b>AC standrd convt. pretr.</b>	<b>AC stndrd green pretrt</b>	<b>Green process</b>	<b>Unit</b>
GWP	IPCC 2013	1.99E+01	1.89E+01	1.76E+01	kg CO2-Eq
land use - competition	CML 2001	2.15E-02	2.01E-02	2.03E-02	m2a
ODP	CML 2001	9.68E-05	9.67E-05	8.46E-05	kg CFC-11-Eq
stratospheric ozone depletion - ODP 20a	CML 2001	1.07E-06	9.80E-07	8.44E-07	kg CFC-11-Eq
HTc	USEtox	6.72E-07	6.42E-07	6.05E-07	CTU
HTnc	USEtox	2.44E-06	2.32E-06	2.27E-06	CTU
PM	Selected LCI results	1.11E-02	1.04E-02	9.28E-03	kg
IR	ILCD 1.0.8 2016	1.65E+00	1.53E+00	1.34E+00	kg U235-Eq
FE	ReCiPe (H)	4.42E-03	4.14E-03	4.11E-03	kg P-Eq
ME	ReCiPe (H)	1.82E-02	1.75E-02	1.61E-02	kg N-Eq
POF	ReCiPe (H)	5.99E-02	5.77E-02	5.56E-02	kg NMVOC
environmental impact - acidification	TRACI	4.95E+00	4.73E+00	4.40E+00	moles of H+-Eq
TA	ILCD 1.0.8 2016	1.14E-01	1.09E-01	1.01E-01	mol H+-Eq
TE	ILCD 1.0.8 2016	1.93E-01	1.86E-01	1.71E-01	mol N-Eq
ET	USEtox	3.20E+01	3.02E+01	3.24E+01	CTU
Rf	Cummulative exergy demand	2.62E+02	2.50E+02	2.52E+02	MJ-Eq
fossil depletion - FDP	ReCiPe (H)	6.38E+00	6.09E+00	6.10E+00	kg oil-Eq
resources - mineral, fossils and renewables	ILCD 1.0.8 2016	1.34E-04	1.27E-04	1.78E-04	kg Sb-Eq



**Table 6.** Environmental impacts after modification of the green approach parameters for the sensitivity analysis study.

<b>Impact category</b>	<b>green</b>	<b>yield 140%</b>	<b>Yield 150%</b>	<b>yield 160%</b>	<b>yield 170%</b>	<b>Unit</b>
climate change - GWP 100a	1.76E+01	1.99E+01	1.89E+01	1.81E+01	1.74E+01	kg CO2-Eq
stratospheric ozone depletion - ODP steady state	8.46E-05	9.68E-05	9.04E-05	8.47E-05	7.98E-05	kg CFC-11-Eq
ecotoxicity - total	3.24E+01	3.20E+01	3.05E+01	2.92E+01	2.81E+01	CTU
human toxicity - carcinogenic	6.05E-07	6.72E-07	6.37E-07	6.08E-07	5.82E-07	CTU
human toxicity - non-carcinogenic	2.27E-06	2.44E-06	2.31E-06	2.20E-06	2.11E-06	CTU
air - particulates, < 2.5 um	9.28E-03	1.11E-02	1.06E-02	1.02E-02	9.85E-03	kg
ecosystem quality - freshwater and terrestrial acidification	1.01E-01	1.14E-01	1.08E-01	1.04E-01	9.93E-02	mol H+-Eq
ecosystem quality - terrestrial eutrophication	1.71E-01	1.93E-01	1.83E-01	1.74E-01	1.67E-01	mol N-Eq
human health - ionising radiation	1.34E+00	1.65E+00	1.58E+00	1.52E+00	1.48E+00	kg U235-Eq
freshwater eutrophication - FEP	4.11E-03	4.42E-03	4.23E-03	4.06E-03	3.92E-03	kg P-Eq
marine eutrophication - MEP	1.61E-02	1.82E-02	1.72E-02	1.64E-02	1.57E-02	kg N-Eq
photochemical oxidant formation - POFP	5.56E-02	5.99E-02	5.66E-02	5.39E-02	5.15E-02	kg NMVOC
fossil - non-renewable energy resources, fossil	2.56E+02	2.68E+02	2.54E+02	2.43E+02	2.33E+02	MJ-Eq

## References

- [1] Y. Ian, Y. Chen, Y. Jiang, L. Zhang. A clean production process of sodium chlorite from sodium chlorate. *Journal of Cleaner Production*, 15 (2007), pp. 920-926.
- [2] Ferreira, C. M. B. Extended environmental life-cycle assessment of munitions: addressing chemical toxicity hazard on human health (Doctoral dissertation, 00500: Universidade de Coimbra) (2017).
- [3] Das, A.M., Ali, A.A., Hazarika, M.P. Synthesis and characterization of cellulose acetate from rice husk: Eco-friendly condition. *Carbohydr. Polym.* 112, 342–349 (2014). <https://doi.org/10.1016/j.carbpol.2014.06.006>.
- [4] Jo, J.S., Jung, J.Y., Byun, J.H., Lim, B.K., Yang, J.K. Preparation of cellulose acetate produced from lignocellulosic biomass. *J. Korean wood Sci. Technol.* 44, 241–252 (2016).

- [5] Coletti, A., Valerio, A., Vismara, E. *Posidonia oceanica* as a renewable lignocellulosic biomass for the synthesis of cellulose acetate and glycidyl methacrylate grafted cellulose. *Materials (Basel)*. 6, 2043–2058 (2013). <https://doi.org/10.3390/ma6052043>.
- [6] Bello, A., Tijjani, M., Olufemi, B.O., Mukhtar, B. Acetylation of Cotton Stalk for Cellulose Acetate Production. *Am. Sci. Res. J. Eng. Technol. Sci.* 15, 137–150 (2016).
- [7] Mostafa, N.A., Tayeb, A.M. Production of biodegradable plastic from agricultural wastes. *Arab. J. Chem.* 11, 546–553 (2018). <https://doi.org/10.1016/j.arabjc.2015.04.008>.
- [8] Cao, L., Luo, G., Tsang, D.C.W., Chen, H., Zhang, S., Chen, J. A novel process for obtaining high quality cellulose acetate from green landscaping waste. *J. Clean. Prod.* 176, 338–347 (2018). <https://doi.org/10.1016/j.jclepro.2017.12.077>